University of Reading

Carbohydrate analysis for biomedical applications-developing integrated workflows for analysing glycans in neurodegenerative disorders.

A thesis submitted to The University of Reading in partial fulfilment for the degree of Doctor of Philosophy

School of Pharmacy

Pornpak Sirathanarun

March 2024

Declaration

I confirm that this is my own work and that all material from other sources has been appropriately acknowledged. This work is original and is not being submitted for any other degree.

PORNPAK SIRATHANARUN

Acknowledgements

Above all, I would like to express my gratitude to my PhD supervisors, Professor Helen Osborn, Dr Graeme Cottrell, and Dr Sarah Allman. Their constant support, guidance, and motivation have been priceless throughout my entire academic journey. From refining my research in each step to submitting my final thesis, their unwavering presence and wealth of knowledge have shaped my academic growth. I highly valued our meetings, which served as checkpoints to keep me on track academically and provided me with plenty of encouragement. I am profoundly grateful for their immeasurable contributions to my development.

In addition to my supervisors, I am indebted to my exceptional lab mates, whose support has been a constant source of motivation. As a pharmacist from Thailand, I have experience in quality control and quality assurance in pharmaceuticals. Chemical synthesis and carbohydrate analysis are new chapters in my academic life. My PhD life in the School of Pharmacy, University of Reading, was passed through quickly with their help. Our collaborative informal chats, whether conducted via screens during lockdowns or in person whenever circumstances allowed, provided a lifeline during the most challenging times. I am proud to say that we became more than just lab partners; we became good friends. Matthew, Oliver and Jessica, thanks for always providing a steady supply of synthesis and analysis techniques for carbohydrate fields. Kathryn, staff, and other PhD students in Hopkins building thank you for being patient with me during the cell culture training for my final thesis Chapter.

A special thanks goes out to all staff of the School of Pharmacy and the Doctoral and Researcher College, University of Reading, for being helpful during my study time at the university. I would like to thank three Thai government sectors for my great opportunity to study in the UK. First, I sincerely thank the Thai government for my scholarship. This grant allowed me to fulfil my achievable life goals in studying abroad. Secondly, The Office of Educational Affairs (OEA), The Royal Thai Embassy in the UK, looked after me during my study period in the UK. Lastly, Walailuk University, Thailand, my workplace, gave me a chance to take educational leave with a full salary payment.

All Thai people in Reading, I appreciate a warm welcome to Thai students. You made my day when I felt homesick—every activity you made me feel at home, especially during the pandemic period.

My close friends in Thailand, Pakawadee, Tassanee, and Chutima, thank you for your constant support and encouragement throughout my studies. Without you, I could not have passed the most challenging academic time.

Finally, I express my deepest gratitude to my family, who believes in my abilities and support. You encouraged me every time I felt terrible. To my mom, dad, and three siblings: Thank you for everything and take care of my cat. My cat, I did not forget you. You are the most motivated to keep going in the PhD life. I dedicate this PhD thesis to all of you.

Abstract

This thesis aims to develop an analytical workflow utilizing HPLC-fluorescence detection for studying *N*- and *O*-linked glycan levels in neurodegenerative disorders *in vitro*. This method was initially validated with simple model samples before being applied to complex *N*-glycan samples from a neuroblastoma cell line *in vitro* (Chapter 5). The *in vitro* application builds on method development for the various stages of the workflow, specifically the labelling (Chapter 2), release (Chapter 3) and enrichment (Chapter 4) of glycans and makes extensive use of HPLC.

The synthesis of an alkyne reagent is described in Chapter 2, which also summarises its use in the CuAAC reaction for successfully labelling *O*-glycans and in a reductive amination reaction for successfully labelling *N*-glycans. The development of methods for simultaneously releasing *O*- and *N*-linked glycans from glycoproteins to allow their simultaneous analysis is described in Chapter 3. However, this could not be achieved despite extensive attempts to achieve complete release of *O*- and *N*-linked glycans to monomer units. The enrichment of labelled *N*-glycans was also probed in Chapter 4, illustrating that Amide SPE and cotton wool SPE demonstrated superior performance compared to other absorbents.

The qualitative and quantitative analysis of *N*-glycans in the SH-SY5Y cell line during differentiation (Chapter 5) using the developed workflow revealed altered expression of *N*-glycans during the differentiation process. These altered glycans can potentially be explored as neurodegenerative disease biomarkers.

Table of Contents

Table of Figures

CHAPTER 6

Table of Tables

Table of Schemes

Abbreviations

2-AA	2-Anthranilic acid
2-AB	2-Aminobenzamide
2-AP	2-Aminopyridine
Aβ	Beta-amyloid
ACN	Acetonitrile
AD	Alzheimer's Disease
ALS	Amyotrophic Lateral Sclerosis
APTS	8-Aminopyrene-1,3,6-trisulfonic acid
Asp	Asparagine
ATRA	All-trans retinoic acid
BBB	Blood-brain barrier
BC	Bacterial Cellulose
BCA	Bicinchoninic acid
BDNF	Brain-derived neurotrophic factor
BTTAA	2-[4-{(Bis[(1-*tert*-buty-1H-1,2,3-triazol-4-yl)methyl]amino)methyl}-1H-1,2,3-triazol-1-yl]acetic acid
CE	Capillary electrophoresis
CNS	Central nervous system
CSF	Cerebrospinal fluid
CT scan	Computed tomography scan
CuAAC	Copper catalysed azide-alkyne 1,3-dipolar cycloaddition
db-cAMP	Dibutyryl cyclic AMP
DCC	*N*,*N*'-Dicyclohexylcarbodiimide
DCM	Dichloromethane
DDW	Distilled deionized water
DMB	1,2-Diamino-4,5-methylenedioxybenzene
DMF	Dimethylformamide
DMSO	Dimethylsulphoxide
DNS	Dansyl chloride
ECM	Extracellular matrix
EOC	Ethoxycarbonylation
EPO	Erythropoietin
ESI	Electrospray ionisation
F12	Nutrient Mixture F-12 Ham
FBS	Foetal bovine serum
FDA	Food and Drug Administration
Fmoc	9-Fluorenylmethyl chloroformate
Fuc	Fucose
Gal	Galactose
GalNAc	*N*-Acetylgalactosamine
GC	Gas Chromatography
Glc	Glucose
GlcNAc	*N*-Acetylglucosamine
GU	Glucose units of carbohydrate
HD	Huntington's disease

HEK	Human embryonic kidney
HILIC	Hydrophilic interaction liquid chromatography
HMC	Human Microglial Cells
HPLC	High performance liquid chromatography
HPTLC	High-performance Thin-layer Chromatography
IR	Infrared spectroscopy
L-PGDS	Lipocalin-type prostaglandin D2 synthase
LAP	Leucine amino peptidase
LC	Liquid chromatography
LU	Luminescence Unit
MALDI	Matrix-assisted laser desorption/ionization
Man	Mannose
MCI	Mild Cognitive Impairment
MEM	Minimum Essential Medium
MO	Methoximation
MRI	Magnetic resonance imaging
MS	Mass spectrometry
NB	Neurobasal medium
Neu5Ac	Sialic acid
NFH	Neurofilament heavy chain
NFL	Neurofilament light chain
NFTs	Neurofibrillary tangles
NHS	Normal horse serum
NMR	Nuclear Magnetic Resonance
OPA	*o*-Phthalaldehyde
p-tau	Phosphorylated tau protein
PABA	4-Aminobenzoic acid
PAGE	Polyacrylamide gel electrophoresis
PBS	Phosphate Buffer saline
PD	Parkinson's Disease
PFA	Paraformaldehyde
PGC	Porous Graphite Carbon
PMP	1-Phenyl-3-methyl-5-pyrazolone
PNGAse F	Peptide: *N*-glycosidase F
RF-MS	RapiFluor-MS
RNase	Ribonuclease
RT	Retention time
SAX	Strong Anion Exchange
SCX	Strong Cation Exchange
SDS	Sodium Dodecyl Sulphate
Ser	Serine
Sia	Sialic acid
SNpc	*Substantia nigra pars compacta*
SPE	Solid Phase Extraction
t-tau	Tau protein
TBTA	tris[1-Benzyl-1H-1,2,3,-triazol-4-yl)methyl]amine
TDMS	*tert*-Butydimethylsily

TEA	Triethylamine
Tf	Transferrin
TFA	Trifluoroacetic acid
THF	Tetrahydrofuran
THPTA	tris[(1-Hydroxypropyl-1H-1,2,3-triazol-4-yl)methyl]amine
Thr	Threonine
TLC	Thin-layer Chromatography
TMS	Tetramethylsilane
TOF	Time of fight
UV	Ultraviolet
WAX	Weak anion exchange
Xyl	Xylose

Chapter 1

Introduction

This thesis aims to devise a glycan analysis workflow to investigate *N*- and *O*-linked glycans for their potential relevance in neurological diseases. The proposed workflow entails the utilisation of a novel technique for analysing *N*- and *O*-linked glycans, exploring alternative enrichment techniques, and examining *N*-glycan profiles in a human neurological cell line as the primary model. Consequently, this introduction emphasises the significance of glycans in health and diseases and summarises the methods and workflow involved in glycan analysis.

1.1 Types of glycosidic bonds

Living cells contain four main types of macromolecules: carbohydrates (glycans), proteins, lipids, and nucleic acids. Carbohydrates can be found either attached to other biological molecules like proteins or lipids (called aglycone) or can exist freely in the cytosol. These macromolecules serve various crucial functions in biological systems. When carbohydrates have covalent bonds with proteins, they participate in essential cellular processes, including adhesion, cell development, and recognition. Glycans are frequently located on the outer surface of cells and play vital roles in facilitating interactions between cells, the extracellular matrix, and other molecules. Glycans exhibit diverse biological functions, which can be influenced by their primary structure and the aglycone to which they are bound. Oligosaccharide chains are attached to proteins through either *N*-glycosidic or *O*-glycosidic bonds, depending on the atom of the amino acids that link the glycan to the aglycone. The common monosaccharide subunit moieties in glycans found in the eukaryotic cells are shown in Figure 1.1 [1, 2]. Numerous studies have demonstrated that the glycan profiles of cells, tissues, organs, and disease states exhibit unique and distinct characteristics, as shown in section 1.2 and 1.3. The variations in the patterns of displayed carbohydrates can serve as crucial indicators, effectively distinguishing between healthy and diseased conditions. Consequently, these changes in glycan patterns hold significant potential as valuable biomarkers for various diseases and medical conditions.

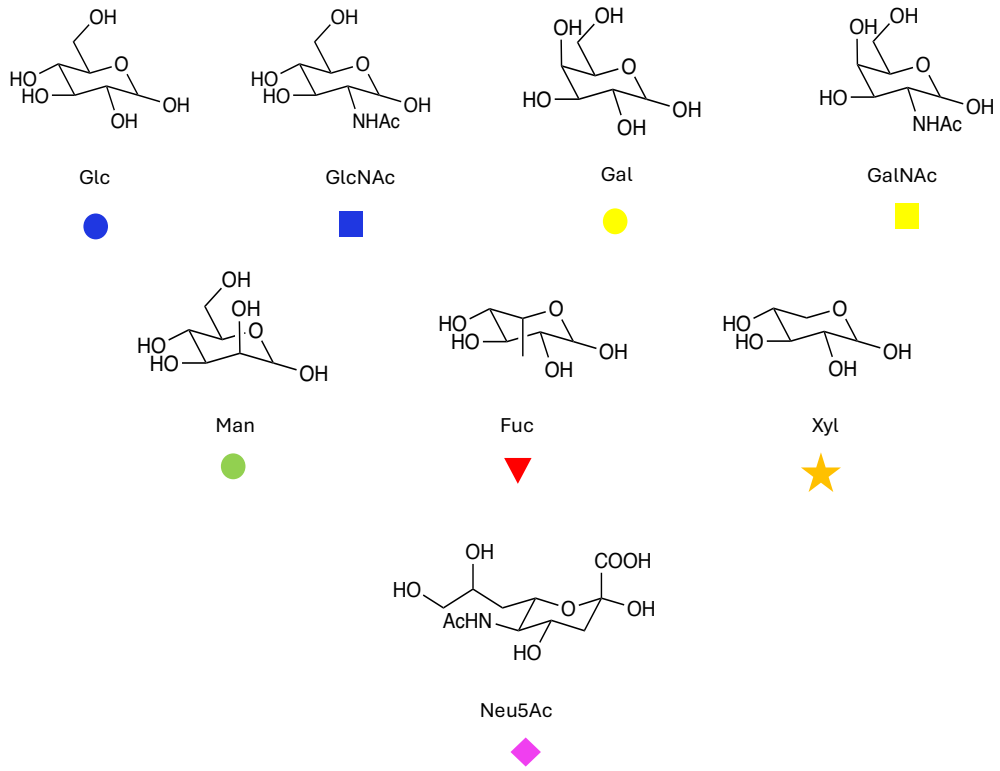

Figure 1.1 The common monosaccharide subunits found in the glycoproteins in the eukaryotic cells. Glycan structures and their corresponding graphical symbols are displayed according to the Symbol Nomenclature for Glycans (SNFG)[3].

1.1.1 *N*-Glycosylation

N-Glycans are sugars linked via a β1-glycosidic covalent bond to the nitrogen atom of an asparagine (Asp) residue (Figure 1.2). *N*-Glycans can be classified into three groups according to the attached monosaccharides. Oligomannosidic glycans contain only two *N*-acetylglucosamine (GlcNAc) residues with a variable number of mannose (Man) (and sometimes glucose (Glc)) residues. Complex-type glycans have various GlcNAc, galactose (Gal), fucose (Fuc), sialic acid (Sia or Neu5Ac) and sometimes *N*-acetylgalactosamine (GalNAc) residues additional to the pentasaccharide core. The final group, hybrid-type glycans, combine motifs that are regarded as oligomannosidic and complex-type. All *N*-glycans share a $Man_3GlcNAc_2$ pentasaccharide core, as shown in Figure 1.2.

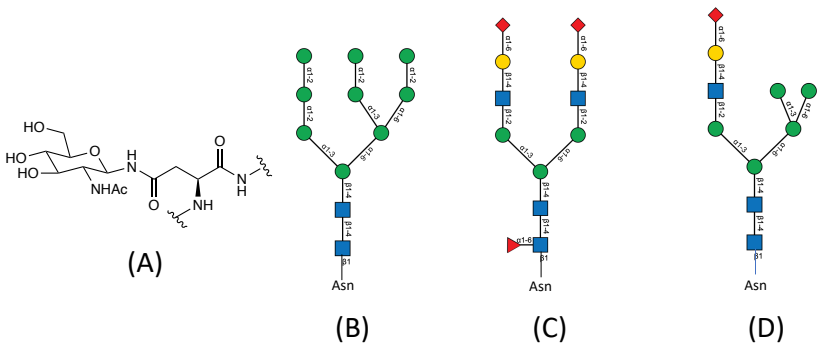

Figure 1.2 Linkage and structure of *N*-linked glycans. (A) GlcNAc linked to asparagine via *N*-link, (B) oligomannose *N*-glycans, (C) complex *N*-glycans, and (D) Hybrid *N*-glycans[4].

1.1.2 *O*-Glycosylation

O-Glycans or mucin-type *O*-glycans involve GalNAc α-linked to the oxygen atom of serine (Ser) or threonine (Thr) residues at the hydroxyl group (Figure 1.3 (A)). Eight types of *O*-glycans present in the mammalian cells, as shown in Figure 1.3 (B), and vary according to their monosaccharide components [5, 6]. The sugars found in *O*-GalNAc glycans include GalNAc, Gal, GlcNAc, Fuc, and Sia, whereas Man, Glc, or xylose (Xyl) residues are not present.

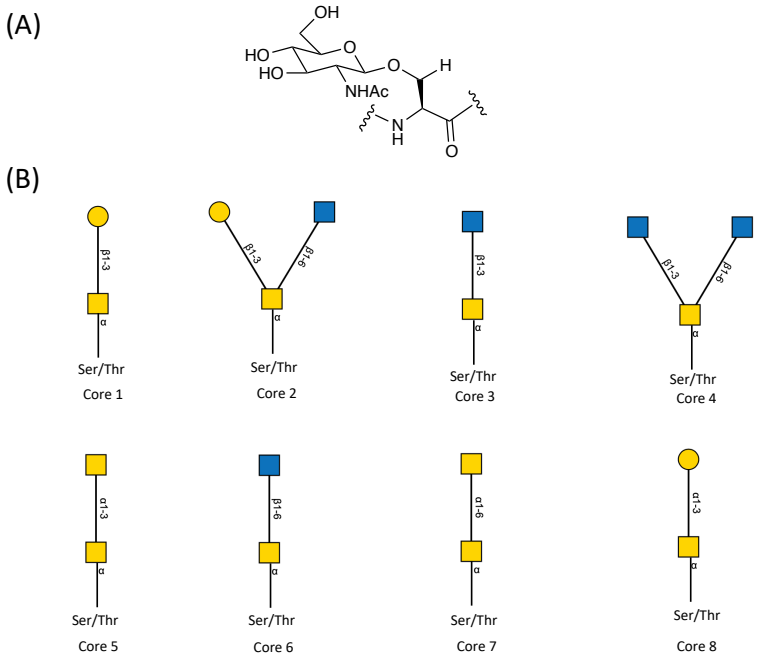

Figure 1.3 Linkage and structure of *O*-linked glycans. (A) GalNAc linked to serine or threonine via *O*-link and (B) *O*-glycans core 1 to 8[4].

1.2 Biological functions of glycans

Glycans play diverse and vital roles in cellular functions, which can be influenced by their primary structure and the aglycone to which they are attached. The biological functions of *N*-glycans within cells encompass essential processes such as protein synthesis and recognition (protein folding, intracellular trafficking, communication between cells, and protein stability)[7-11], modulation of the immune system (Immunoglobulins; IgA, IgD, IgE, IgG, and IgM)[12-18], facilitation of brain development and function, such as neurotransmission release and synaptic transmission [19-26], as shown in Figure 1.4. On the other hand, the mucin-type *O*-glycans are found in the epithelial cells (figure 1.4), such as the airway, digestive surface, saliva, gum and teeth, and skin [27-34]. As a dense mucin layer, *O*-glycoproteins serve roles such as physical protection and tissue elasticity and coat the epithelial surface providing protection from microorganism invasion[35, 36]. The mucin *O*-glycans are associated with human blood groups via antigens T, sialyl T, Tn, and sialyl Tn [37, 38]. In the neurological setting, *O*-glycosylation is found in the amyloid-β (1-42) peptides (Aβ)[39, 40]. The *N*- and *O*-glycosylated proteins are found in internal body fluids such as blood plasma and cerebrospinal fluid (CSF). As glycosylated proteins have hydrophobic, hydrophilic and acidic parts, these macromolecules can contribute between blood and CSF via blood-brain barriers (BBB) [41].

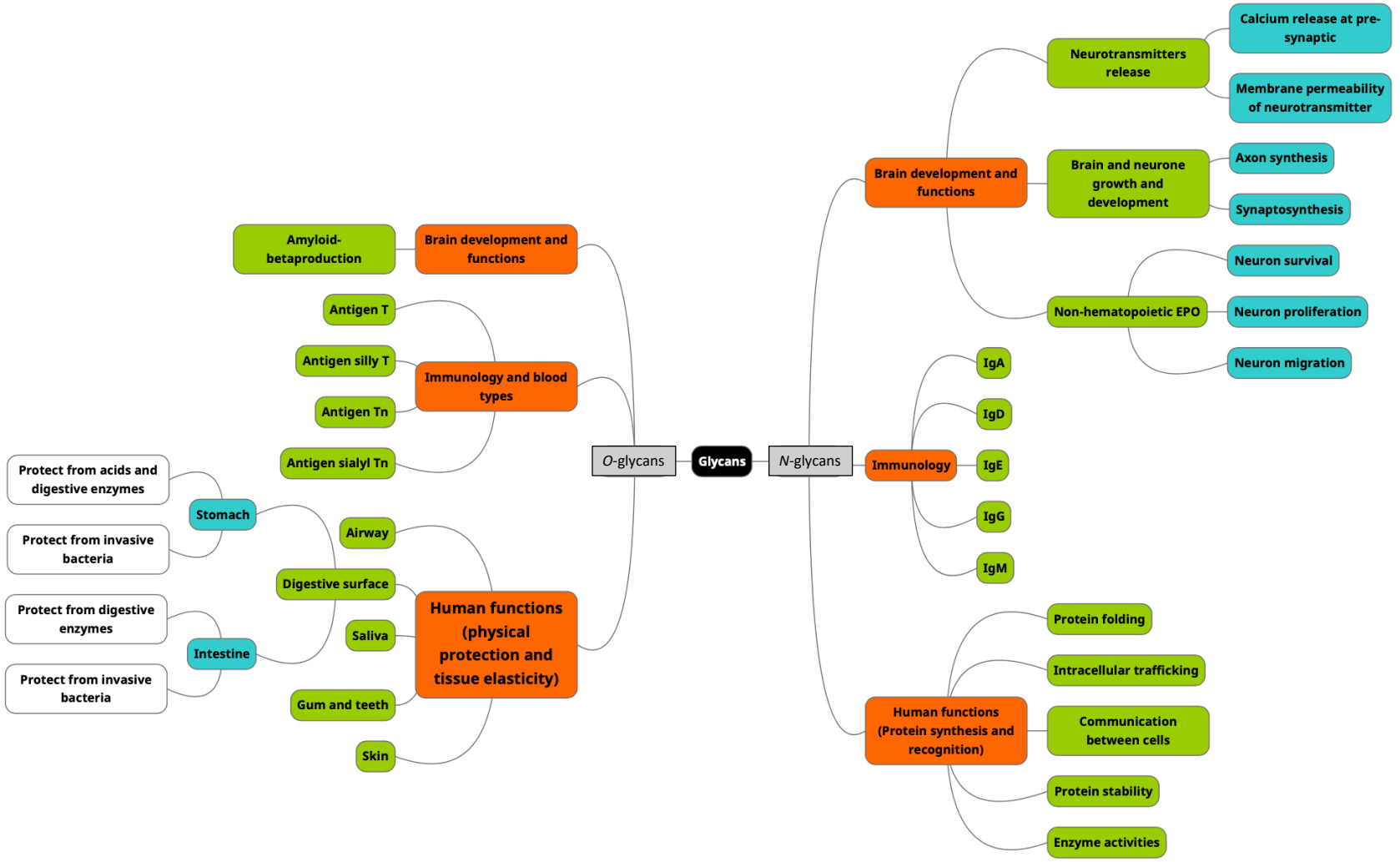

Figure 1.4 A summary of the biological function of *N*- and *O*-glycans.

Moreover, glycosylation determines ligand affinity for endogenous mammalian lectins (carbohydrate-binding proteins). Lectins are highly selective for specific glycan structures. These lectins are very useful for studying glycan functions. Glycan-lectin interactions are important for enzyme or antibody activity. The glycan moieties affect the binding between ligands and substrates [42-48]. A graphical demonstration of glycan-lectin activity is shown in Figure 1.5. The ligand can attach to specific glycoproteins at the target site. After binding, the target organ is then activated. This phenomenon can be used to develop specific ligands for therapeutic applications [49-51]. Furthermore, drug delivery systems and targeted therapeutics can be developed using this knowledge.

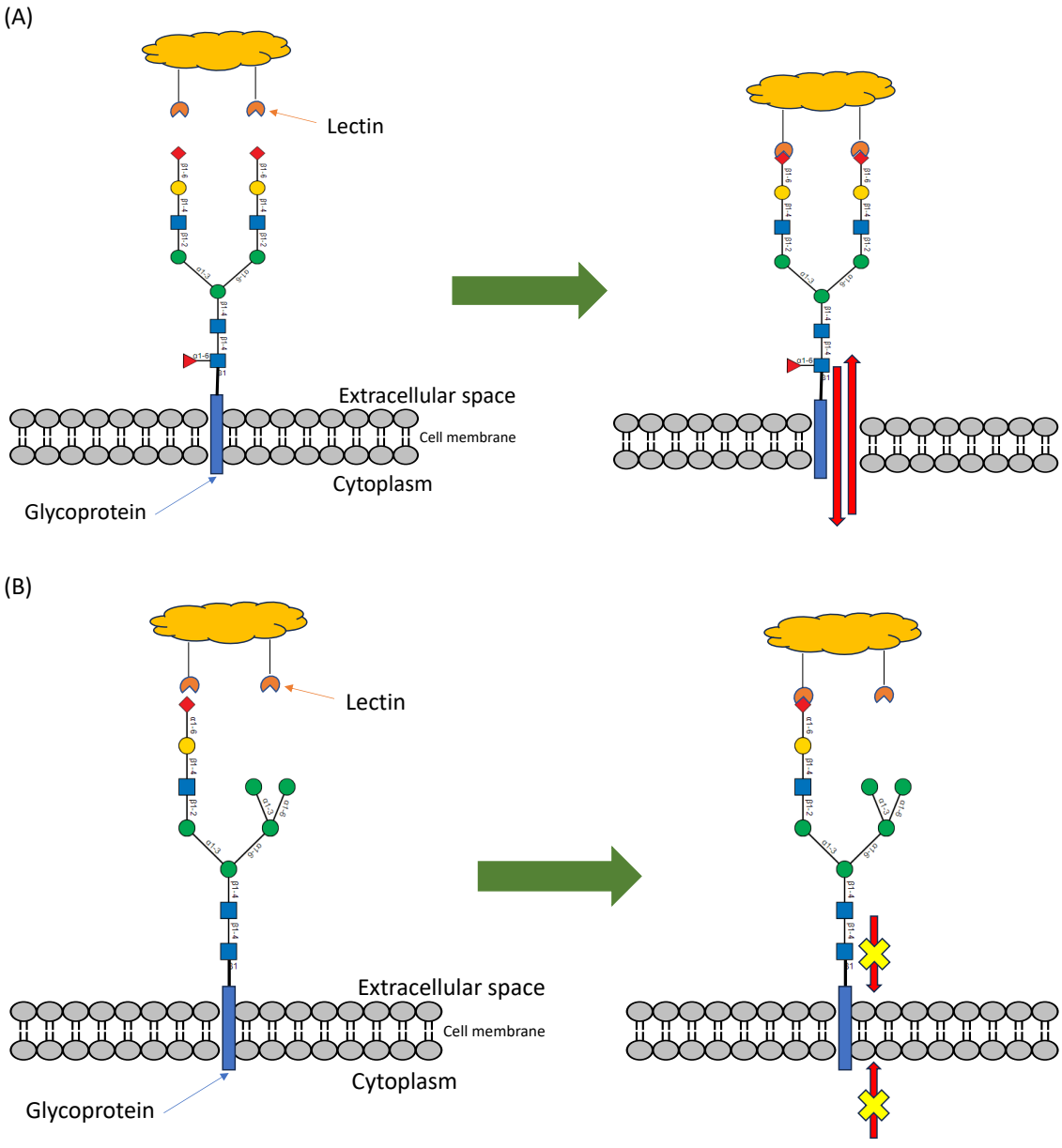

Figure 1.5 Demonstration of glycan-lectin activity in cell function. (A) The specific interaction of two sugar moieties with the ligand on the cell wall activates the cell. (B) In contrast, the cell is not activated if only one sugar moiety can interact with the ligand.

1.3 Glycans as biomarkers for neurodegenerative diseases

Studying differences in the glycan profile between healthy and disease states can allow glycan-based biomarkers for diseases to be developed. The U.S. Food and Drug Administration (FDA) has approved the use of glycoproteins in serum, such as *O*-glycosylated mucin glycoproteins of carbohydrate antigens (CA125 for ovarian, CA27.29 and CA15.3 for breast, CA19.9 for pancreatic cancers) and *N*-glycosylated glycoproteins (α-fetoprotein for hepatocellular carcinoma, prostate-specific antigen for prostate cancer), as biomarkers for cancer [13, 14, 52-65].

In neurodegenerative diseases, various biomarkers have been studied in clinical trials, such as protein, DNAs, and RNAs mutation in various diseases such as Parkinson's disease (PD), Alzheimer's disease (AD), Huntington's disease (HD), mild cognitive impairment (MCI), amyotrophic lateral sclerosis, frontotemporal dementia, and multiple sclerosis. The diagnosis of neurodegenerative diseases usually uses brain imaging scans and markers from CSF. The method for taking the CSF from the patients is invasive. The discovery of glycans as biomarkers from the blood or serum in these diseases could replace the CSF method. The results show the different levels of glycans between CSF and blood in patients with disease and healthy people [66, 67].

The characterisation of AD and PD is the progression of specific symptoms. AD is the progressive loss of cognitive function, behavioural impairment (e.g., mood change), problems with communication and reasoning, and cerebral deposit of senile plaques; Aβ peptide in extracellular fluid and neurofibrillary tangles (NFTs) in intracellular fluid from CSF [68]. PD is the progressive degeneration of dopaminergic neurons in the *Substantia nigra pars compacta* (SNpc), resulting in typical motor symptoms such as resting tremor, rigidity, bradykinesia, gait, and balance dysfunction [69]. This eventually results in near-total immobility, hyposmia, constipation, hallucination, depression, anxiety, and sleep dysfunction. Nowadays, the detection of PD uses various methods; the most popular is clinical observation combined with imaging.

It has also been reported that specific glycans could perhaps be potential neurodegenerative biomarkers. Studies considering the glycome as the biomarker in neurodegenerative diseases focus on the transferrin (Tf) attached to the *N*-glycans, such as GlcNAc-Tf, Sia-Tf, Man-Tf and Lipocalin-type prostaglandin D2 synthase (L-PGDS) and mannose and glucuronylation for *O*-glycans. The studies focused on *O*-glycan levels in CSF. The levels of Man-Tf increased in the AD, PD and MCI patients. The GlcNAc-Tf levels increased in AD and dementia patients. The sia-Tf increased in AD and MCI patients. However, the Sia-fucosylated and *O*-glycosylated mannose core levels decreased in the MCI and AD patients [41, 70-76], as summarised in Table 1.1. The study of the relationship between tau proteins (T-tau and P-tau) in the brain of AD patients shows the corresponding level between tau and *N*-glycans in CSF [71, 76, 77]. *N*-Glycans in CSF can be used to replace brain biopsy to analyse the tau proteins for diagnosis of AD from this relationship. From the glycome studies of neurodegenerative diseases, analysing glycans as biomarkers is an important process for identifying and quantifying the profiles of carbohydrates and tracking the progression of the disease.

Table 1.1 Comparison of glycan levels between AD, PD, MCI patients and healthy groups

Glycans type	Glycan levels in patients compared to healthy group			References
	AD	PD	MCI	
Mannose	increase	increase	increase	[70, 73, 76]
High mannose	increase	N/A	decrease	[66, 75]
GlcNAc	increase	N/A	increase	[70, 71]
Sialic acid	increase	increase	increase	[66, 71, 75, 78]
Sia-fucosylated	decrease	N/A	decrease	[66]
Fucosylated glycan	N/A	N/A	decrease	[66]
O-Glycosylated mannose core	decrease	increase	decrease	[75, 78]

1.4 Glycan and glycoprotein analysis

The majority of research in the field of glycan analysis focuses on characterising and quantifying the level of *N*-glycans in biological samples. This is because *N*-glycans can be released from proteins using specific enzymes, enabling more straightforward analysis. Numerous reports have investigated the qualitative and quantitative aspects of *N*-glycans, revealing their relevance to health and various disease states [18, 23, 54, 61, 74, 79-89]. On the other hand, there needs to be more research on the relationship between *O*-glycans and health or disease. The intricate structure of *O*-glycans and the challenges involved in their analysis pose significant barriers to studying their levels in biological samples. Most existing reports on *O*-glycans describe the vast diversity of *O*-glycan structures or differences between *O*-glycan fragments rather than their direct associations with specific health conditions or diseases. As a result, *O*-glycan analysis remains an area that requires further exploration and understanding to uncover its potential significance in biological contexts.

As previously mentioned, glycoproteins are valuable biomarkers in various disease conditions. The development of glycoprotein analysis is crucial for qualitative and quantitative identification and monitoring of diseases. Several techniques are available for glycoprotein analysis, as listed in Table 1.2. Examples of glycoprotein separation include Sodium Dodecyl Sulphate-Polyacrylamide Gel Electrophoresis (SDS-PAGE) and 2-dimensional (2D) PAGE. Staining or blotting techniques and advanced mass spectrometric methods can be used to identify glycoproteins. Notably, glycoprotein structures lack chromophores and fluorophores, making them less efficiently ionised. Nevertheless, Matrix-Assisted Laser Desorption/Ionisation Time-Of-Flight (MALDI-TOF) Mass Spectrometry (MS) has been developed for glycoprotein analysis, often in conjunction with Gas Chromatography (GC) and High-Performance Liquid Chromatography (HPLC).

Table 1.2 Summary and critical appraisal of glycoprotein analysis techniques

Technique	Method/Detector	Advantages	Disadvantages	References
SDS-PAGE/Gel electrophoresis	SDS-PAGE 2D-PAGE	- This method can digest the samples in the gel before analysis. - This method can develop proper capture materials for specific analysis (such as only *O*-glycosylated proteins) and can be developed for higher affinity to glycoproteins. - Sometimes, this method is used for purification of samples before analysis by HPLC. - This method can be used to study protein-glycoprotein interactions.	- This method requires fluorescence labelling for visualisation. - This method requires enzymatic or chemical reactions to release glycans before conducting the analysis. - This method requires a staining reagent for developing bands during visualisation. - Identification is primarily based on the molecular weight fragments of the glycans.	[20, 21, 61, 79, 90-93]
Microarray	Lectin microarray	- This method is used for glycan profile patterns. - This method can analyse both *N*- and *O*-glycans at the same time. - This method can be used as high throughput for glycan profile therapeutic proteins when coupled with a sophisticated detection system.	- This method needs a labelling reagent. - Lectin from a natural source displays weak binding affinity to a spectrum of glycans. - This method needs enzyme or chemical reactions to release glycans before analysis.	[74, 81-83, 93-98]
Capillary Electrophoresis (CE)	MS/MS	- This method is of high sensitivity and resolution.	- Some labelling reagents are incompatible with CE (e.g., 2-Anthranilic acid (2-AA) and 8-aminopyrene-1,3,6-trisulfonate (APTS)).	[84, 99, 100]

Technique	Method/Detector	Advantages	Disadvantages	References
			- This method is not suitable for all size of glycans. This method can use for small more than large glycans size. - This method needs enzyme or chemical reactions to release glycans before analysis.	
HPLC	Fluorescence MS (MALDI, TOF, MALDI-TOF, MS/MS)	- This method can use various detectors - This method can analyse samples of low concentrations. - This method is precise, accurate, of high-resolution and reproducible. - This method can identify the structure of glycans - Various fluorescence labelling reagents can be used for HPLC analysis.	- This method requires labelling reagents before analysis to increase detection sensitivity. - This method requires purification methods for clean up before analysis. - This method requires the enzyme or chemical reactions to release glycans before analysis. -The MS-ESI detector has low sensitivity.	[26, 54, 85, 94, 99, 101, 102] [8, 21, 22, 26, 86, 87, 94, 103]
MS	MS MS/MS MALDI MALDI-TOF MALDI-TOF/TOF MALDI-FT-ICR	- This method can analyse both *N*- and *O*-glycans at the same time. - This method can be used for structure determination. - This method can analyse various biological samples (blood, plasma, CFS, etc.)	- Some samples need labelling reagents for increasing detection sensitivity. - Some biological samples require pre-separation by SDS, LC or CE before being introduced into MS	[74] [18, 19, 72] [104] [95, 105] [88, 89, 93, 96, 106, 107] [108, 109]

1.5 Glycoproteins' Analytical Workflow

Developing methods for analysis of glycoproteins is important for qualitative and quantitative identification and disease monitoring. As glycoprotein structures are less efficiently ionised than other biomolecules, MALDI-TOF MS combined with GC and HPLC is the first-choice method for glycoprotein analysis. The workflow for glycan analysis in biological samples requires digesting samples into small fragments, releasing the glycans (using a specific enzyme or chemical reactions), derivatising (for increased ionisation or adding chromophore or fluorophore), purifying, enriching the labelled glycans, and analysis. For example, a typical glycan analysis workflow is illustrated in Figure 1.6.

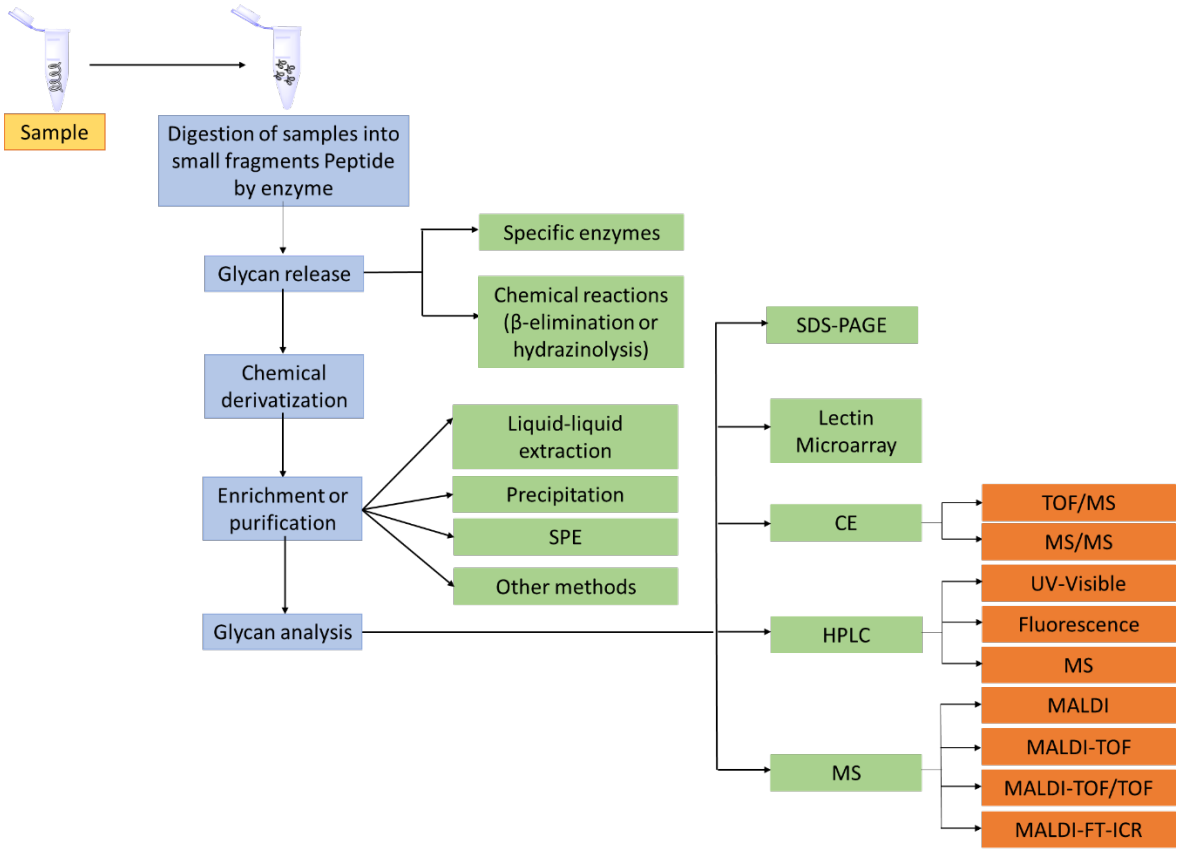

Figure 1.6- General overview of the *N*- and *O*-glycan analysis workflow.

Figure 1.6 illustrates the *N*- and *O*-glycan analysis workflow. The workflow starts with the sample being digested into small peptide fragments by enzymes. The glycans are released from the backbone by specific enzymes or chemical reactions and labelled with the reagent for easy detection. Enrichment or purification of labelled glycans is needed before the analysis step to remove unnecessary chemicals from the labelling reaction. Depending on the qualitative or quantitative detection method, various analytical techniques can be conducted on the labelled glycans.

1.5.1 Methods to release glycans

Most analytical methods for glycoproteins use proteolytic enzymes (e.g., trypsin or pronase) to digest proteins into small peptide fragments before releasing carbohydrates from the core. Different *N*- and *O*-linked glycan sizes (*O*-glycans vary significantly in size but can be smaller than *N*-glycans) also influence the choice of labelling methods for analysis.

1.5.1.1 *N*-Glycan release

Most of the research in glycan analysis focuses on *N*-linked glycoproteins. *N*-Glycans can be released by chemical reaction (hydrazinolysis) [110] or enzymatically using Peptide: *N*-glycosidase F enzyme (PNGase F) [111-113], as demonstrated in Scheme 1.1. In contrast to *N*-linked glycoprotein analyses, *O*-linked glycoprotein analyses are challenging because no specific enzyme releases all *O*-linked glycoproteins from the polypeptide backbone. Researchers use enzymes to cleave glycoproteins into shorter peptide bonds before releasing *O*-glycans from the core. However, developing universal methods that can release all types of core *O*-glycans from the protein backbone remains challenging.

1.5.1.2 *O*-Glycan release

a. By enzymes

The enzyme for the release of *O*-glycans from glycopeptides is called *O*-glycanase or *O*-glycosidase. This method uses enzymes from natural sources. Nowadays, the enzyme releasing *O*-glycans can cleave core 1 and 3 from the backbone between the serine or threonine at the β1-3 linkage to Gal (core 1) or GlcNAc (core 3). Various examples and the origins of *O*-glycanase are shown in Table 1.3. An endo-*α*-*N*-acetylgalactosaminidase or endo-α-GalNAcase is used for specific cleavage of core 1 and an GalNAc from the backbone. One example of this enzyme is the glycoside hydrolase family or GH101 [114]. One example of GH101, called EngBF, from *Bifidobacterium longum* is a highly specific enzyme that effects cleavage to core 1 of *O*-glycans [115, 116]. The GH101 from *Tyzzerella nexilis*, specific to core 1 [117], and GH31 from *Enterococcus faecalis* (or Nag31s) in the human gut are used for cleaving *O*-glycan at core 1 and core 3 [118]. Another example of *O*-glyconase from human gut microbiota is endo-β1,4-galactosidase (GH16). This enzyme is specific to Galβ1,4GlcNAc linkage in the poly-*N*-acetyl-lactosamine (polyLacNAc) chains of *O*-glycans [119]. The *enterococcus faecalis* (endoEF) enzyme can release core 1, core 2, and core 3 [90, 120]. Research focusing on new universal enzymes to release *O*-glycans is ongoing. OpeRATOR is an example of a specific *O*-protease (*O*-endoproteinase/*O*-endopeptidase) from intestinal bacteria. This enzyme digests the core 1 mucin type from the protein backbone via the *N*-terminal. However, this enzyme limits activity for core 3 *O*-glycans [121, 122]. The benefit of using enzymes for releasing the *O*-glycans from the backbone is the mild conditions (mild base or acids and at a temperature between 30-37^{o}C) and the opportunity to identify more sub-types of enzymes from the natural sources or mutation of bacteria to modify the activity of the enzymes. On the other hand, the activity of enzymes depends on the types, sources, and methods for enrichment and purification of enzymes. However, the remaining challenge of enzyme release for *O*-glycans is to find the universal enzyme for all cores, similar to *N*-glycans.

Table 1.3 Examples of enzymes used for *O*-glycans release.

Name of enzymes	Origins	Target site	Advantages	Disadvantages	References
Endo-*α*-*N*-acetylgalactosaminidase (GH101)	*Bifidobacterium longum*	Highly specific to core 1 *O*-glycoproteins.	- These enzymes found in various types of bacteria. - The bacteria can be mutants to modify the activity of enzymes.	- The activity of enzymes depends on the source of bacteria.	[115, 116]
	Tyzzerella nexilis from human gut	Specific to core 1 *O*-glycoproteins.			[117]
	Enterococcus faecalis (endoEF)	Specific to core 1 and core 3 *O*-glycoproteins.			[90, 120]
Endo-β1,4-galactosidase (GH16)	Human gut microbiota	Specific to Galβ1,4GlcNAc linkage *O*-glycans.	- There are many subtypes. - this enzyme can use both endo- and exo-acting enzyme.	- The activity depended on the kind of subtypes.	[119]
α-*N*-Acetylgalactosaminidases (EC 3.2.1.49) (GH31, Nag31s)	*Enterococcus faecalis* from the human gut	Specific to GalNAc in *O*-glycoproteins, low activity to Tn antigen.	- The bacteria can be mutant to modify the activity of enzymes.	- This enzyme can be used for core 1 and 3 only.	[118]
OpeRATOR	Human intestinal bacteria expressed in *Escherichia coli*	Specific to core 1 and limit activity to core 3 *O*-glycoproteins.	- The enzyme specifically binds to *O*-glycans on native glycoproteins at the *N*-terminal end of *O*-glycans.	-Need trypsin to cleave the glycoproteins to small molecules and PNGase F to remove *N*-glycans before using this enzyme to release *O*-glycans	[121, 122]

b. By Chemical reaction

A major problem in *O*-glycan research is that no single enzyme can release all types of cores. To release all cores of the *O*-glycans at the same time, a chemical reaction must be used. *O*-Linked glycoprotein analysis most commonly employs β-elimination reactions and hydrazinolysis reactions for release as reducing sugars before labelling. The β-elimination reaction for release of *O*-linked glycoproteins is under alkali conditions (pH>10) through the linkage between GalNAc and β-carbon bond hydroxyl groups of serine or threonine, as shown in Scheme 1.1. The reductive β-elimination reaction occurs under strong alkali conditions, and the 'peeling reaction' appears and decreases free *O*-glycans' yield by converting free sugar to alditol molecules [123]. The alditols are unavailable for labelling with the fluorophore or chromophore. This reaction starts with the hydroxide ions attacking the β-carbon of the GalNAc molecules, releasing, and destroying the end GalNAc from the whole molecule. Reducing agents are added to the reaction, such as sodium borohydride ($NaBH_4$), potassium borohydride (KBH_4), and 1-phenyl-3-methyl-5-pyrazolone (PMP), to prevent peeling by converting the reducing end of the terminal monosaccharide of the released sugar to an alditol (GalNAcol) [124]. The peeling rate is 0-10% after reducing agents are added to the reactions [125]. The condition of this reaction is 40-50^{o}C, and the incubation period is 4-24 hours. It has proved to be more effective for core 1 and core 2 *O*-glycans than others [126-131]. Using mild bases, such as ammonia, ethylamine, or lithium hydroxide, to hydrolyse the *O*-glycans from the peptides is called non-reductive β-elimination. The reaction requires more than 40 hours. Unfortunately, these methods still produce undesirable peeling (0-60%), depending on the conditions used [124, 125]. Typically, the reaction conditions are 50-70^{o}C and 1-24 hours [124, 131-134]. To reduce the reaction times, microwave-assisted nonreductive β-elimination has been developed. The condition uses microwave radiation at 70^{o}C for 12 minutes [74].

Hydrazinolysis (or β-elimination using anhydrous hydrazine) is used in *N*-linked glycans[135] and has been developed further for *O*-linked glycoprotein release [136]. The reducing glycans are converted to hydrazones in this reaction. The chemical reaction for releasing glycans cleaves the amide component of the *N*-glycosidic bonds and deacetylates GlcNAc, GalNAc, and neuramic acids. The reaction still has peeling for both *N*- and *O*-glycans (6-71%) [137] but produces a higher yield of released *O*-glycans than the β-elimination reaction. This reaction requires 60-100^{o}C and an incubation period of 5-18 hours [131, 136, 138, 139]. However, this reaction is extremely toxic and hazardous due to the hydrazine for *O*-glycan release.

There are reports of releasing *O*-glycan strategies that do not require strong basic conditions and hence avoid peeling. For example, hydroxylamine (50% by weight in the water) and an organic superbase (1,8-diazabicyclo[5.4.0]undec-7-ene) combined with hydrazinolysis have been reported. The hydroxylamine reaction's condition is 37-50^{o}C, 20-60 minutes. This reaction has higher yields than the hydrazinolysis reaction, and the peeling yields are lower (0-10%) [125, 138].

In summary, the enzymatic approach for releasing *O*-glycans brings the benefit of requiring mild conditions without effecting peeling. However, this method must be further developed to be efficient for the release of all *O*-glycan cores. The chemical releasing method can release more core than the enzymatic method but results in low yields due to peeling and the formation of alditol products. The overarching challenge for *O*-glycan release is to develop a universal method for releasing all core *O*-glycans in one step. After the release step, *O*- glycans must then be labelled for increased detection, and the sample must be cleaned up before analysis.

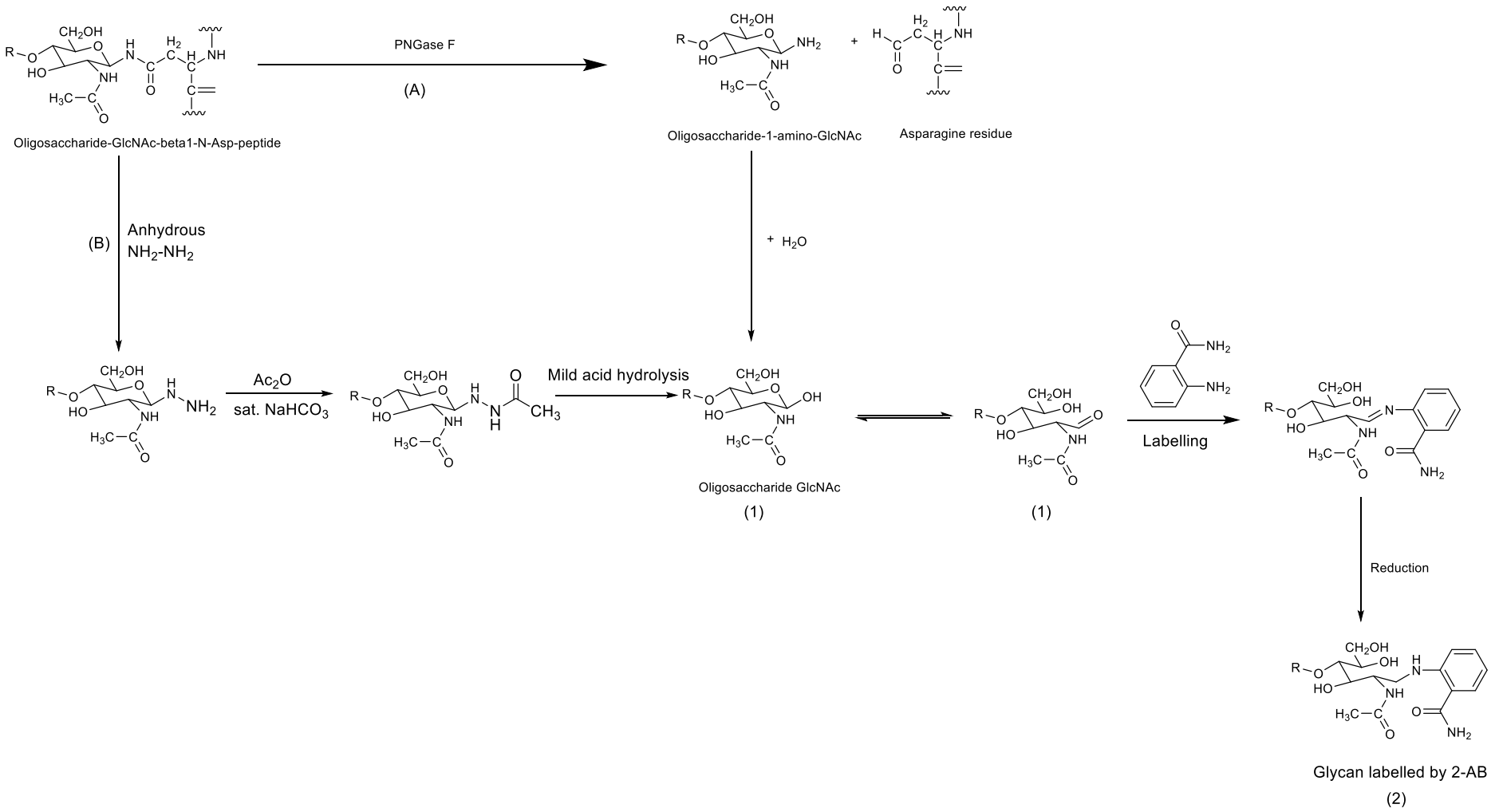
PNGase F
(A)
Oligosaccharide-GlcNAc-beta1-N-Asp-peptide
Oligosaccharide-1-amino-GlcNAc
Asparagine residue
(B)
Anhydrous
NH2-NH2
+ H2O
Ac2O
sat. NaHCO3
Mild acid hydrolysis
Oligosaccharide GlcNAc
(1)
(1)
Labelling
Reduction
Glycan labelled by 2-AB
(2)

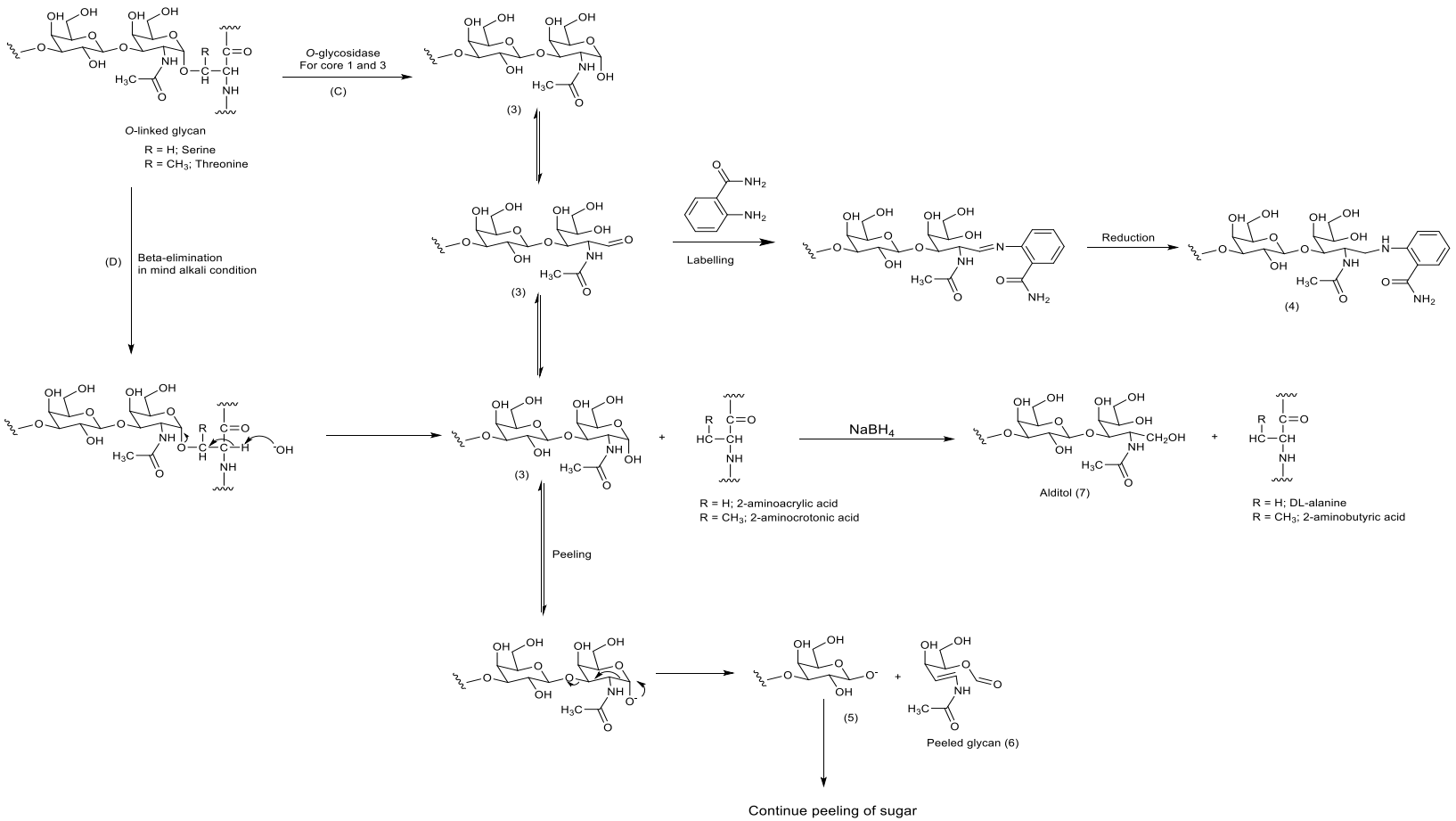

Scheme 1.1 Releasing *N*-glycans (A-B) and *O*-glycans (C-D) from the cores; (A) *N*-Glycans release by PNGase F from the asparagine backbone to afford GlcNAc, (1) oligosaccharide GlcNAc equilibration between keto-enol form, (2) 2-AB labelled *N*-glycans, (B) *N*-Glycan release by hydrazinolysis reactions to afford GlcNAc in mild acid condition to (1), (C) *O*-glycans released by *O*-glycosidase form the serine or threonine backbone, (D) *O*-glycans released by reductive β-elimination, (3) free *O*-glycan equilibrates between keto-enol form, (4) 2-AB labelled *O*-glycans, (5-6) peeling rection of free *O*-glycans in enol form, (7) using reducing agents to minimise peeling, converting the free *O*-glycans in enol form to Alditol.

1.5.2 Methods to derivatise glycans

As glycans lack chromophores and fluorophores, they are difficult to detect. Derivatisation is, therefore, an option to make glycans detectable. This is usually achieved by derivatising the sugar released from *N*- and *O*-linked glycans with a fluorophore labelling reagent to enable fluorescent detection. The labelling reaction that is most often used is reductive amination using aromatic amines such as 2-anthranilic acid (2-AA or *o*-aminobenzoic acid), 2-aminobenzamine (2-AB), 2-aminopyridine (2-AP), procainamide, 8-Aminopyrene-1,3,6-trisulphonic acid (APTS), 1,2-Diamino- 4,5-methylenedioxybenzene (DMB), or RapiFluor-MS. These reagents react with the reducing end of the oligosaccharide under mild conditions (Figure 1.7). Detection with fluorescence at various excitation wavelengths (230-488 nm) and emission wavelengths (320-550 nm) is possible. Table 1.4 provides the structures and fluorophore detection parameters for fluorescence labelling reagents commonly used for glycan analysis.

Table 1.4 Examples of labelling reagents for glycan/glycoprotein analysis by HPLC using Fluorescence or MS as the detector

Name of Labelling reagents	Structure	Method of detections			References
		The wavelength for fluorophore detection		MS	
		Excitation wavelength (nm)	Emission wavelength (nm)		
2-AA	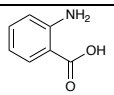	330-360	420-425	✓	[87, 111, 131, 138]
2-AB	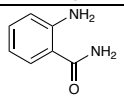	250-330	420-430	✓	[26, 54, 74, 86, 94, 102, 124, 133]
2-AP		310-320	370-400	✓	[112, 136, 140, 141]
Procainamide	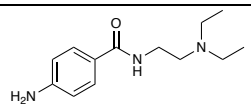	310	370	✓	[85, 103, 111, 133, 142]
APTS	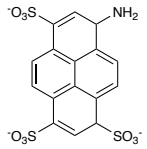	488	520	✓	[143-145]
DMB	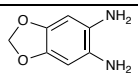	370-375	440-460	✓	[146-148]
RapiFluor-MS	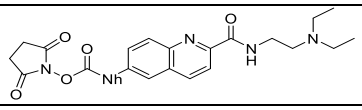	265	425	✓	[134, 149, 150]

1.5.3 Purification of released glycans and labelled glycans prior to HPLC analysis

After the glycans are released from the core, the next crucial step involves enriching and purifying the free glycans. Enrichment at this stage aims to remove impurities such as deglycosylated proteins, salts, and other unwanted components. Various purification methods are employed, including precipitation with organic solvents like acetone, and Solid Phase Extraction (SPE) using C18, porous graphite carbon (PGC), and Hydrophilic Interaction Chromatography (HILIC) modes [151-153]. The resulting sample from this enrichment step can then be analysed using MS for qualitative and quantitative analysis of glycans without the need for fluorescence labelling. Due to the inherent characteristics of glycans, such as the lack of chromophores, fluorophores, and low ionisation properties, they require labelling reagents to facilitate their detection during HPLC analysis. These labelling reagents enhance the sensitivity and selectivity of the method, allowing for the accurate and reliable identification and quantification of glycans in complex biological samples. Once the sample has been labelled, it is important to eliminate any unreacted labelling reagents. Various enrichment methods are used to achieve this, such as precipitation using organic solvent (acetone), SPE with HILIC mode, or alternative methods like cotton wool or magnetic beads. An alternative enrichment method was developed to increase precise, accurate, and environmentally safe protocols, and decrease the cost and time of sample preparation. These techniques help purify and concentrate the labelled glycans for additional analysis [99, 151, 154-156].

1.5.4 Analysis of glycans by HPLC

HPLC is a powerful analytical technique known for its accuracy, precision, high resolution, and rapidity in analysing pharmaceuticals, biopharmaceuticals, and biomarkers. In glycan research encompassing *N*-linked and *O*-linked glycans, HPLC is commonly employed with various detectors like fluorescence, MS, or MS/MS. These methods can identify by-products of *O*-linked glycan releasing steps, such as peeling or alditol formation. LC-MS or LC-MS/MS can achieve qualitative and quantitative analysis of *N*- and *O*-linked glycans within the same samples. However, their different sizes mean that both cannot be analysed simultaneously in one injection, requiring separate injections for each glycan type. Glycan assays often use HPLC with fluorescence detection, which can increase sensitivity when combined with MS techniques (ESI, MALDI). Different modes of analysis have been reported for both unlabelled and labelled glycans. Unlabelled glycans are commonly separated using the reverse phase (C18) [8, 72] and porous graphitised carbon (PGC) HPLC columns [18, 19, 74, 99, 157]. On the other hand, labelled glycans are typically separated using HILIC [21, 54, 74, 94, 102, 103, 157, 158], C18 [85-87], and weak anion exchange (WAX) HPLC columns [26, 74, 94]. These diverse column types allow researchers to effectively separate and characterise glycans in various biological samples, contributing to a comprehensive understanding of their structural and functional properties.

1.6 Glycan analysis in the neuroblastoma cell line as an *in vitro* model

In the study of neurodegenerative biomarkers, *in vitro* models are often selected as alternatives to invasive procedures involving patients. Cell line cultures were chosen to replace biological samples from the patients. The SH-SY5Y cell line is a thrice cloned cell line from a bone marrow metastatic neuroblastoma and is commonly used for neurodegenerative studies, especially for AD and PD biomarkers and treatment studies. Studies usually focus on drug treated or stressed cells and examine the activity of the enzyme (e.g., β-galactosidase), production of protein (e.g., Aβ, P-tau and T-tau), genes (mRNA) expression, cell morphology, and the cell cycle [159-166]. The glycoprotein or glycan analysis that is studied in SH-SY5Y includes total monosaccharides, terminal *N*-glycans, total *N*-glycans, and total carbohydrate production. The analysis methods of the glycan levels studied in SH-SY5Y cell cultures involve HPLC-MS/MS [167-169], MS [170], microarray or lectin blotting [169-171]. The study of glycan profiles in these cell cultures is

ongoing, with the aim that in the future, these data may find applications in representing disease progression and evaluating drug treatments *in vivo*, offering valuable insights into potential therapeutic strategies.

1.7 Aim and Objectives

This thesis aims to create and integrate a simple *N*- and *O*-glycoprotein analysis method using an HPLC with fluorescence labelling analytical workflow. The method is initially developed for using simple model samples before being applied to complex samples derived from a neuroblastoma cell line *in vitro*.

The alkyne fluorescence labelling reagent (**5**) is used to label both *N*- and *O*-glycans in different reactions for HPLC analysis, reductive amination for *N*-glycans and click reaction for *O*-glycans. The objective is to confirm that **5** can be used for labelling *N*- and *O*-linked glycans using lactose (2GU, **14**) as a model substrate for the *N*-glycan by reductive amination reaction and a commercial azido-sugar (**24**) as the *O*-glycan model compound by CuAAC reaction. These results are presented in Chapter 2.

The optimised methods to simultaneously analyse *N*- and *O*-linked glycans without releasing the glycans from the core are developed by hydrolysis of the protein portion of glycoproteins to a single amino acid. A fluorescence labelling reagent was used to label the functional groups of amino acids and amino glycans of the amide before HPLC analysis. The objective is optimizing the hydrolysis of a protein model to individual amino acids, which involves combining various enzymes and chemical reactions. Ribonuclease A (RNase A) is chosen as a simple protein model. The optimized process from a simple protein model will be applied to bovine fibrinogen (complex glycoproteins) for *N*- and *O*-glycoproteins analysis. These results are presented in Chapter 3.

The development and optimisation of the enrichment of labelled glycans using various brands of SPE (PGC, C8, C18, polystyrene DVB, amide, SAX, SCX, and Superco discovery glycans) and comparing the results with enrichment using cotton wool is studied by using the lactose (**14**) derivatised with a commercially available label (2AB, **26**) and a synthetic alkyne labelling reagent, **5** as the glycans standard model. The objective is to compare the enrichment conditions from SPE and cotton wool results and repeat them with the more complex glycans (maltotriose and dextran ladder). These results are presented in Chapter 4.

Finally, the developed glycan analysis workflow from Chapter 4 is used to analyse the glycan profile from a complex biological sample, namely undifferentiated and differentiated SH-SY5Y cells, as the model system to fulfil the aim and objectives of this thesis. Compound **26** is chosen as the glycan labelling reagent. These results are presented in Chapter 5.

This thesis structure is summarised in Figure 1.7, which outlines the schemes of work carried out within each chapter.

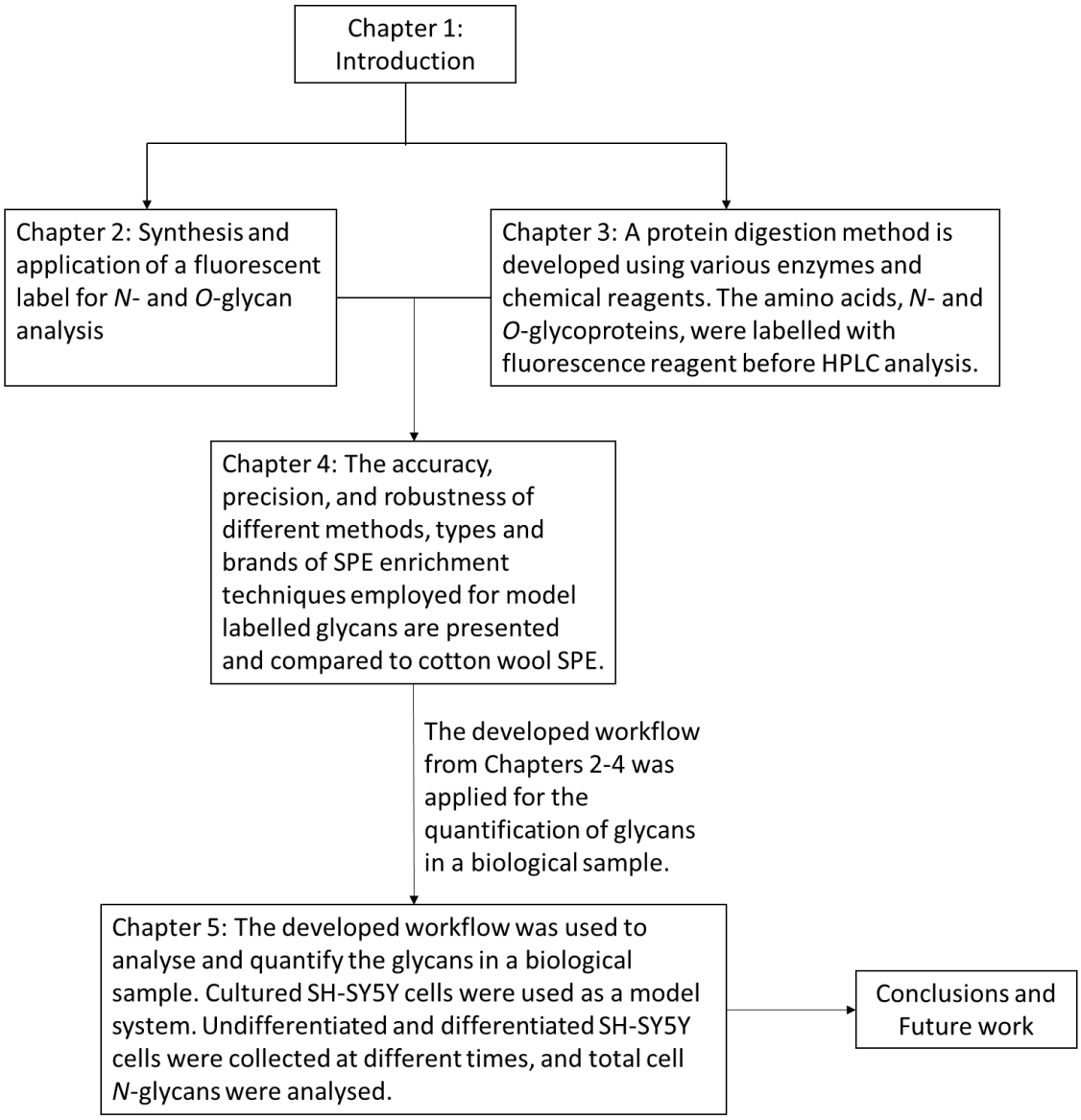

Figure 1.7 - Schematic representation of the content within this thesis.

1.8 References

1. Fogarty, C.A., et al., *How and why plants and human N-glycans are different: Insight from molecular dynamics into the "glycoblocks" architecture of complex carbohydrates.* Beilstein Journal of Organic Chemistry, 2020. **16**: p. 2046-2056.
2. Varki, A., *Biological roles of glycans.* Glycobiology, 2017. **27**(1): p. 3-49.
3. Neelamegham, S., et al., *Updates to the Symbol Nomenclature for Glycans guidelines.* Glycobiology, 2019. **29**(9): p. 620-624.
4. Mehta, A.Y. and R.D. Cummings, *GlycoGlyph: a glycan visualizing, drawing and naming application.* Bioinformatics, 2020. **36**(11): p. 3613-3614.
5. Brockhausen, I., et al., *O-GalNAc Glycans*, in *Essentials of Glycobiology*, A. Varki, et al., Editors. 2022, Cold Spring Harbor Laboratory Press Copyright © 2022 The Consortium of Glycobiology Editors, La Jolla, California; published by Cold Spring Harbor Laboratory Press; doi:10.1101/glycobiology.4e.10. All rights reserved.: Cold Spring Harbor (NY). p. 117-28.
6. Diepeveen, L., et al., *Glycosylation-related Diagnostic and Therapeutic Drug Target Markers in Hepatocellular Carcinoma.* Journal of gastrointestinal and liver diseases: JGLD, 2015. **24**: p. 349-357.
7. Hirata, T., et al., *Recognition of glycan and protein substrates by N-acetylglucosaminyltransferase-V.* Biochimica et Biophysica Acta (BBA) - General Subjects, 2020. **1864**(12): p. 129726.
8. Hall, M.K., et al., *Limited N-Glycan Processing Impacts Chaperone Expression Patterns, Cell Growth and Cell Invasiveness in Neuroblastoma.* Biology (Basel), 2023. **12**(2): p.293.
9. Esmail, S. and M.F. Manolson, *Advances in understanding N-glycosylation structure, function, and regulation in health and disease.* European Journal of Cell Biology, 2021. **100**(7): p. 151186.
10. Kuribara, T. and K. Totani, *Structural insights into N-linked glycan-mediated protein folding from chemical and biological perspectives.* Current Opinion in Structural Biology, 2021. **68**: p. 41-47.
11. Rahman, M., et al., *Specific N-glycans regulate an extracellular adhesion complex during somatosensory dendrite patterning.* EMBO reports, 2022. **23**(7): p. e54163.
12. Krištić, J., G. Lauc, and M. Pezer, *Immunoglobulin G glycans – Biomarkers and molecular effectors of aging.* Clinica chimica acta, 2022. **535**: p. 30-45.
13. Iwamura, H., et al., *Machine learning diagnosis by immunoglobulin N-glycan signatures for precision diagnosis of urological diseases.* Cancer Science, 2022. **113**(7): p. 2434-2445.
14. Kodama, H., et al., *N-glycan signature of serum immunoglobulins as a diagnostic biomarker of urothelial carcinomas.* Cancer Medicine, 2021. **10**(4): p. 1297-1313.
15. Wang, B., et al., *Immunoglobulin G N-glycan, inflammation and type 2 diabetes in East Asian and European populations: a Mendelian randomization study.* Mol Med, 2022. **28**(1): p. 114.
16. Wang, W., et al., *N-glycan profiling alterations of serum and immunoglobulin G in immune thrombocytopenia.* Journal of Clinical Laboratory Analysis, 2022. **36**(2): p. e24201.

17. Petrov, V.A., et al., *Association Between Human Gut Microbiome and N-Glycan Composition of Total Plasma Proteome.* Front Microbiol, 2022. **13**: p. 811922.
18. Alvarez, M.R.S., et al., *N-Glycan and Glycopeptide Serum Biomarkers in Philippine Lung Cancer Patients Identified Using Liquid Chromatography–Tandem Mass Spectrometry.* ACS Omega, 2022. **7**(44): p. 40230-40240.
19. Helm, J., et al., *Bisecting Lewis X in Hybrid-Type N-Glycans of Human Brain Revealed by Deep Structural Glycomics.* Analytical Chemistry, 2021. **93**(45): p. 15175-15182.
20. Bradberry, M.M., et al., *Molecular Basis for Synaptotagmin-1-Associated Neurodevelopmental Disorder.* Neuron, 2020. **107**(1): p. 52-64.e7.
21. Bradberry, M.M. and E.R. Chapman, *All-optical monitoring of excitation–secretion coupling demonstrates that SV2A functions downstream of evoked Ca2+ entry.* The Journal of Physiology, 2022. **600**(3): p. 645-654.
22. Lee, J., et al., *Spatial and temporal diversity of glycome expression in mammalian brain.* Proceedings of the National Academy of Sciences, 2020. **117**(46): p. 28743-28753.
23. Williams, S.E., et al., *Mammalian brain glycoproteins exhibit diminished glycan complexity compared to other tissues.* Nature Communications, 2022. **13**(1): p.275.
24. Bürgi, M., et al., *Novel erythropoietin-based therapeutic candidates with extra N-glycan sites that block hematopoiesis but preserve neuroplasticity.* Biotechnology Journal, 2021. **16**(5): p. 2000455.
25. Yale, A.R., et al., *Regulation of neural stem cell differentiation and brain development by MGAT5-mediated N-glycosylation.* Stem Cell Reports, 2023. **18**(6): p. 1340-1354.
26. Helm, J., L. Hirtler, and F. Altmann, *Towards Mapping of the Human Brain N-Glycome with Standardized Graphitic Carbon Chromatography.* Biomolecules, 2022. **12**(1): p. 85.
27. Dabelsteen, S., et al., *Essential Functions of Glycans in Human Epithelia Dissected by a CRISPR-Cas9-Engineered Human Organotypic Skin Model.* Developmental cell, 2020. **54**(5): p. 669-684.e7.
28. Benktander, J., et al., *Stress Impairs Skin Barrier Function and Induces α2-3 Linked N-Acetylneuraminic Acid and Core 1 O-Glycans on Skin Mucins in Atlantic Salmon, Salmo salar.* International Journal of Molecular Sciences, 2021. **22**(3): p. 1488.
29. Madunić, K., et al., *Specific (sialyl-)Lewis core 2 O-glycans differentiate colorectal cancer from healthy colon epithelium.* Theranostics, 2022. **12**(10): p. 4498-4512.
30. Boschiero, C., et al., *Differentially CTCF-Binding Sites in Cattle Rumen Tissue during Weaning.* International Journal of Molecular Sciences, 2022. **23**(16): p. 9070.
31. Matos, R., et al., *Mycobacterium tuberculosis Infection Up-Regulates Sialyl Lewis X Expression in the Lung Epithelium.* Microorganisms, 2021. **9**(1): p.99.
32. Guindolet, D., et al., *Glycogene Expression Profile of Human Limbal Epithelial Cells with Distinct Clonogenic Potential.* Cells, 2022. **11**(9): p.1575
33. Luis, A.S., et al., *A single sulfatase is required to access colonic mucin by a gut bacterium.* Nature, 2021. **598**(7880): p. 332-3,337A-337N.

34. Huang, L., et al., *Elevated miR-124-3p in the aging colon disrupts mucus barrier and increases susceptibility to colitis by targeting T-synthase.* Aging Cell, 2020. **19**(11): p. e13252.
35. Chahal, G., et al., *A Complex Connection Between the Diversity of Human Gastric Mucin O-Glycans, Helicobacter pylori Binding, Helicobacter Infection and Fucosylation.* Mol Cell Proteomics, 2022. **21**(11): p. 100421.
36. González-Morelo, K.J., M. Vega-Sagardía, and D. Garrido, *Molecular Insights Into O-Linked Glycan Utilization by Gut Microbes.* Frontiers in Microbiology, 2020. **11**: p.591568.
37. Dotz, V. and M. Wuhrer, *Histo-blood group glycans in the context of personalized medicine.* Biochimica et Biophysica Acta (BBA) - General Subjects, 2016. **1860**(8): p. 1596-1607.
38. Janković, M., *Glycans as Biomarkers: Status and Perspectives.* Journal of Medical Biochemistry, 2011. **30**: p.213-223
39. Liu, D., et al., *O-Glycosylation Induces Amyloid-β To Form New Fibril Polymorphs Vulnerable for Degradation.* Journal of the American Chemical Society, 2021. **143**(48): p. 20216-20223.
40. Akasaka-Manya, K. and H. Manya, *The Role of APP O-Glycosylation in Alzheimer's Disease.* Biomolecules, 2020. **10**(11): p.1569.
41. Hoshi, K., et al., *Brain-Derived Major Glycoproteins Are Possible Biomarkers for Altered Metabolism of Cerebrospinal Fluid in Neurological Diseases.* International Journal of Molecular Sciences, 2023. **24**(7): p. 6084.
42. Manabe, Y., et al., *Improvement of Antibody Activity by Controlling Its Dynamics Using the Glycan–Lectin Interaction.* Angewandte Chemie International Edition, 2023. **62**(30): p. e202304779.
43. Donahue, T.C., et al., *Catanionic Vesicles as a Facile Scaffold to Display Natural N-Glycan Ligands for Probing Multivalent Carbohydrate–Lectin Interactions.* Bioconjugate Chemistry, 2023. **34**(2): p. 392-404.
44. Szydlak, R., et al., *Bladder Cancer Cells Interaction with Lectin-Coated Surfaces under Static and Flow Conditions.* International Journal of Molecular Sciences, 2023. **24**(9): p. 8213.
45. *Comprehensive analysis of lectin-glycan interactions reveals determinants of lectin specificity*, in *Obesity, Fitness & Wellness Week*. 2021. p. 1469.
46. Lenza, M.P., et al., *Structural Characterization of N-Linked Glycans in the Receptor Binding Domain of the SARS-CoV-2 Spike Protein and their Interactions with Human Lectins.* Angewandte Chemie International Edition, 2020. **59**(52): p. 23763-23771.
47. Nangarlia, A., et al., *Irreversible Inactivation of SARS-CoV-2 by Lectin Engagement with Two Glycan Clusters on the Spike Protein.* Biochemistry, 2023. **62**(14): p. 2115-2127.
48. Lete, M.G., et al., *Molecular Recognition of Glycan-Bearing Glycomacromolecules Presented at Membrane Surfaces by Lectins: An NMR View.* ACS Omega, 2023. **8**(19): p. 16883-16895.
49. Hooper, J., et al., *Polyvalent Glycan Functionalized Quantum Nanorods as Mechanistic Probes for Shape-Selective Multivalent Lectin-Glycan Recognition.* ACS Applied Nano Materials, 2023. **6**(6): p. 4201-4213.

50. Kitaguchi, D., et al., *Lectin drug conjugate therapy for colorectal cancer.* Cancer Science, 2020. **111**(12): p. 4548-4557.
51. Hayashi, Y., et al., *The therapeutic capacity of bone marrow MSC-derived extracellular vesicles in Achilles tendon healing is passage-dependent and indicated by specific glycans.* FEBS Letters, 2022. **596**(8): p. 1047-1058.
52. Silva, M.L.S. and C. Ramírez Martínez, *A Phaseolus vulgaris Leukoagglutinin Biosensor as a Selective Device for the Detection of Cancer-associated N-glycans with Increased β1→6 Branching.* Electroanalysis (New York, N.Y.), 2021. **33**(12): p. 2490-2501.
53. Jezkova, P., et al., *Differentiation of Sialyl Linkages Using a Combination of Alkyl Esterification and Phenylhydrazine Derivatization: Application for N-Glycan Profiling in the Sera of Patients with Lung Cancer.* Analytical chemistry, 2022. **94**(18): p. 6736-6744.
54. Gilgunn, S., et al., *Glycosylation in Indolent, Significant and Aggressive Prostate Cancer by Automated High-Throughput N-Glycan Profiling.* Int J Mol Sci, 2020. **21**(23): p.9233.
55. Alvarez, M.R.S., et al., *N-Glycan and Glycopeptide Serum Biomarkers in Philippine Lung Cancer Patients Identified Using Liquid Chromatography–Tandem Mass Spectrometry.* ACS omega, 2022. **7**(44): p. 40230-40240.
56. Taniguchi, N., et al., *N-glycan branching enzymes involved in cancer, Alzheimer's disease and COPD and future perspectives.* Biochemical and biophysical research communications, 2022. **633**: p. 68-71.
57. Liu, S., et al., *N-glycan structures of target cancer biomarker characterized by two-dimensional gel electrophoresis and mass spectrometry.* Analytica chimica acta, 2020. **1123**: p. 18-27.
58. Gu, Y., et al., *Serum IgG N-glycans enable early detection and early relapse prediction of colorectal cancer.* International journal of cancer, 2023. **152**(3): p. 536-547.
59. Cong, X., et al., *Silencing GnT-V reduces oxaliplatin chemosensitivity in human colorectal cancer cells through N-glycan alteration of organic cation transporter member 2.* Experimental and therapeutic medicine, 2021. **21**(2): p. 128-128.
60. Arnold, J.N., et al., *Novel Glycan Biomarkers for the Detection of Lung Cancer.* Journal of Proteome Research, 2011. **10**(4): p. 1755-1764.
61. Liang, Y., et al., *Stage-associated differences in the serum N- and O-glycan profiles of patients with non-small cell lung cancer.* Clinical Proteomics, 2019. **16**: p.20.
62. Lan, Y., et al., *Serum glycoprotein-derived N- and O-linked glycans as cancer biomarkers.* American journal of cancer research, 2016. **6**(11): p. 2390-2415.
63. Gizaw, S.T., S. Gaunitz, and M.V. Novotny, *Highly Sensitive O-Glycan Profiling for Human Serum Proteins Reveals Gender-Dependent Changes in Colorectal Cancer Patients.* Analytical Chemistry, 2019. **91**(9): p. 6180-6189.
64. Gam, L.H., *Breast cancer and protein biomarkers.* World J Exp Med, 2012. **2**(5): p. 86-91.
65. Charkhchi, P., et al., *CA125 and Ovarian Cancer: A Comprehensive Review.* Cancers (Basel), 2020. **12**(12): p.3730

66. Reyes, C.D.G., et al., *LC-MS/MS Isomeric Profiling of N-Glycans Derived from Low-Abundant Serum Glycoproteins in Mild Cognitive Impairment Patients.* Biomolecules, 2022. **12**(11): p.3730.
67. Baerenfaenger, M., et al., *Glycoproteomics in Cerebrospinal Fluid Reveals Brain-Specific Glycosylation Changes.* Int J Mol Sci, 2023. **24**(3): p.1937.
68. Kumar A, S.J., Goyal A, et al. *Alzheimer Disease.* 2022 Updated 2022 Jun 5 [cited 2024 9 Feb]; Available from: https://www.ncbi.nlm.nih.gov/books/NBK499922/.
69. DeMaagd, G. and A. Philip, *Parkinson's Disease and Its Management: Part 1: Disease Entity, Risk Factors, Pathophysiology, Clinical Presentation, and Diagnosis.* P t, 2015. **40**(8): p. 504-32.
70. Zhang, X., et al., *Association of dementia with immunoglobulin G N-glycans in a Chinese Han Population.* npj Aging and Mechanisms of Disease, 2021. **7**(1): p. 3.
71. Schedin-Weiss, S., et al., *Glycan biomarkers for Alzheimer disease correlate with T-tau and P-tau in cerebrospinal fluid in subjective cognitive impairment.* The FEBS Journal, 2020. **287**(15): p. 3221-3234.
72. Baerenfaenger, M., et al., *Glycoproteomics in Cerebrospinal Fluid Reveals Brain-Specific Glycosylation Changes.* International Journal of Molecular Sciences, 2023. **24**(3): p. 1937.
73. Odaka, H., et al., *Platelet-derived extracellular vesicles are increased in sera of Alzheimer's disease patients, as revealed by Tim4-based assays.* FEBS Open Bio, 2021. **11**(3): p. 741-752.
74. Wilkinson, H., et al., *The O-Glycome of Human Nigrostriatal Tissue and Its Alteration in Parkinson's Disease.* Journal of Proteome Research, 2021. **20**(8): p. 3913-3924.
75. Shirotani, K., et al., *The role of TREM2 N-glycans in trafficking to the cell surface and signal transduction of TREM2.* The Journal of Biochemistry, 2022. **172**(6): p. 347-353.
76. Hoshi, K., et al., *Transferrin Biosynthesized in the Brain Is a Novel Biomarker for Alzheimer's Disease.* Metabolites, 2021. **11**(9):p.616.
77. Hoshi, K., et al., *Brain-Derived Major Glycoproteins Are Possible Biomarkers for Altered Metabolism of Cerebrospinal Fluid in Neurological Diseases.* Int J Mol Sci, 2023. **24**(7): p.6084.
78. Wilkinson, H., et al., *The O-Glycome of Human Nigrostriatal Tissue and Its Alteration in Parkinson's Disease.* J Proteome Res, 2021. **20**(8): p. 3913-3924.
79. Jiang, Y., et al., *Aberrant O-glycosylation contributes to tumorigenesis in human colorectal cancer.* Journal of cellular and molecular medicine, 2018. **22**(10): p. 4875-4885.
80. Wilson, M.P., et al., *CAMLG-CDG: a novel congenital disorder of glycosylation linked to defective membrane trafficking.* Human Molecular Genetics, 2022. **31**(15): p. 2571-2581.
81. Kazuno, S., et al., *O-glycosylated clusterin as a sensitive marker for diagnosing early stages of prostate cancer.* The Prostate, 2021. **81**(3): p. 170-181.
82. Yu, H., et al., *Integrated glycomics strategy for the evaluation of glycosylation alterations in salivary proteins associated with type 2 diabetes mellitus.* RSC Advances, 2020. **10**(65): p. 39739-39752.

83. Itakura, Y., N. Sasaki, and M. Toyoda, *Glycan characteristics of human heart constituent cells maintaining organ function: relatively stable glycan profiles in cellular senescence.* Biogerontology, 2021. **22**(6): p. 623-637.
84. Belczacka, I., et al., *Urinary Glycopeptide Analysis for the Investigation of Novel Biomarkers.* Proteomics Clin Appl, 2019. **13**(3): p. e1800111.
85. Moran, A.B., et al., *Serum N-Glycosylation RPLC-FD-MS Assay to Assess Colorectal Cancer Surgical Interventions.* Biomolecules, 2023. **13**(6): p. 896.
86. Kimura, K., et al., *Glycoproteomic analysis of the changes in protein N-glycosylation during neuronal differentiation in human-induced pluripotent stem cells and derived neuronal cells.* Sci Rep, 2021. **11**(1): p. 11169.
87. Gaunitz, S., L.O. Tjernberg, and S. Schedin-Weiss, *The N-glycan profile in cortex and hippocampus is altered in Alzheimer disease.* Journal of Neurochemistry, 2021. **159**(2): p. 292-304.
88. Wu, Y., et al., *N-glycomic profiling reveals dysregulated N-glycans of peripheral neuropathy in type 2 diabetes.* J Chromatogr B Analyt Technol Biomed Life Sci, 2023. **1220**: p. 123662.
89. Bai, R., et al., *The expression and functional analysis of the sialyl-T antigen in prostate cancer.* Glycoconjugate Journal, 2020. **37**(4): p. 423-433.
90. Wu, Z.L. and J.M. Ertelt, *Fluorescent glycan fingerprinting of SARS2 spike proteins.* Scientific Reports (Nature Publisher Group), 2021. **11**(1): p.20428.
91. Liu, D., et al., *Rapid glycosylation analysis of mouse serum glycoproteins separated by supported molecular matrix electrophoresis.* Journal of Proteomics, 2021. **234**: p. 104098.
92. Fukui, A., et al., *Dual impacts of a glycan shield on the envelope glycoprotein B of HSV-1: evasion from human antibodies in vivo and neurovirulence.* mBio. **0**(0): p. e00992-23.
93. Williams, S.E., et al., *Mammalian brain glycoproteins exhibit diminished glycan complexity compared to other tissues.* Nature Communications, 2022. **13**(1): p. 275.
94. Samal, J., et al., *Region-Specific Characterization of N-Glycans in the Striatum and Substantia Nigra of an Adult Rodent Brain.* Analytical Chemistry, 2020. **92**(19): p. 12842-12851.
95. Wilson, M.P., et al., *CAMLG-CDG: a novel congenital disorder of glycosylation linked to defective membrane trafficking.* Hum Mol Genet, 2022. **31**(15): p. 2571-2581.
96. Yang, J., et al., *Abnormal Galactosylated-Glycans recognized by Bandeiraea Simplicifolia Lectin I in saliva of patients with breast Cancer.* Glycoconj J, 2020. **37**(3): p. 373-394.
97. Yokose, T., et al., *O-Glycan-Altered Extracellular Vesicles: A Specific Serum Marker Elevated in Pancreatic Cancer.* Cancers, 2020. **12**(9): p. 2469.
98. Bertok, T., et al., *Analysis of serum glycome by lectin microarrays for prostate cancer patients - a search for aberrant glycoforms.* Glycoconjugate Journal, 2020. **37**(6): p. 703-711.
99. García-Artalejo, J.A., et al., *Characterizing a novel hyposialylated erythropoietin by intact glycoprotein and glycan analysis.* J Pharm Biomed Anal, 2022. **213**: p. 114686.

100. Cowper, B., et al., *Comprehensive glycan analysis of twelve recombinant human erythropoietin preparations from manufacturers in China and Japan.* J Pharm Biomed Anal, 2018. **153**: p. 214-220.
101. Bradberry, M.M., et al., *N-glycoproteomics of brain synapses and synaptic vesicles.* Cell Reports, 2023. **42**(4): p. 112368.
102. Gu, Y., et al., *Serum IgG N-glycans enable early detection and early relapse prediction of colorectal cancer.* Int J Cancer, 2023. **152**(3): p. 536-547.
103. Park, C.S., et al., *Fragmentation stability and retention time-shift obtained by LC-MS/MS to distinguish sialylated N-glycan linkage isomers in therapeutic glycoproteins.* Journal of Pharmaceutical Analysis, 2023. **13**(3): p. 305-314.
104. Huang, C., et al., *Identification of carbohydrate peripheral epitopes important for recognition by positive-ion MALDI multistage mass spectrometry.* Carbohydrate Polymers, 2020. **229**: p. 115528.
105. Kameyama, A., et al., *Alteration of mucins in the submandibular gland during aging in mice.* Archives of Oral Biology, 2021. **121**: p. 104967.
106. Jezková, P., et al., *Differentiation of Sialyl Linkages Using a Combination of Alkyl Esterification and Phenylhydrazine Derivatization: Application for N-Glycan Profiling in the Sera of Patients with Lung Cancer.* Analytical Chemistry, 2022. **94**(18): p. 6736-6744.
107. Takada, H., T. Katayama, and T. Katoh, *Sialylated O-Glycans from Hen Egg White Ovomucin are Decomposed by Mucin-degrading Gut Microbes.* Journal of applied glycoscience, 2020. **67**(2): p.31-39.
108. Samal, J., et al., *Enhanced Detection of Charged N-Glycans in the Brain by Infrared Matrix-Assisted Laser Desorption Electrospray Ionization Mass Spectrometric Imaging.* Analytical Chemistry, 2023. **95**(29): p. 10913-10920.
109. Li, W., et al., *Developmental O-glycan profile analysis shows pentasaccharide mucin-type O-glycans are linked with pupation of Tribolium castaneum.* Archives of Insect Biochemistry and Physiology, 2022. **109**(1): p. e21852.
110. Kamerling, J.P. and G.J. Gerwig, *2.01 - Strategies for the Structural Analysis of Carbohydrates*, in *Comprehensive Glycoscience*, H. Kamerling, Editor. 2007, Elsevier: Oxford. p. 1-68.
111. Kim, W., et al., *Qualitative and quantitative characterization of sialylated N-glycans using three fluorophores, two columns, and two instrumentations.* Analytical Biochemistry, 2019. **571**: p. 40-48.
112. Kishimoto, Y., et al., *Analysis of 2-aminopyridine labeled glycans by dual-mode online solid phase extraction for hydrophilic interaction and reversed-phase liquid chromatography.* J Chromatogr A, 2020. **1625**: p. 461194.
113. Gebrehiwot, A.G., et al., *Healthy human serum N-glycan profiling reveals the influence of ethnic variation on the identified cancer-relevant glycan biomarkers.* PloS one, 2018. **13**(12): p. e0209515-e0209515.
114. Wardman, J.F., et al., *Discovery and Development of Promiscuous O-Glycan Hydrolases for Removal of Intact Sialyl T-Antigen.* ACS Chemical Biology, 2021. **16**(10): p. 2004-2015.
115. Hansen, A.L., et al., *Identification of a Catalytic Nucleophile-Activating Network in the endo-α-N-Acetylgalactosaminidase of Family GH101.* Biochemistry, 2021. **60**(45): p. 3398-3407.

116. Hansen, D.K., J.R. Winther, and M. Willemoës, *Steady state kinetic analysis of O-linked GalNAc glycan release catalyzed by endo-α-N-acetylgalactosaminidase.* Carbohydrate Research, 2019. **480**: p. 54-60.
117. Kulinich, A., et al., *Biochemical characterization of the endo-α-N-acetylgalactosaminidase pool of the human gut symbiont Tyzzerella nexilis.* Carbohydrate Research, 2020. **490**: p. 107962.
118. Miyazaki, T., M. Ikegaya, and S. Alonso-Gil, *Structural and mechanistic insights into the substrate specificity and hydrolysis of GH31 α-N-acetylgalactosaminidase.* Biochimie, 2022. **195**: p. 90-99.
119. Crouch, L.I., et al., *Prominent members of the human gut microbiota express endo-acting O-glycanases to initiate mucin breakdown.* Nature Communications, 2020. **11**(1): p. 4017.
120. Morio, A., et al., *Expression, purification, and characterization of highly active endo-α-N-acetylgalactosaminidases expressed by silkworm-baculovirus expression system.* Journal of Asia-Pacific Entomology, 2019. **22**(2): p. 404-408.
121. Yang, S., et al., *Optimization of O-GIG for O-Glycopeptide Characterization with Sialic Acid Linkage Determination.* Analytical Chemistry, 2020. **92**(16): p. 10946-10951.
122. Yang, S., et al., *Deciphering Protein O-Glycosylation: Solid-Phase Chemoenzymatic Cleavage and Enrichment.* Analytical Chemistry, 2018. **90**(13): p. 8261-8269.
123. Anumula, K.R., *Advances in fluorescence derivatization methods for high-performance liquid chromatographic analysis of glycoprotein carbohydrates.* Analytical Biochemistry, 2006. **350**(1): p. 1-23.
124. Li, M., et al., *DiLeuPMP: A Multiplexed Isobaric Labeling Method for Quantitative Analysis of O-Glycans.* Analytical Chemistry, 2021. **93**(28): p. 9845-9852.
125. de Haan, N., et al., *In-Depth Profiling of O-Glycan Isomers in Human Cells Using C18 Nanoliquid Chromatography–Mass Spectrometry and Glycogenomics.* Analytical Chemistry, 2022. **94**(10): p. 4343-4351.
126. Vreeker, G.C.M., et al., *O- and N-glycosylation analysis of cell lines by ultrahigh resolution MALDI-FTICR-MS.* International Journal of Mass Spectrometry, 2020. **448**: p. 116267.
127. Zhang, X., et al., *Highly sialylated mucin-type glycopeptide from porcine intestinal mucosa after heparin extraction: O-glycan profiling and immunological activity evaluation.* Glycoconjugate Journal, 2021. **38**(5): p. 527-537.
128. Kurz, S., et al., *Separation and Identification of Permethylated Glycan Isomers by Reversed Phase NanoLC-NSI-MSn.* Molecular & Cellular Proteomics, 2021. **20**: p. 100045.
129. Flowers, S.A., C.S. Lane, and N.G. Karlsson, *Deciphering Isomers with a Multiple Reaction Monitoring Method for the Complete Detectable O-Glycan Repertoire of the Candidate Therapeutic, Lubricin.* Anal Chem, 2019. **91**(15): p. 9819-9827.
130. Xu, G., et al., *Deep Structural Analysis and Quantitation of O-Linked Glycans on Cell Membrane Reveal High Abundances and Distinct Glycomic Profiles Associated with Cell Type and Stages of Differentiation.* Analytical Chemistry, 2020. **92**(5): p. 3758-3768.

131. Goso, Y., et al., *Comparison of Methods to Release Mucin-Type O-Glycans for Glycomic Analysis.* Analytical Chemistry, 2017. **89**(17): p. 8870-8876.
132. Wang, C.-Y., et al., *Surface Shave: Revealing the Apical-Restricted Uroglycome.* Journal of Proteome Research, 2022. **21**(2): p. 360-374.
133. Kim, J., et al., *Structural and Quantitative Characterization of Mucin-Type O-Glycans and the Identification of O-Glycosylation Sites in Bovine Submaxillary Mucin.* Biomolecules, 2020. **10**(4): p. 636.
134. Furuki, K., T. Toyo'oka, and K. Ban, *Highly sensitive glycosylamine labelling of O-glycans using non-reductive β-elimination.* Analytical and Bioanalytical Chemistry, 2017. **409**(9): p. 2269-2283.
135. Yan, S., et al., *Core Richness of N-Glycans of Caenorhabditis elegans: A Case Study on Chemical and Enzymatic Release.* Analytical Chemistry, 2018. **90**(1): p. 928-935.
136. Vanbeselaere, J., et al., *The parasitic nematode Oesophagostomum dentatum synthesizes unusual glycosaminoglycan-like O-glycans.* Glycobiology (Oxford), 2018. **28**(7): p. 474-481.
137. Kozak, R.P., et al., *Improved nonreductive O-glycan release by hydrazinolysis with ethylenediaminetetraacetic acid addition.* Analytical Biochemistry, 2014. **453**: p. 29-37.
138. Kameyama, A., et al., *A practical method of liberating O-linked glycans from glycoproteins using hydroxylamine and an organic superbase.* Biochemical and Biophysical Research Communications, 2019. **513**(1): p. 186-192.
139. King, S.R., E.S. Hecht, and D.C. Muddiman, *Demonstration of hydrazide tagging for O-glycans and a central composite design of experiments optimization using the INLIGHT™ reagent.* Analytical and bioanalytical chemistry, 2017. **410**(5): p. 1409-1415.
140. Fukunaga, T., et al., *Characterization of N- and O-linked galactosylated oligosaccharides from fission yeast species.* Journal of Bioscience and Bioengineering, 2020. **130**(2): p. 128-136.
141. Hasehira, K., et al., *Quantitative structural analysis of glycans expressed within tumors derived from pancreatic cancer patient-derived xenograft mouse models.* Biochemical and Biophysical Research Communications, 2021. **534**: p. 310-316.
142. Guo, L., et al., *Glycine additive enhances sensitivity for N- and O-glycan analysis with hydrophilic interaction chromatography-electrospray ionization-mass spectrometry.* Analytical Biochemistry, 2021. **635**: p. 114447.
143. Huang, Y.P., R.C. Robinson, and D. Barile, *Food glycomics: Dealing with unexpected degradation of oligosaccharides during sample preparation and analysis.* J Food Drug Anal, 2022. **30**(1): p. 62-76.
144. Kinoshita, M., et al., *A rapid and facile preparation of APTS-labeled N-glycans by combination of ion pair-assisted extraction and HILIC-SPE for routine glycan analysis.* Journal of Pharmaceutical and Biomedical Analysis, 2021. **195**: p. 113875.
145. Reider, B., M. Szigeti, and A. Guttman, *Evaporative fluorophore labeling of carbohydrates via reductive amination.* Talanta, 2018. **185**: p. 365-369.

146. Dold, J.E.G.A. and V. Wittmann, *Metabolic Glycoengineering with Azide- and Alkene-Modified Hexosamines: Quantification of Sialic Acid Levels.* ChemBioChem, 2021. **22**(7): p. 1243-1251.
147. Flynn, R.A., et al., *Small RNAs are modified with N-glycans and displayed on the surface of living cells.* Cell, 2021. **184**(12): p. 3109-3124.e22.
148. Miura, Y. and T. Endo, *Glycomics and glycoproteomics focused on aging and age-related diseases — Glycans as a potential biomarker for physiological alterations.* Biochimica et Biophysica Acta (BBA) - General Subjects, 2016. **1860**(8): p. 1608-1614.
149. Cowper, B., et al., *Glycan analysis of erythropoiesis-stimulating agents.* Journal of Pharmaceutical and Biomedical Analysis, 2020. **180**: p. 113031.
150. Messina, A., et al., *HILIC-UPLC-MS for high throughput and isomeric N-glycan separation and characterization in Congenital Disorders Glycosylation and human diseases.* Glycoconjugate journal, 2021. **38**(2): p. 201-211.
151. Kim, B.J. and D.C. Dallas, *Systematic examination of protein extraction, proteolytic glycopeptide enrichment and MS/MS fragmentation techniques for site-specific profiling of human milk N-glycoproteins.* Talanta (Oxford), 2021. **224**: p. 121811-121811.
152. Barboza, M., et al., *Region-Specific Cell Membrane N-Glycome of Functional Mouse Brain Areas Revealed by nanoLC-MS Analysis.* Molecular & cellular proteomics, 2021. **20**: p. 100130-100130.
153. Wang, Y., et al., *Glycan reductive amino acid coded affinity tagging (GRACAT) for highly specific analysis of N-glycome by mass spectrometry.* Analytica chimica acta, 2019. **1089**: p. 90-99.
154. Zhang, Y., et al., *A rapid 2AB-UHPLC method based on magnetic beads extraction for N-glycan analysis of recombinant monoclonal antibody.* Journal of chromatography. B, Analytical technologies in the biomedical and life sciences, 2022. **1192**: p. 123139-123139.
155. Selman, M.H.J., et al., *Cotton HILIC SPE Microtips for Microscale Purification and Enrichment of Glycans and Glycopeptides.* Analytical Chemistry, 2011. **83**(7): p. 2492-2499.
156. Han, J., et al., *Purification of N- and O-glycans and their derivatives from biological samples by the absorbent cotton hydrophilic chromatographic column.* Journal of Chromatography A, 2020. **1620**: p. 461001.
157. Liew, C.Y., et al., *Identification of the High Mannose N-Glycan Isomers Undescribed by Conventional Multicellular Eukaryotic Biosynthetic Pathways.* Analytical Chemistry, 2023. **95**(23): p. 8789-8797.
158. Aoyama, M., et al., *Effects of terminal galactose residues in mannose α1-6 arm of Fc-glycan on the effector functions of therapeutic monoclonal antibodies.* mAbs, 2019. **11**(5): p. 826-836.
159. Mei Chou, L., et al., *A Bibenzyl Component Moscatilin Mitigates Glycation-Mediated Damages in an SH-SY5Y Cell Model of Neurodegenerative Diseases through AMPK Activation and RAGE/NF-κB Pathway Suppression.* Molecules, 2020. **25**(19): p. 4574.
160. Snoderly-Foster, L.J., et al., *Regulation of Parkinson's disease-associated genes by Pumilio proteins and microRNAs in SH-SY5Y neuronal cells.* PLoS One, 2022. **17**(9): p.e0275235

161. Pokusa, M., et al., *Vulnerability of Subcellular Structures to Pathogenesis Induced by Rotenone in SH-SY5Y Cells.* Physiological Research, 2021. **70**(1): p. 89-99.
162. Chen, Y., et al., *Dexmedetomidine protects SH-SY5Y cells against MPP+-induced declining of mitochondrial membrane potential and cell cycle deficits.* European Journal of Neuroscience, 2021. **54**(1): p. 4141-4153.
163. Guyon, A., et al., *The protective mutation A673T in amyloid precursor protein gene decreases Aβ peptides production for 14 forms of Familial Alzheimer's Disease in SH-SY5Y cells.* PLoS One, 2020. **15**(12): p.e0237122
164. Blanco-Míguez, A., et al., *Microbiota-Derived β-Amyloid-like Peptides Trigger Alzheimer's Disease-Related Pathways in the SH-SY5Y Neural Cell Line.* Nutrients, 2021. **13**(11): p. 3868.
165. Radagdam, S., et al., *Evaluation of dihydrotestosterone and dihydroprogesterone levels and gene expression of genes involved in neurosteroidogenesis in the SH-SY5Y Alzheimer disease cell model.* Frontiers in Neuroscience, 2023. **17**: p.1163806
166. Costanti, F., et al., *A Deep Learning Approach to Analyze NMR Spectra of SH-SY5Y Cells for Alzheimer's Disease Diagnosis.* Mathematics, 2023. **11**(12): p. 2664.
167. Zhu, D., et al., *Structure-activity relationship analysis of Panax ginseng glycoproteins with cytoprotective effects using LC-MS/MS and bioinformatics.* International Journal of Biological Macromolecules, 2020. **158**: p. 1352-1361.
168. Hu, Y., et al., *N-linked glycan profiling in neuroblastoma cell lines.* Journal of proteome research, 2015. **14**(5): p. 2074-2081.
169. Demir, R., U. Şahar, and R. Deveci, *Determination of terminal glycan and total monosaccharide profiles of reelin glycoprotein in SH-SY5Y neuroblastoma cell line by lectin blotting and capillary liquid chromatography electrospray ionization-ion trap tandem mass spectrometry system.* Biochim Biophys Acta Proteins Proteom, 2021. **1869**(2): p. 140559.
170. Losev, Y., et al., *Novel model of secreted human tau protein reveals the impact of the abnormal N-glycosylation of tau on its aggregation propensity.* Scientific reports, 2019. **9**(1): p. 2254-2254.
171. Birol, M., et al., *Identification of N-linked glycans as specific mediators of neuronal uptake of acetylated α-Synuclein.* PLOS Biology, 2019. **17**(6): p. e3000318.

Chapter 2

O-Linked glycan analysis by CuAAC using a synthetic labelling reagent

2.1 Introduction

Click reactions were first employed for functionalising biological molecules by Sharpless *et al.* [1] as they proceed under mild aqueous conditions. There are two common click cycloaddition reactions between alkynes and azides, specifically Huisgen's 1,3-dipolar cycloaddition and the copper catalysed azide-alkyne 1,3-dipolar cycloaddition (CuAAC) reaction, as shown in Scheme 2.1. CuAAC is milder than Huisgen's reaction and produces only one isomer of the product [2, 3]. The click reaction is chosen for many research studies in materials science, biomedicine, nanotechnology, chemical biology, drug delivery, targeted bioorthogonal study, cell biology, and tissue engineering fields [4-9], because these reactions proceed under aqueous conditions and do not damage cells or organelles.

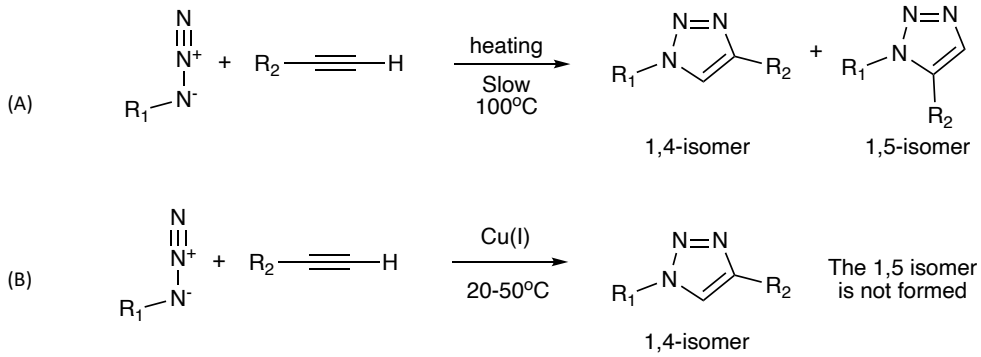

Scheme 2.1 Click reaction involving Huisgen's 1,3-dipolar cycloaddition reaction and CuAAc reaction. (A) Huisgen's 1,3-dipolar cycloaddition reaction, and (B) CuAAC reaction.

The click reaction requires ligands that are designed to enhance the binding of the azido group to the copper centre, hence increasing the yields of the reaction and the water-solubility of the Cu (I) component. Many kinds of ligands have been used, such as TBTA (tris[1-benzyl-1H-1,2,3,-triazol-4-yl)methyl]amine) [10, 11], THPTA (tris[(1-hydroxypropyl-1H-1,2,3-triazol-4-yl)methyl]amine) [9, 12], and BTTAA (2-[4-{(bis[(1-tert-buty-1H-1,2,3-triazol-4-yl)methyl]amino)methyl}-1H-1,2,3-triazol-1-yl]acetic acid) [13], as illustrated in Figure 2.1.

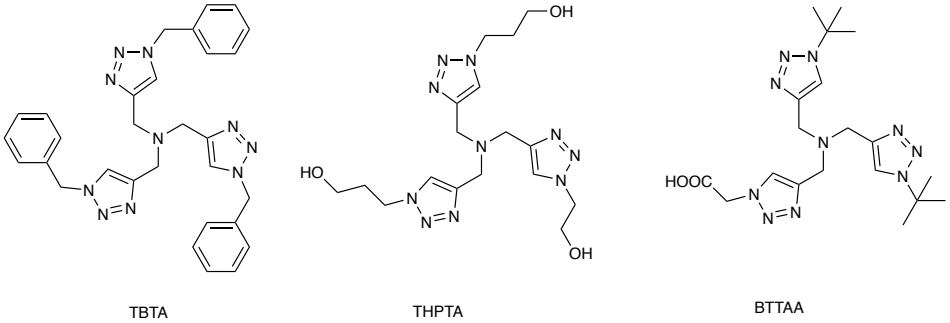

Figure 2.1 TBTA, THPTA and BTTAA structures.

2.1.1 Application of CuAAC to studies of biomolecules

The CuAAC reaction is widely used in biological studies using a chromophore or fluorophore bearing alkyne to react with the azide functional group that can be introduced in living cells. However, Cu (I) is toxic to living cells, so a combination of $CuSO_4$ with sodium ascorbate and ligand is more often used as this is biocompatible. Specific applications of the click reaction are presented below.

2.1.1.1 DNA and RNA Fluorescence Labelling

In DNA, RNA, or microRNA studies, the click reaction was used to selectively add a fluorophore to living cells' DNA/RNA sequences compared to normal and tumour cells [7, 9, 14]. The different targets for the click reaction were studied with a focus on developing drug-targeted therapy [15-22].

2.1.1.2 Tracking biomarker levels and living cell changes

Biomarkers in living cells can be detected by using the click reaction to deliver fluorescence tags to the cells. An example of using the CuAAC reaction to track biomarkers focuses on detecting hydrogen sulphide (H_2S), which is an endogenous cellular signalling molecule, and abnormal production is linked to many diseases (AD, cancer, and Down syndrome). The traditional detection of H_2S used a sensing method that was non-accurate, non-precise, and had high detection limits, such as colorimetry, electrochemical analysis, and sulphide precipitation [23-26]. The CuAAC was developed for H_2S detection by introducing an azide fluorophore. The synthetic azide reacted with the H_2S to form the amine group. The total azide is detected by a click reaction with a fluorescent alkyne. The decrease in fluorescence detection can be used for quantitative analysis of the H_2S [8, 27-29].

Antibodies (such as IgG and IgM) are also used as biomarkers for various kinds of diseases. The click reaction has been developed to increase the sensitivity of detection at low concentrations of the biomarkers. Examples of where this has been successfully applied include the detection of biomarkers for cancer [22, 30-35], infection [36-38], and inflammation [39]. The target cells are diagnosed by the specific azide probe uptake to the target cells, without uptake to the normal cells, and subsequent click reaction with fluorescent alkyne reagents.

The CuAAC reaction has also been used to study the diversity of glycans in humans. Due to the toxicity of copper, the mapping of *O*-glycosylation used gold nanoparticles to replace copper for the click reaction to introduce a fluorophore to the glycans [40]. The diversity of the glycan pattern was studied by introducing the azide functional group to the cell surface before introducing an alkyne fluorophore [31, 35, 41-51]. These results can be used to detect the progress of diseases or the effectiveness of treatments.

2.1.1.3 Drug delivery

Cells engineered to display the azide functional group within cell surface glycans or oligosaccharides can be developed for site-selective modification by introducing an alkyne group and using a drug with an azide group [48, 52]. For example, this has allowed the development of drug delivery systems to enhance the absorption and improve the release of hydrophobic drugs using the click reaction between drugs and polymer. The natural, non-toxic polymer chitosan and oligosaccharide/alginate were chosen as the polymer base. Releasing mechanism factors that were studied included the swelling properties, pH, maximum drug loading capacity, drug release and stability [53-55]. Injection drug formulations have used hyaluronic acid as the safety polymer. The click reaction between the hydrophobic drug and hydrogel increases the water solubility of the medicine [56, 57]. For the chemotherapy drug delivery system, the click reaction between the medicine and tumour cells, or specific pH at the

target site, or photodynamic release is used to decrease the offsite toxicity in normal cells [58-64].

2.1.2 Application of CuAAC in glycan analysis

Various methods can be used to analyse changing glycan levels in biological samples. Introducing azide to the glycans for click reaction with a fluorophore alkyne can increase the level of detection [65]. The click reaction adds the fluorophore to the azide-glycan structure for structure-activity relationship studies by high-throughput screening for *O*-linked glycosylation studies [66, 67], and for microplate reader (fluorescence scanning) [48, 66, 67], Ultraviolet (UV)/Visible spectroscopy [47], or MS [68, 69]. HPLC was used for following the conjugation of radio-labelled monoclonal antibodies [70]. Azide is introduced to living cells using the azide sugar inserted into the cells during the cell metabolic process [46, 69, 71-75]. The summary process of using the click reaction for *O*-glycan analysis in living cells is shown in Figure 2.2. Examples of azide sugars [42, 44, 65-67, 74, 76-79] are shown in Figure 2.3.

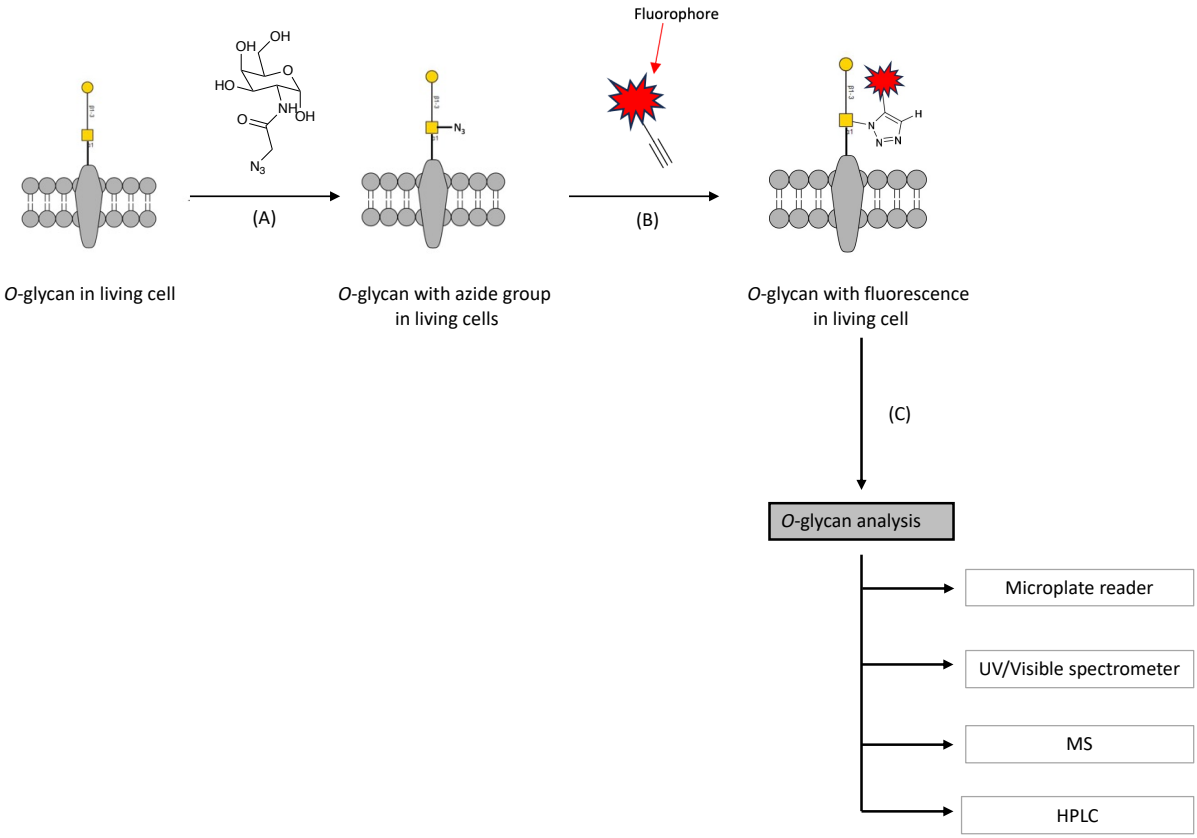

Figure 2.2 The process of using CuAAC reaction to introduce the fluorophore functional group to the sugar of living cells. (A) introducing the azido-sugar to living cells in the metabolism pathway, (B) adding alkyne with fluorophore functional group to azido-sugar by Click reaction, and (C) analysis of *O*-glycan.

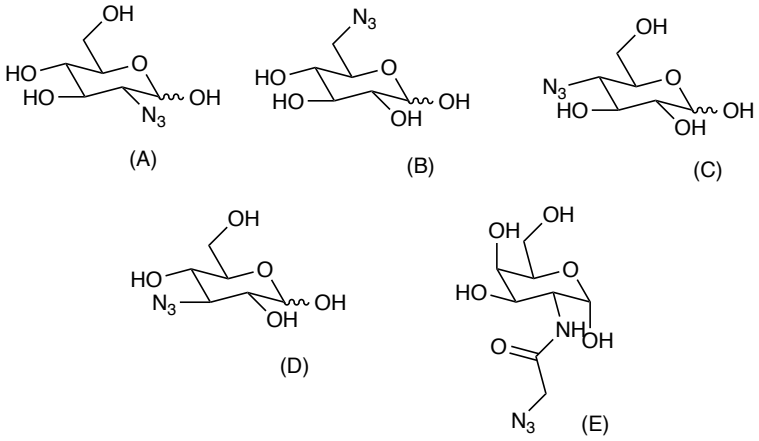

Figure 2.3 Examples of azide sugars for *O*-glycosylation study (A-D) azido glucose [51] and (E) azido GalNAc [80].

The application of the click reaction for *O*-glycan analysis was studied by introducing an azide to the sugar moieties. However, when labelling the *O*-glycans by CuAAC reaction or reductive amination reaction, the glycan must be released from the core before using HPLC, and the HPLC analysis for all core *O*-glycans is still challenging.

In general, glycan analysis using commercial fluorescent labels requires a functional handle to enable the coupling of the sugar with the label. If the process is to be carried out on glycosyl amino acids rather than free or enzymatically released glycans, a novel label must be developed to enable selective reaction with an amino acid coupling partner. The reaction must also be suitable to be carried out in aqueous media. To enable this, it is envisaged that if the mixture of amino acids obtained by proteolytic cleavage can be converted to the corresponding azides, this will install a functional group that can react selectively with an alkyne functionalised label. Azides are not commonly found in proteins. Hence, choosing this modification reduces the risk of unwanted side reactions.

2.2 Aim and Objectives

This work aims to determine whether an alkyne functionalised fluorescence labelling reagent (**5**) can be used for the analysis of *N*- and *O*-linked glycans using HPLC equipped with a fluorescence detector. It is proposed that *N*-linked glycans will be labelled by a reductive amination reaction, and *O*-glycans will be labelled by the CuAAC reaction.

The work in this chapter, therefore, sets out to fulfil three main objectives. The first objective is to synthesize, purify, and characterise the alkyne fluorescence labelling reagent (**5**) and the ligand required for the click reaction (**12**).

The second objective is the synthesis, purification and characterisation of an azide *O*-linked glycan mimic based on protected glucose (1 Glucose Unit (GU), **20**) and Boc-L-serine methyl ester (**19**).

The final objective is to confirm that **5** can be used for labelling *N*- and *O*-linked glycans using lactose (2GU, **14**) as a model substrate for the *N*-glycan and a commercial azido-sugar (**24**) as the *O*-glycan model compound.

This research is summarised in Figure 2.4, which outlines the schemes of work carried out within this chapter.

(A)

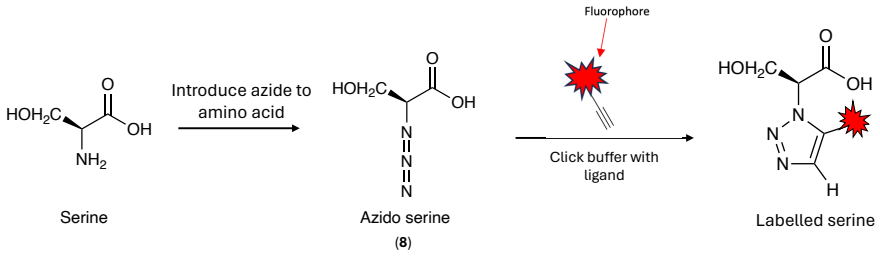

(B)

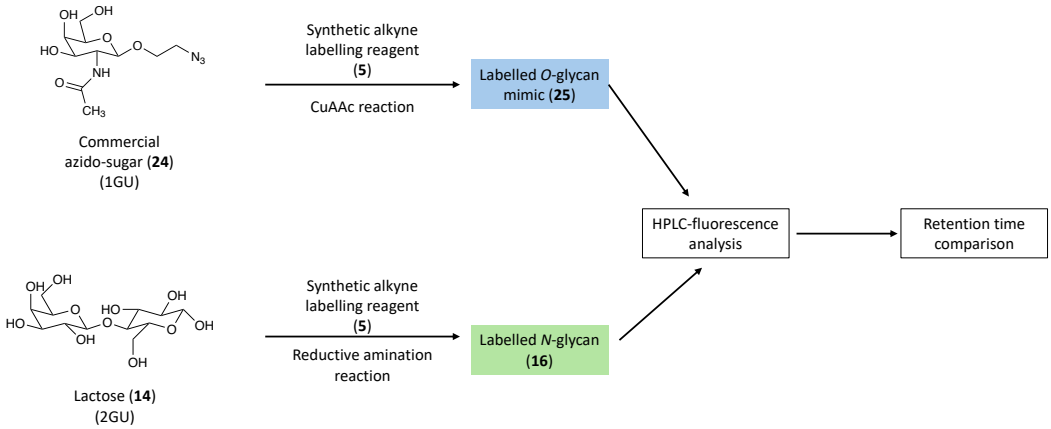

Figure 2.4 Workflow for labelled *O*- and *N*-glycans using synthetic alkyne labelling reagent before HPLC-fluorescence analysis. (A) Serine, with no chromophore or fluorophore in the structure, was chosen as the model for the introduced azide before Click reaction with the synthetic labelling reagent. (B) Reaction of the *O*-glycan mimic and the disaccharide with the synthetic alkyne labelling reagent.

2.3 Results and Discussion

2.3.1 Synthesis of an alkyne label - synthesis of 4-amino-*N*-(pent-4-yn-1-yl)benzamide (5) as the synthetic fluorescence labelling reagent [81]

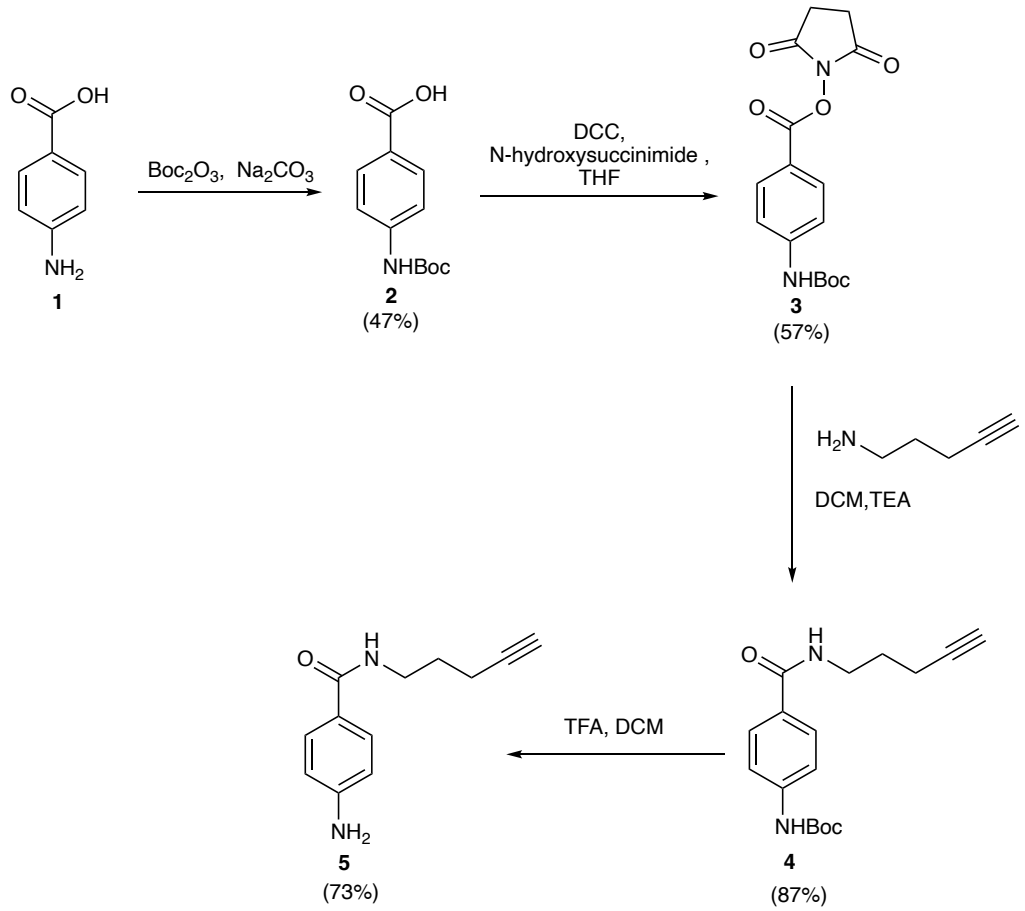

Scheme 2.2 Synthesis of fluorescence label **5**.

Scheme 2.2 shows the approach taken to synthesise the glycan fluorescence labelling reagent (**5**). The synthesis started from 4-aminobenzoic acid (PABA) **1**. The amine was first protected by adding a Boc group to yield **2**. The reaction between **2** and *N*-hydroxysuccinimide converts the carboxylic to a better leaving group within **3**. The reaction between **3** and 4-pentyn-1-amine hydrochloride allows introduction of the alkyne group into the structure, affording **4**. The final step is removing the Boc group using trifluoroacetic acid (TFA) in dichloromethane (DCM) (1:6 v/v) and amberlite IRA-57® in methanol (MeOH) for neutralisation, affording **5**. Compound **5** is an alkyne fluorophore labelling reagent suitable for the click reaction. All intermediates were purified by flash column chromatography and characterized by ^{1}H NMR, ^{13}C NMR, and IR spectroscopy. The compound **5** was characterized by ^{1}H NMR, ^{13}C NMR spectroscopy, IR spectroscopy and MS.

2.3.2 Synthesis of azido-serine (8)

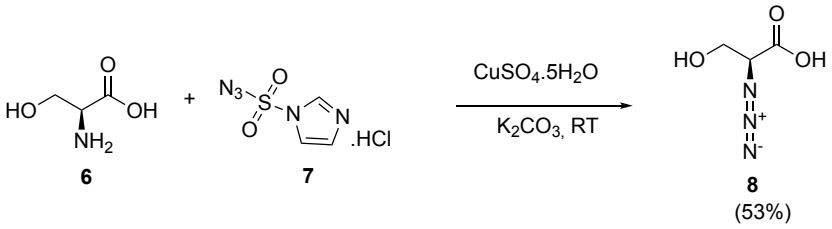

Scheme 2.3 Synthesis of azido-serine (**8**).

Scheme 2.3 shows a reaction for synthesising azido-serine (**8**) [82]. The reaction required a diazo transfer reaction to add the azide group to the amino acid structure. Stick reagent (imidazole-1-sulfonyl azide HCl) (**7**) was used to add the azide group to L-serine (**6**) and optimise the reaction conditions. When the reaction was conducted at room temperature, the product was formed after 10 days. The product was purified by column chromatography, using 1-butanol:glacial acetic acid:water (12:3:5) as the mobile phase, and this afforded **8** as a pale yellow oil in 84% yield. The azide **8** was characterised by ^{1}H NMR, ^{13}C NMR, and IR spectroscopy.

2.3.3 Synthesis of tris((1-benzyl-1H-1,2,3-triazol-4-yl)methyl)amine. (TBTA) (12) [81]

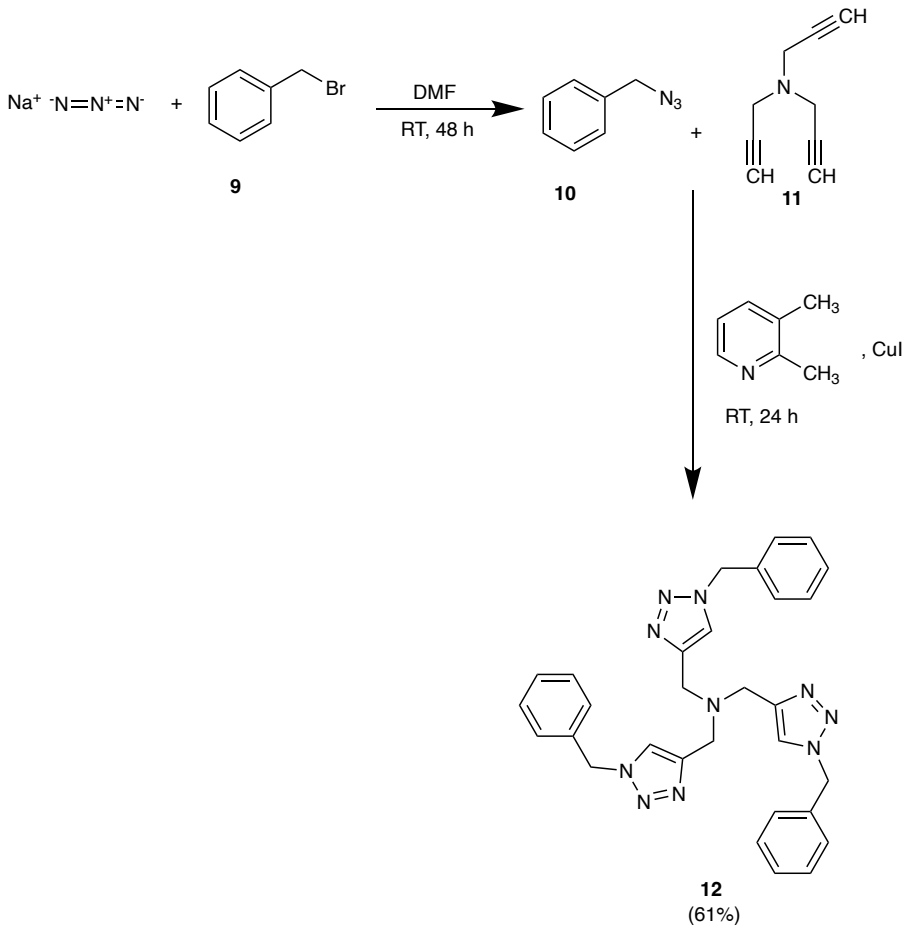

Scheme 2.4 Synthesis of TBTA (**12**).

Scheme 2.4 shows a reaction for TBTA (**12**) synthesis. TBTA is used for the ligand in the click buffer. The synthesis was carried out in two steps. First, the reaction between sodium azide and benzyl bromide (**9**) was conducted at room temperature. The product was benzyl azide (**10**). The second step was the reaction between benzyl azide and tripropargyl amine (**11**), using

copper iodide and 2,3-lutidine as catalysts. Compound **12** was characterized by ^{1}H NMR, ^{13}C NMR spectroscopy, IR spectroscopy and MS.

2.3.4 Optimisation of click reaction between alkyne 5 and azide 8

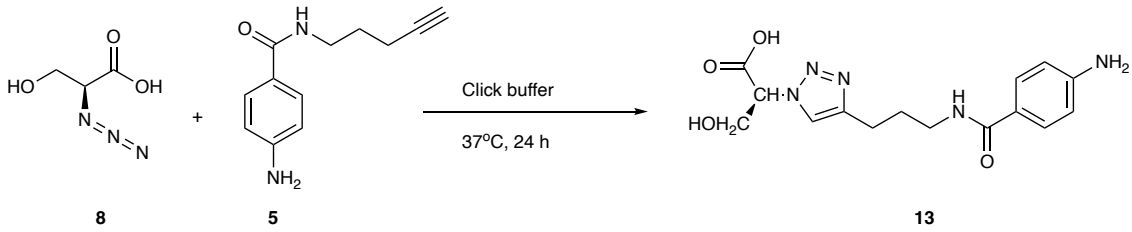

8 5 13

Scheme 2.5 Click reaction between **5** and **8**.

The click reaction between **5** and **8** (Scheme 2.5) was investigated using 200 μL of 1 mM of **5** and 200 μL of 0.5 mM of **8** added to 600 μL of click buffer (table 2.4). The reaction equivalent was 1:0.5 between **5** and **8**, respectively. The mixture was incubated at 37°C for at least 24 hours and checked for completion of the reaction by monitoring the consumption of **8** by TLC (DCM:ethyl acetate (EtOAc):MeOH(8:1:1) detected by UV light and ninhydrin. The reaction in this work is completed in 24 hours.

2.3.5 Optimisation of labelling between Lactose (14) and 5 [81]

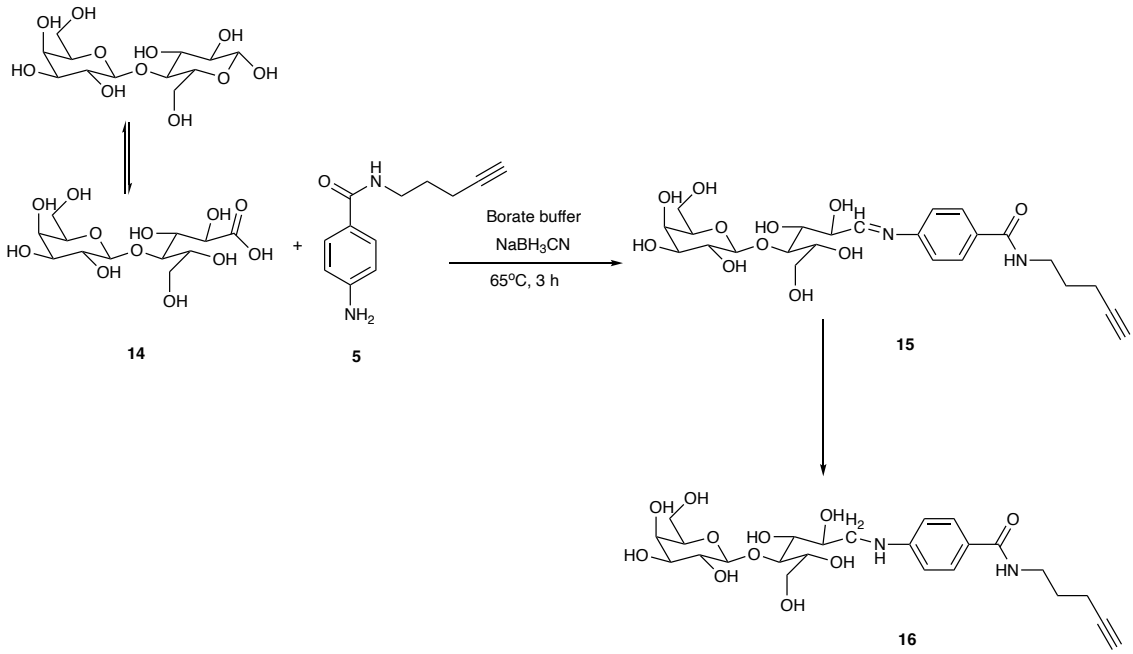

14 5 15 16

Scheme 2.6 Reaction of lactose (**14**) with **5** by reductive amination reaction.

Lactose (**14**) was dissolved in water, and sodium cyanoborohydride in borate acetate buffered MeOH was added, as shown in Scheme 2.6. Compound **5** in MeOH was added to the reaction. The reaction mixture was then vortexed and centrifuged for 10 seconds before being heated at 65°C for at least 3 hours. Completion of the reaction was ascertained by TLC analysis (acetonitrile(ACN):water (3:1)).

2.3.6 Synthesis of Boc-L-serine methyl ester (19)

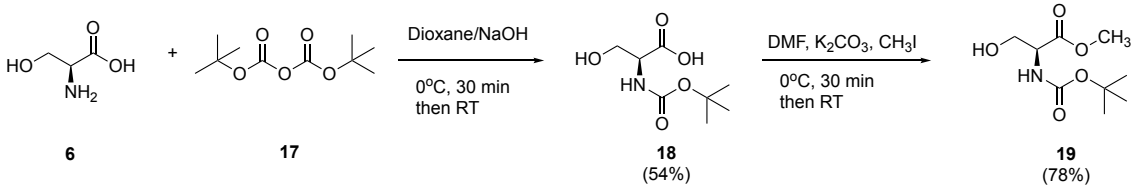

6 17 **18** (54%) **19** (78%)

Scheme 2.7 Synthesis of Boc-L-serine methyl ester (**19**).

Scheme 2.7 shows the approach followed for the synthesis of Boc-L-serine methyl ester (**19**). The first step is Boc-protection of the amine functional group in serine to afford **18**. The reaction was run at 0°C for 30 minutes in basic dioxane and was then warmed to room temperature with monitoring via TLC analysis until the reaction was complete. Compound **18** was then reacted without purification with methyl iodide at 0°C for 30 minutes in dimethylformamide (DMF) with potassium carbonate, and then at room temperature until the reaction was complete. Compounds **18** and **19** were characterised by ^{1}H NMR, ^{13}C NMR spectroscopy, IR spectroscopy and MS.

2.3.7 Synthesis of (*2R,3R,5R,6R*)-2-(acetoxymethyl)-6-(2-((tert-butoxycarbonyl)amino)-3-methoxy-3-oxopropoxy)tetrahydro-2H-pyran-3,4,5-triyl triacetate (21)

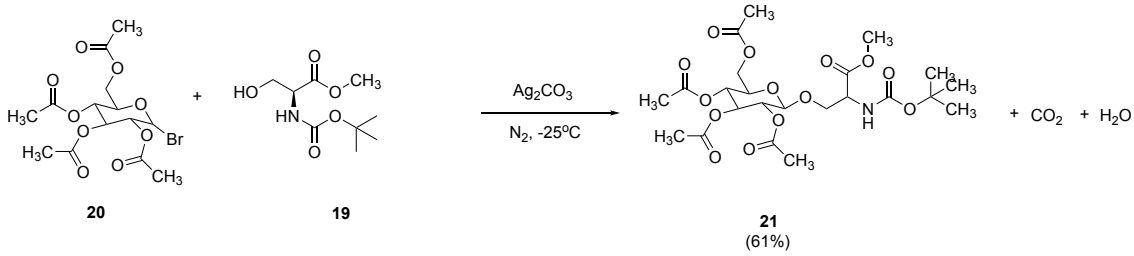

20 19 **21** (61%)

Scheme 2.8 Synthesis of (*2R,3R,5R,6R*)-2-(acetoxymethyl)-6-(2-((tert-butoxycarbonyl)amino)-3-methoxy-3-oxopropoxy)tetrahydro-2H-pyran-3,4,5-triyl triacetate (**21**).

Scheme 2.8 shows the synthesis of **21**. Compound **19** was reacted with compound **20** in dry toluene under an inert atmosphere. Silver carbonate was added to the mixture, and this was stirred at -25°C until the reaction was complete. Compound **21** was characterised by ^{1}H NMR, ^{13}C NMR spectroscopy and MS.

2.3.8 De-protection of (*2R,3R,5R,6R*)-2-(acetoxymethyl)-6-(2-((tert-butoxycarbonyl)amino)-3-methoxy-3-oxopropoxy)tetrahydro-2H-pyran-3,4,5-triyl triacetate to *O*-((*2R,3R,5S,6R*)-3,4,5-trihydroxy-6-(hydroxymethyl)tetrahydro-2H-pyran-2-yl)serine (23)

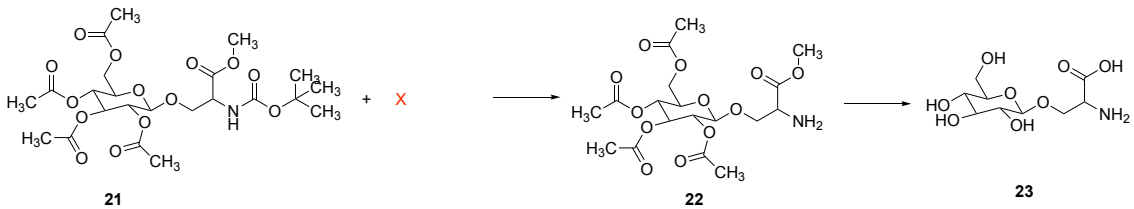

21 22 23

Scheme 2.9 Synthesis of *O*-((*2R,3R,5S,6R*)-3,4,5-trihydroxy-6-(hydroxymethyl)tetrahydro-2H-pyran-2-yl)serine (**23**). The X in the Scheme represented the chemical reagents for removal of the protecting groups from **21**.

Scheme 2.9 shows a reaction for the synthesis of **23,** which is an *O*-glycosylation mimic that can be converted to an azide-functionalised glycoside. To protect the decomposition of the azide during the synthesis reaction, the azide is introduced to the *O*-glycosylation mimic in the last

step. The methods investigated for the removal of the Boc protecting group from within **21** are summarised in Table 2.1. In all cases, ^{1}H NMR spectroscopic analysis indicated that the Boc group was still present, suggesting that none of the conditions successfully removed the Boc-protecting group.

Table 2.1 Summary of the methods investigated for removal of the Boc protecting group from **21**

Reaction procedure	Reagents	Results	Reference
2.0 equivalent of $FeCl_3$ was added to the DCM solution of **21**, stirring at room temperature. Purification by column chromatography using DCM:MeOH 95:5 as mobile phase	$FeCl_3$ (2 equivalent) in DCM	- Boc peak still present in the ^{1}H NMR spectrum - MS analysis did not afford data consistent with the required product	[83]
A solution of K_2CO_3 (0.414 g, 3 mmol) in MeOH-H_2O (3:1, 15 mL) containing **21** (1 mmol) was heated at reflux on a steam bath. Purification by column chromatography using DCM:MeOH 95:5.	K_2CO_3 (3 mmol) in MeOH:water (3:1)	- Boc peak still present in the ^{1}H NMR spectrum - MS analysis did not afford data consistent with the required product	[84]
1 mmol of **21** was stirred in 1:6 TFA/DCM at room temperature. Purification by column chromatography using 95:5 DCM:MeOH.	TFA/DCM 1:6	- Boc peak still present in the ^{1}H NMR spectrum - MS analysis did not afford data consistent with the required product	[83]
A solution **21** in HCl/dioxane (0.2 mmol) was stirred in an ice bath for 30 minutes and then the reaction was kept at room temperature. The reaction mixture was condensed by rotary evaporation under a high vacuum at room temperature. The residue was then washed with dry diethyl ether and collected by filtration.	HCl/dioxane	- Boc peak still present in the ^{1}H NMR spectrum - MS analysis did not afford data consistent with the required product	[85]
1 mmol of **21** stirred in 5 mL of DCM. 5 mol% of $ZnBr_2$ was added and stirred at room temperature. Purification by column chromatography using EtOAc:hexane 1:1 containing 1% acetic acid as mobile phase	$ZnBr_2$/DCM	- Boc peak no longer present in ^{1}H NMR spectrum - MS analysis did not afford data consistent with the required product	[86]

However, the process of removing Boc and acetyl groups from **21**, as shown in Table 2.1, did not produce **23**. The commercial 2-azidoethyl 2- acetamido-2-deoxy-β-D-galactopyranoside (**24**) was therefore used instead to probe the ability to use a click reaction between **24** and **5** for HPLC-fluorescence analysis.

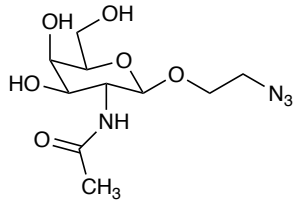

24

Figure 2.5 The structure of 2-azidoethyl 2- acetamido-2-deoxy-β-D-galactopyranoside (**24**).

2.3.9 Optimisation of click reaction between 5 and 24

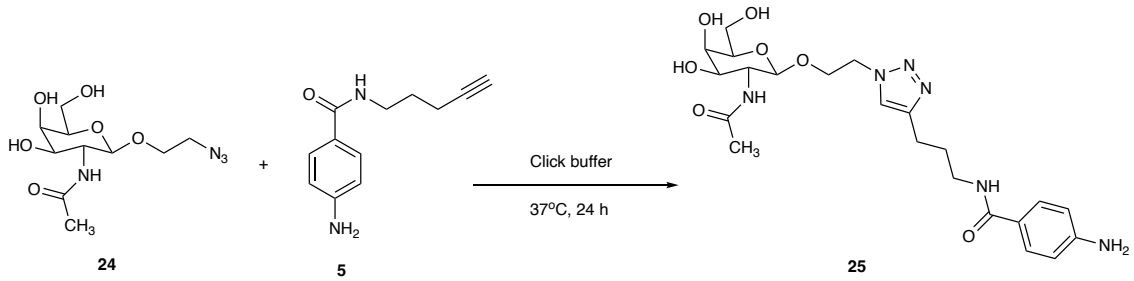

24 **5** **25**

Scheme 2.10 Click reaction between **5** and **24**.

Optimised condition from 2.3.4 were used for the click reaction between **5** and **24**. Compound **25** was analysed by HPLC-fluorescence.

2.3.10 HPLC-fluorescence retention times for compounds 5, 16 and 25

Compound **5** at a concentration of 1 nmol/ml in MeOH, and labelled compounds **16** and **25** diluted to 1 mL with HPLC water were analysed by Agilent 1100 HPLC system. A 4.6x250 mm column packed with 5 µM Amide-80 HR column (Tosah bioscience) was used as the stationary phase. The mobile phase A was 50 mM ammonium formate (pH 4.4), and ACN was phase B. The column temperature was set at 40°C. Samples were injected at 2 µL per injection. The retention times for 3 compounds are shown in Table 2.2 and Figure 2.7.

Table 2.2 Retention times of **5**, **16**, and **25**

Compound	Retention time (minutes)
5	3.5
16	6.5
25	5.3

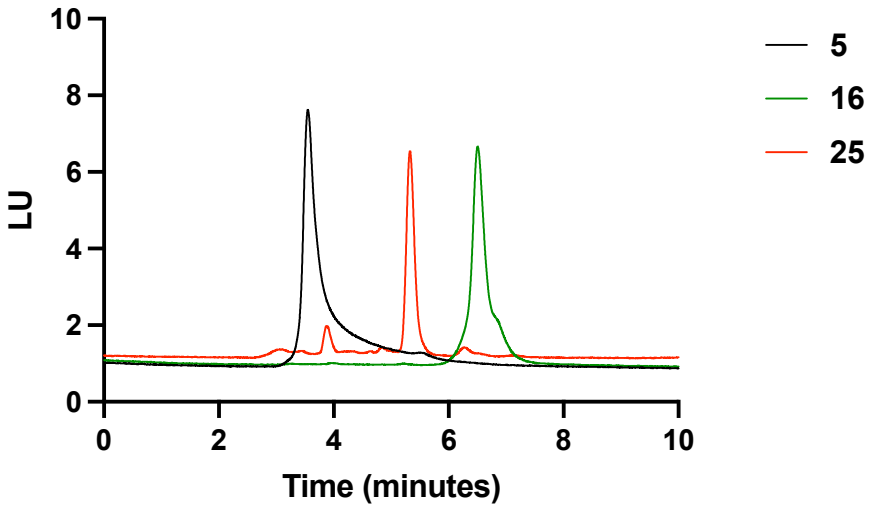

Figure 2.6 The HPLC chromatograms for **5**, **16,** and **25**.

The HPLC data show that the alkyne labelling reagent **5** can be used to label *N*- and *O*-glycans in different reactions. The chromatogram shows the product from the different retention times (6.5 and 5.3 minutes, for **16** and **25**, respectively) for the different glycosidic bond types.

Figure 2.6 confirmed that Compound **5** can labelled *N*-linked glycan by a reductive amination reaction and *O*-linked glycan by the CuAAC reaction for HPLC-fluorescent detection. Compound **5** separated fastest, and Compounds **25** and **16**, respectively. This HPLC system used a HILIC column for separation. The sequence of separation from the column depends on the polarity of the structures. Compound **5**, the labelling reagent, has the most polarity than Compounds **16** and **25**. Comparing Compounds **16** and **25**, Compound **25** has more polarity than **16**. Because Compound **16** has more sugar units than Compound **25**, 2 sugar units for Compound **16** and 1 sugar unit for Compound **25**.

2.4 Conclusions and Future Work

The synthetic alkyne fluorescence labelling reagent (**5**) has been developed for the multifunction labelling of *N*- and *O*-glycoproteins in different reactions for HPLC-fluorescence analysis. Compound **5** can label the *N*-glycans by a reductive amination reaction at the primary amine functional group without carbohydrate modification. On the other hand, *O*-glycans require labelling with **5** by the click reaction.

Compound **5** and the click ligand (**12**) were synthesised in 4 and 2 steps, respectively. It was then demonstrated that a click reaction can occur between an azido derivative of serine (**8**) and the fluorescent label (**5**) in 24 hours. This result was extended to probe whether a click reaction could also occur between (**5**) and a model azide compound (**24**).

The HPLC chromatograms compared between labelling reagents, labelled *N*-glycans and labelled *O*-azido sugar (**5**, **16** and **25**) are shown in Figure 2.6. Compounds **16** and **25** have different retention times for the different sugar types (2GU and 1GU, respectively).

Future work could focus on using the CuAAC reaction for the analysis of more complex glycoproteins by HPLC**.** This method should be started by cleaving the peptide bond to single amino acids, enriching all glycans from amino acids, and introducing the azide to the amine group at the glycans' amino acid before using a click reaction for HPLC-fluorescence or HPLC-MS analysis, as illustrated in Figure 2.8**.** This can be used for HPLC analysis of all *N*- and *O*-glycan cores using the same labelling reagent**.**

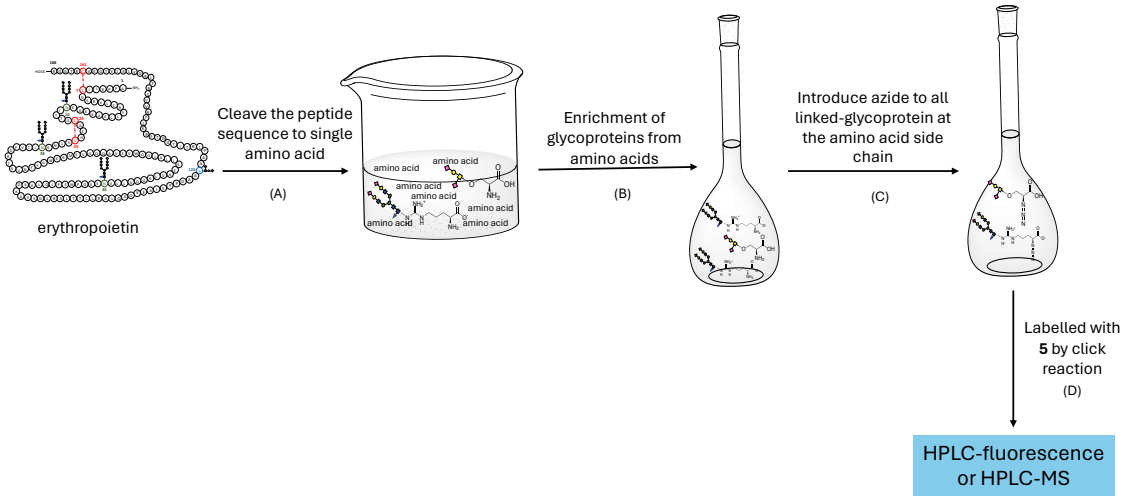

Figure 2.7 Workflow using CuAAC for labelled *N*- and *O*-glycans for HPLC analysis at the same time. (A) Erythropoietin is cleaved into single amino acids and single glycoproteins. (B) The *N*- and *O*-glycoproteins are enriched before introducing the azide to the amino acid side chain (C). (D) The azide glycoproteins are labelled with **5** by click reaction before analysis by HPLC-fluorescence or HPLC-MS.

2.5 Experimental

2.5.1 General experiment

All chemicals used were analytical or HPLC grade, purchased from commercial sources (Sigma-Aldrich, Merk, Fisher Scientific, Alfa Aesar and Acros Organics), and used without further purification. Anhydrous solvents including DCM, DMF, toluene and diethyl ether were purchased from Acros organics in Acro-seal bottled store over molecular sieves. HPLC analytical column (TSKgel Amide-80 HR column) was purchased from Tosoh Bioscience GmbH (Germany). Monitoring of reactions via TLC used aluminium backed 60 F254 silica TLC plates (Sigma Merk). Visualisation was then carried out under UV light (λ= 254 nm), followed by staining with Ninhydrin.

2.5.2 Analytical Equipment

Nuclear Magnetic Resonance
^{1}H and ^{13}C NMR spectroscopic analysis was carried out using a Bruker DPC 400MHz NMR, and spectra were collected in $CDCl_3$, MeOD, and acetone-d, and analysed using MestreNova NMR software. Chemical shifts are reported as ppm (δ) and referenced to the solvents' signals ($CDCl_3$ 7.26 ppm; MeOD 3.66 and 3.43 ppm; acetone-d 1.80 ppm). Splitting patterns are designated as s, singlet; d, doublet; t, triplet; m, multiplet. Coupling constants (*J*) are reported in Hz. All NMR solvents were purchased from Merk or Fluorochem.

Infrared Spectroscopy
IR spectra were obtained using a Perkin Elmer spectrum 100 FTIR instrument with a 2.5mm compression tip. Data was collected using the Perkin Elmer Spectrum 10 software package. Functional group absorbance peaks are reported in cm^{-1} and characterised as Asymm, Bend, Rock, Stretch, Symm, and Wing. Peak shapes are designated as Strong, S: Medium, M; Weak, W; Broad, B: Narrow, N; Variable, V.

Mass Spectrometry
Electrospray Ionization Fourier Transform Mass Spectrometry (FTMS+p ESI) were obtained by either LCMS or direct infusion on a Thermofisher Scientific Orbitrap XL mass spectrometer in ESI+ mode. The scan range is full scan (mass 80.00-2000.00).

High performance liquid chromatography
HILIC mode HPLC was performed on an Agilent 1100 series HPLC system linked to an Agilent G1321A FLD detector and an G1314A variable wavelength detector. Amide HILIC allowed the separation of labelled sugars on a TSKgel Amide-80 HR column (250 x 4.6 mm, 5 µM particle size) filled with a TSKgel Amide-80 guard column (15 x 3.2 mm, 5 µM particle size). Solvent A was composed of ammonium formate buffer (50 mMol pH 4.4), while solvent B consisted of ACN. The flow rate was set at 0.8 mL/ min, and the column was maintained at 40^{o}C for the duration of the run.
Separation of samples took place over 35 minutes with a linear gradient beginning with 65% phase B at 1 minute, with a further gradient to 50% in 10 minutes, to 45% in 5 minutes, to 10% in 3 minutes, maintaining 10% for 2 minutes before returning to injection condition of 65% B between 34-35 minutes. The column was conditioned with 65% B, 5 minutes before the next injection. The injection volume was 2 µL per injection. The fluorescence detection used the excitation wavelength 240 nm and emission wavelength 420 nm. The Fluorescence absorptivity detection was reported as luminescence unit (LU) represent to the Agilent system.

2.5.3 Solvents and Buffer

2 M Ammonium formate buffer stock solution pH 4.4
Formic acid (184.12 g, 4 mol) was combined with water (1 L) and cooled to 0°C in an ice bath. 25% Ammonium solution (200 mL) was then added in 50 mL increments. The pH was adjusted to 4.4 by the 25% ammonium solution. The stock solution was then diluted to 2 L to a final concentration 50 mM and used as a HILIC phase modifier.

Click buffer
The click buffer was prepared according to Table 2.3 [81].

Table 2.3 Click buffer for a total of 1 mL

Reagent	Stock	Volume (µL)	pipetting sequence
Tris/HCl pH8.5	1 M	50	1
18Ω H2O	-	728	2
Glycerol	50% v/v	200	3
Sodium ascorbate	1 M	10	4
$CuSO_4.5H_2O$	1 M	2	5
TBTA in DMSO	100 mM	2	6 Mix TBTA and 1-BuOH first, then add into the final solution
1-BuOH	-	8	
Total volume		1000	

Labelling agent stock solution
Compound **5** was weighed and diluted in MeOH to a final concentration of 1 mM.

Labelling buffer solution
Boric acid (3 g, 0.04 mol) and sodium acetate trihydrate (6 g, 0.045 mol) were dissolved in MeOH (100 mL).

Sodium cyanoborohydride solution
Sodium cyanoborohydride solution was prepared at 0.42 mM in the labelling buffer solution.

2.5.4 Synthesis of 4(*tert*-Butoxycarbonylamino)benzoic acid (2) [81]

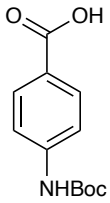

4-Aminobenzoic acid (**1**) (200 mg, 1.5 mmol) was dissolved in water (1.6 mL), and dioxane (3.2 mL), to this triethylamine (0.26 mL) and di-*tert*-butyl dicarbonate (426 mg) were added, and the solution was stirred at room temperature for 24 hours. The solution was removed under reduced pressure to leave a thick, colourless oil. 3 M HCl (6 mL) was added and stirred until a white precipitate had formed. The precipitate was collected via filtration and washed with water (3 x 5 mL) followed by petroleum ether (3 x 5 mL). The white solid was collected and dried to afford pure Boc-4-aminobenzoic acid (**2**) (166 mg, 0.7 mmol, 47%).

^{1}H NMR (400 MHz, Acetone, TMS**)** δ 8.79 **(**s, 1H, HN**)**, 7.98 **(**d, *J* **=** 8.8 Hz, 2H, 2xAr H**)**, 7.69 **(**d, *J* **=** 8.8 Hz, 2H, 2xAr H**)**, 1.51 **(**s, 9H, Boc**)**, **^{13}C NMR** (101 MHz, Acetone) δ 166.46 (-C=OOH), 152.57 (NCO), 144.13 (CH Ar), 130.67 (CH Ar), 117.18 (CH Ar), 79.77 ($3CH_3$-**C**-O), 27.55 ($3CH_3$), **IR** V_{max}/cm^{-1} 3411.06, M (C-H, Ar stretch), 3321.32 VB (O-H stretch), 1691.91 S (C=O stretch),

1525.00 M (C-C, Ar stretch) 1058.50 S (C-O, Stretch) 763.91 SB (N-H), **FTMS** ESI+p $C_{12}H_{15}NO_4$ expected [M+Na] 260.0893 found: 260.0895 [M+Na].

2.5.5 Synthesis of 2,5-Dioxopyrrolidin-1-yl 4-(*tert*-Butoxycarbonylamino)benzoate (3) [81]

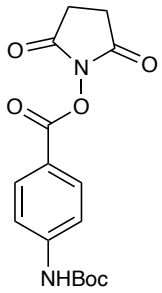

Compound **2** (2.37 g, 10 mmol) and *N*-hydroxysuccinimide (1.15 g, 10 mmol) were added to THF (50 mL). A solution of *N*,*N*'-Dicyclohexylcarbodiimide (DCC) (2.06 g, 10 mmol) in THF (10 mL) was added. The solution was stirred at room temperature for 20 hours. After 20 hours, the solution was filtered to remove 1,3-Dicyclohexyl urea. The solvents were removed under reduced pressure, and the white solid was purified *via* flash chromatography (EtOAc: petroleum ether, 1:1). Compound **3** was isolated as a white solid (1.92 g, 5.74 mmol, 57%).

^{1}H NMR (400 MHz, Acetone, TMS**)** δ 9.00 **(**s, 1H, HN**)**, 8.07 **(**d, *J* = 8.8 Hz, 2H, 2xAr H**)**, 7.79 **(**d, *J* = 8.6 Hz, 2H, 2xAr H**)**, 2.96 **(**s, 4H 2x CH_3**)**, 1.52 **(**s, 9H, Boc**)**, **^{13}C NMR** (101 MHz, Acetone) δ 169.81 (2 ONC=O), 166.40 (Ar-COO), 152.41 (C=O), 146.15 (CH Ar), 131.42 (CH Ar), 118.29 (CH Ar), 80.25 ($3CH_3$-**C**-O), 27.50 ($3CH_3$), 25.47 (2 CH_2), **IR** V_{max}/cm^{-1} 3247.14 M (C-H, Ar stretch), 1676.94 S (C=O, Stretch), 1504.54 M (C-C, Ar stretch), 1211.98 S (C-O, Stretch), **FTMS** ESI+p $C_{16}H_{18}N_2O_6$ expected [M+Na] 357.1057 found: 357.1058 [M+Na].

2.5.6 Synthesis of 4-(*tert*-Butoxycarbonylamino)benzoate (4) [81]

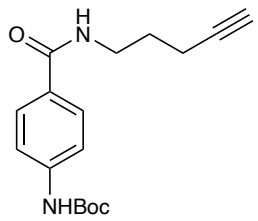

Compound **3** (100 mg, 0.3 mmol) was dissolved in dry DCM (7.5 mL), followed by the addition of 4-pentyn-1-amine hydrochloride (54 mg, 0.66 mmol) and triethylamine (300 µL). The solution was stirred at room temperature overnight. The reaction mixture was concentrated and purified by flash column chromatography (petroleum ether: EtOAc, 1:1) to obtain the compound **4** as a white solid (73 mg, 0.26 mmol, 87% yield).

^{1}H NMR (400 MHz, $CDCl_3$**)** δ 7.64 **(**d, *J* = 8.6 Hz, 2H, 2xAr H**)**, 7.36 **(**d, *J* = 8.6 Hz, 2H, Ar 2xCH**)**, 6.57 **(**s, 1H, NH**)**, 3.51 **(**q, *J* = 6.5 Hz, 2H CH_2**)**, 2.25 **(**td, *J* = 6.8, 2.6 Hz, 1H, C*H*$_2$C≡CH**)**, 1.95 **(**t, *J* = 2.6, 5.0 Hz, 1H, ≡C*H***)**, 1.79 **(**d, *J* = 6.8 Hz, 2H, CH_2**)**, 1.46 **(**s, 9H, Boc**). ^{13}C NMR** (101 MHz, $CDCl_3$) δ 166.93 (C=O), 152.27 (C-NH_2 Ar), 128.74 (**C**H-C=O Ar), 127.99 (CH Ar), 117.70 (2CH Ar), 83.74 (CH_2-**C**≡CH**)**, 81.14 ($3CH_3$-**C**-O), 69.33 (C≡**C**H**)**, 39.33 ($NHCH_2$), 28.25 ($3xCH_3$), 28.05 (**C**H_2C≡CH**)**, 16.34 (CH_2**C**H_2CH_2), **IR** V_{max}/cm^{-1} 3304 M (N-H, stretch), 3287 M (C-H, Ar stretch), 1702 S (C=O, Stretch), 1629 M (N-H, Ar bend), 1507 M (C-C, Ar stretch), 1235 V (C-N, stretch), 1148 S (C=O, stretch), **FTMS** ESI+p $C_{17}H_{22}N_2O_3$ expected [M+H] 303.1703 found: 303.1703 [M+H].

2.5.7 Synthesis of 4-amino-*N*-(pent-4-yn-1-yl)benzamide (5) [81]

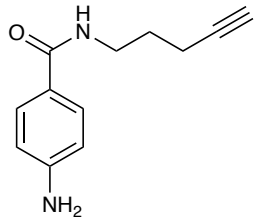

Compound **4** (250 mg, 0.83 mmol) was dissolved in a mixture of TFA and DCM 1:6 v/v (2 mL) and left stirring at room temperature for 1.5h. DCM was removed, and 15 mL of MeOH was added. The reaction mixture was quenched with Amberlite® IRA-67 (Sigma Aldrich), filtered and concentrated, followed by purification by flash column chromatography (DCM:CH_3OH, 9:1). The title compound was obtained as a white solid **5** (124 mg, 0.61 mmol, 73% yield).

^{1}H NMR (400 MHz, MeOD, TMS**)** δ 7.49 **(**d, *J* = 8.5 Hz, 2H, 2xAr H**)**, 6.56 **(**d, *J* = 8.5, Hz, 2H, 2xAr H**)**, 3.32 **(**t, *J* = 7.0 Hz, 2H CH_2**)**, 3.21 **(**s, 2H, CH_2**)**, 2.15 **(**t, *J*=6.0 Hz, 1H, ≡C*H***)**, 1.95 **(**t, *J* = 2.6, 2H, ≡C*H***)**, **^{13}C NMR** (101 MHz, $CDCl_3$) δ 167.35 (C=O), 149.54 (C-NH_2 Ar), 128.62 (CH Ar), 124.14 (CH-**C**=O Ar), 114.15 (2xCH Ar), 83.80 (C**≡C**-H), 69.20 (**C≡**CH**)**, 39.12 ($NHCH_2$), 28.19 (CH_2**C**H_2C**≡C)**, 16.27 (CH_2**C**H_2CH_2), **IR** V_{max}/cm^{-1} 3320.67 M (N-H, stretch), 3295.0 NS (C-H, stretch), 2929.10 M (C-H, Ar stretch), 1677.94 S (C=O, Stretch), 1544.69 M (C-C, Ar stretch), 1182.22 V (C-N, stretch), 1149.48 V (C-N stretch), 836.96 SB (N-H), **FTMS** ESI+p $C_{12}H_{14}N_2O$ expected [M+H] 203.1179 found: 203.1178 [M+H]. The retention time is 3.5 minutes.

2.5.8 Synthesis of azido-serine (8) [82]

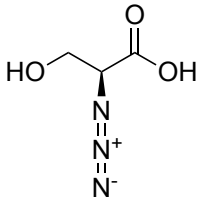

Imidazole-1-sulfonyl azide hydrochloride (125 mg,0.6 mol, 1.2 equiv.) and L-serine (50 mg,0.5 mol, 1 equiv.) were added to a solution of K_2CO_3 (199 mg, 1.4 mol, 3 equiv.) and $CuSO_4.5H_2O$ (60 mg., 0.2 mol, 0.5 equiv.) in MeOH/ H_2O (15 mL /4 mL). The mixture was stirred at room temperature for 10 days. Upon completion of the reaction (as monitored by TLC, 1-butanol:acetic acid:water (12:3:5)), the mixture was concentrated under reduced pressure. The residue was washed with water (20 mL) and extracted with EtOAc (3 × 10 mL). The combined organic layers were dried over magnesium sulphate ($MgSO_4$), the solvents were removed under reduced pressure, and the residue was purified *via* flash chromatography (1-butanol:acetic acid:water, 12:3:5). The compound **8** was isolated as a pale-yellow oil (42 mg, 0.32 mmol, 53% yield).

^{1}H NMR (400 MHz, MeOD, TMS**)** δ 4.99 **(**s, 1H alcohol**)**, 3.90 **(**s, 2H, β-carbon H**)**, 3.78 **(**s, 1H α-carbon H**)**, 3.33-3.08 **(**m, 1H α-carbon H**)**, **^{13}C NMR** (101 MHz, MeOD) δ 178.47 (O=C-OH), 78.00 (C-OH), 62.27 (C-N), **IR** V_{max}/cm^{-1} 2923.06 S (O-H, stretch), 2897.0 M (C=O carboxylic acid, stretch), 2165.0 M (N=N=N azide, stretch), 1558.72 M (C-H, bend), 1408.90 M (C-H, bend), 1153.75 N (O-H, stretch), 1049.12 SV (C-O, stretch), 1027.0 V (C-N, stretch)

2.5.9 Synthesis of tris((1-benzyl-1H-1,2,3-triazol-4-yl)methyl)amine. (TBTA) (12) [81]

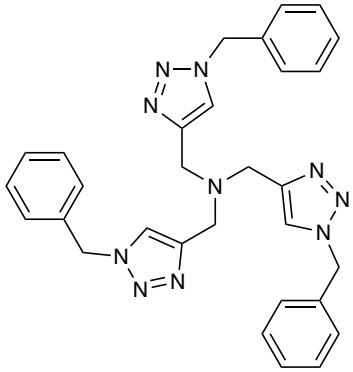

Sodium azide (2.66 g, 40.9 mmol) was suspended in dry DMF (5.0 mL), and benzyl bromide (3.25 mL, 27.3 mMol) was added. The suspension was stirred at room temperature for 48 hours. The reaction mixture was poured into water (50 mL) and extracted with diethyl ether (4x25 mL). The combined organic layer was washed with brine (20 mL), dried over $MgSO_4$ and concentrated under reduced pressure to an approximate volume of 7-8 mL. Tripropargyl amine (0.53 g, 4.1 mmol) was added to a solution of benzyl azide in diethyl ether (5.0 mL, 18.3 mmol, as prepared above). 2,6-Lutidine (0.47 mL, 4.1 mmol) in dry ACN (6.0 mL) was added to the stirred mixture, followed by copper (I) iodide (16 mg, 0.08 mmol). The reaction mixture was stirred at room temperature for 24 hours. The solidified mixture was then filtered, washed with cold acetonitrile (25 mL), and dried under vacuum to afford **12** as a white powder (13.23 g, 24.95 mmol, 61% yield).

^{1}H NMR (400 MHz, MeOD, TMS**)** δ 7**.**62 **(**s, 3H, CH**(**Ar**))**, 7**.**25 **(**t, *J*=8**.**6 Hz, 3H, Ph**)**, 7**.**18 **(**dd, *J* **=** 6**.**9, 4**.**9 Hz, 12H, Ph**)**, 5**.**42 **(**s, 6H, NCH_2Ph**)**, 3**.**65 **(**s, 6H, N-CH_2-triazole**)**, **^{13}C NMR** (101 MHz, $CDCl_3$) δ 144.07 (3x CH_2-**C** Ar), 134.74 (C=**C**-N), 129.09 (6xCH Ar), 128.69 (6xCH Ar), 128.02 (3xCH Ar), 124.00 (3xCH=CH-N), 54.18 (3xC-N), **IR** V_{max}/cm^{-1} 3060 M (C-H, stretch), 2930 M (C-H, stretch), 2824 M (C-H, stretch), 1496 M (C=C, stretch), 1455 M (C-C, Ar stretch). **FTMS** ESI+p $C_{30}H_{30}N_{10}$ expected [M+H] 531.2728 found: 531.2715 [M+H].

2.5.10 Synthesis of Boc-L-serine (18)

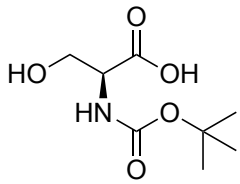

L-Serine (2.1 g, 20 mmol, 1 eq.) was added to aqueous sodium hydroxide (15 mL, 1 M). Di-*tert*-butyl dicarbonate (4.80 g, 22 mmol, 1.2 eq.) was added in 10 mL of cold dioxane (4-5^{o}C). The mixture was stirred at 5^{o}C for 30 min, then warmed to room temperature for 30 min, and stirred at room temperature for 6 h. Upon completion of the reaction (as monitored by TLC, 1-butanol:acetic acid:water, 12:3:5), the mixture was concentrated under reduced pressure, and the residue was washed with diethyl ether (2x 30 mL). The aqueous layer was acidified to pH 2-3 by slowly adding concentrated sulphuric acid (H_2SO_4). The aqueous solution was extracted with EtOAc (3x50 mL). The combined organic layers were washed with brine (1x30 mL), dried over $MgSO_4$, and filtered. The solvents were removed under reduced pressure to give Boc-L-serine (2.2 g, 10.72 mmol, 54% yield) as a colourless, sticky foam used without further purification.

^{1}H NMR (400 MHz, $CDCl_3$, TMS) δ 3.83 (d, *J*=11.6 Hz 1H, α-carbon), 4.40-3.50 (m, 2H, β-carbon), 1.45 (s, 9H, methyl-Boc), **^{13}C NMR** (101 MHz, $CDCl_3$) δ 172.92 (C=O, carboxylic acid), 155.21 (C=O, Boc), 79.48 (C, Boc), 61.94 (CH, α-carbon), 59.49 (C, β-carbon), 27.27 (CH_3, Boc).

2.5.11 Synthesis of Boc-L-serine methyl ester (19)

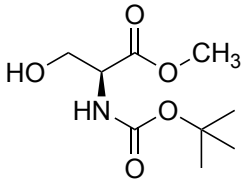

Compound **18** (2.05g, 10 mmol, 1 eq.) was added to cold DMF (4-5°C, 15 mL). K_2SO_4 (1.65 g, 12 mmol, 1.2 eq.) was added and stirred for 10 min in an ice bath. Methyl iodide (1.35 mL, 3.12 g, 22 mmol, 1eq.) was added. The mixture was stirred at 5°C for 30 min, then allowed to come to room temperature for 30 min and stirred at room temperature for 6 h. Upon completion of the reaction, water (30 mL) was added to the mixture reaction and filtered. The solution was extracted with EtOAc (1x30 mL). The organic layers were washed with brine (2x30 mL), dried over the $MgSO_4$ and filtered. Solvents were removed under reduced pressure, and the residue was purified *via* flash chromatography (petroleum ether:EtOAc 7:3). Boc-L-serine methyl ester was isolated as a pale amber oil (1.7 g, 7.75 mmol, 78% yield).

^{1}H NMR (400 MHz, $CDCl_3$, TMS) δ 5.60 (d, *J*=6.0 H, 1H, amine), 4.38 (s, 1H, hydroxyl), 3.87 (dt, *J*=10.0, 5.3 Hz, 1H, α-carbon), 4.00-3.92 (m, 2H, β -carbon), 3.78 (s, 3H, O-methyl), 1.45 (s, 9H, Boc), **^{13}C NMR** (101 MHz, $CDCl_3$) δ 171.41 (C=O, carboxylic acid), 155.82 (C=O, Boc), 63.34 (α-carbon), 55.76 (β-carbon), 52.59 (O-methyl), 28.30 (CH_3, Boc), **IR** V_{max}/cm^{-1} 3336 B (O-H, stretch), 2955 M (NH, stretch), 1684 S (O=C-OCH_3, stretch), **FTMS** ESI+p $C_9H_{17}NO_5$ expected [M+Na] 242.0999 found: 242.0997 [M+Na].

2.5.12 Synthesis of (*2R,3R,5R,6R*)-2-(acetoxymethyl)-6-(2-((tert-butoxycarbonyl)amino)-3-methoxy-3-oxopropoxy)tetrahydro-2H-pyran-3,4,5-triyl triacetate (21)

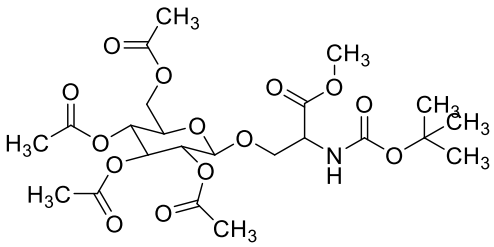

Compound **19** (0.3288 g, 1.5 mmol, 15 eq.) was added to dry toluene (30 mL) under nitrogen. Tetra-*O*-acetyl-α-D-glucopyronosyl bromide (0.0411g, 0.1 mmol, 1 eq.) and silver carbonate (0.0358 g, 0.13 mmol, 1.3 eq.) were added. The mixture was stirred at -25°C for 6 h. Upon completion of the reaction, EtOAc (30 mL) was added, and the suspension was filtered, and dried over $MgSO_4$, the solvents were removed under reduced pressure, and the residue was purified via flash chromatography (petroleum ether:EtOAc 1:1). Compound **21** was isolated as a colourless oil (0.5025 g, 0.91 mmol, 61% yield).

^{1}H NMR (400 MHz, $CDCl_3$, TMS) δ 5.60-5.44 (m, 2H, C1 and C3-carbohydrate), 5.27 (t, *J* = 9.6 Hz, 1H, C2-carbohydrate), 5.09 (t, *J* = 9.7 Hz, 1H, C4-carbohydrate), 4.96-4.83 (m, 1H, C5-carbohydrate), 4.25 (dd, *J* = 16.3, 6.8 Hz, 1H α-carbon), 4.14 (t, *J*=9.3 Hz, 2H, C6-carbohydrate), 3.78 (d, *J*=11.3 Hz, 3H, O-methyl), 3.54-3.43 (m, 2H, β-carbon), 2.18 – 1.93 (m, 12H, CH_3-C=O, carbohydrate), 1.56 (s, 9H, Boc), **^{13}C NMR** (101 MHz, $CDCl_3$) δ 171.22 (C=O, serine), 170.73

(C=O, sugar), 69.79 (CH, C3), 68.41 (CH, C2), 67.30 (CH, C4), 63.68 (CH, C5), 61.91 (CH_2, C6), 55.62 (CH_2, α-carbon), 52.70 (CH_3, O-acetyl), 28.29 (CH_3, Boc), 20.60 (CH_3, acetyl of sugar), **FTMS** ESI+p $C_{23}H_{35}NO_{14}$: 572.1950 [$M+Na^+$], found 572.1948 [$M+Na^+$].

2.5.16 General procedure for click reaction between azide (8 or 24) and 5.

Compound **5** (200 µL of a 1 mM in MeOH) was added to azide **8** or **24** (200 µL of a 1.0 mM in MeOH) in the 1.5 mL tube. Click buffer (600 µL) was added to the reaction tube. The mixture was incubated at 37°C for 24 hours. The click product from **8** was detected at the completion of the reaction by TLC for optimisation of the reaction time. The click product from **24** was transferred for enrichment with Amide SPE before HPLC analysis. The spe-ed2 Amide SPE column was pre equilibrated with MeOH (2 ml). The sample was loaded and allowed to drip through under gravity. The sample was then washed with 99% ACN (aq) (5 x 1 ml) followed by 97% ACN (aq) (5 x 1 ml). The purified sample was then eluted with HPLC water (800 µl). The eluted solution from the enrichment method was dried and kept at -20°C until redissolved with 0.5 mL of HPLC water for HPLC analysis. The retention time of **25** is 5.3 minutes.

2.5.17 General labelling procedure between Lactose and 5.

Lactose solution (1 mM in MeOH), 100 µL, was applied to a 1.5 mL tube and mixed with the 100 µL of labelling buffer and 15 µL of sodium cyanoborohydride (15 µL). Compound **5** solution (1 mM in MeOH) was added (100 µL). The reaction mixture was then vortexed for 10 seconds before being heated at 65°C for 180 minutes. The reaction solution was quenched with the addition of ACN (950 µL), producing a white precipitate. The quenched solution was transferred for enrichment with Amide SPE. The spe-ed2 Amide SPE column was pre equilibrated with MeOH (2 ml). The sample was loaded and allowed to drip through under gravity. The sample was then washed with 99% ACN (aq) (5x1 ml) followed by 97% ACN (aq) (5x1 ml). The purified sample was then eluted with HPLC water (800 µL). The eluted solution from the enrichment method was dried and kept at -20°C until redissolved with 0.5 mL of HPLC water for HPLC analysis. The retention time of **16** is 6.5 minutes.

2.6 References

1. Kolb, H.C., M.G. Finn, and K.B. Sharpless, *Click Chemistry: Diverse Chemical Function from a Few Good Reactions.* Angewandte Chemie International Edition, 2001. **40**(11): p. 2004-2021.
2. Liang, L. and D. Astruc, *The copper(I)-catalyzed alkyne-azide cycloaddition (CuAAC) "click" reaction and its applications. An overview.* Coordination Chemistry Reviews, 2011. **255**(23): p. 2933-2945.
3. Kalra, P., et al., *Metals as "Click" catalysts for alkyne-azide cycloaddition reactions: An overview.* Journal of organometallic chemistry, 2021. **944**: p. 121846.
4. Yang, G., et al., *Water-soluble Cu30 nanoclusters as a click chemistry catalyst for living cell labeling via azide-alkyne cycloaddition.* Nano Research, 2023. **16**(1): p. 1748-1754.
5. Liu, H., et al., *Tug-of-war: molecular dynamometers against living cells for analyzing sub-piconewton interaction of a specific protein with the cell membrane.* Chemical science (Cambridge), 2021. **12**(43): p. 14389-14395.
6. Yang, Y., et al., *O -GlcNAcylation mapping of single living cells by in situ quantitative SERS imaging.* Chemical science (Cambridge), 2022. **13**(33): p. 9701-9705.
7. You, Y., et al., *DNA-based platform for efficient and precisely targeted bioorthogonal catalysis in living systems.* Nature communications, 2022. **13**(1): p. 1459-1459.
8. Saha, S., et al., *Comparative Study of Nitro- and Azide-Functionalized ZnII-Based Coordination Polymers (CPs) as Fluorescent Turn-On Probes for Rapid and Selective Detection of H2S in Living Cells.* Chemistry – A European Journal, 2022. **28**(9): p. e202103830.
9. Liu, K., et al., *CLICK-17, a DNA enzyme that harnesses ultra-low concentrations of either Cu+ or Cu2+ to catalyze the azide-alkyne 'click' reaction in water.* Nucleic acids research, 2020. **48**(13): p. 7356-7370.
10. Hoffmann, P., et al., *A mesoporous metal–organic framework used to sustainably release copper(ii) into reducing aqueous media to promote the CuAAC click reaction.* RSC advances, 2022. **12**(41): p. 26825-26833.
11. Xia, X., et al., *Probe and dye design through copper-mediated reactions of N-arylhydroxylamines.* Organic & biomolecular chemistry, 2022. **20**(46): p. 9234-9240.
12. Garlatti, L., R. Huet, and K. Alvarez, *Efficient access to 3'-deoxy-3'-(4-substituted-1,2,3-triazol-1-yl)-thymidine derivatives via ligand-promoted CuAAC.* Tetrahedron, 2021. **92**: p. 132252.
13. Besanceney-Webler, C., et al., *Increasing the Efficacy of Bioorthogonal Click Reactions for Bioconjugation: A Comparative Study.* Angewandte Chemie International Edition, 2011. **50**(35): p. 8051-8056.
14. Chen, M., et al., *Antifouling peptides combined with recognizing DNA probes for ultralow fouling electrochemical detection of cancer biomarkers in human bodily fluids.* Biosensors & bioelectronics, 2022. **206**: p. 114162-114162.
15. Wang, Z., et al., *Cu(I)-Catalyzed Click Reaction-Triggered 3D DNA Walker for Constructing an "OFF–ON" Fluorescent Biosensor for Cu2+ Detection.* ACS applied bio materials, 2021. **4**(4): p. 3571-3578.
16. Zhang, A., et al., *DNA Strand Displacement with Base Pair Stabilizers: Purine-2,6-Diamine and 8-Aza-7-Bromo-7-Deazapurine-2,6-Diamine Oligonucleotides Invade Canonical DNA and New Fluorescent Pyrene Click Sensors Monitor the Reaction.* Chemistry : a European journal, 2022. **28**(72): p. e202202412
17. Saha, P., D. Panda, and J. Dash, *Nucleic acids as templates and catalysts in chemical reactions: target-guided dynamic combinatorial chemistry and click chemistry and DNA/RNA induced enantioselective reactions.* Chemical Society reviews, 2023. **52**(13): p. 4248-4291.

18. Hu, J., et al., *Construction of an enzyme-free biosensor utilizing CuO nanoparticles enriched in DNA polymer to catalyze a click chemistry reaction for SERS detection of the p53 gene.* Analytica chimica acta, 2022. **1222**: p. 339958-339958.
19. Spampinato, A., et al., *trans-Cyclooctene- and Bicyclononyne-Linked Nucleotides for Click Modification of DNA with Fluorogenic Tetrazines and Live Cell Metabolic Labeling and Imaging.* Bioconjugate chemistry, 2023. **34**(4): p. 772-780.
20. Rezaei, H., M. Hosseini, and S. Radfar, *A dual-signaling electrochemical ratiometric strategy combining "signal-off" and "signal-on" approaches for detection of MicroRNAs.* Analytical biochemistry, 2021. **632**: p. 114356-114356.
21. Hu, L., Y. Takezawa, and M. Shionoya, *Cu-II-mediated DNA base pairing of a triazole-4-carboxylate nucleoside prepared by click chemistry.* Chemical Communications (Cambridge, England), 2023. **59**(7): p. 892-895.
22. Wang, J.J., et al., *Prostate cancer extracellular vesicle digital scoring assay – a rapid noninvasive approach for quantification of disease-relevant mRNAs.* Nano today, 2023. **48**: p. 101746.
23. Zhang, X., et al., *Flexible Metal–Organic Framework-Based Mixed-Matrix Membranes: A New Platform for H2S Sensors.* Small, 2018. **14**(37): p. 1801563.
24. Smith, M.K. and K.A. Mirica, *Self-Organized Frameworks on Textiles (SOFT): Conductive Fabrics for Simultaneous Sensing, Capture, and Filtration of Gases.* Journal of the American Chemical Society, 2017. **139**(46): p. 16759-16767.
25. Cui, J., et al., *Pd Uptake and H2S Sensing by an Amphoteric Metal–Organic Framework with a Soft Core and Rigid Side Arms.* Angewandte Chemie International Edition, 2014. **53**(52): p. 14438-14442.
26. Lawrence, N.S., et al., *The Electrochemical Analog of the Methylene Blue Reaction: A Novel Amperometric Approach to the Detection of Hydrogen Sulfide.* Electroanalysis, 2000. **12**(18): p. 1453-1460.
27. Pose, M., et al., *Fluorescent detection of hydrogen sulfide (H(2)S) through the formation of pyrene excimers enhances H(2)S quantification in biochemical systems.* J Biol Chem, 2022. **298**(10): p. 102402.
28. Zhang, R., et al., *Switchable Nanochannel Biosensor for H2S Detection Based on an Azide Reduction Reaction Controlled BSA Aggregation.* Analytical Chemistry, 2019. **91**(9): p. 6149-6154.
29. Biswas, B., et al., *Triggered emission for rapid detection of hydrogen sulfide chaperoned by large Stokes shift.* Journal of Photochemistry and Photobiology A: Chemistry, 2019. **371**: p. 264-270.
30. Chen, M., et al., *Click reaction-assisted construction of antifouling immunosensors for electrochemical detection of cancer biomarkers in human serum.* Sensors and actuators. B, Chemical, 2022. **363**: p. 131810.
31. Liu, X., et al., *Cancer cell-targeted cisplatin prodrug delivery in vivo via metabolic labeling and bioorthogonal click reaction.* Biomaterials science, 2021. **9**(4): p. 1301-1312.
32. Wu, K., et al., *Click activated protodrugs against cancer increase the therapeutic potential of chemotherapy through local capture and activation.* Chemical science (Cambridge), 2021. **12**(4): p. 1259-1271.
33. d'Orchymont, F. and J.P. Holland, *Asymmetric rotaxanes as dual-modality supramolecular imaging agents for targeting cancer biomarkers.* Communications chemistry, 2023. **6**(1): p. 107-107.
34. Hu, D., et al., *Development of nanosensor by bioorthogonal reaction for multi-detection of the biomarkers of hepatocellular carcinoma.* Sensors and actuators. B, Chemical, 2021. **334**: p. 129653.

35. Parle, D.R., et al., *Metabolic Glycan Labeling of Cancer Cells Using Variably Acetylated Monosaccharides.* Bioconjugate chemistry, 2022. **33**(8): p. 1467-1473.
36. Hironaka, K., et al., *Conjugation of antibody with temperature-responsive polymer via in situ click reaction to enable biomarker enrichment for increased diagnostic sensitivity.* Biomaterials science, 2021. **9**(14): p. 4870-4879.
37. Tran, V.V., et al., *Development strategies of conducting polymer-based electrochemical biosensors for virus biomarkers: Potential for rapid COVID-19 detection.* Biosensors & bioelectronics, 2021. **182**: p. 113192-113192.
38. Xiong, Y., et al., *Target Enzyme-Triggered Click Chemistry and Hybridization Chain Reaction for Fluorescence Nonculture Homogeneous Analysis of E. coli in Bloodstream Infections.* ACS applied materials & interfaces, 2023. **15**(23): p. 27687-27695.
39. Goncin, U., et al., *Rapid Copper-free Click Conjugation to Lipid-Shelled Microbubbles for Ultrasound Molecular Imaging of Murine Bowel Inflammation.* Bioconjugate chemistry, 2022. **33**(5): p. 848-857.
40. Yang, Y., et al., *O-GlcNAcylation mapping of single living cells by in situ quantitative SERS imaging.* Chemical science (Cambridge), 2022. **13**(33): p. 9701-9705.
41. Smirnov, I., et al., *A Strategy for Tumor Targeting by Higher-Order Glycan Pattern Recognition: Synthesis and In Vitro and In Vivo Properties of Glycoalbumins Conjugated with Four Different N-Glycan Molecules.* Small (Weinheim an der Bergstrasse, Germany), 2020. **16**(46): p. e2004831.
42. Fan, X.-M., et al., *Metabolic integration of azide functionalized glycan on Escherichia coli cell surface for specific covalent immobilization onto magnetic nanoparticles with click chemistry.* Bioresource technology, 2021. **324**: p. 124689.
43. Zhang, X., et al., *Site-Specific Chemoenzymatic Conjugation of High-Affinity M6P Glycan Ligands to Antibodies for Targeted Protein Degradation.* ACS chemical biology, 2022. **17**(11): p. 3013-3023.
44. Suttapitugsakul, S., et al., *Surface Glycoproteomic Analysis Reveals That Both Unique and Differential Expression of Surface Glycoproteins Determine the Cell Type.* Analytical chemistry (Washington), 2019. **91**(10): p. 6934-6942.
45. Jaiswal, M., et al., *A metabolically engineered spin-labeling approach for studying glycans on cells.* Chemical science (Cambridge), 2020. **11**(46): p. 12522-12532.
46. Agrawal, A., et al., *Click-Chemistry-Based Free Azide versus Azido Sugar Detection Enables Rapid In Vivo Screening of Glycosynthase Activity.* ACS chemical biology, 2021. **16**(11): p. 2490-2501.
47. Sapozhnikova, K.A., et al., *Detection of the PRAME Protein on the Surface of Melanoma Cells Using a Fluorescently Labeled Monoclonal Antibody.* Russian journal of bioorganic chemistry, 2021. **47**(5): p. 1077-1085.
48. Qian, H., et al., *Dual-aptamer-engineered M1 macrophage with enhanced specific targeting and checkpoint blocking for solid-tumor immunotherapy.* Molecular therapy, 2022. **30**(8): p. 2817-2827.
49. Smirnov, I., et al., *Importance of local glycan heterogeneity for in vivo cancer targeting.* Tetrahedron letters, 2021. **72**: p. 153089.
50. Norman, J., S. Tommasone, and P.M. Mendes, *Selective oligosaccharide recognition with phenylboronic acid through Cu(I)-catalysed click imprinted surfaces.* Materials today chemistry, 2022. **24**: p. 100939.
51. Liu, F., et al., *Azido Groups Hamper Glycan Acceptance by Carbohydrate Processing Enzymes.* ACS central science, 2022. **8**(5): p. 656-662.
52. Lam, Y.Y., et al., *Systematic Investigation of Metabolic Oligosaccharide Engineering Efficiency in Intestinal Cells Using a Dibenzocyclooctyne-Monosaccharide Conjugate.* Chembiochem : a European journal of chemical biology, 2023. **24**(12): p. e202300144

53. Hoang, H.T., et al., *Dual cross-linked chitosan/alginate hydrogels prepared by Nb-Tz 'click' reaction for pH responsive drug delivery.* Carbohydrate polymers, 2022. **288**: p. 119389-119389.
54. Tao, Y., et al., *Modular synthesis of amphiphilic chitosan derivatives based on copper-free click reaction for drug delivery.* International journal of pharmaceutics, 2021. **605**: p. 120798-120798.
55. Niu, Y. and Y. Lu, *Construction of pH-responsive core crosslinked micelles via thiol-yne click reaction.* Journal of applied polymer science, 2022. **139**(32): p. e52753
56. Joo, S.-B., et al., *Fast Absorbent and Highly Bioorthogonal Hydrogels Developed by IEDDA Click Reaction for Drug Delivery Application.* Materials, 2022. **15**(20): p. 7128.
57. Vu, T.T., et al., *Injectable and biocompatible alginate-derived porous hydrogels cross-linked by IEDDA click chemistry for reduction-responsive drug release application.* Carbohydrate polymers, 2022. **278**: p. 118964-118964.
58. Liu, P., P. Huang, and E.-T. Kang, *pH-Sensitive Dextran-Based Micelles from Copper-Free Click Reaction for Antitumor Drug Delivery.* Langmuir, 2021. **37**(44): p. 12990-12999.
59. Zhang, N., et al., *Construction of hyperbranched and pH-responsive polymeric nanocarriers by yne-phenol click-reaction for tumor synergistic chemotherapy.* Colloids and surfaces, B, Biointerfaces, 2021. **204**: p. 111790-111790.
60. Zhu, J.Q., et al., *Responsive Hydrogels Based on Triggered Click Reactions for Liver Cancer.* Advanced materials (Weinheim), 2022. **34**(38): p. e2201651
61. Hoang, H.T., et al., *Dual pH-/thermo-responsive chitosan-based hydrogels prepared using "click" chemistry for colon-targeted drug delivery applications.* Carbohydrate polymers, 2021. **260**: p. 117812.
62. Bo, Y., et al., *Leveraging intracellular ALDH1A1 activity for selective cancer stem-like cell labeling and targeted treatment via in vivo click reaction.* Proceedings of the National Academy of Sciences - PNAS, 2023. **120**(36): p. e2302342120-e2302342120.
63. Gao, Z., et al., *Bacteria-Mediated Intracellular Click Reaction for Drug Enrichment and Selective Apoptosis of Drug-Resistant Tumor Cells.* ACS applied materials & interfaces, 2022. **14**(10): p. 12106-12115.
64. Wang, P., et al., *Nanovoid-confinement and click-activated nanoreactor for synchronous delivery of prodrug pairs and precise photodynamic therapy.* Nano research, 2022. **15**(10): p. 9264-9273.
65. Moh, E.S.X., N. Sayyadi, and N.H. Packer, *Chemoenzymatic glycan labelling as a platform for site-specific IgM-antibody drug conjugates.* Analytical biochemistry, 2019. **584**: p. 113385-113385.
66. Jaiswal, M., et al., *Enzymatic glycoengineering-based spin labelling of cell surface sialoglycans to enable their analysis by electron paramagnetic resonance (EPR) spectroscopy.* Analyst (London), 2022. **147**(5): p. 784-788.
67. Yang, X., et al., *Fluorometric visualization of mucin 1 glycans on cell surfaces based on rolling-mediated cascade amplification and CdTe quantum dots.* Microchimica Acta, 2019. **186**(11): p.721
68. Deslignière, E., et al., *State-of-the-art native mass spectrometry and ion mobility methods to monitor homogeneous site-specific antibody-drug conjugates synthesis.* Pharmaceuticals (Basel, Switzerland), 2021. **14**(6): p. 498.
69. Luo, Y., et al., *"Two Birds One Stone" Strategy for the Site-Specific Analysis of Core Fucosylation and O-GlcNAcylation.* Journal of the American Chemical Society, 2023. **145**(29): p. 15879-15887.
70. Bhise, A., et al., *Optimizing and determining the click chemistry mediated Cu-64 radiolabeling and physiochemical characteristics of trastuzumab conjugates.* Biochemical and biophysical research communications, 2023. **638**: p. 28-35.

71. Han, J., et al., *Metabolic glycan labeling immobilizes dendritic cell membrane and enhances antitumor efficacy of dendritic cell vaccine.* Nature Communications, 2023. **14**(1): p. 5049-5049.
72. Kizuka, Y., *Metabolic utilization and remodeling of glycan biosynthesis using fucose analogs.* Biochimica et biophysica acta. General subjects, 2022. **1866**(12): p. 130243-130243.
73. Shivatare, V.S., et al., *Probing the Internalization and Efficacy of Antibody-Drug Conjugate via Site-Specific Fc-Glycan Labelling of a Homogeneous Antibody Targeting SSEA-4 Bearing Tumors.* Israel journal of chemistry, 2023. **63**(10-11): p. e202300042.
74. Jaiswal, M., et al., *Enzymatic glycoengineering-based spin labelling of cell surface sialoglycans to enable their analysis by electron paramagnetic resonance (EPR) spectroscopy.* Analyst, 2022. **147**(5): p. 784-788.
75. Ai, X., et al., *Surface Glycan Modification of Cellular Nanosponges to Promote SARS-CoV-2 Inhibition.* Journal of the American Chemical Society, 2021. **143**(42): p. 17615-17621.
76. Jaiswal, M., et al., *Different Biophysical Properties of Cell Surface α2,3- and α2,6-Sialoglycans Revealed by Electron Paramagnetic Resonance Spectroscopic Studies.* The journal of physical chemistry. B, 2023. **127**(8): p. 1749-1757.
77. Wu, Z.L., et al., *Direct fluorescent glycan labeling with recombinant sialyltransferases.* Glycobiology (Oxford), 2019. **29**(11): p. 750-754.
78. Ou, C., et al., *Synthesis, binding affinity, and inhibitory capacity of cyclodextrin-based multivalent glycan ligands for human galectin-3.* Bioorganic & medicinal chemistry, 2022. **72**: p. 116974-116974.
79. Chinoy, Z.S., K.W. Moremen, and F. Friscourt, *A Clickable Bioorthogonal Sydnone-Aglycone for the Facile Preparation of a Core 1 O-Glycan-Array.* European journal of organic chemistry, 2022. **2022**(27): p. e202200271
80. Tomás, R.M.F. and M.I. Gibson, *Covalent cell surface recruitment of chemotherapeutic polymers enhances selectivity and activity.* Chemical science (Cambridge), 2021. **12**(12): p. 4557-4569.
81. Hancox, O.G.A., *Integrated workflows for Carbohydrate Analysis - Artificial Glycoconjugates as Tools for Glycan Analysis*, in *School of Pharmacy*. 2023, University of Reading. p. 242.
82. Yang, J.W., et al., *A unique and rapid approach toward the efficient development of novel protein tyrosine phosphatase (PTP) inhibitors based on 'clicked' pseudo-glycopeptides.* Bioorg Med Chem Lett, 2011. **21**(4): p. 1092-6.
83. Giri, R.S., et al., *FeCl3-Mediated Boc Deprotection: Mild Facile Boc-Chemistry in Solution and on Resin.* ChemistrySelect, 2020. **5**(6): p. 2050-2056.
84. Chakrabarty, M., T. Kundu, and Y. Harigaya, *Mild Deprotection of tert-Butyl Carbamates of NH-Heteroarenes under Basic Conditions.* Synthetic Communications, 2006. **36**(14): p. 2069-2077.
85. Han, G., M. Tamaki, and V.J. Hruby, *Fast, efficient and selective deprotection of the tert-butoxycarbonyl (Boc) group using HCl/dioxane (4 m).* The journal of peptide research, 2001. **58**(4): p. 338-341.
86. Kaul, R., et al., *Selective tert-Butyl Ester Deprotection in the Presence of Acid Labile Protecting Groups with Use of ZnBr2.* The Journal of Organic Chemistry, 2004. **69**(18): p. 6131-6133.

Chapter 3

Development of Protein hydrolysis methodology for *N*- and *O*-glycan analysis

3.1 Introduction

Precise and accurate HPLC analytical methods are available for quantifying all types of *N*-glycans in biological samples, for example, using HPLC-fluorescence [1-3] and HPLC-MS [1, 4, 5]. This contrasts with methods for quantifying all types of *O*-glycans, where more methods are needed and hence research is ongoing. This is because the specific enzymes or chemicals required for releasing the *O*-linked glycan from the core are unavailable. *N*-Glycan analysis usually uses *N*-glycosidase or PNGase F enzymes to break the linkage between the sugar and the amino acids [6-9]. However, *O*-glycan cores have no specific release enzymes, with only cores 1, 2, and 3 being able to be analysed this way [10, 11]. Therefore, the usual method for *O*-glycan release uses a chemical reaction; hydrazine, reductive β-elimination, and non-reductive β-elimination [12-16]. However, the available chemical methods cannot release all *O*-linked cores and have a peeling reaction producing by-products that decrease yields [15, 17]. Indeed, one of the most significant challenges in glycan analysis is using HPLC to accurately quantify all core *N*- and *O*-linked glycans simultaneously in the same sample.

One approach for simultaneous *N*- and *O*-glycan analysis could be combining enzymes and chemicals to cut and digest the proteins into single amino acids. Aminoglycans would then be present in the digestion products. Figure 3.1 demonstrates a proposed workflow of *N*- and *O*-glycan analysis using erythropoietin as the substrate of interest, as it contains amino acid sequences, including aminoglycans, as shown in Figure 3.1 (A). *N*-Glycans are present in the sequence at Asp residues 24, 38 and 83, and *O*-glycans are present at Ser residue 126. The erythropoietin is digested into small peptide fragments using an enzyme or chemical reaction; these smaller peptides are hydrolysed into single amino acids. All amino acids and glycoproteins in the sample are labelled with a fluorophore and analysed with an HPLC-fluorescence detector.

(A)

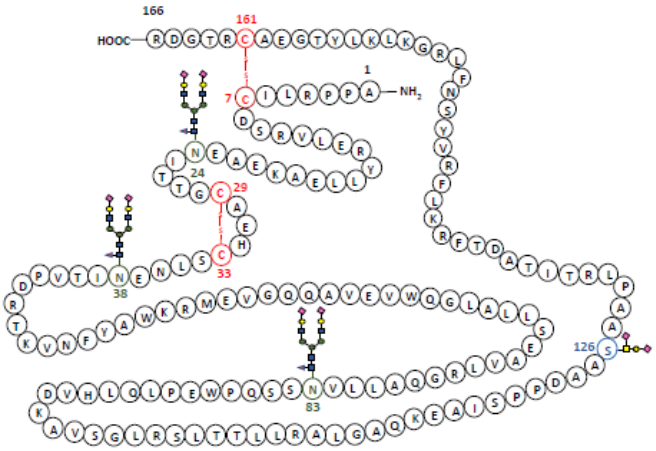

(B)

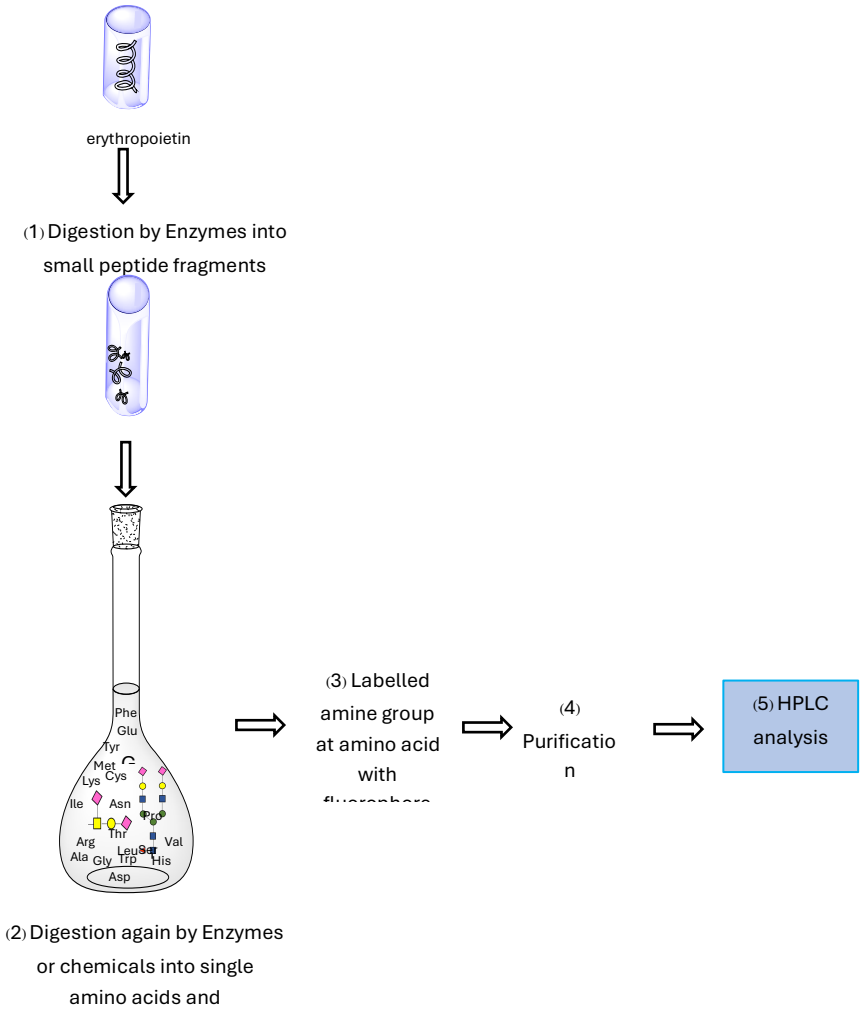

Figure 3.1 The proposed *N*- and *O*-glycan analytical method by labelling at the amino acid's side chain. (A) The amino acid sequence of core Erythropoietin (EPO) shows the position of *N*-linked (green) and *O*-linked (blue) glycans and disulphide bonds (red). (B) The aminoglycan analysis workflow (1) digestion of the protein to small peptides, (2) digestion of the peptides to single amino acids and aminoglycans, (3) labelling of the amino acids and aminoglycans with the fluorophore, (4) purification of the sample, and (5) HPLC analysis.

3.1.1 Protein digestion and hydrolysis methods

In vitro, protein digestion to afford small peptide fragments has afforded information on the protein's structure and the total amount of specific amino acids present. The method of first choice is to use enzymes such as trypsin, pepsin, chymotrypsin, and pronase [18-20]. The second choice for the hydrolysis of proteins to small peptide fragments is using chemical reagents [21-23] or combining enzymes and chemicals as simulated gastrointestinal reagents [24-27]. Figure 3.2 illustrates the protein digestion and hydrolysis steps for the small peptide or amino acids.

3.1.1.1 Enzyme digestion

In glycoprotein analysis, enzymes are used to digest the sample to afford small peptide fragments before using specific enzymes or chemical reactions to release the glycan before analysis. Trypsin is the most often-used enzyme [28, 29]. The natural structures of proteins include folding, which affects the shapes of proteins and affords two main types of proteins. The first type is the fibrous proteins that contain a structure fixed by the disulphide bond between the amino acids in the sequence, as shown in Figure 3.1(A). The second type is the globular proteins, such as albumin, which are spherical due to the polypeptides coiling around themselves, as shown in Figure 3.2. These are usually soluble in water. Therefore, using enzymes to denatured proteins and cut disulphide bonds before further digestion is important. Protein denaturing and disulphide bond-cutting steps use high temperatures or chemicals (such as HEPES, urea, guanidine, 0.1-10% SDS, 1% sodium deoxycholate or commercial denaturing buffer) [28-31]. There are many kinds of enzymes that can affect *in vitro* protein digestion. Examples of protein digestion with enzymes are shown in Table 3.1. The disadvantages of using multiple enzymes for protein digestion are self-hydrolysis and hydrolysis between enzymes. This phenomenon will produce the wrong results of the total percentage of each amino acid. In order to stop the digestion reaction, heating (80-110^{o}C) is applied for at least 10 minutes [19, 32, 33], or the solution is acidified (pH<2.5) [24, 30, 31].

3.1.1.2 Chemical hydrolysis

Chemical reagents are an alternative method for protein digestion and can be used with or without enzymes. A combination of enzymes (normally pepsin) and chemical reagents (usually HCl) are used in simulated gastric fluid [25, 34]. When only acid is used, this is usually 1-6 M HCl, 20% v/v trichloroacetic acid, 0.1-1.0 M acetic acid and 25% v/v TFA. The conditions for chemical hydrolysis require the temperature to be between 25-110^{o}C for between 0.5-24 hours [19, 21, 22, 35, 36].

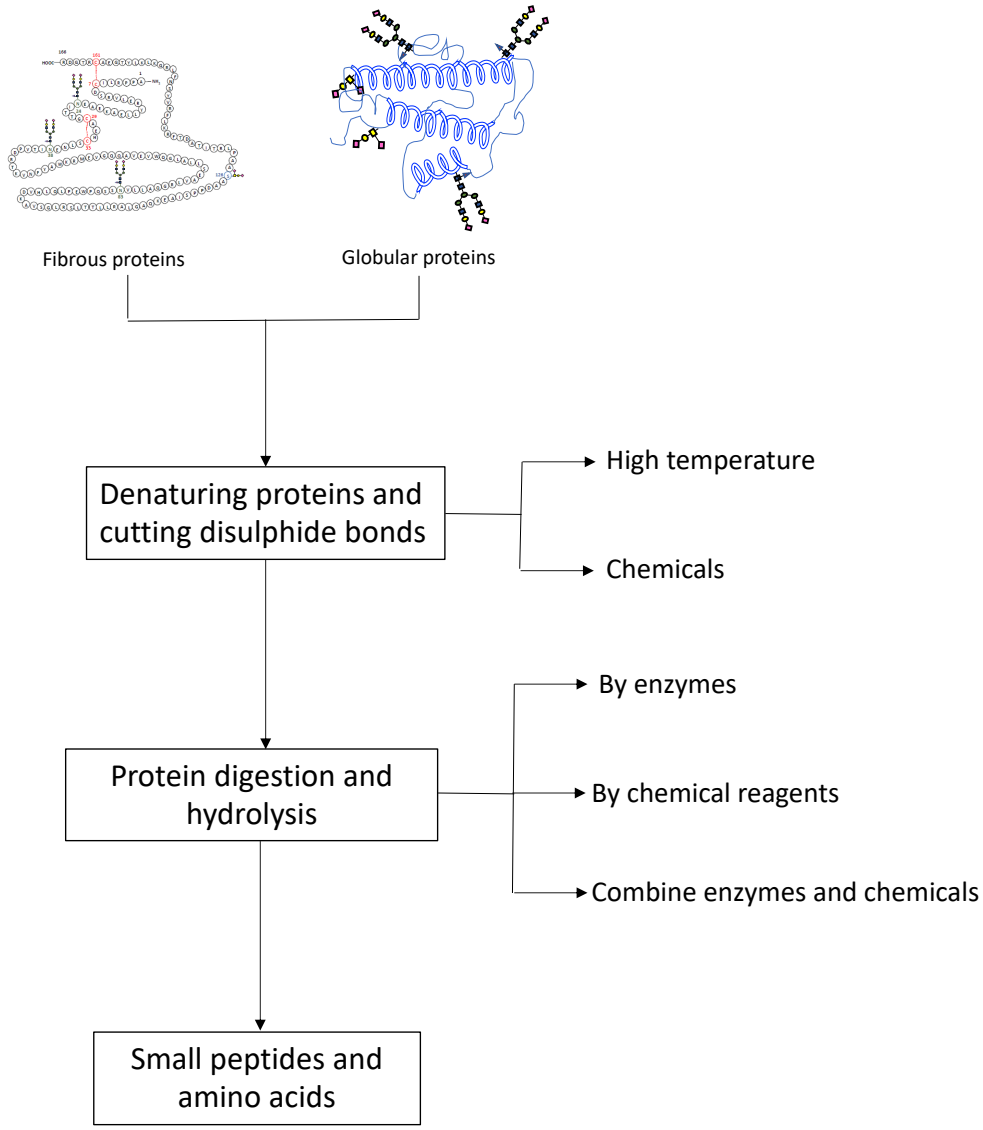

Figure 3.2 The protein digestion and hydrolysis steps to afford small peptides or amino acids

Table 3.1 Examples of enzymes used for protein hydrolysis.

Enzyme name	Source	Cleavage site	Working concentration	Enzyme:Substrate Ratio (w/w)	Optimum condition		Time (h)	Examples	References
					pH	Temperature (°C)			
Pepsin	Porcine gastric mucosa	At the C-terminal site of Phenylalanine, Leucine, Tyrosine, and Tryptophan.	0.05-0.5 mg/mL	1:100 to 1:20	1.0-30	37	1-18	To study the antioxidant activity of proteins and hydrolysate collected from newborn pigs' livers using pepsin, papain, and trypsin in digestion. The molecular mass of the product from the trypsin hydrolysis has a higher molecular weight (>3000 Da) than the products from pepsin and papain hydrolysis [33].	[19, 32, 33, 37-39]
Acalase	*Bacillus licheniformis*	Broad enzyme activity.	5000 U/g protein	-	7.0-8.5	50-75	6-12	To study *Harpa ventricose* (Gastropod) hydrolysis by acalase, pepsin and trypsin for testing the anti-inflammatory activity of the peptide fragments <10 kDa. The results show that the hydrolysis time increases from pepsin to acalase to trypsin [35].	[32, 35, 40]
Pancreatin	Porcine pancreas	Broad spectrum enzyme contains	2-14 U/mL	1:100 to 1:20	7.0-7.2	30-50	6-24	To study the angiotensin I-converting enzyme	[33, 37, 39, 40]

Enzyme name	Source	Cleavage site	Working concentration	Enzyme:Substrate Ratio (w/w)	Optimum condition		Time (h)	Examples	References
					pH	Temperature (°C)			
		trypsin, amylase and lipase, ribonuclease, and protease						(ACE) inhibition from the longan seed protein used papain and pancreatin. The results show that the protein fragment <3 kDa has the highest activity. [37].	
Trypsin	Porcine pancreas, bovine pancreatic	At the C-terminal site of lysine and arginine amino acid residues	1 mg/mL	1:100 to 1:20	7.0-9.0	25-65	2-24	To study fibrin proteins from the plasma of patients with venous thromboembolism using endoproteinase (LysC), trypsin and α-chymotrypsin. The result shows digestion yield from trypsin> α-chymotrypsin>LysC [41].	[19, 32, 33, 38, 41, 42]
α-Chymotrypsin	Bovine pancreas	Selectively hydrolyses peptide bonds on the C-terminal side of tyrosine, phenylalanine, tryptophan, and leucine.	0.5-1.0 µ	1:200 to 1:20	7.0-9.0	25	2-18	To study the antioxidant activity from the velvet antler using pepsin, trypsin, α-chymotrypsin, neutrase and acalase. The result shows the yield after hydrolysis α-chymotrypsin> Trypsin>acalase>neutrase>pepsin [32].	[19, 32, 38]
Pronase/ proteases	*Streptomyces griseus*	Non-specific protease contains	0.5-2 mg/mL	1:100 to 1:20	7.0-8.0	40-60	6-24	The study used enzymes to remove the	[31, 34, 37]

Enzyme name	Source	Cleavage site	Working concentration	Enzyme:Substrate Ratio (w/w)	Optimum condition		Time (h)	Examples	References
					pH	Temperature (°C)			
		neutral protease, chymotrypsin, trypsin, carboxypeptidase, aminopeptidase and neutral and alkaline phosphatases.						proteinaceous templates in the development of molecularly imprinted polymers. Protease was chosen for optimisation in the template removal step for creating selective binding sites. [31].	
Leucine amino peptidase (LAP)	*Burkholderia pseudomallei*, Porcine kidney	At the N-terminal of leucine residues.	0.01-0.1 mg/mL	1:100 to 1:10	7.0-9.0	37-60	2-24 h	To use LAP to detect *Escherichia coli* (*E. coli)* [43].	[43-45]
Papain	*Carica papaya*	Broad specificity, cleaving peptide bonds of basic amino acids, leucine, or glycine	$\geq$ 10 units/mg protein	-	6.0-7.0	35-65	6-24	To study the antioxidant activity and iron (II) chelating activity from milk using pepsin, pancreatin, trypsin, α-chymotrypsin, papain and pronase. The result shows the degree of hydrolysis from pepsin <papain< trypsin < α-chymotrypsin<pancreatin< pronase. [46].	[46]

3.1.2 Amino acid analysis methods

Proteomics is the large-scale study of proteins, particularly their functions and structures. There are two methods used in proteomics, top-down and bottom-up workflows. Top-down proteomics is used in the protein mixture that has a mass of less than 50 kDa. Bottom-up proteomics is used in the protein mixture in the unspecific protein molecular mass. Bottom-up proteomics is a widely used approach for studying proteins within complex biological samples. The workflow starts from the protein digestion by enzymes, such as trypsin, into smaller peptides, then separated by the specific LC column, and finally identified the peptides by MS or MS/MS [47]. These spectra are then compared against online protein databases, such as MASCOT and UniProt, to determine the identity of the proteins.

There are many analysis methods for proteins, peptides, and amino acids. The simplest peptide and amino acid analysis methods include SDS-PAGE, Thin-layer Chromatography (TLC), High-performance Thin-layer Chromatography (HPTLC), MS, GC, and HPLC. SDS-PAGE, TLC, and HPTLC need to stain or derivatize the fragment for detection by the molecular mass of proteins. MS is used for mapping amino acid sequences in the protein or peptide samples. This technique does not require the protein structure to be derivatised. GC is the technique of choice for analysing amino acids and fatty acids in biological samples with MS or MS/MS detectors. HPLC is the other choice for protein separation and analysis with various types of detectors.

Although some amino acids include a chromophore in their structure, not all amino acids can be detected under UV-Visible spectroscopy. Therefore, detection methods for amino acids usually use labelling reagents to introduce colour, a chromophore, or a fluorophore, as shown in Table 3.2. Most chromophore or fluorophore labelling reagents react with the amine group ($-NH_2$) within the amino acids' structures. Examples of fluorescence labelling reagents for amino acids in HPLC analysis are dansyl chloride (DNS), *o*-phthalaldehyde (OPA), and 9-fluorenylmethyl chloroformate chloride (Fmoc-Cl). The reactions between a representative amino acid (serine) and labelling reagents are shown in Scheme 3.1. DNS has more advantages than OPA. OPA can only label primary amines, whereas DNS can react with primary and secondary amines.

Table 3.2 Examples of labelling reagents for amino acid analysis using various techniques.

Name of Labelling reagents	Structure	Method of detection						References
		TLC	SDS	The wavelength for UV-visible detection (nm)	The wavelength for fluorophore detection		MS	
					Excitation wavelength (nm)	Emission wavelength (nm)		
Ninhydrin	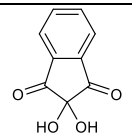	√		440,570				[48, 49]
Coomassie Brilliant Blue G-250	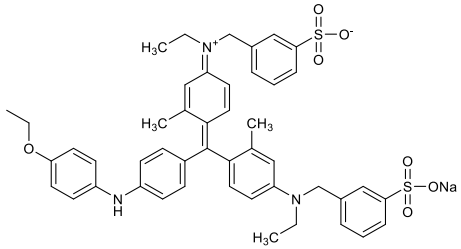		√					[24, 39]
Fluorescamine	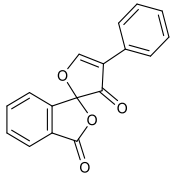				Max. 390	Max. 480		[25, 50]
4-Fluoro-7-nitro-2,1,3-benzoxadiazole (NBD-F)	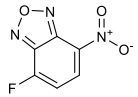				470-490	535-550		[51, 52]

Name of Labelling reagents	Structure	Method of detection						References
		TLC	SDS	The wavelength for UV-visible detection (nm)	The wavelength for fluorophore detection		MS	
					Excitation wavelength (nm)	Emission wavelength (nm)		
DNS	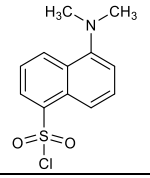			Diode-array	310-350	500-550	√	[53-57]
OPA	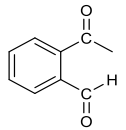				340-360	440-460		[25, 58-61]
Fmoc-Cl	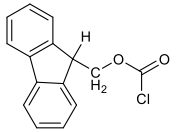			Diode-array	220-270	300-320	√	[25, 62, 63]
6-Aminoquinolyl-*N*-hydroxysuccinimidyl-carbamate	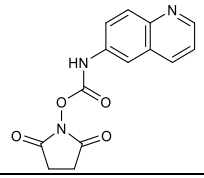				245	395		[64]

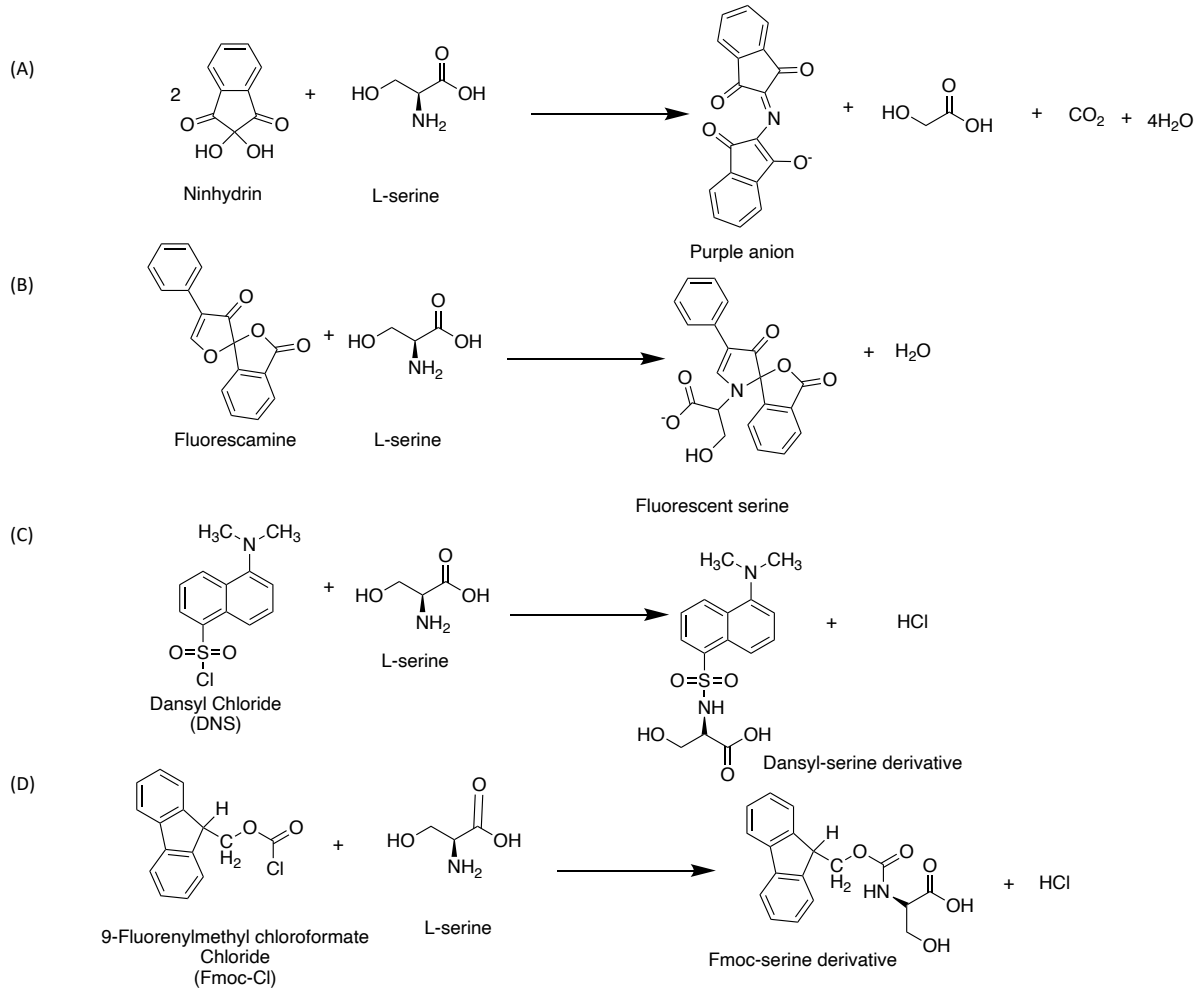

Scheme 3.1 Examples of reactions between serine and labelling reagent: (A) Ninhydrin, (B) Fluorescamine, (C) DNS, and (D) Fmoc-Cl.

3.1.2.1 Peptide/amino acid analytical instruments.

A summary of peptide fragments and amino acid analytical methods is presented in Table 3.3. The details of each instrument are described below.

3.1.2.1.1 TLC/HPTLC

TLC is used to identify compounds by comparing their R_f with a standard. TLC's separation potential depends on the polarity between the stationary and mobile phases. TLC must be combined with other instruments (such as a densitometer) for quantitation. The peptide fragments cannot be directly visualised without staining with a dye. Normally, ninhydrin reagent is the first choice. This reagent reacts with the amine group in the amino acid's structure [65]. The product's colour will depend on the type of amino acids, but it is usually dark purple. A combination of TLC with MS has been reported for the qualitative and quantitative analysis of labelled amino acids [48].

3.1.2.1.2 SDS-PAGE/Gel electrophoresis

SDS-PAGE is another routine method for separating peptide fragments by molecular weight. The molecular mass suitable for this method is between 5 – 250 kDa. The SDS-PAGE surfactant charges the peptide/amino acids according to its mass. The peptide fragments cannot be detected by visualisation. Staining reagents (or dyes), such as Coomassie Brilliant Blue G-250, are necessary for detection. Western blot is a gel electrophoresis technique that separates

molecules based on their molecular weight. It involves transferring peptides from a gel to a membrane, where target proteins are detected using specific antibodies[39, 51]. The mass of proteins is compared with specific mass makers that run at the same time.

3.1.2.1.3 MS

MS is used in amino acid analysis without connection to other instruments. Electrospray ionisation (ESI) is the first amino acid MS detection choice. Stand-alone MS usually uses MS/MS [66]. Some MS research uses a guard column for a short separation before the MS step using the same instrument without modification [67].

3.1.2.1.4 GC

Amino acid analysis by GC requires derivatisation of the amino acids for the selected ion monitoring reagents. Examples of derivatising strategies include ethoxycarbonylation (EOC), methoximation (MO), and *tert*-butydimethylsilylation (TDMS) [68, 69]. GC's amino acid analysis is usually combined with MS or MS/MS as the detector [68, 70].

3.1.2.1.5 HPLC

Reverse-phase HPLC is most commonly used to separate and analyse each amino acid. The HPLC columns include ion-exchange (anion- or cation-exchange) [71], C8 [58], C18 [54-57, 61, 64, 67, 72], chiral column [73], and HILIC [53]. The detectors for amino acids include UV-Visible, fluorescence and mass spectrometry, depending on the purpose of the research. However, derivatisation for UV is necessary for amino acids that do not have a chromophore or fluorescence label [64] in order for them to be used in association with a fluorescence detector, as shown in Table 3.2. Another kind of detector used in amino acid analysis with HPLC is MS. HPLC-MS, or MS/MS, is used for amino acid analysis in biological samples, such as plasma, urine, or CSF [64, 67, 71, 72]

Table 3.3 Summary of amino acid analysis technique

Technique	Method/Detector	Benefit	Limitation	References
TLC/HPTLC	Visualised by using specific reagents for amino acids or amine moieties (such as ninhydrin)	- This method is inexpensive, highly sensitive, and quick. - Selection involves various types of stationary phases (NP, RP, or size exclusion).	- This method needs coloured reagents for the detection of some amino acids. - Quantitative analysis needs extra instruments, such as a densitometer.	[48, 65, 74]
SDS-PAGE, Gel electrophoresis	Visualised by using specific stains for proteins (such as Coomassie brilliant blue R-250)	- This method can be combined with MS for genome sequencing.	- This method uses toxic reagents for the gel page and staining reagents.	[19, 22, 24, 34, 39, 75, 76]
MS	MS (ESI, MALDI) MS/MS	- This method can be used for amino acid sequencing. - The sample can be analysed without derivatisation. - MS can be used for qualitative and quantitative analysis of enantiomers.	- Asparagine and methionine have less sensitivity to MS than other amino acids. - This method destroys the samples.	[35, 42, 66, 67, 69, 76]
GC	MS MS/MS	- This method can analyse essential biological substances from the same sample, such as amino acids, fatty acids, and volatile substances.	- The amino acids need derivatisation for selected ion monitoring.	[68-70]
HPLC	UV-Visible spectroscopy	- This method can be used for peptide purification on a small scale. - This detector can be combined with MS to determine the structure.	- Some amino acids need to be derivatised with chromophore increased detection.	[19, 34, 53, 54, 57, 62]

Technique	Method/Detector	Benefit	Limitation	References
	Fluorescence	- The fluorescence labelling reagents can detect all amino acids without interference by solvents or foreign substances. - A labelling range of labelling reagents are available. - This detector can be combined with MS to determine the structure.	- This approach needs two steps before analysis (labelling and clean-up step). - Some labelling reagents can label only primary amines.	[25, 55, 58, 60]
	MS (e.g., ESI, MALDI) MS/MS (e.g., MS/MS, MALDI-TOF)	- The sample can be analysed without derivatisation.	- This method needs a mobile phase that is compatible with MS.	[21, 22, 24, 30, 31, 38, 41, 67, 71-73]

3.2 Aim and Objectives

This work aims to optimise methods to simultaneously analyse *N*- and *O*-linked glycans without the need to release the glycans from the core. Hydrolysis of the protein portion of glycoproteins to single amino acids will be achieved using various enzymes (pepsin, trypsin, LAP and pronase) and chemical reactions. It is hypothesised that after breaking down the protein into single amino acids, the sample will contain *N*- and *O*-linked glycans alongside the free amino acids. Labelling of the released amine functional group within these single amino acids, and within the *N*- and *O*-linked glycans, will then be achieved by reaction with DNS. Reverse-phase HPLC can then be used for qualitative and quantitative analysis allowing for simultaneous analysis of the *N*- and *O*-linked glycans without the need to release the glycans from the core.

The work in this chapter sets out to fulfil three main objectives. The first objective is to improve the labelling of amino acid standards using DNS by determining the minimum concentration of DNS and minimum reaction time that are required prior to HPLC-fluorescence analysis.

The second objective is to optimise the conditions required for hydrolysis of a simple protein model (ribonuclease A, RNase A) into individual amino acids using a combination of different enzymes and chemical reactions.

The final objective is to apply the optimised labelling and hydrolysis conditions established for the simple protein model to a more complex glycoprotein, Bovine fibrinogen.

This research is summarised in Figure 3.3, which outlines the schemes of work carried out within this chapter.

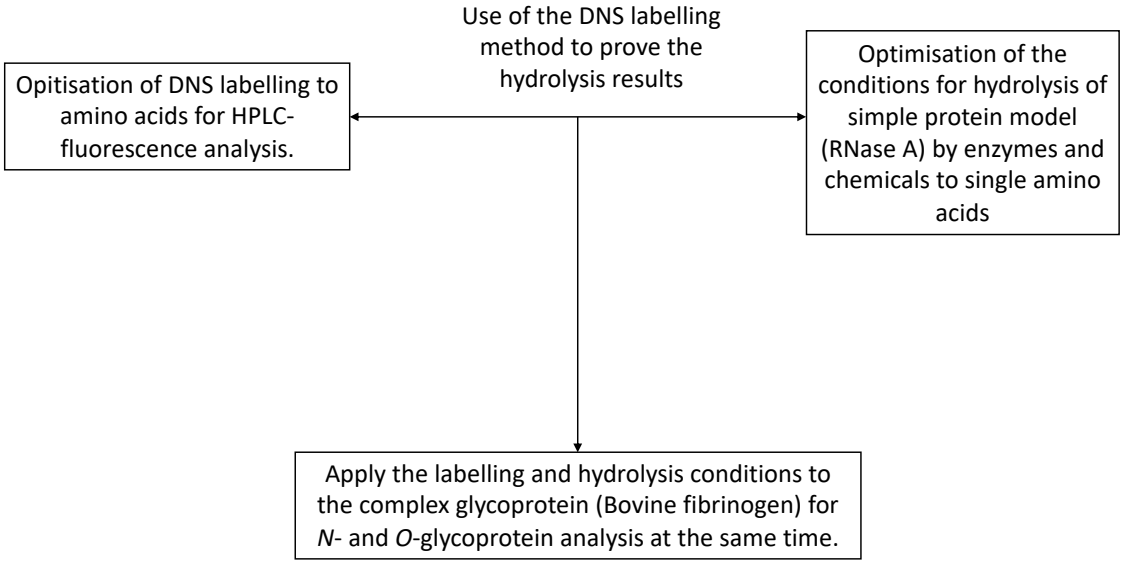

Figure 3.3 Working flow for optimization condition of DNS labelling and protein hydrolysis to a single amino acid for *N*- and *O*-glycoproteins HPLC-fluorescence analysis.

3.3 Results and Discussion

3.3.1 Optimisation of labelling condition between the amino acids and DNS

As not all amino acids have chromophores, commercial fluorophores are introduced to facilitate their analysis. In this study, DNS was chosen as the labelling reagent as it produces products that can be analysed by HPLC in conjunction with UV-visible, fluorescence and MS detectors. Labelling of the amino acids using DNS was optimised based on the method from Si-Jin Liu *et al* [77] prior to HPLC analysis. Our study sought to optimise the number of equivalents, reaction time, pH and temperature, using valine as a representative model amino acid, as shown in Scheme 3.2 below. Valine was chosen as the amino acid model due to its lack of chromophore and fluorophore.

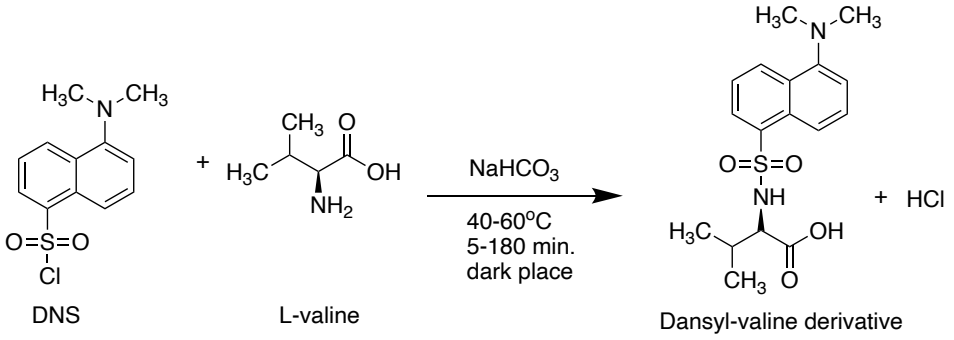

Scheme 3.2 The reaction of DNS with L-valine.

The DNS labelling reaction requires basic conditions, and the reaction time correlates with the reaction temperature. The reaction was conducted between 40-60°C, at a pH greater than 9.5, and in the dark. Si-Jin Liu *et al* [77] methodology used 500 μL of 5 g/L in acetone of DNS (19 mM) and 300 μL of 20 g/L of sodium hydrogen carbonate (approximate pH 8.8-9.0) added to 100 μL of the mixed biogenic amine samples from various foods. The mixture was incubated at 45°C in a shaking box in the dark for 60 minutes. The reaction was stopped by adding 100 μL of 25% (w/v) ammonium hydroxide to remove the excess DNS. The conditions explored to optimise the labelling of valine are shown in Tables 3.4, 3.5 and 3.6. The optimisation focuses on the concentration of DNS, temperature and pH of the labelling conditions for amino acid, using 1 mmol/mL in 0.1 M HCl of L-valine as the model. The progress of all of the reactions was followed by TLC using either isopropyl alcohol:DCM:acetic acid (7:2:1) or isopropyl alcohol:DCM:acetic acid (7:1:2) as the mobile phase, and detection was achieved using UV irradiation (254 nm) and staining with ninhydrin solution. This allowed the endpoint of the reaction to be determined as the point when no L-valine was detectable.

Table 3.4 Optimisation of the concentration of DNS with 20 g/L of sodium hydrogen carbonate without adjusting pH at 60°C

Concentration of DNS (mM)	Reaction time (hours)
20	>6.0
100	4.0
200	3.0

However, the 200 mM of DNS solution in acetone appeared slightly turbid due to approaching the maximum solubility of DNS in acetone. 100 mM DNS in acetone was therefore used for subsequent reactions.

Table 3.5 Optimisation of the reaction temperature using the 100 mM of DNS with 20 g/L of sodium hydrogen carbonate without adjusting pH

Temperature (^{o}C)	Reaction time (hours)
40	3.0
50	2.5
60	2.0
70	1.5
80	<1.0

A reaction temperature of 60^{o}C was chosen due to this being the shortest reaction time that falls around the boiling point of acetone (58-59^{o}C).

Table 3.6 Optimisation of the reaction pH using 100 mM of DNS at 60^{o}C with 20 g/L of sodium hydrogen carbonate

pH	Reaction time (minutes)
9.4	60
9.5	60
9.6	45
9.7	45
9.8	45

The optimised labelling conditions between DNS and L-valine from Table 3.4-3.6 used 500 µL of 100 mM of DNS solution in acetone, 100 µL of 1 mmol/mL of L-valine in 0.1 M HCl, and 300 µL of 20 g/L of sodium hydrogen carbonate (adjust pH to 9.6), incubated in a shaking box in the dark at 60^{o}C. The reaction was stopped by adding 500 µL of 25% (w/v) ammonium hydroxide. This optimised condition was applied to the other 18 amino acids individually and a mixture of 0.02-1 mmol/mL in 0.1 M HCl 19 amino acids (alanine, arginine, asparagine, aspartic acid, cysteine, glutamic acid, glycine, histidine, isoleucine, leucine, lysine, methionine, phenylalanine, proline, serine, threonine, tryptophan, tyrosine, and valine), used as HPLC standards for the next experiment, labelling with DNS. The mixture of amino acids labelled with DNS was completed in 1.5 hours. Figure 3.4 illustrates the summary of DNS labelling condition optimisation.

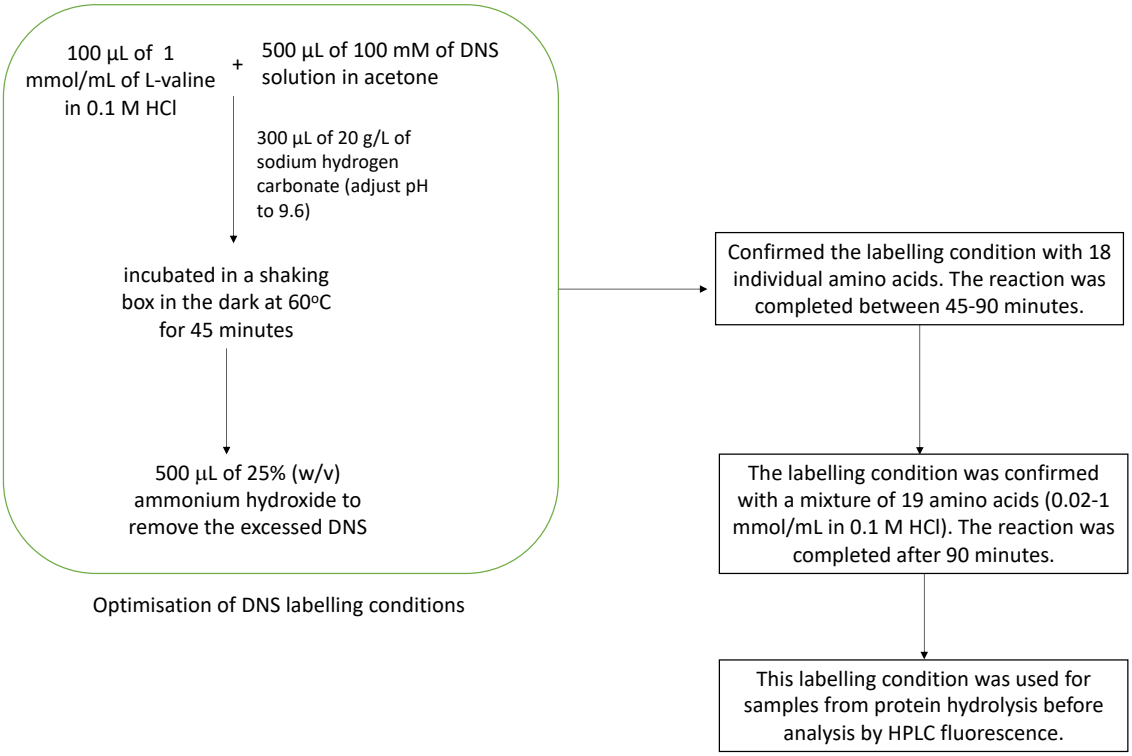

Figure 3.4 Summary of DNS labelling condition optimisation.

3.3.2 Optimisation of conditions for HPLC analysis of the amino acid standards labelled with DNS

The HPLC analytical method was modified based on the procedure from Jiaxi Yao *et al*. [78]. The C18 and guard columns in this study were different from the literature hence the HPLC analysis needed to be optimised with the other brand of the C18 column. The chromatogram of all the labelled amino acid standards is shown in Figure 3.5. The retention time of each labelled amino acid is presented in Table 3.7.

(A)

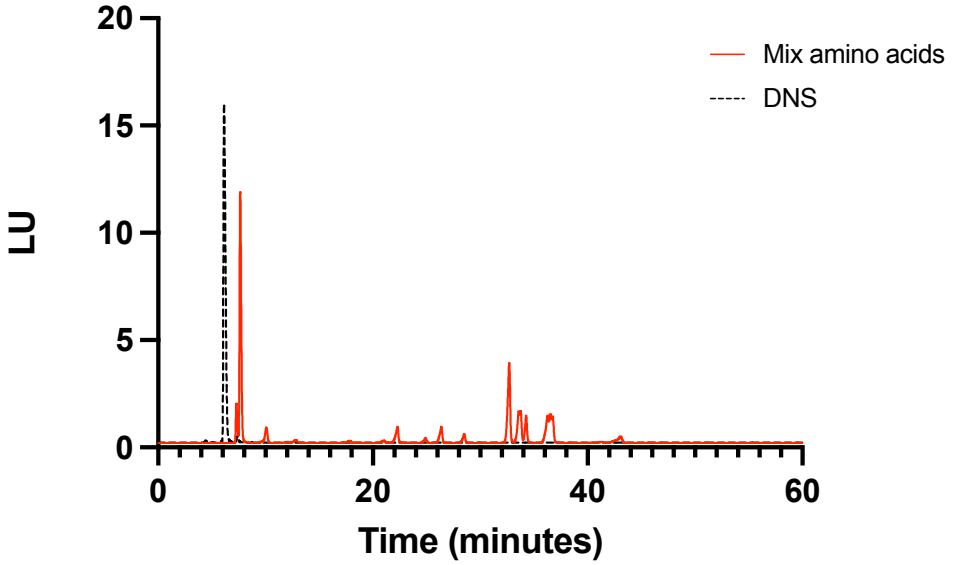

(B)

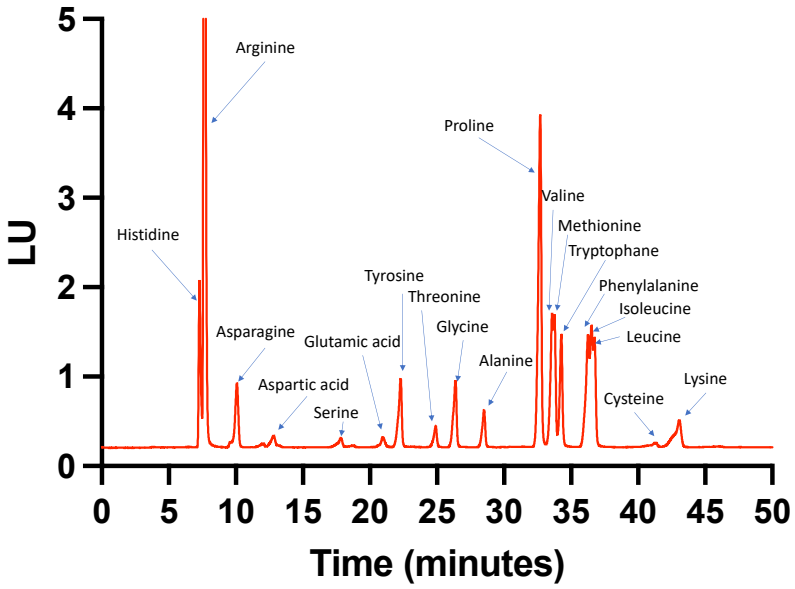

Figure 3.5 HPLC Chromatogram of 19 labelled amino acids. (A) Comparison of DNS and mixed amino acids retention time (B) Chromatogram of 19 amino acids in the mixed solution.

Table 3.7 The retention times of the individual 19 DNS-labelled amino acids by HPLC analysis

Amino acid	Retention time (minutes)
Histidine	7.3
Arginine	7.6
Asparagine	10.1
Aspartic acid	12.8
Serine	17.8
Glutamic acid	21.0
Tyrosine	22.3
Threonine	24.9
Glycine	26.4
Alanine	28.5
Proline	32.7
Valine	33.5
Methionine	33.7
Tryptophan	34.3
Phenylalanine	36.2
Isoleucine	36.5
Leucine	36.7
Cysteine	41.5
Lysine	43.0

3.3.3 Optimision of hydrolysis of a model protein, RNase A, using enzymes and chemical hydrolysis

The bovine pancreatic RNase A was chosen as the model protein due to its relatively short and uncomplex structure and lack of glycan. The advantage of the protein model without glycans is that the HPLC results will not be complicated by *N*- and *O*-glycoproteins and small peptides. The results can prove that the hydrolysis was completed by the optimisation method in the study. This protein contains 124 amino acids and 4 disulphide bonds between cysteine residues 26 and 84, 40 and 95, 58 and 110, and 65 and 72, as shown in Figure 3.6. The theoretical percentage of each amino acid that should be detected if complete hydrolysis of the protein is shown in Figure 3.7. Figures 3.8 reflects that for trypsin, hydrolysis is predicted to occur at 13 cleavage sites at positions 1, 7, 10, 31, 33, 37, 39, 61, 66, 85, 91, 98, and 104 [79]. Predictions also suggest that using trypsin alone will not affect the cleavage of the RNase A into single amino acids. A combination of various enzymes that effect cleavage at other sites was used to hydrolyse this protein to single amino acids.

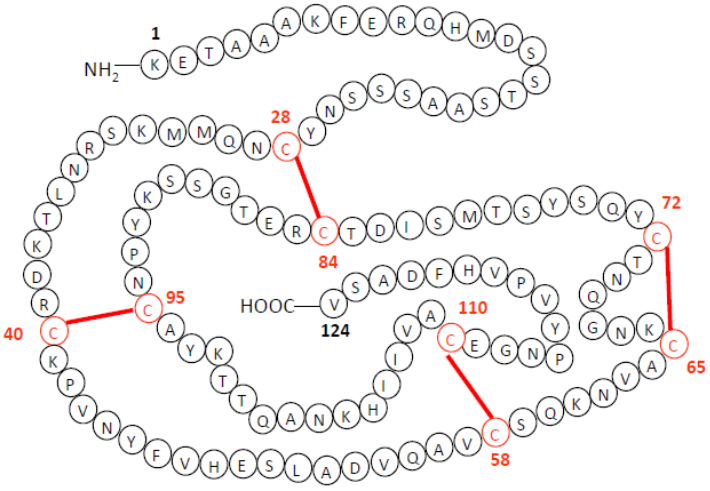

Figure 3.6 The amino acid sequence of RNase A, from bovine pancreas (EC 3.1.27.5 Transferred entry; 4.6.1.18) showing the position of disulphide bonds (red line).

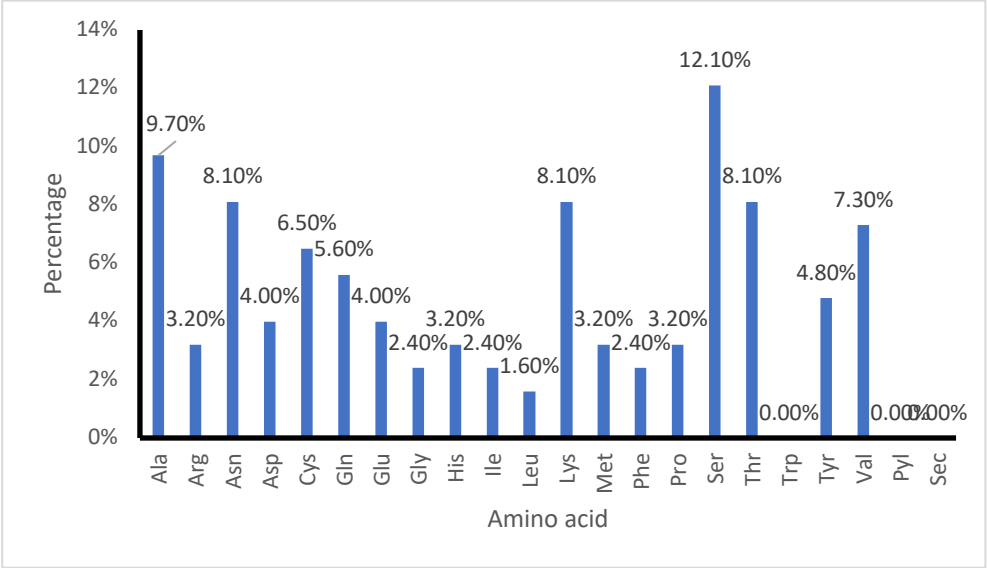

Figure 3.7 The percentage of each amino acid in bovine pancreatic RNase A. The data was generated from Figure 3.6

Figure 3.8 The RNase A cleavage site prediction used trypsin. The prediction is from the website web.expasy.org/peptide_cutter [80]

3.3.3.1 Enzymatic hydrolysis

The enzymes used in this study were pepsin, trypsin, LAP, and pronase. These enzymes were chosen from the different cleavage sites, as shown in Table 3.1. Experiments sought to optimise the pH, temperature, time, and sequence of enzymes added to effect cleavage of the proteins into single amino acids. The hydrolysis reaction used enzymes:proteins at a ratio of 1:20 (by concentration). RNase A was denatured by heating it at 95^{o}C for 1 hour and cooling it down, adding 1 M guanidine to denaturated the disulphide bond before digestion. This approach had two stages. The first stage started with the optimisation of the digestion condition of each enzyme (pH, temperature, and time). The second stage used the condition from the first stage in combination with enzyme digestion. All hydrolysis stages are done in triplicate. The sequence of the enzyme combination digestion starts from pepsin to break down the protein model into smaller peptides. Trypsin (C-terminal of lysine and arginine residue) and LAP (N-terminal of leucine residue) are used as specific site cleavage. Pronase was used last as a non-specific site cleavage enzyme.

After collection, the digestion reaction of the samples was stopped by heating them at 95^{o}C for 20 minutes. The peptide fragments and amino acids were detected by labelling them with DNS and using HPLC-fluorescence for analysis under the condition outlined in section 3.3.2. The completion of digestion was detected using the sample solution's HPLC retention time compared with standard amino acids from Table 3.7. The peaks with retention times not related to the amino acid standard were detected as peptide fragments. The Chemstation detected the peaks for the LC 3D System and Agilent Technology. All enzyme condition tests were collected in triplicate.

3.3.3.1.1 Optimisation of pepsin digestion time

Pepsin has the best activity under acidic conditions (pH<2.5), 37^{o}C. This enzyme is deactivated by pH <5 and temperature>40^{o}C [81]. Pepsin was diluted from the stock using 1 mM HCl as a

working solution. The sample solution added 0.1 M HCl until the concentration of HCl in the sample was 0.04 M before adding the pepsin. The ratio between enzyme and substrate was 1:20. The duration of the digestion test was 1, 2, 4, 6, 18 and 24 hours. The number of peaks in the chromatogram after digestion compared with the digestion time is shown in Table 3.8 (the number of peaks' detection by the program from Agilent) and Figure 3.9. Figure 3.10 shows the chromatograms resulting from the various digestion times.

Table 3.8 The total HPLC peaks of RNase A digestion by pepsin. The condition of the reaction was pH <2, 37°C, and all data were collected in triplicate.

Time (h)	Total peaks found
1	13±2.08
2	11±4.16
4	12±3.51
6	12±1.73
18	10±1.53
24	14±3.06

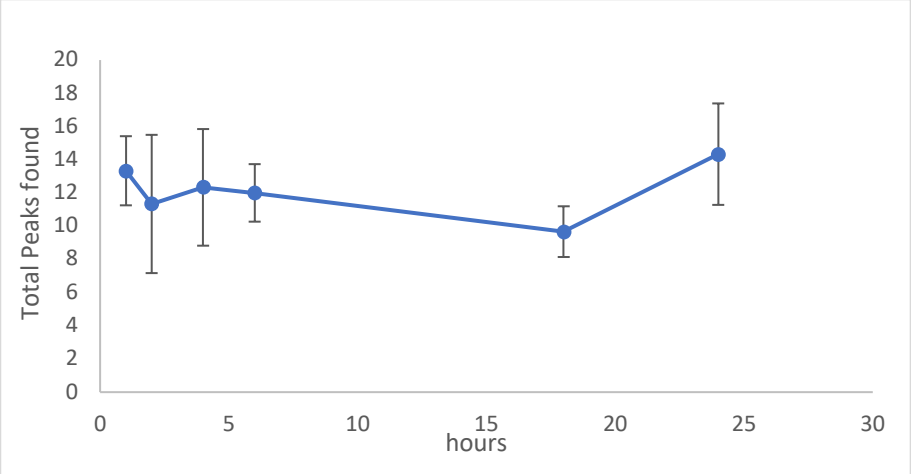

Figure 3.9 The total peaks found from RNase A digested by pepsin for 24 hours. The reaction condition was 37°C in an acidic solution.

(A)

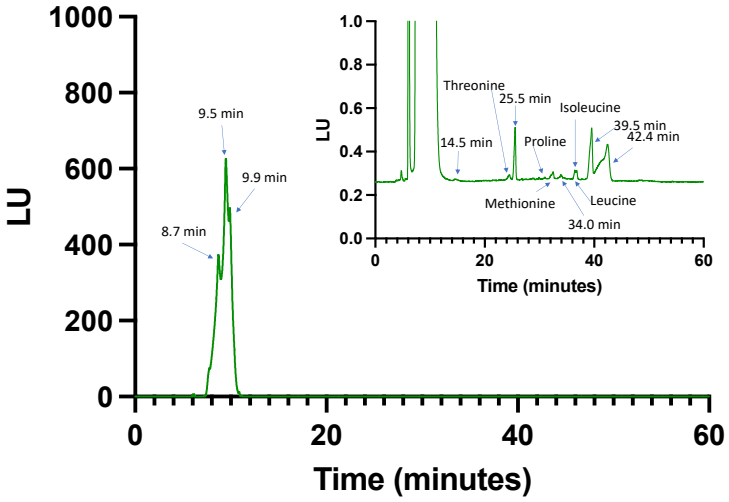
LU
Time (minutes)
9.5 min
9.9 min
8.7 min
Threonine
25.5 min
Isoleucine
39.5 min
42.4 min
14.5 min
Proline
Methionine
Leucine
34.0 min

(B)

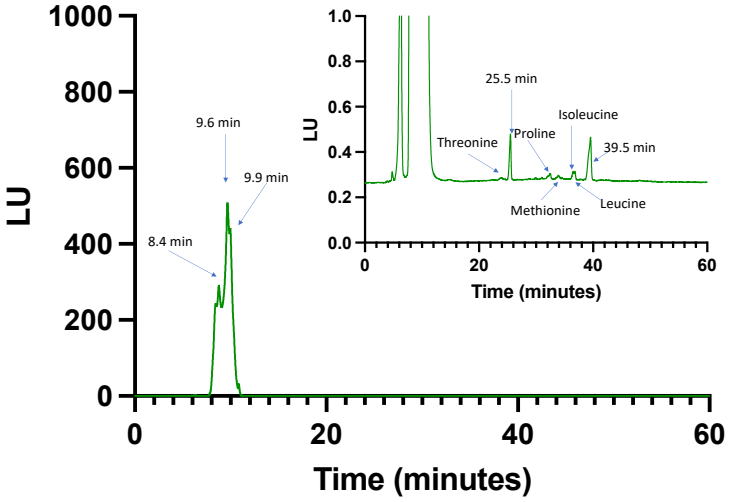
LU
Time (minutes)
9.6 min
9.9 min
8.4 min
25.5 min
Isoleucine
Threonine
Proline
39.5 min
Methionine
Leucine

(C)

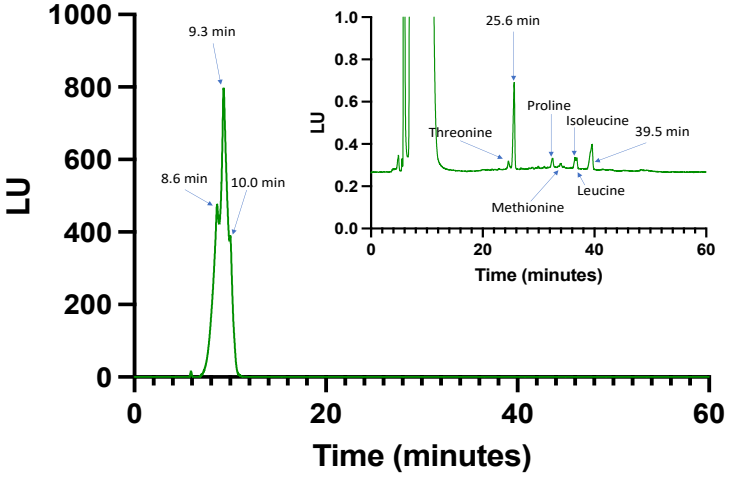
LU
Time (minutes)
9.3 min
8.6 min
10.0 min
25.6 min
Proline
Isoleucine
Threonine
39.5 min
Leucine
Methionine

(D)

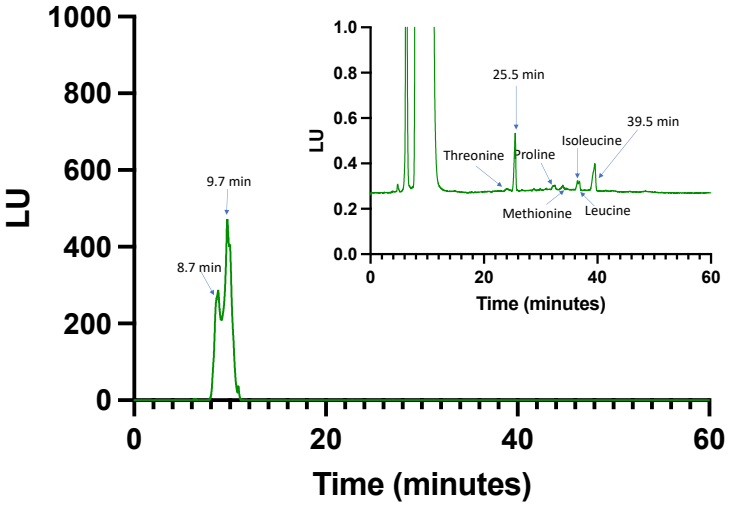

(E)

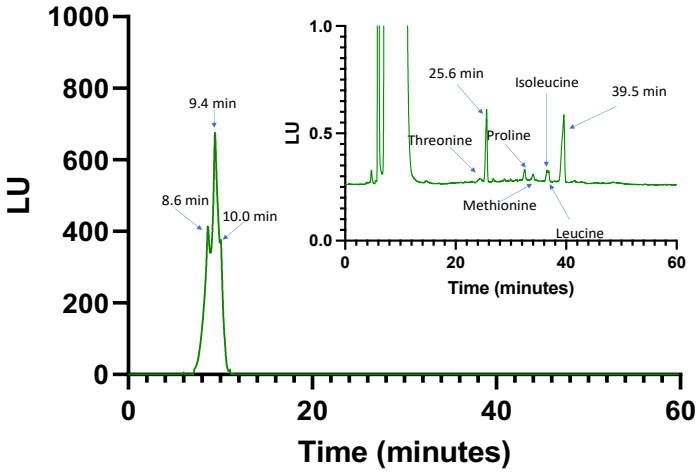

(F)

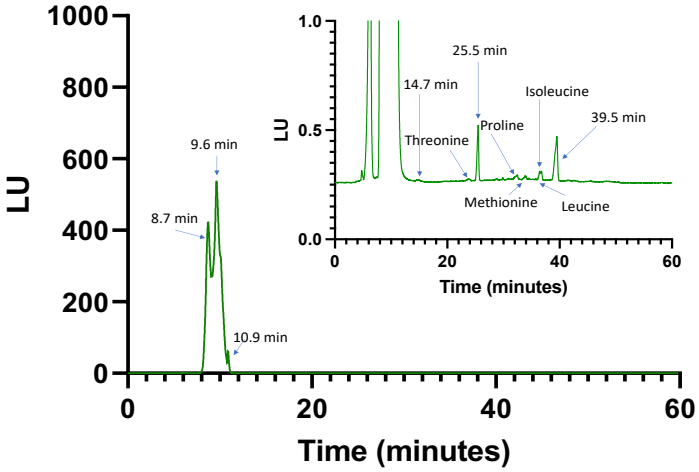

Figure 3.10 HPLC chromatogram of RNase A digestion by pepsin at various times: (A) 1 hour, (B) 2 hours, (C) 4 hours, (D) 6 hours, (E) 18 hours, and (F) 24 hours at 37^{o}C.

The results show that most peaks are peptide fragments. The peaks at 24.9, 32.5, 33.9, 36.4, and 36.7 minutes could be amino acids (threonine, proline, methionine, isoleucine, and leucine, respectively). The largest peak between the retention time at 8-12 minutes decreased when using longer digestion time. However, the peak height of the largest peak remains the same after 18 hours of digestion. So, the condition of pepsin digestion from these results used pH<2, 37^{o}C in 24 hours before adding the following enzymes.

3.3.3.1.2 Optimisation condition (temperature and pH) of Pronase, Trypsin and LAP

Pronase, trypsin, and LAP can be used in various pH and temperature conditions, as shown in Table 3.1. The solution pH 7.5 was chosen to study temperature optimisation over 24 hours using the ratio of enzyme: substate of 1:20. The results from temperature optimisation in each enzyme were used to optimise pH in the next section. The experiment used 1 M Tris at pH 7.5, 8.0, and 8.5 to prepare the protein model solution to adjust the pH of the reaction condition. The results of temperature optimisation are shown as the number of peaks in Table 3.9 and Figure 3.11. The peak height of the highest peak (peak A) is illustrated in Figure 3.12, and the average height of peak A is shown in Table 3.10.

Table 3.9 Effect of temperature on the activity of RNase A digestion, and all data were collected in triplicate.

Temperature	Total peaks found in chromatogram		
	Pronase	Trypsin	LAP
37^{o}C	25±2.31	18±3.21	24±2.52
50^{o}C	20±2.52	25±3.51	20±3.06
55^{o}C	19±1.53	27±3.06	26±2.31
60^{o}C	25±1.73	36±3.21	20±2.52
65^{o}C	24±2.08	15±2.65	16±2.08

(A)

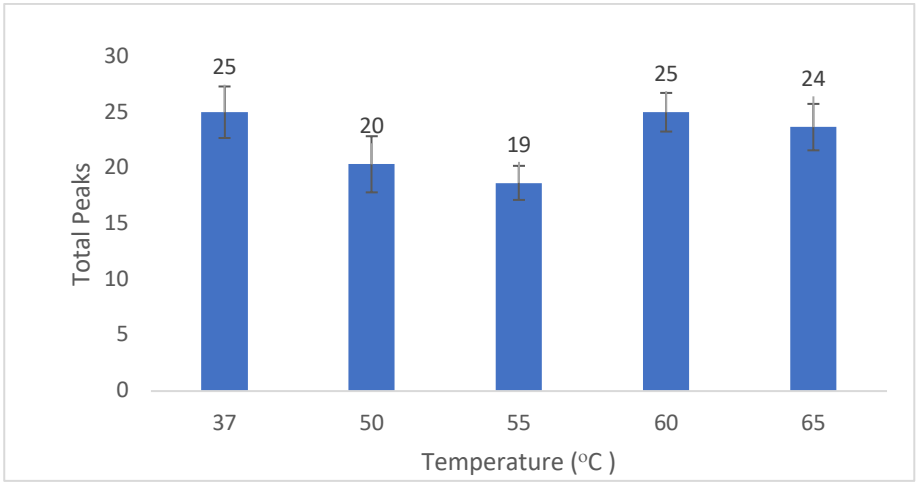

(B)

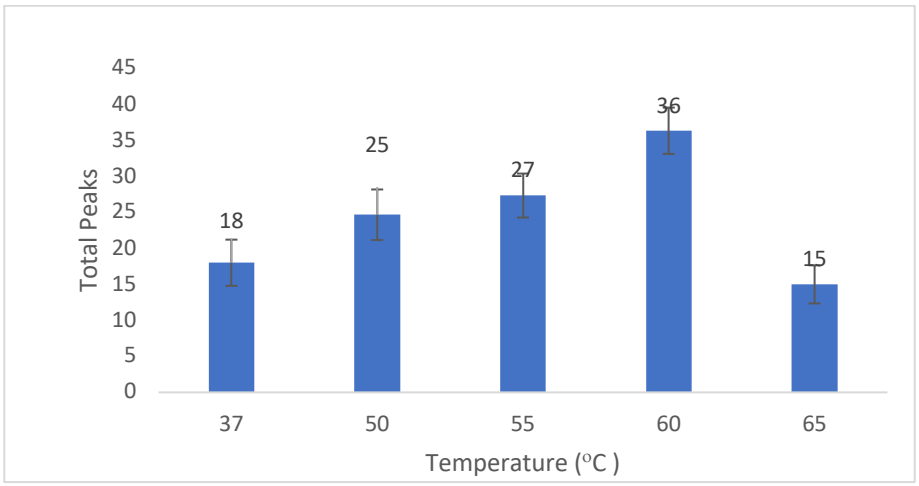

(C)

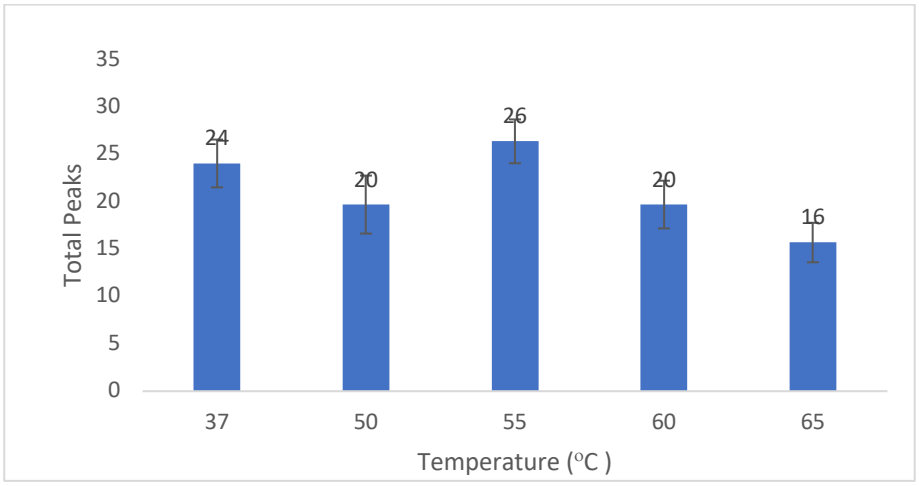

Figure 3.11 The total peaks from RNase A digested by pronase, trypsin and LAP, (A) pronase, the condition of the reaction is pH 7.5, over 24 hours compared to the temperature effect, (B) trypsin, the condition of the reaction is pH 7.5, over 24 hours compared the temperature effect, and (C) LAP, the condition of the reaction is pH 7.5, over 24 hours compared the temperature effect.

Table 3.10 The average peak height of the peak A after digestion by various pronase, trypsin, and LAP vary temperatures at pH 7.5, and all data were collected in triplicate.

Temperature	The average peak height of peak A		
	Pronase	Trypsin	LAP
37°C	47 ± 3.51	69 ± 7.09	1065 ± 58.13
50°C	47 ± 6.03	53 ± 5.69	897 ± 23.16
55°C	48 ± 5.13	53 ± 4.04	853 ± 22.72
60°C	41 ± 4.51	48 ± 3.51	898 ± 23.26
65°C	45 ± 5.51	52 ± 6.24	890 ± 23.52

(A)

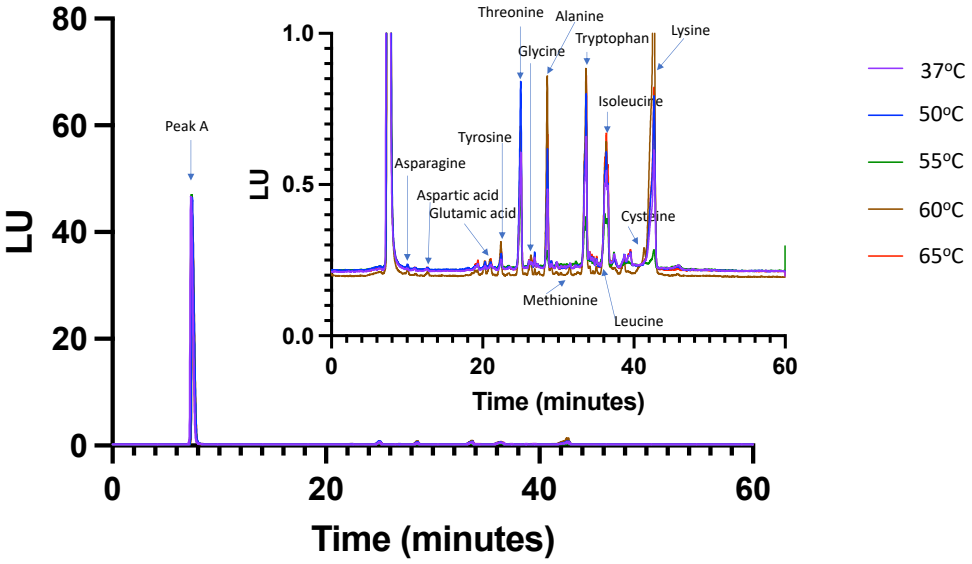

(B)

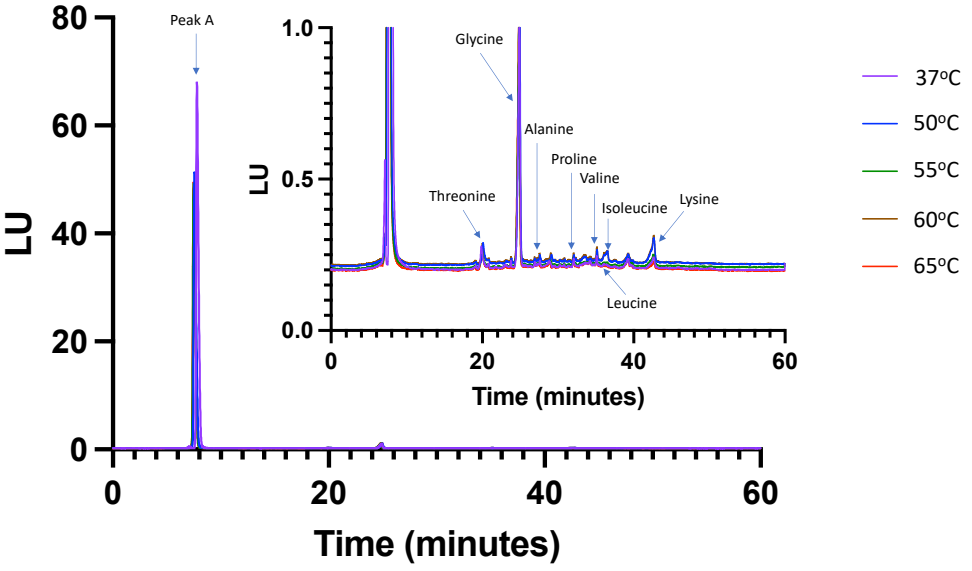

(C)

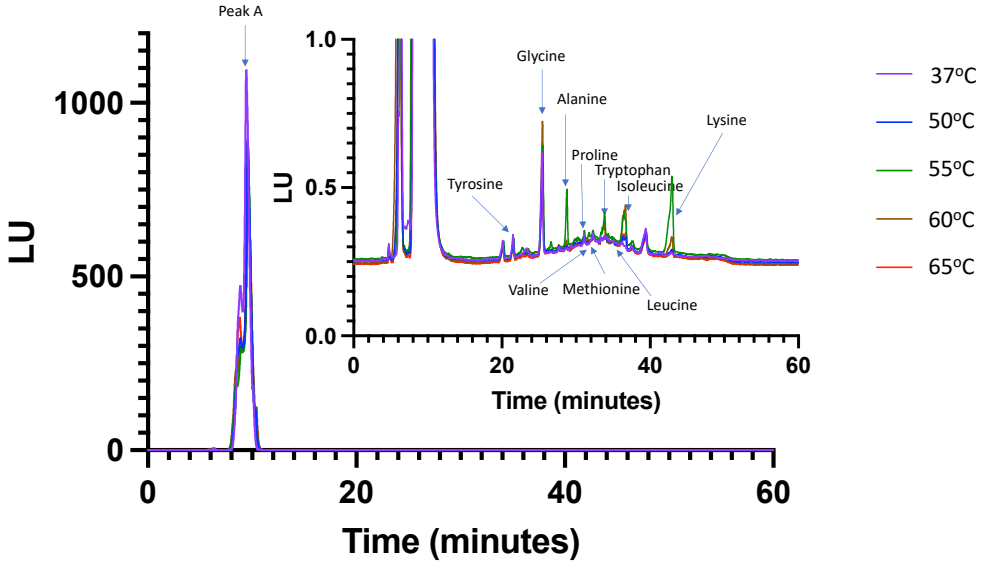

Figure 3.12 HPLC chromatogram of RNase A digestion at various temperatures by (A) pronase, (B) trypsin, and (C) LAP.

From the chromatogram in Figure 3.12, the peaks at 10.1, 12.5, 21.0, 22.3, and 24.9. 26.4, 28.5, 32.7, 33.5, 36.2 36.5, 36.7, 41.5 and 43.0 minute are amino acids (asparagine, aspartic acid, glutamic acid, tyrosine, threonine, glycine, alanine, proline, valine, methionine, tryptophan, phenylalanine, isoleucine, leucine, cysteine, and lysine, respectively). The temperatures used in the next step were 60, 60, and 55°C for pronase, trypsin, and LAP, respectively. The temperature was selected from the total peaks found and the lowest peak height of peak A after digestion. The data from Tables 3.9 and 3.10 show a correlation between the peak height of peak A and the total peaks found. The data show the lowest peak height of peak A and the most total peaks in the chromatogram. The selected temperature was used to optimise the pH of the digestion condition over 24 hours in the following experiment. The results of pH optimisation were shown as the number of peaks in Table 3.11 and Figure 3.13. The peak height of the biggest peak (peak B) is illustrated in Figure 3.14, and the average height of peak B is in Table 3.12.

Table 3.11 Effect of pH on the enzyme's activity for RNase A digestion at 60°C for pronase and trypsin and 55°C for LAP, and all data were collected in triplicate.

pH	Total peaks found in chromatogram		
	Pronase	Trypsin	LAP
7.5	25±1.73	36±3.21	26±2.31
8.0	30±2.08	27±2.00	19±2.52
8.5	31±2.52	36±3.61	25±3.51
9.0	25±3.06	29±3.51	20±1.53

(A)

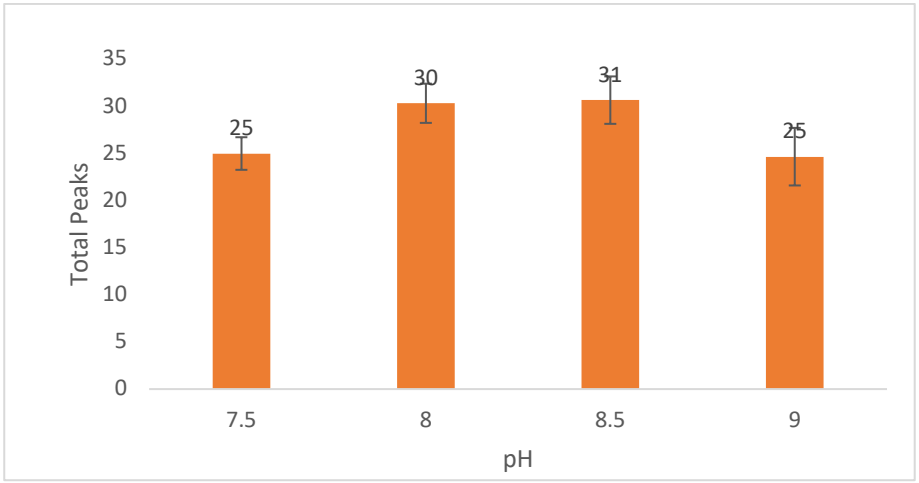

(B)

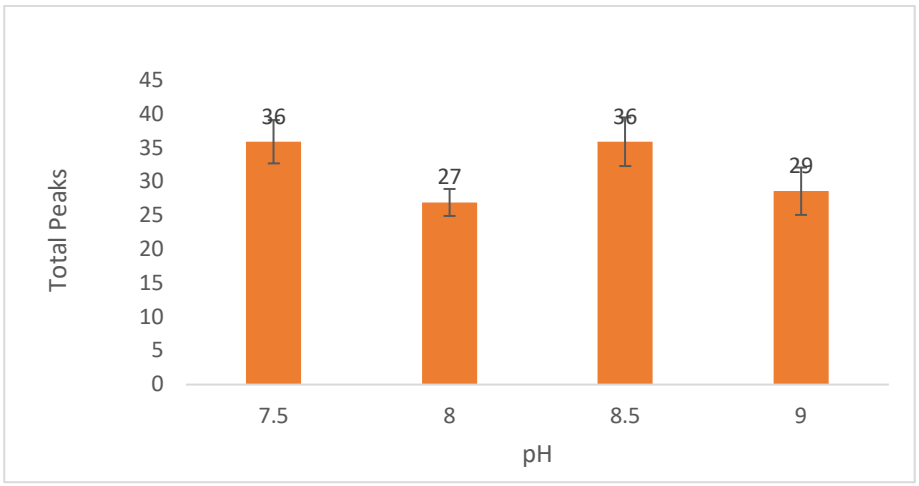

(C)

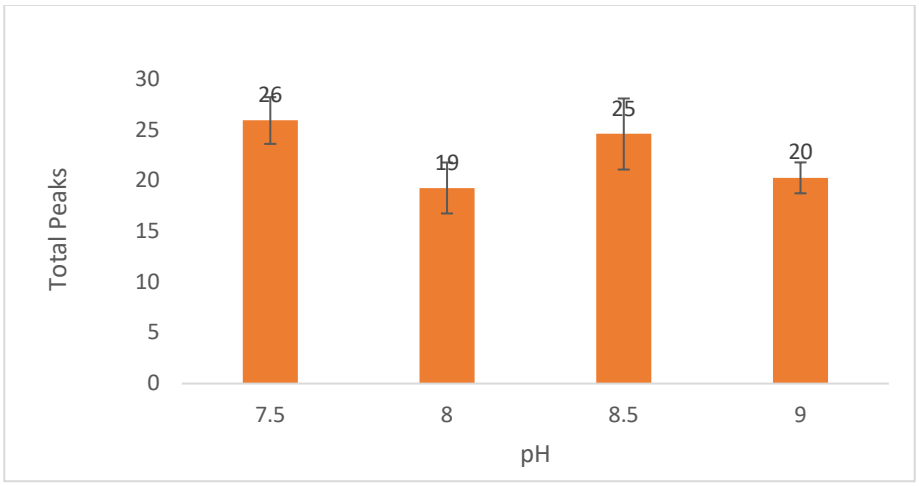

Figure 3.13 The total peaks from RNase A digested by (A) Pronase, the condition of the reaction is 60°C, 24 hours compared to the pH effect; (B) Trypsin, the condition of the reaction is 60°C, 24 hours compared to the pH effect, and (C) LAP, the condition of the reaction is 55°C, 24 hours compared the pH effect.

Table 3.12 The average peak height of the peak B various pH on the activity of the enzyme for RNase A digestion at 60°C for pronase and trypsin and 55°C for LAP, and all data were collected in triplicate.

pH	The average peak height of peak B		
	Pronase	Trypsin	LAP
7.5	41 ± 4.51	48 ± 3.51	853 ± 22.72
8.0	29 ± 3.00	56 ± 8.12	1416 ± 137.88
8.5	15 ± 2.27	46 ± 6.26	837 ± 61.34
9.0	19 ± 2.80	69 ± 4.16	1402 ± 102.21

(A)

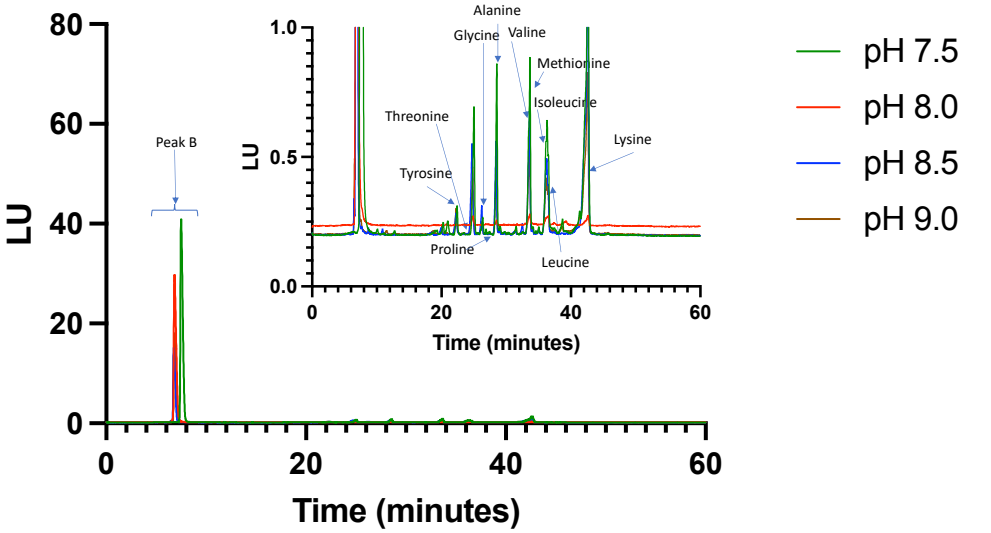

(B)

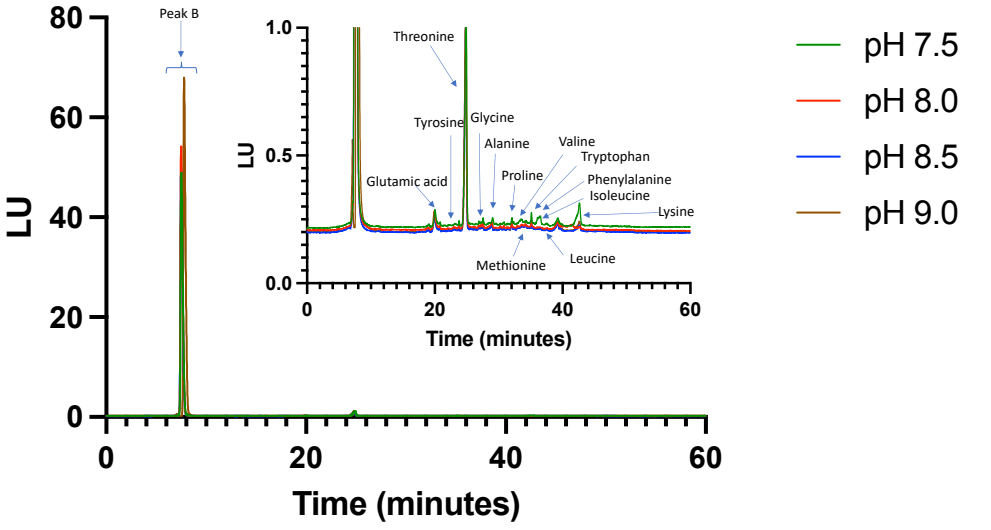

(C)

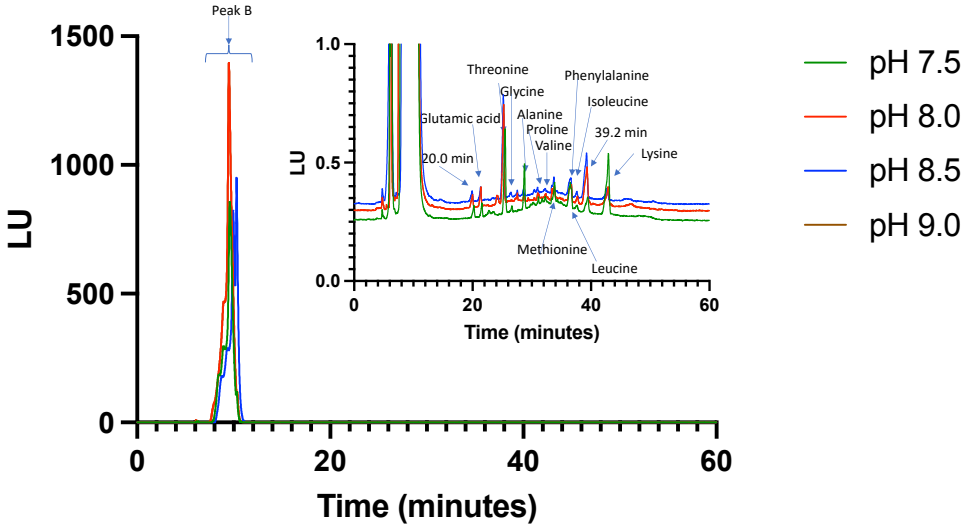

Figure 3.14 HPLC chromatogram of RNase A digestion at various pH by (A) Pronase at 60°C, 24 hours, (B) Trypsin at 60°C, 24 hours, and (C) LAP at 55°C, 24 hours.

From the chromatogram in Figure 3.14, the peak at 21.0, 22.3, 24.9, 26.4, 28.5, 32.7, 33.5, 33.7, 34.3, 36.2, 36.5, 36.7, and 43.0 minute are amino acids (glutamic acid, tyrosine, threonine, glycine, alanine, proline, valine, methionine, tryptophan, phenylalanine, isoleucine, leucine, and lysine, respectively). The pH data of digestion conditions found at pH 8.5 of all enzymes have the lowest peak B. However, the average number of total peaks between pH 7.5 and 8.5 of trypsin and LAP are the same.

3.3.3.1.3 Optimisation of Pronase digestion time and protocol

Pronase is the non-specific cleavage site enzyme containing neutral protease, chymotrypsin, trypsin, carboxypeptidase, aminopeptidase, and neutral and alkaline phosphatases. This enzyme is active at pH between 7-8 and temperature between 40-60°C. Most of the studies of protein digestion used pronase and added more enzymes every 24 hours until finished [31, 34, 37]. In this experiment, the study started with the digestion results of adding more enzymes every 24 hours for 3 days compared to adding enzyme once and leaving the reaction for 3 days. The result of the number of peaks in the chromatogram after digestion for 3 days is shown in Table 3.13 and Figure 3.15.

Table 3.13 The total peaks of RNase A after digestion by pronase with and without adding more enzyme. Hydrolysis was performed at pH 8.5, 60°C, and all data were collected in triplicate.

Time (h)	Total peaks found	
	Pronase is only added at the beginning of the reaction	Pronase is added every 24 hours for 72 hours.
1	22±3.61	22±3.61
2	26±2.25	26±2.25
4	29±2.08	29±2.08
6	29±1.53	29±1.53
24	25±2.31	25±2.31
48	20±2.08	22±2.89
72	16±2.08	25±2.52

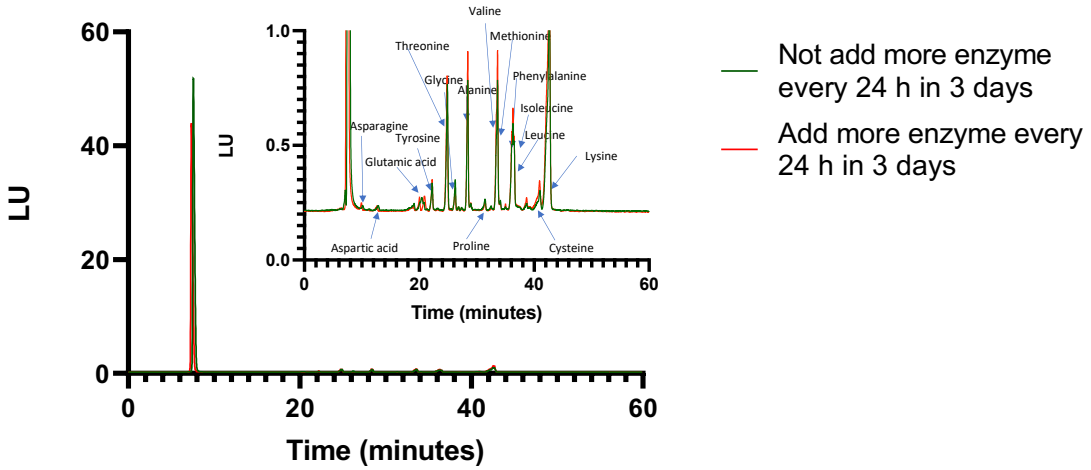

Figure 3.15 Comparison of chromatogram RNase A digestion using pronase for 3 days. The chromatogram shows that the peak height of the amino acid peaks in adding more enzymes every 24 hours is higher than when not adding more enzymes in the same condition.

From the results in Figure 3.15, the chromatogram between 20.0-21.0 minutes shows that adding more enzymes can digest the peptide at a retention time of 20.4 minutes to 2 peaks (19.0 and 20.9 minutes, green circle). The peak at 20.4 minutes is not related to the amino acid standard. It is defined as a peptide fragment. The peak at 20.9 minutes is related to glutamic acid standard retention time.

The results show that adding the enzyme every 24 hours to digest the RNase A can increase the hydrolysis more than adding the enzyme once at the start. Adding additional enzyme can replace the inactivated enzyme.

The summary of each enzyme digestion condition is shown in Table 3.14.

Table 3.14 Summary of enzyme digestion conditions

Enzyme	Digestion conditions		
	Temperature (^{o}C)	pH	Time (hours)
Pepsin	37	<2	24
Trypsin	60	8.5	24
LAP	55	8.5	24
Pronase	60	8.5	72*

* adding more enzyme every 24 hours.

3.3.3.1.4 Using a combination of enzymes

Each enzyme in the study has a specific cleavage site, as shown in Table 3.1. The data from section 3.3.3.1.1-3.3.3.1.3 show that using a single enzyme cannot cleave the protein into single amino acids, which is required to meet the aims of this work. It was, therefore, hypothesized that a combination of enzymes could be used to effect cleavage to single amino acid residues. Denaturing of the disulphide bond could also be affected chemically prior to enzyme mediated hydrolysis. From the results described above, pepsin requires different optimised conditions for the other enzymes. The study was divided into two groups, as shown in Figure 3.16. The first group involves enzymes using the same pH condition, starting from trypsin, LAP and pronase. The second group started with pepsin and then adjusted the pH of the sample to 8.5 before adding trypsin, LAP and pronase.

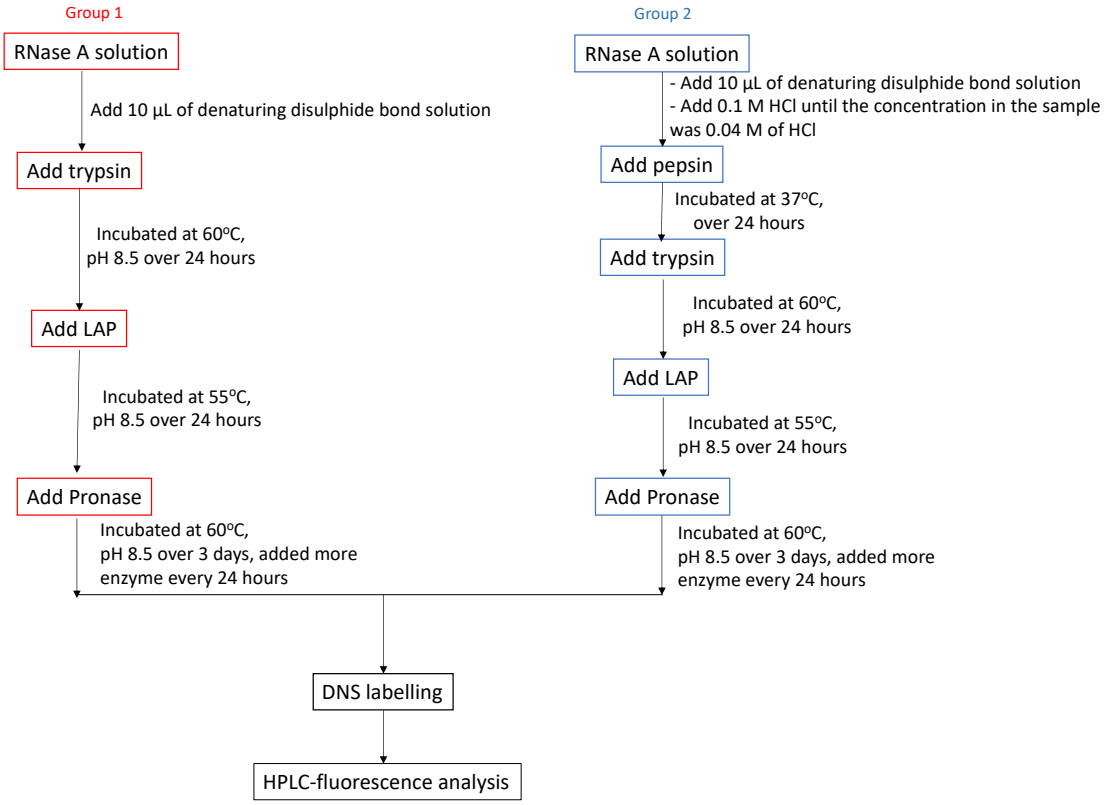

Figure 3.16 The workflow of using the combination of enzymes in RNase A digestion.

The results from the two approaches show that neither approach was effective for cleaving the protein sample to single amino acids, as presented in Figures 3.17 and 3.18.

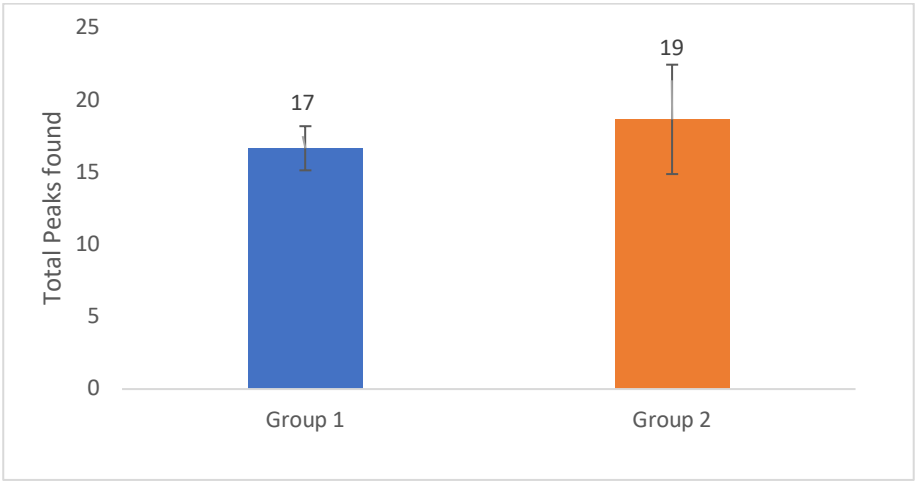

Figure 3.17 Comparison of the average total peaks found in the chromatogram of RNase A after digestion by 3 and 4 enzymes, and all experiments were done in triplicate.

(A)

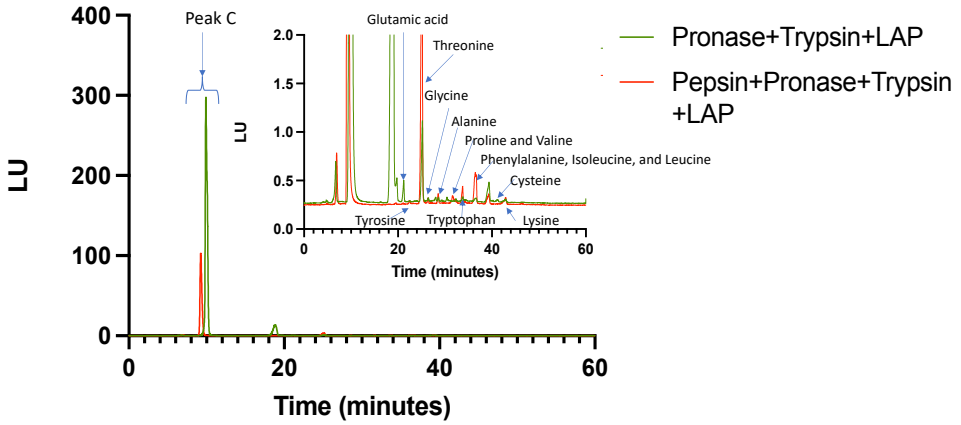

(B)

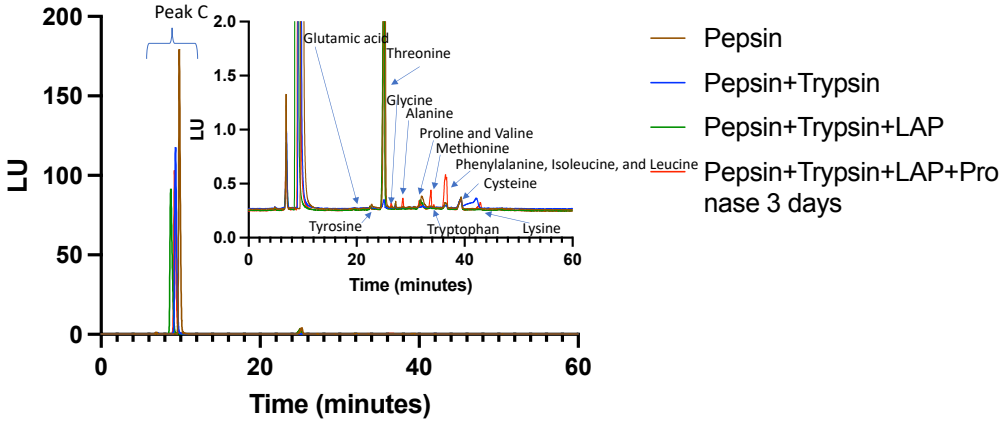

Figure 3.18 Comparison of chromatogram RNase A digestion by using the enzymes in sequence. (A) Comparison between using 3 and 4 enzymes as the sequence. (B) The digestion solution chromatogram results in the sequence starting from pepsin, trypsin, LAP and pronase after 3 days

The results from section 3.3.3.1.4 used the enzymes in a sequence that can cleave the protein sample from the peptide to a smaller size better than using a single enzyme from the optimisation steps (3.3.3.1.1 – 3.3.3.1.3). The peak height of peak C from using the enzymes in the sequence is smaller than peaks A and B from using individual enzymes for cleavage of the protein. This phenomenon can explain why pepsin (at the C-terminal site of phenylalanine, leucine, tyrosine, and tryptophan) cleaved RNase A to peptide fragments and some amino acids (threonine, proline, methionine, leucine, and isoleucine). Trypsin was used as the second enzyme. Trypsin causes specific cleavage at the C-terminal site of lysine and arginine amino acid residues: the third enzyme, LAP cleaved at the N-terminal of leucine residues. Pronase (a mix of protease enzyme and non-specific site cleavage) is chosen to cleave the small peptides to amino acids in the previous step. However, combination enzymes cannot digest RNase A to a single amino acid. The results from HPLC chromatograms (Figure 3.18 (B)) show a large peak C at 9.0-10.0 minutes, defined as a peptide fragment, which decreased but was still found in the sample. The results show that using four kinds of enzymes cannot cleave the protein model to a single amino acid.

3.3.3.1.5 Chemical hydrolysis

From the enzyme digestion results, the protein sample cannot be digested to a single amino acid using enzymes alone. Chemical hydrolysis was therefore also studied in order to effect complete hydrolysis of the peptide fragments that resulted from enzyme digestion. The chemical reagents were selected with consideration for compatibility requirements when the method is applied to more complex glycoprotein samples for future study. 1 M HCl and 1 M acetic acid were selected. The 100 µL of sample solution was added with 100 µL of each acid at 70°C. The sample was analysed at various time points between 1-24 hours. The reaction was stopped by adding 1 M NaOH to basify the solution to pH 9.5 before analysis. The results demonstrate that 1 M HCl produces a solution with more fragments than that from treatment with 1 M acetic acid, as shown in Figures 3.19 and 3.20.

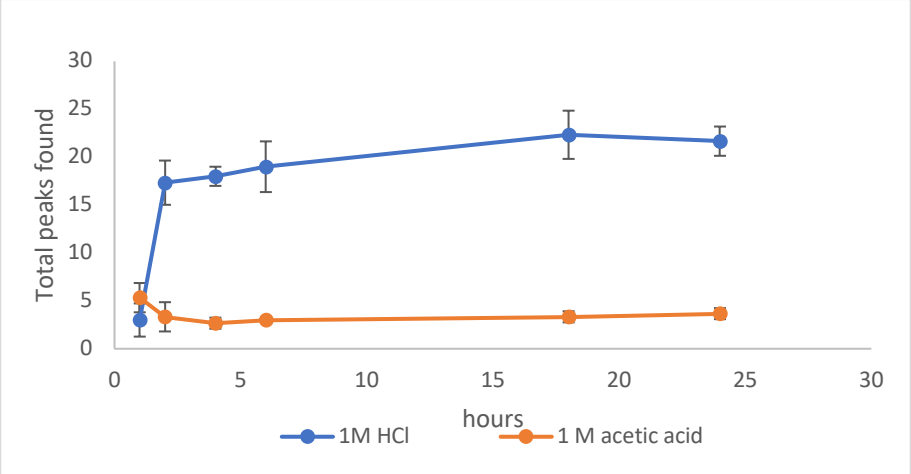

Figure 3.19 Comparison of the total peaks of RNase A after hydrolysis with either 1 M HCl or 1 M acetic acid at 70°C after 24 hours, and all data were collected in triplicate.

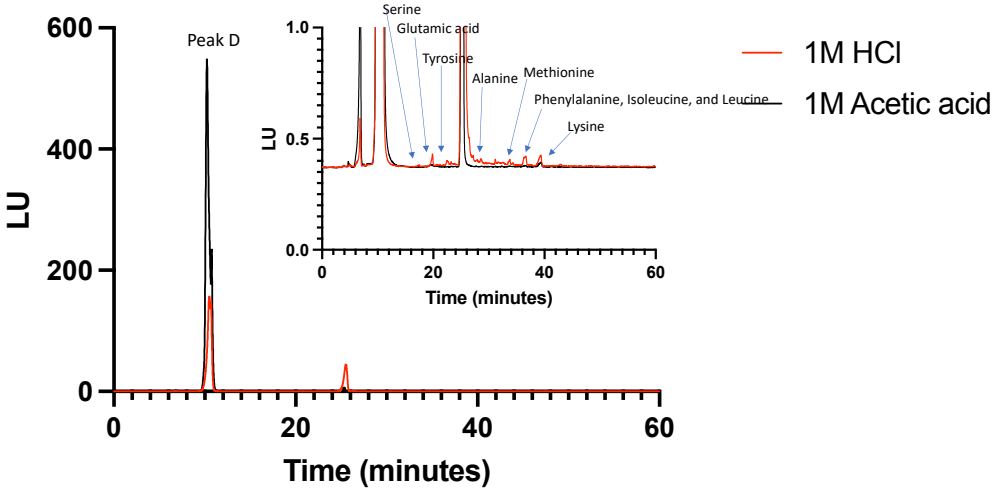

Figure 3.20 Comparison of chromatogram RNase A hydrolysis by 1 M HCl and 1 M acetic acid.

Figures 3.19 and 3.20 show that 1 M HCl is more effective in RNase A hydrolysis than 1 M acetic acid. The biggest peak (peak D) is smaller when using 1 M HCl than 1 M acetic acid. The total peaks found in the 1 M HCl hydrolysis sample were more than 1 M acetic acid. 1 M HCl was chosen for hydrolysis of the sample after the enzyme digestion in the previous step. However, a temperature of 70°C can damage the sugar in the glycan [82, 83]. The conditions were further investigated to identify whether lower temperatures of 40-60°C would allow effective

hydrolysis. This was again to identify conditions that would be compatible with more complex glycoprotein samples.

The reaction was stopped by adding 1 M NaOH to basify the solution to pH 9.5 before labelling with DNS. Using 1 M HCl at 60 and 70°C produces the most fragments in 90 minutes, as shown in Figures 3.21 and 3.22. The average peak height of peak E in the various temperatures is shown in Table 3.1. The temperature was chosen at 60°C.

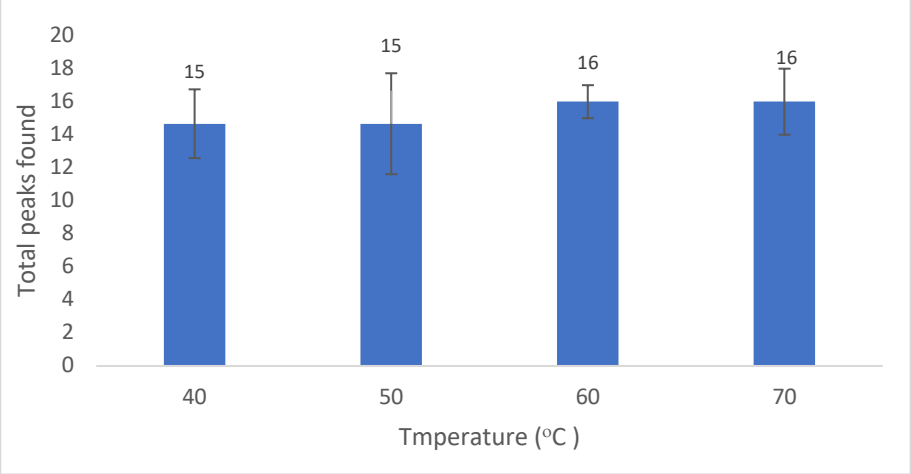

Figure 3.21 The total peaks found of RNase A after digestion by 1 M HCl with various temperatures, and all data were collected in triplicate.

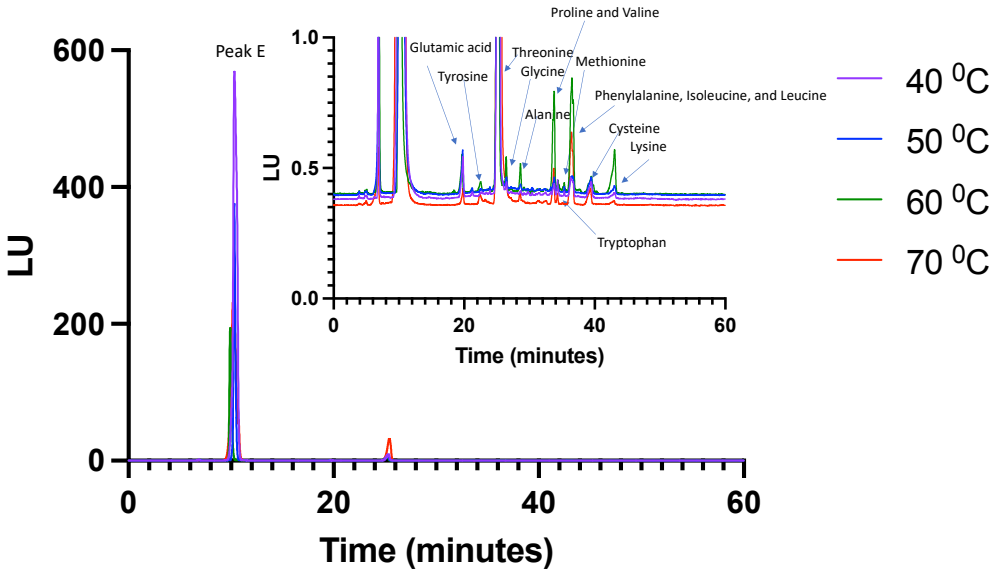

Figure 3.22 HPLC chromatogram of RNase A digestion at various temperatures by 1 M HCl.

Table 3.15 The average peak height of the peak E various temperatures for RNase A digestion with 1 M HCl in 90 minutes, and all data were collected in triplicate.

Temperature (^{o}C)	The average peak height of the peak E
40	589 ± 80.88
50	369 ± 33.06
60	199 ± 23.90
70	354 ± 28.62

3.3.3.1.6 Combining enzyme digestion and acid hydrolysis

The next step was to combine the optimized enzyme digestion protocol from section 3.3.3.1 with optimized acid hydrolysis studies using 1 M HCl. The combined method did not break down RNase A into individual amino acids even after exposure to four enzymes and 1 M HCl for 72 hours, as the HPLC chromatogram shown in Figure 3.23.

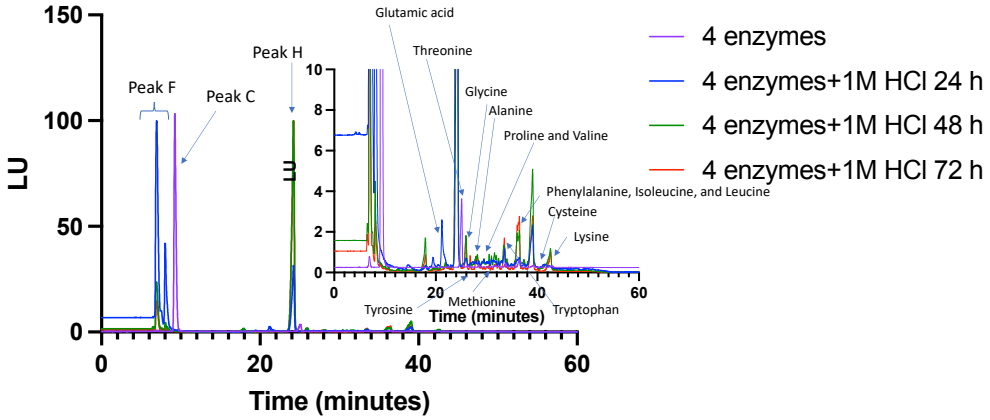

Figure 3.23 HPLC chromatogram of RNase A digestion at various times by 1 M HCl after enzyme digestion.

The data of RNase A hydrolysis using the combination of four enzymes and 1 M HCl show that the peak C from enzyme digestion decreased when adding 1 M HCl for 24 hours. Peak F appeared in acid hydrolysis. This peak decrease is related to the duration of hydrolysis. However, peak H appeared in the acid hydrolysis after enzyme digestion. This peak is related to peak F. The more peak F decreases, the more peak H increases. The peak height of peak H after hydrolysis for 48 and 72 h is not different, as shown in Table 3.16 below.

Table 3.16 The average peak height of the peak E at various times for RNase A digestion with 1 M HCl at 60^{o}C after four enzyme digestion, and all data were collected in triplicate.

Time (h)	The average peak height	
	Peak F	Peak H
24	80 ± 8.74	34 ± 9.45
48	25 ± 6.11	100 ± 11.14
72	16 ± 5.03	100 ± 11.24

The results from using 1 M HCl hydrolysis after digestion using four enzymes show no difference in the largest peptide fragments (peak F and H) after 48 hours of the hydrolysis reaction. The effect on hydrolysis of increasing HCl concentration between 2-5 M was also studied. In all

cases, this was studied subsequent to the digestion using four enzymes, and the results are shown in Figure 3.24, 3.25 and Table 3.17.

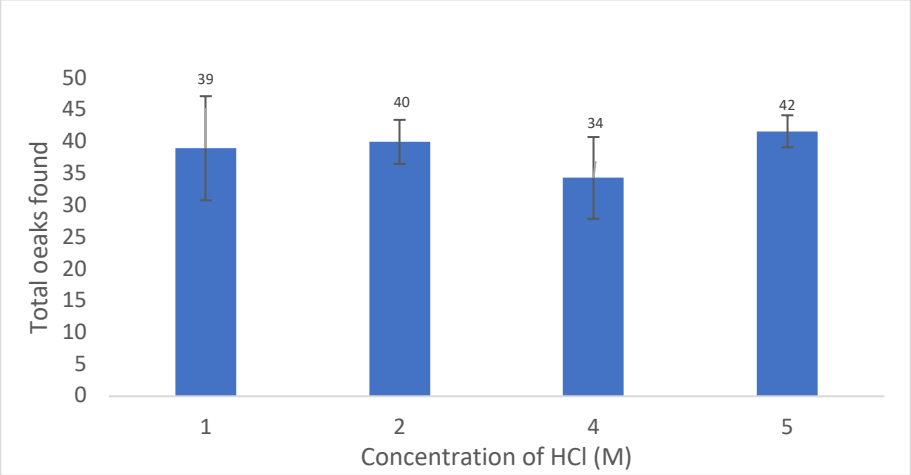

Figure 3.24 The total peaks of RNase A were found after digestion by four enzymes and HCl with various concentrations for 72 hours of acid hydrolysis, and all experiments were done in triplicate.

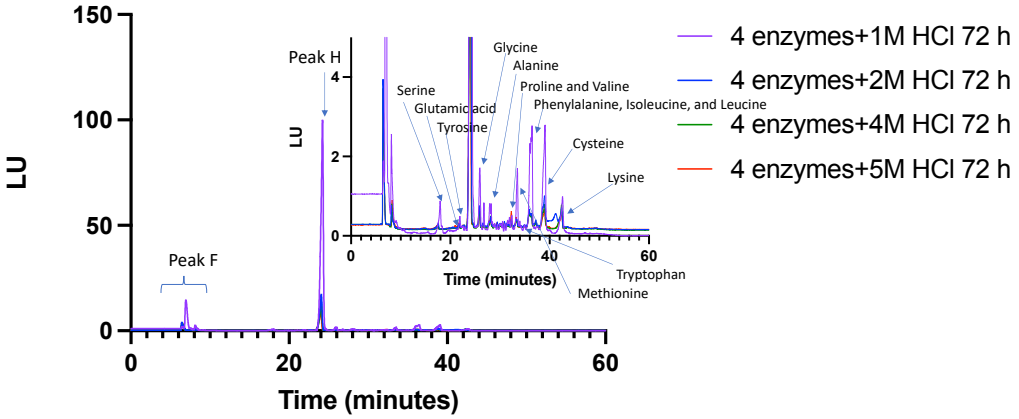

Figure 3.25 HPLC chromatogram of fragments RNase A digested by four enzymes and 1-5 M HCl.

Table 3.17 The average peak height of the peak E at various times for RNase A digestion with 1 M HCl at 60°C, 72 hours after four enzymes digestion, and all experiments were done in triplicate.

Concentration of HCl (M)	The average peak height	
	Peak F	Peak H
1	16 ± 5.03	100 ± 11.24
2	4 ± 1.53	17 ± 3.00
4	4 ± 1.00	13 ± 4.04
5	4 ± 1.53	10 ± 4.04

The results of varied HCl concentration (1-5 M) for hydrolysis after using four enzymes for digestion of RNase A show that with increased concentration of HCl, the peptide peaks (peak F and H) decreased. However, increasing the concentration of HCl to 5 M cannot hydrolyse RNase A into single amino acid fragments. Figure 3.4 shows RNase A should have histidine, arginine,

asparagine, and aspartic acid (the retention time in chromatograms 7.3, 7.6, 10.1, and 12.8, respectively). But the results in Figure 3.25 show peak F at 6.6-7.2 and 8.2-9.1 minutes. The peaks related to histidine, arginine, asparagine, and aspartic acids do not appear in the chromatograms. Peak H has a retention time of 24.0-24.5 minutes. This peak has a retention time near threonine (24.9 minutes). When the acid concentration increases, the peak height of peak H decreases, as shown in Table 3.17. However, the threonine peak does not appear.

The results show that all concentrations of hydrochloric acid studied cannot produce complete hydrolysis of RNase A to single amino acid fragments.

3.4 Conclusions and Future Work

N- and *O*-glycans are attached to amino acids in the peptide chain of protein sequences. An ongoing challenge in glycome analysis is developing a method that effects the release of all core *O*-glycans as well as the subsequent simultaneous analysis of *N*- and *O*-glycans in the same HPLC sample. In this study, we hypothesized that if proteins within glycoproteins could be digested into single amino acids, the amines of the released amino acids, and the *N*- and *O*-linked amino acid glycans could be labelled with a fluorophore. These could then be analysed and quantified by HPLC in conjunction with a fluorescence detector, with each *N*- and *O*-linked amino acid glycan having a different retention time in the HPLC system. Using this approach, it was hypothesized that the qualitative and quantitative HPLC analysis of all glycans could be achieved in one injection.

DNS was chosen as a labelling reagent as it can label primary and secondary amines. Labelling amino acids with DNS was optimized using valine by considering the concentration of DNS, temperature and pH of the reaction condition. The labelling condition with valine was applied to 18 amino acids individually and then confirmed in the 19 amino acids mixture solution. The labelling condition was 500 μL of 100 mM of DNS solution in acetone, 100 μL of 19 amino acids mixture solution (0.02-1 mmol/mL in 0.1 M HCl), and 300 μL of 20 g/L of sodium hydrogen carbonate (adjust pH to 9.6), incubated in a shaking box in the dark at 60^{o}C. The reaction was stopped by adding 500 μL of 25% (w/v) ammonium hydroxide. The reaction was completed in 1.5 hours and reverse-phase HPLC was used to determine the retention times of the labelled amino acids. Some labelled amino acids could not be completely separated (phenylalanine, isoleucine and leucine). The retention time of labelled amino acid standards was compared to the model protein sample hydrolysis experiment results.

Hydrolysis of a simple (non-glycoprotein) protein sample (RNase A) was studied as a model system, using various enzymes and mild acids considered compatible with *N*- and *O*-glycans. The optimisation of each enzyme's digestion conditions was first studied with respect to the temperature, pH, and reaction time. The benefit of the efficiency of the reaction of adding additional enzymes throughout the reaction was also probed. Except for pronase, adding more enzymes daily for at least 3 days caused more effective hydrolysis [31, 34, 37]. Using a single enzyme proved ineffective for hydrolysing the protein to single amino acid residues. Hence, sequential usage of a range of enzymes was used in an attempt to digest the model system RNase A to smaller peptides and amino acids. The results show that four enzymes (pepsin, trypsin, LAP, and pronase) cannot hydrolyse the RNase A to single amino acid fragments. Acid hydrolysis (1-5 M HCl) was investigated after enzyme hydrolysis. The peak hight of the largest peaks from the enzyme's hydrolysis decreased, but not completely hydrolysis to the single amino acid.

Future work will focus on improving the protein hydrolysis method from the biological mimic to complete the protein digestion to single amino acids. This approach can then analyse the *N*- and *O*-amino glycans in the protein sequences.

3.5 Experimental

3.5.1 General experiment

All chemicals used were analytical or HPLC grade, purchased from commercial sources (Sigma-Aldrich, Merk, Fisher Scientific, Alfa Aesar and Acros Organics), and used without further purification. HPLC analytical column (Columbus, C18) was purchased from Phenomenex (UK). The experiments were monitored by TLC using aluminium-backed 60 F254 silica plates (Sigma Merk). Visualisation was then carried out under UV light (λ= 254 nm) or via ninhydrin solution with heating to effect staining.

3.5.2 Analytical Equipment

Thin-layer Chromatography
The progress of all the labelling reactions was followed by TLC using either isopropanol:DCM:acetic acid (7:2:1) or isopropyl alcohol:DCM:acetic acid (7:1:2) as the mobile phase, and detection was achieved using UV irradiation (254 nm) and staining with ninhydrin solution. This allowed the end of the reaction to be determined as the point when no amino acid standard was detectable.

High-performance liquid chromatography
Reverse phase mode HPLC was performed on an Agilent 1100 series HPLC system linked to an Agilent G1321A FLD detector and a G1314A variable wavelength detector. A Columbus C18 column (250 x 4.6 mm, 5 μM particle size) with a C18 guard column (15 x 3.2 mm, 5 μM particle size) was used for the separations. Solvent A was composed of 0.1% Formic acid in water, while solvent B consisted of 0.1% Formic acid in ACN. The flow rate was set at 0.6 mL/ min, and the column was maintained at 45^{o}C for the duration of the run.

Separation of labelled amino acids took place over 60 minutes with a linear gradient beginning with 20% phase B at 10 minutes, with a further gradient to 60% in 20 minutes, maintaining 60% for 15 minutes before returning to injection condition of 20% B between 5 minutes, maintain 20% for 10 minutes before the next injection. The column was conditioned with 20% B, 5 minutes before the next injection. The injection volume was 2 μL per injection. The fluorescence detection used the excitation wavelength of 330 nm and emission wavelength of 500 nm. The Fluorescence absorptivity detection was reported as luminescence unit (LU) represent to the Agilent system.

3.5.3 Solvents and Buffer

Working DNS solution
DNS stock solution was weighed and diluted in acetone to a final concentration of 100 mM. The solution was stored in a dark container at -20^{o}C.

Sodium hydrogen carbonate solution
Sodium hydrogen carbonate was weighed and diluted in water to a final concentration of 20 g/L, and pH was adjusted to 9.6 with 1 M NaOH solution. The solution was stored in a closed container at room temperature.

Amino acid standard solution
The 19 amino acids standard solution mixture was prepared at concentrations between 0.02-1.0 mmol/mL in 0.1 M HCl.

RNase A solution
The RNase A solution was prepared at a 1 mg/mL concentration in 0.01 M Tris solution, pH 8.5. The sample solution was heated to 100^{o}C for 15 minutes and slowly cooled to room temperature. The sample was stored in closed containers at -20^{o}C.

Working LAP
The stock LAP was prepared in 10 mg/mL concentration in 0.1 M phosphate buffer pH 7.0. The stock solution was kept at -20^{o}C before use. The working LAP was prepared using 1 µL of stock solution and adjusted volume to 100 µL with 5 mM of magnesium chloride solution in 5 mM of Tris solution, pH 8.5. The working solution must be pretreated at 40^{o}C for 30 minutes before use.

Working Pepsin
The stock pepsin was prepared at 10 mg/mL in 1 mM hydrochloric acid (pH<2.0). The stock solution was kept at -20^{o}C before use. The working pepsin was prepared using 500 µL of stock solution and adjusted volume to 1000 µL with water, as pepsin works at low pH conditions. This experiment adjusted the sample solution by 1 M hydrochloric acid until the concentration of hydrochloric acid in the sample was 0.04 M, for the temperature optimisation was 37^{o}C.

Working Pronase
The stock pronase was prepared in water at a 10 mg/mL concentration. The stock solution was kept at -20^{o}C before use. The solution of working pronase was prepared using 100 µL of stock solution, adding 100 µL of 100 mM calcium chloride solution in water and adjusting the volume to 1000 µL with 0.1 M Tris solution, pH 8.5.

Working Trypsin
The stock trypsin was prepared in 1 mg/mL concentration in 1 mM hydrochloric acid. The stock solution was kept at -20^{o}C before use. The working trypsin was prepared using 100 µL of stock solution, adding 100 µL of 100 mM calcium chloride solution in water and adjusting the volume to 1000 µL with 0.1 M Tris solution, pH 8.5. The working solution must be pretreated at 57^{o}C for 15 minutes and then 37^{o}C for 1 hour before use.

Denaturing disulphide bonds solution.
2-Mercaptoethanol was weighed and diluted in water to a final concentration of 5% (w/v).

3.5.4 General labelling procedure for amino acids/peptides with DNS
The amino acid or peptide samples (100 µL) were added to a 1.5 mL dark centrifuge tube and mixed with the 300 µL sodium hydrogen carbonate solution pH 9.6. The DNS working solution was added (500 µL) to the reaction tube. The sample was incubated at 60^{o}C in a shaking box for 2 hours. The excess labelling reagent was removed with 500 µL of 25% ammonium hydroxide solution. The reaction solution was dried and kept at -20^{o}C until redissolved with 1% formic acid in HPLC water before HPLC analysis. The retention time of amino acids is shown in Table 3.7.

3.5.6 General enzymes hydrolysis of RNase A
The RNase A solution 1 mL was added to the 1.5 mL centrifuged tube. The denaturing disulphide solution (10 µL) was added. The hydrolysis reaction used enzymes to proteins at a ratio of 1:20 (by concentration). The sample digestion by pepsin was addition of 0.1 M HCl until the concentration of HCl in the sample was 0.04 M and incubated at 37^{o}C, pH<2 over 24 hours. The sample digestion by trypsin, LAP and pronase has adjusted the pH to 8.5 before adding enzymes. The sample with trypsin was incubated at 60^{o}C, pH 8.5 over 24 hours. The sample with LAP was incubated at 55^{o}C, pH 8.5 over 24 hours. The sample with pronase was incubated

at 60°C, pH 8.5 over 24 hours. Before collecting the sample, the sample tubes were heated to stop the digestion reaction (95°C, 20 minutes for pepsin, 100°C, 5 minutes for trypsin and LAP, and 85°C, 20 minutes for pronase). The sample solution (100 µL) was then labelled with DNS before HPLC analysis.

3.5.7 General acid hydrolysis of RNase A

The RNase A solution (100 µL) was added to the 1.5 mL centrifuged tube. The denaturing disulphide solution (10 µL) was added. 100 µL of 1 M HCl was added to the reaction tube and incubated in the shaking box at 60°C for 72 hours. The reaction was stopped by adding 1 M NaOH to adjust the pH to approximately 8.5. The solution from the hydrolysis tube (100 µL) was taken to a 1.5 mL dark centrifuge tube and labelled with DNS before HPLC analysis.

3.5.8 General sequence enzyme hydrolysis of RNase A

The RNase A solution (100 µL) was added to the 1.5 mL centrifuged tube. The denaturing disulphide solution (10 µL) was added. The pH of the sample solution was adjusted by the addition of 0.1 M HCl until the concentration of HCl in the sample was 0.04 M. The first enzyme was 5 µL of working pepsin. The tube was incubated at 37°C for 24 hours, and then 0.1 M of NaOH was added to adjust the pH to approximately 8.5. The second enzyme was 50 µL of working trypsin, and the sample was incubated at 60°C for 24 hours. The third enzymes was 8 µL of working LAP, incubated at 55°C for 24 hours. The last enzyme in the sequence was 5 µL of working pronase by adding the working pronase every 24 hours for 3 days and incubated at 60°C. The hydrolysis reaction was stopped by heating at 100°C for 20 minutes after 3 days of the pronase. The sample solution was taken 100 µL to a 1.5 mL dark centrifuge tube and labelled with DNS before HPLC analysis.

3.5.9 General sequence enzyme and acid hydrolysis of RNase A

The RNase A solution (100 µL) was added to the 1.5 mL centrifuged tube. The denaturing disulphide solution (10 µL) was added. The pH of the sample solution was adjusted by the addition of 1 M HCl until the concentration of hydrochloric acid in the sample was 0.04 M. 5 µL of working pepsin was added to the reaction tube. The tube was incubated at 37°C for 24 hours. 0.1 M of NaOH was added to adjust the pH to approximately 8.5. 50 µL of working trypsin was then added, and the sample was incubated at 60°C for 24 hours. The reaction tube was cooled to 55°C before adding 8 µL of working LAP. The tube was incubated at 55°C for 24 hours. 5 µL of working pronase was added to the reaction tube every 24 hours for 3 days and incubated at 60°C. The reaction was stopped by heating at 100°C for 20 minutes. After cooling, 100 µL of 1-5 M HCl was added to the reaction tube and incubated in the shaking box at 60°C for 72 hours. The reaction was stopped by adding 1 M NaOH to adjust the pH of approximately 8.5. The sample solution was taken 100 µL to a 1.5 mL dark centrifuge tube and labelled with DNS before HPLC analysis.

3.6 References

1. Helm, J., L. Hirtler, and F. Altmann, *Towards Mapping of the Human Brain N-Glycome with Standardized Graphitic Carbon Chromatography.* Biomolecules, 2022. **12**(1): p. 85.
2. Samal, J., et al., *Region-Specific Characterization of N-Glycans in the Striatum and Substantia Nigra of an Adult Rodent Brain.* Analytical Chemistry, 2020. **92**(19): p. 12842-12851.
3. García-Artalejo, J.A., et al., *Characterizing a novel hyposialylated erythropoietin by intact glycoprotein and glycan analysis.* Journal of Pharmaceutical Biomedical Analysis, 2022. **213**: p. 114686.
4. Hall, M.K., et al., *Limited N-Glycan Processing Impacts Chaperone Expression Patterns, Cell Growth and Cell Invasiveness in Neuroblastoma.* Biology (Basel), 2023. **12**(2): p.293.
5. Bradberry, M.M. and E.R. Chapman, *All-optical monitoring of excitation–secretion coupling demonstrates that SV2A functions downstream of evoked Ca2+ entry.* The Journal of Physiology, 2022. **600**(3): p. 645-654.
6. Kim, W., et al., *Qualitative and quantitative characterization of sialylated N-glycans using three fluorophores, two columns, and two instrumentations.* Analytical Biochemistry, 2019. **571**: p. 40-48.
7. Kishimoto, Y., et al., *Analysis of 2-aminopyridine labeled glycans by dual-mode online solid phase extraction for hydrophilic interaction and reversed-phase liquid chromatography.* J Chromatogr A, 2020. **1625**: p. 461194.
8. Wu, Y., et al., *Flowing on-line preparation of deglycosylation, labeling and purification for N-glycan analysis.* Talanta, 2022. **249**: p. 123652.
9. Kasim, M., et al., *Seamless Coupling of Chemical Glycan Release and Labeling for an Accelerated Protein N -Glycan Sample Preparation Workflow.* Bioengineering (Basel), 2023. **10**(6): p. 651.
10. Wu, Z.L. and J.M. Ertelt, *Fluorescent glycan fingerprinting of SARS2 spike proteins.* Scientific Reports, 2021. **11**(1): p.20428.
11. Morio, A., et al., *Expression, Purification, and Characterization of highly active Endo-α-Nacetylgalactosaminidases expressed by Silkworm-Baculovirus Expression System.* Journal of Asia-Pacific Entomology, 2019. **22**: p.404-408
12. Yan, S., et al., *Core Richness of N-Glycans of Caenorhabditis elegans: A Case Study on Chemical and Enzymatic Release.* Analytical Chemistry, 2018. **90**(1): p. 928-935.
13. Vreeker, G.C.M., et al., *O- and N-glycosylation analysis of cell lines by ultrahigh resolution MALDI-FTICR-MS.* International Journal of Mass Spectrometry, 2020. **448**: p. 116267.
14. Kurz, S., et al., *Separation and Identification of Permethylated Glycan Isomers by Reversed Phase NanoLC-NSI-MSn.* Molecular & Cellular Proteomics, 2021. **20**: p. 100045.
15. de Haan, N., et al., *In-Depth Profiling of O-Glycan Isomers in Human Cells Using C18 Nanoliquid Chromatography–Mass Spectrometry and Glycogenomics.* Analytical Chemistry, 2022. **94**(10): p. 4343-4351.
16. Wang, C.-Y., et al., *Surface Shave: Revealing the Apical-Restricted Uroglycome.* Journal of Proteome Research, 2022. **21**(2): p. 360-374.

17. Li, M., et al., *DiLeuPMP: A Multiplexed Isobaric Labeling Method for Quantitative Analysis of O-Glycans.* Analytical Chemistry, 2021. **93**(28): p. 9845-9852.
18. Perreault, V., et al., *Pretreatment of flaxseed protein isolate by high hydrostatic pressure: Impacts on protein structure, enzymatic hydrolysis and final hydrolysate antioxidant capacities.* Food Chem, 2017. **221**: p. 1805-1812.
19. Oussaief, O., et al., *Dromedary Milk Protein Hydrolysates Show Enhanced Antioxidant and Functional Properties.* Food Technol Biotechnol, 2020. **58**(2): p. 147-158.
20. Draher, J., *HPLC Determination of Total Tryptophan in Infant Formula and Adult/Pediatric Nutritional Formula Following Enzymatic Hydrolysis, Multilaboratory Testing Study: Final Action 2017.03.* J AOAC Int, 2019. **102**(5): p. 1567-1573.
21. Shimamoto, S., et al., *Chemical Digestion of the -Asp-Cys- Sequence for Preparation of Post-translationally Modified Proteins.* Protein Journal, 2020. **39**(6): p. 711-716.
22. Pane, K., et al., *Chemical Cleavage of an Asp-Cys Sequence Allows Efficient Production of Recombinant Peptides with an N-Terminal Cysteine Residue.* Bioconjugate Chemistry, 2018. **29**(4): p. 1373-1383.
23. Bae, J.W., et al., *Chemical RNA digestion enables robust RNA-binding site mapping at single amino acid resolution.* Nature Structural and Molecular Biology, 2020. **27**: p. 678-682.
24. Di Stasio, L., et al., *In vitro gastroduodenal and jejunal brush border membrane digestion of raw and roasted tree nuts.* Food Research International, 2020. **136**: p. 109597.
25. Štreimikytė, P., et al., *Formulating protein-based beverages for the dysphagia diets of the elderly: viscosity, protein quality, in vitro digestion, and consumers acceptability.* Journal of the Science of Food and Agriculture, 2020. **100**(10): p. 3895-3901.
26. Wu, T., et al., *Effects of chemical composition and baking on in vitro digestibility of proteins in breads made from selected gluten-containing and gluten-free flours.* Food Chemistry, 2017. **233**: p. 514-524.
27. Grancieri, M., H.S.D. Martino, and E. Gonzalez de Mejia, *Digested total protein and protein fractions from chia seed (Salvia hispanica L.) had high scavenging capacity and inhibited 5-LOX, COX-1-2, and iNOS enzymes.* Food Chemistry, 2019. **289**: p. 204-214.
28. Wang, Q., et al., *Comprehensive N- and O-Glycoproteomic Analysis of Multiple Chinese Hamster Ovary Host Cell Lines.* Journal of Proteome Research, 2022. **21**(10): p. 2341-2355.
29. You, X., et al., *Chemoenzymatic Approach for the Proteomics Analysis of Mucin-Type Core-1 O-Glycosylation in Human Serum.* Analytical Chemistry, 2018. **90**(21): p. 12714-12722.
30. Zheng, Y.Z. and M.L. DeMarco, *Manipulating trypsin digestion conditions to accelerate proteolysis and simplify digestion workflows in development of protein mass spectrometric assays for the clinical laboratory.* Clinical Mass Spectrometry, 2017. **6**: p. 1-12.

31. Erdőssy, J., et al., *Enzymatic digestion as a tool for removing proteinaceous templates from molecularly imprinted polymers.* Analytical Methods, 2017. **9**(31): p. 4496-4503.
32. Ding, Y., et al., *Protective Effects of Novel Antioxidant Peptide Purified from Alcalase Hydrolysate of Velvet Antler Against Oxidative Stress in Chang Liver Cells in Vitro and in a Zebrafish Model In Vivo.* Int J Mol Sci, 2019. **20**(20): p.5187
33. Zhang, R., et al., *Antioxidant capacity of proteins and hydrolysates from the liver of newborn piglets, and their inhibitory effects on steatosis in vitro.* Food technology and biotechnology, 2020. **58**(4): p. 455-464.
34. Costantini, A., et al., *How cereal flours, starters, enzymes, and process parameters affect the in vitro digestibility of sourdough bread.* Food research international, 2022. **159**: p. 111614-111614.
35. Joshi, I., S. Sudhakar, and R.A. Nazeer, *Anti-inflammatory Properties of Bioactive Peptide Derived from Gastropod Influenced by Enzymatic Hydrolysis.* Appl Biochem Biotechnol, 2016. **180**(6): p. 1128-1140.
36. Orsini, S., et al., *Characterization of Degraded Proteins in Paintings Using Bottom-Up Proteomic Approaches: New Strategies for Protein Digestion and Analysis of Data.* Analytical Chemistry, 2018. **90**(11): p. 6403-6408.
37. Nuchprapha, A., et al., *Two novel ACE inhibitory peptides isolated from longan seeds: purification, inhibitory kinetics and mechanisms.* RSC advances, 2020. **1**(22): p. 12711-1272.
38. Guapo, F., et al., *Fast and efficient digestion of adeno associated virus (AAV) capsid proteins for liquid chromatography mass spectrometry (LC-MS) based peptide mapping and post translational modification analysis (PTMs).* Journal of pharmaceutical and biomedical analysis, 2022. **207**: p. 114427-114427.
39. Edwards, T.S., et al., *A simple method to generate β-casomorphin-7 by in vitro digestion of casein from bovine milk.* Journal of functional foods, 2021. **85**: p. 104631.
40. Hou, C., et al., *Purification and Identification of Antioxidant Alcalase-Derived Peptides from Sheep Plasma Proteins.* Antioxidants (Basel), 2019. **8**(12): p.592
41. Stachowicz, A., et al., *Optimization of quantitative proteomic analysis of clots generated from plasma of patients with venous thromboembolism.* Clinical Proteomics, 2017. **14**(1): p. 38.
42. Kailash, V., et al., *SPACEPro: A Software Tool for Analysis of Protein Sample Cleavage for Tandem Mass Spectrometry.* Journal of Proteome Research, 2021. **20**(4): p. 1911-1917.
43. Park, S., et al., *Wash-Free Amperometric Escherichia coli Detection via Rapid and Specific Proteolytic Cleavage by Its Outer Membrane OmpT.* Analytical chemistry (Washington), 2022. **94**(11): p. 4756-4762.
44. Wanat, W., et al., *Phosphonic acid analogues of phenylglycine as inhibitors of aminopeptidases: Comparison of porcine aminopeptidase N, Bovine Leucine aminopeptidase, tomato acidic leucine aminopeptidase and aminopeptidase from barley seeds.* Pharmaceuticals (Basel, Switzerland), 2019. **12**(3): p. 139.
45. Morelos-Castro, R.M., et al., *Expression analyses of digestive enzymes during early development and in adults of the chame fish Dormitator latifrons.* Aquaculture research, 2020. **51**(1): p. 265-275.

46. Oussaief, O., et al., *Dromedary Milk Protein Hydrolysates Show Enhanced Antioxidant and Functional Properties.* Food technology and biotechnology, 2020. **58**(2): p. 147-158.
47. Al-Amrani, S., et al., *Proteomics: Concepts and applications in human medicine.* World J Biol Chem, 2021. **12**(5): p. 57-69.
48. Esparza, C., et al., *Suitable analysis of α-amino acids by a direct combination of thin-layer chromatography and matrix-assisted laser desorption/ionization mass spectrometry in conjunction with post-chromatographic fixed-charge derivatization.* Journal of Chromatography A, 2020. **1626**: p. 461335.
49. Michel, M., et al., *Method comparison of HPLC-ninhydrin-photometry and UHPLC-PITC-tandem mass spectrometry for serum amino acid analyses in patients with complex congenital heart disease and controls.* Metabolomics, 2020. **16**(12): p. 128-128.
50. Aubrey, A., et al., *The Urey Instrument: An Advanced In Situ Organic and Oxidant Detector for Mars Exploration.* Astrobiology, 2008. **8**: p. 583-95.
51. Onozato, M., et al., *Amino acid analyses of the exosome-eluted fractions from human serum by HPLC with fluorescence detection.* Practical Laboratory Medicine, 2018. **12**: p. e00099.
52. Alnajjar, A.O., et al., *Utilization of 4-fluoro-7-nitro-2,1,3-benzoxadiazole (NBD-F) as a fluorogenic reagent for the development of a spectrofluorometric assay method for taurine in energy drinks.* Journal of Chemical Research, 2022. **46**(5): p. 17475198221114760.
53. Kirkan, E. and C. Aydogan, *Free Amino Acid Analysis in Honey Samples by Hydrophilic Interaction Liquid Chromatography with UV Detection Using Precolumn Derivatization with Dansyl Chloride.* Chromatographia, 2021. **84**(2): p. 127-133.
54. Ai, Y., et al., *Determination of biogenic amines in different parts of lycium barbarum L. By HPLC with precolumn dansylation.* Molecules (Basel, Switzerland), 2021. **26**(4): p. 1046.
55. Mir-cerdà, A., et al., *Data Fusion Approaches for the Characterization of Musts and Wines Based on Biogenic Amine and Elemental Composition.* Sensors (Basel, Switzerland), 2022. **22**(6): p. 2132.
56. Mir-Cerdà, A., et al., *Oenological processes and product qualities in the elaboration of sparkling wines determine the biogenic amine content.* Fermentation (Basel), 2021. **7**(3): p. 144.
57. Esposito, F., et al., *Level of biogenic amines in red and white wines, dietary exposure, and histamine-mediated symptoms upon wine ingestion.* Molecules (Basel, Switzerland), 2019. **24**(19): p. 3629.
58. Iwata, N., et al., *A Novel Determination Method of Thirty-Seven o-Phthalaldehyde-Derivatized D/L-Amino Acids with Complementary Use of Two Chiral Thiols by High Performance Liquid Chromatography.* CHROMATOGRAPHY, 2021: p. 2021.012.
59. Furusho, A., et al., *High-Performance Liquid Chromatographic Determination of Chiral Amino Acids Using Pre-Column Derivatization with o-Phthalaldehyde and N-tert-Butyloxycarbonyl-D-cysteine and Application to Vinegar Samples.* CHROMATOGRAPHY, 2020. **41**(3): p. 147-151.

60. Gkantiri, A.-M., et al., *HPLC method with post-column derivatization for the analysis of endogenous histidine in human saliva validated using the total-error concept.* Amino acids, 2022. **54**(3): p. 399-409.
61. Li, J.S., et al., *The variation in the levels of 18 amino acids in the cortex and plasma of cerebral ischemia C57BL/6 mice.* Biomedical chromatography, 2021. **35**(6): p. e5084.
62. Kahsay, B.N., et al., *Development and Validation of a Simple, Selective, and Accurate Reversed-Phase Liquid Chromatographic Method with Diode Array Detection (RP-HPLC/DAD) for the Simultaneous Analysis of 18 Free Amino Acids in Topical Formulations.* Chromatographia, 2022. **85**(7): p. 665-676.
63. Micikas, R., et al., *A Scalable Synthesis of the Blue Fluorescent Amino Acid 4-Cyanotryptophan and the Fmoc Derivative: Utility Demonstrated with the Influenza M2 Peptide Tetramer.* Organic Letters, 2021. **23**(4): p. 1247-1250.
64. Naffa, R., et al., *Comparison of liquid chromatography with fluorescence detection to liquid chromatography-mass spectrometry for amino acid analysis with derivatisation by 6-aminoquinolyl-N-hydroxysuccinimidyl-carbamate: Applications for analysis of amino acids in skin.* Arabian journal of chemistry, 2020. **13**(2): p. 3997-4008.
65. Mohammad, A., et al., *Detection reagents used in on-plate identification of amino acids by thin layer chromatography: A review.* Journal of Liquid Chromatography & Related Technologies, 2018. **41**(10): p. 595-603.
66. Pickens, C.A. and K. Petritis, *High resolution mass spectrometry newborn screening applications for quantitative analysis of amino acids and acylcarnitines from dried blood spots.* Analytica chimica acta, 2020. **1120**(C): p. 85-96.
67. Fernández-del-Campo-García, M.T., et al., *Rapid and reliable analysis of underivatized amino acids in urine using tandem mass spectrometry.* Microchemical journal, 2022. **172**: p. 106914.
68. Seo, C., et al., *Metabolomic analysis of amino acids and organic acids in aging mouse eyes using gas chromatography–tandem mass spectrometry.* Biomedical chromatography, 2022. **36**(3): p. e5298.
69. Lee, H.-S., et al., *Characterization of Ripening Bananas by Monitoring the Amino Acid Composition by Gas Chromatography-Mass Spectrometry With Selected Ion Monitoring and Star Pattern Analysis.* Analytical letters, 2019. **52**(16): p. 2496-2505.
70. Farcas, A.C., et al., *Analysis of Fatty Acids, Amino Acids and Volatile Profile of Apple By-Products by Gas Chromatography-Mass Spectrometry.* Molecules (Basel, Switzerland), 2022. **27**(6): p. 1987.
71. Desmons, A., et al., *Direct liquid chromatography tandem mass spectrometry analysis of amino acids in human plasma.* JOURNAL OF CHROMATOGRAPHY A, 2020. **1622**: p. 461135.
72. Phipps, W.S., et al., *Quantitative amino acid analysis by liquid chromatography-tandem mass spectrometry using low cost derivatization and an automated liquid handler.* JIMD reports, 2020. **51**(1): p. 62-69.
73. Raimbault, A., A. Noireau, and C. West, *Analysis of free amino acids with unified chromatography-mass spectrometry—application to food supplements.* JOURNAL OF CHROMATOGRAPHY A, 2020. **1616**: p. 460772.

74. Yousefinejad, S., et al., *Structure–retardation factor relationship of natural amino acids in two different mobile phases of RP-TLC.* Journal of Liquid Chromatography & Related Technologies, 2020. **43**(15-16): p. 580-588.
75. Sun, B., et al., *Probing the Proteomics Dark Regions by VAILase Cleavage at Aliphatic Amino Acids.* Analytical Chemistry, 2020. **92**(3): p. 2770-2777.
76. Espinosa, L.A., et al., *In-solution buffer-free digestion allows full-sequence coverage and complete characterization of post-translational modifications of the receptor-binding domain of SARS-CoV-2 in a single ESI–MS spectrum.* Analytical and bioanalytical chemistry, 2021. **413**(30): p. 7559-7585.
77. Liu, S.-J., et al., *A comparative analysis of derivatization strategies for the determination of biogenic amines in sausage and cheese by HPLC.* Food Chemistry, 2018. **266**: p. 275-283.
78. Yao, J., et al., *A sensitive method for the determination of the gender difference of neuroactive metabolites in tryptophan and dopamine pathways in mouse serum and brain by UHPLC-MS/MS.* Journal of Chromatography B, 2018. **1093-1094**: p. 91-99.
79. Zhang, X., et al., *Synthesis and Evaluation of Three Azide-Modified Disaccharide Oxazolines as Enzyme Substrates for Single-Step Fc Glycan-Mediated Antibody-Drug Conjugation.* Bioconjugate chemistry, 2022. **33**(6): p. 1179-1191.
80. Su, Y., et al., *All-in-One azides: empowered click reaction for in vivo labeling and imaging of biomolecules.* Chemical Communications, 2016. **52**(10): p. 2185-2188.
81. Minoru, K., *Temperature and pH dependency of pepsin activity in the gastric juice of farmed Pacific bluefin tuna Thunnus orientalis.* Aquaculture Science, 2015. **63**: p. 459-461.
82. Kwon, J., et al., *Glycan Stability and Flexibility: Thermodynamic and Kinetic Characterization of Nonconventional Hydrogen Bonding in Lewis Antigens.* Journal of the American Chemical Society, 2023. **145**(18): p. 10022-10034.
83. Radovani, B., G. Lauc, and I. Gudelj, *Storage stability and HILIC-UHPLC-FLR analysis of immunoglobulin G N-glycome from saliva.* Analytical and Bioanalytical Chemistry, 2023. **415**(28): p. 6985-6993.

Chapter 4
Enrichment methods for labelled glycans

4.1 Introduction

Glycan profiles can be used as biomarkers in many diseases, such as neurodegenerative diseases, cancers, cardiovascular disease, and metabolic syndrome [1-4]. Analysis of the glycan's profile in the biological samples usually uses HPLC combined with various detectors. The structures of the glycans lack chromophores or fluorophores and are often not amenable for ionisation. The derivatisation of the structure of the glycans to facilitate detection must, therefore, be developed. HPLC-MS or HPLC-MS/MS have been used for non-derivatised and derivatised glycans. This method is usually used for glycan mapping and identification of the unknown glycan samples in the biological samples [5-8]. HPLC-fluorescence is usually used for the derivatised glycans. The most important part of the HPLC glycan analysis workflow is the enrichment or purification of the sample before HPLC analysis. This step is necessary for both unlabelled and labelled glycans. This step aims to remove any interference, impurities, desalting, or excess labelling reagents from the sample. This removal of the interfering substances increases the accuracy, and precision, of the analysis methods and also increases the HPLC column lifetime.

4.1.1 Purification of glycans prior to HPLC analysis

Widely used methods for glycan purification include precipitation with acetone [4, 9], solid phase extraction (SPE), and modified methods for example using cotton wool [10, 11], bacterial cellulose [12], and magnetic capture microspheres [13-15].

4.1.1.1 Precipitation with acetone

The use of organic solvents for precipitation and extraction of glycans was developed for large-scale sample purification. This method uses an organic solvent to precipitate the target molecules from impurities. Cold acetone has been used as the organic solvent for precipitating before centrifuging the glycans into pellets and discarding the organic solvent. This method can be used for unlabelled and labelled glycans [9, 16-18]. The workflow of acetone precipitation is shown in Figure 4.1. The study using this method reported recovery of the unlabelled and labelled glycans in the acetone fraction. The percentage of the samples in the acetone extract depends on the type of labelling reagents and the weight of the glycans. The high molecular weight (such as high mannose), and longer peptide backbone (more than 15 amino acids) glycans have recovery results from the acetone precipitation process that are lower than for glycans of low molecular weight or containing short peptide backbones. However, the average of hydrophobicity calculated from the amino acid composition of the peptide backbone does not affect enrichment recovery.

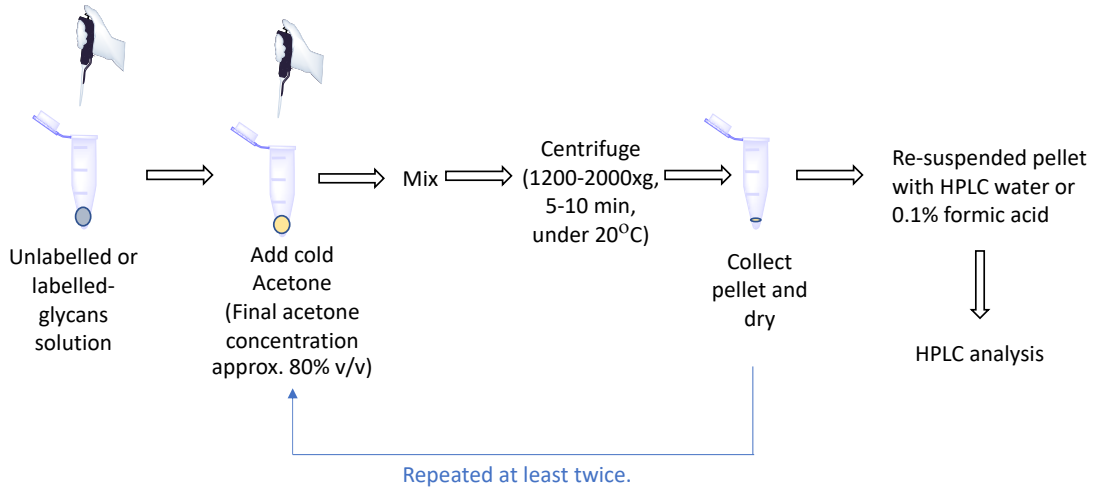

Figure 4.1 General approach for purification of glycans via precipitation with acetone.

4.1.1.2 Solid Phase Extraction (SPE)

SPE is commonly used in the glycans' analysis workflow and uses a solid absorbent in the cartridge. The kind of absorbent selected is dependent on the target molecules. The separation steps of SPE are equilibration, condition, loading, wash, and elute. The equilibration and condition steps activate and prepare the absorbent in the cartridge for binding with the target molecules. The target molecules are retained in the cartridge by binding with the absorbent, whilst impurities pass through with the solvent in the washing step. The eluting step uses an alternative solvent to break the bond between the target molecules and the absorbent. The target molecules then pass through with the eluting solvent without the impurities. The types of SPE absorbents are normal phase, reverse phase, HILIC, ion exchange, and porous graphite, and they are specific for target molecules. In glycan analysis, various types of SPE are used, such as PGC [14, 17, 19-22], C18 [17], HILIC [14, 17, 23-25], and Strong Anion Exchange (SAX) [26]. Some studies use a mixed mode of SPE and C18 before PGC [21, 27] to remove the residual peptides and lipids. HILIC SPE is usually used for fluorescence-labelled glycans. The purification workflow of SPE is illustrated in Figure 4.2. The summary of purification methods of glycans by various types of SPE is shown in Table 4.1.

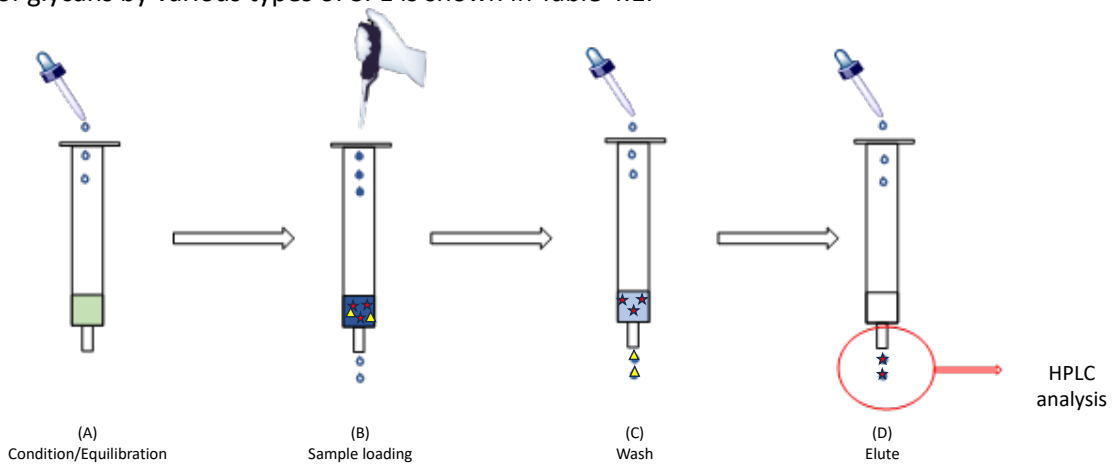

Figure 4.2 General SPE purification of glycans workflow. (A) Condition and equilibration for activating the absorbent, (B) Load the sample solution to the cartridge, (C) Wash the impurities from the cartridge, and (D) Elute the target molecules by using the solvent to break the bond with the absorbent.

Table 4.1 The purification conditions for each type of SPE cartridge

SPE type	Condition	Equilibration	Load	Wash	Elute	Application	Enrichment efficiency	References
PGC	80% ACN in water with 0.1% TFA or 80% ACN in water	Water or 0.1% TFA in water	sample in the buffer solution or water	water	20% ACN in water 40% ACN in water, 10% ACN containing acid, 40% ACN containing acid or 0.1% TFA in 80% ACN deepened on the type of glycans	The studies using PGC SPE reported unlabelled glycans.	91-95%	[14, 17, 19-22, 27]
C18	80% ACN in water with 0.1% TFA or 60-80% ACN in water	Water or 0.1% TFA in water	sample in the buffer solution or water	water	20% ACN in water 40% ACN in water, 10% ACN containing acid, 40% ACN containing acid or 0.1% TFA in 80% ACN deepened on the type of glycans	The studies using the C18 column reported unlabelled and labelled *O*- and *N*-linked glycans.	74-100%	[17, 25, 27, 28]
HILIC	1% TFA in water, water, 70-100% methanol, or 70% ethanol.	80-96% ACN	sample 90-100% ACN	90-99% ACN or 1% FA in 90% ACN	0.1-1% TFA in water, ammonium acetate buffer, or water.	The studies using the HILIC SPE reported labelled glycans.	90-96%	[14, 17, 23-25, 29]
SAX	ACN, 100nM triethylammonium acetate and water	1% TFA in 95% ACN	sample in the buffer solution or water	1% TFA in 95% ACN	0.1% TFA in 50% ACN	The SAX SPE studies reported unlabelled and labelled *N*- and *O*-linked glycans. Suitable for *N*-linked glycans that *O*-linked glycans. The sialic acid can ionisation in the conditions of SAX SPE.	75-93%	[25]

4.1.1.3 Modified Methods

Today, glycan purification methods are developed to increase precision, accuracy, and decrease cost and time. Natural or synthetic materials, such as cotton and bacterial cellulose, are explored. The current trends in glycan purification are illustrated below.

a. Cotton wool

Cotton wool is one kind of natural hydrophilic cellulose. The cellulose structure is loose and porous, with hydroxyl groups at the surface [30]. Studies have reported using the cotton wool adsorbent via a HILIC mechanism. The preparation of cotton wool used 3-100 mg of cotton wool packed into pipette tips (2-200 µL). The micropipettes passed the solvents through the cotton wool in each step. The mobile phase in each step (condition, equilibration, load, wash, and elute) was modified from HILIC SPE. Most cotton wool purification studies have been developed for unlabelled *N*- and *O*-linked glycans. The study of labelled *N*-glycans with 2-AA shows low recovery in high water content solvents [10]. For other labelling reagents, such as PMP, cotton wool can remove the excess labelling reagent in *N*- and *O*-linked glycans [31]. There are reports of using cotton wool to purify glycans in biological sample analysis [30-32], and this method can be used for low molecular weight glycans (less than 200 Da)[10, 33]. The capacity of glycan purification with cotton depended on the hydroxyl and carboxyl groups on the glycans. Han J. *et al.* [31] reported that acidic glycans have more absorbability with cotton wool than neutral glycans with similar molecular weight. The variation of the results with unlabelled glycans depended on the weight and the method of cotton wool preparation. The absorption capacity of cotton wool for unlabelled glycans increases when the weight of cotton wool increases [33].

Table 4.2 The purification conditions of the cotton wool study

Weight of cotton wool	Type of glycans	Condition	Equilibration	Load	Wash	Elute	References
500 ug-100 mg	Unlabelled glycans	water	80-85% ACN	Sample in 80-100% ACN	0.1% TFA in 80-85% ACN	water	[10, 30, 33-35]
	Labelled glycans - 2AA	water	83%ACN	sample in 90% ACN	0.1% TFA in 90% ACN	water	[10]
	- PMP	N/A	N/A	Glycans in water and dried in a vacuum at 30°C for 30 min.	Gradient elution with 0.1% TFA in 100% ACN, 0.1% TFA in 90% ACN in water	water	[31]

b. Bacterial cellulose

Bacterial cellulose (BC) is a natural hydrophilic polymer from microorganisms. The BC structure is like plant cellulose, in nano-size. BC can be used to purify glycans and glycoproteins in biological samples [12]. The BC purification mechanism relies on bond formation between the hydrophilic part of glycans/glycoproteins and the porous residues of BC. The BC imprint of specific glycan/glycoprotein sites can separate the impurity from target glycans/glycoproteins. The different buffers in the wash and elute steps purify the glycans and glycoproteins from the samples. The desalting process before enrichment is necessary. However, only *N*-linked glycans and *N*-linked glycopeptides were studied in BC enrichment.

c. Magnetic capture microspheres for glycans

Modified magnetic microspheres are synthesised to capture glycans or glycoproteins [14, 15]. The principle of this method is using the buffer and magnetic field to alter the glycans/glycoproteins absorbed into the microsphere. A magnet captures the microspheres with glycans, and the solvent with the impurities is discarded. Finally, an appropriate solvent breaks the link between the glycans/glycoproteins and microspheres without the magnetic fields; the purified glycans/glycoproteins dissolve in the solvents.

The summarised advantages, disadvantages, and enrichment efficiency of the glycan purification methods for analysis are shown in Table 4.3 below.

Table 4.3 Comparison between purification methods for glycan analysis

Method	Advantage	Disadvantage	Enrichment efficiency
Acetone precipitation	- This method can be used for both unlabelled and labelled glycans. - Rapid	- Some glycans are also extracted into the acetone. - Low precision - Acetone is a toxic solvent.	5-100%
SPE	- High robustness and precision. - C18 SPE can remove peptides and lipids before the purification of glycans by PGC SPE. - There are various studies about the development of absorbent types, especially for glycans.	- The eluting solvents have to be selected based on the size and charge of glycans. - Some SPE types have less recovery (less than 90%) - PGC SPE is not suitable for glycopeptide enrichment.	90-96%
Cotton wool	- Low cost. - Low usage of solvents - Quick - This method can be used for both N- and O-linked glycans	- The recovery of some labelled glycans is low. - This method cannot be used for glycans with a molecular weight of more than 2000 Da. - There are no commercial pre-packed columns.	53-96%
Bacterial cellulose	- This method can be used for both glycans and glycopeptides. - Environmentally friendly as it is biodegradable. - Quick	- Salts affect the purification property.	56-87%
Magnetic beads	- Magnetic beads can be prepared that are specific for glycans or glycoproteins.	- These have not been reported for use with O-linked glycans.	70-103%

4.2 Aims and Objectives.

This work aims to develop and optimise the enrichment of labelled glycans using various brands of SPE (PGC, C8, C18, Polystyrene DVB, Amide, SAX, SCX, and Superco discovery glycans) and compare the results with enrichment using cotton wool. The study focuses on lactose (**14**) derivatised with a commercially available label (2AB, **26**) and a synthetic alkyne labelling reagent, **5**. HPLC fluorescence is used for quantitative analysis.

The work in this chapter sets out to fulfil three main objectives. The first objective is to optimise the enrichment methods and investigate the purification process of **27** from the excess labelling reagent **26** to achieve high precision and accuracy.

The second objective is to optimise the enrichment conditions using cotton wool with standard **27**. This work focuses on optimising cotton wool's condition and capacity for enrichment. The best conditions will then be used to investigate the absorbance capacity and recovery using three brands of cotton wool that are widely available.

The final objective is to confirm that the selected SPE and cotton wool conditions can be used with different labelling reagent types and sugar units. Standard **16** is used in the optimised conditions for SPE and cotton wool to confirm whether the results from standard **27** can be repeated with other derivatives. Furthermore, **5** and **26** are used to label maltotriose, the dextran ladder (mixture of linear glucose oligomers obtained by the partial hydrolysis of dextran) will be used to test the applicability of the selected enrichment method of SPE and cotton wool further.

These research objectives will therefore enable the development of an enrichment method for labelled *N*-linked glycans within the broader analysis workflow. This is an important part of the analysis of complex samples, as enrichment must be accurate and precise.

This research is summarised in Figure 4.3, which outlines the schemes of work carried out within this chapter.

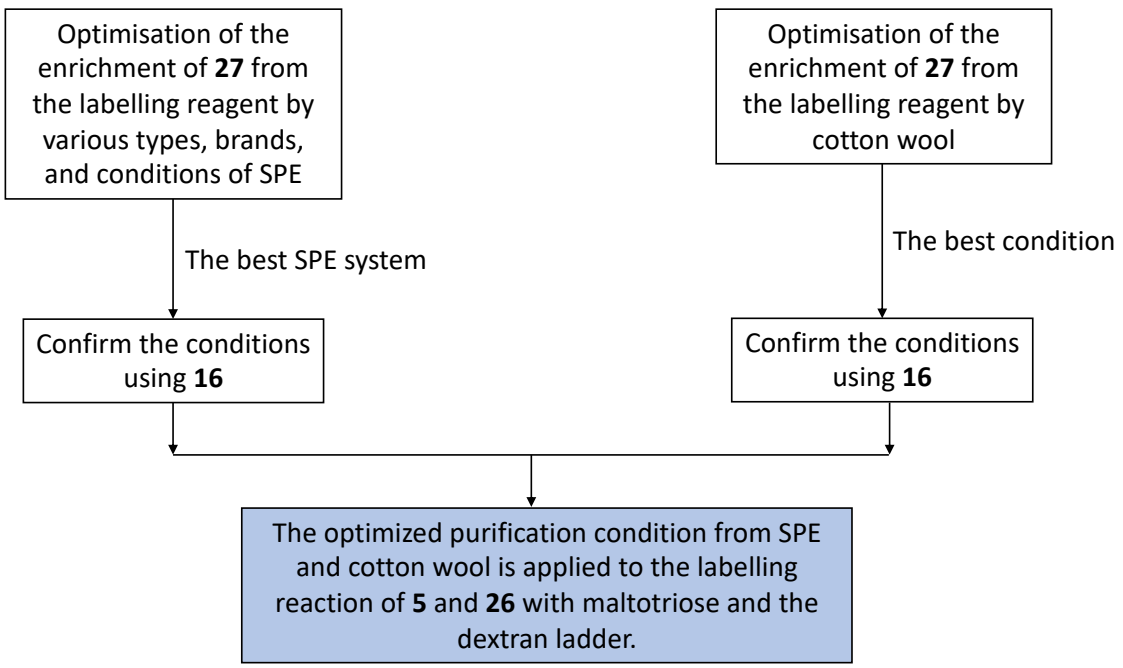

Figure 4.3 Workflow for optimisation condition enrichment by SPE and cotton wool.

4.3 Results and Discussion

4.3.1 Synthesis of the fluorescence labelled *N*-glycan standards (compound 16 and 27) [29]
The fluorescence labelled *N*-glycan standards, compounds **16** and **27**, were prepared using the synthetic alkyne labelling reagent from Chapter 2 (**5**) and commercially available labelling reagents 2AB (**26**) with lactose (**14**) by the labelling reaction from section 2.3.5. The labelling reactions are presented in Scheme 4.1. The labelling reaction involved reductive amination of the aromatic amine of the labelling reagents at the oligosaccharide reducing end of the glycan. These standards were used to test the enrichment method by SPE and cotton wool in each step.

(A)

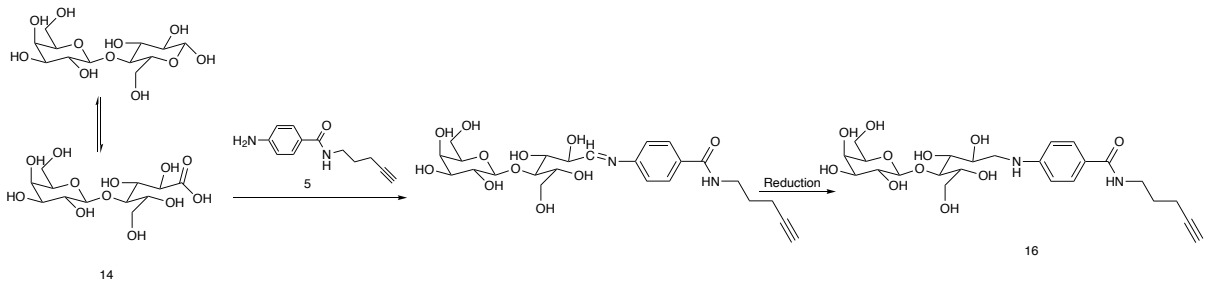

(B)

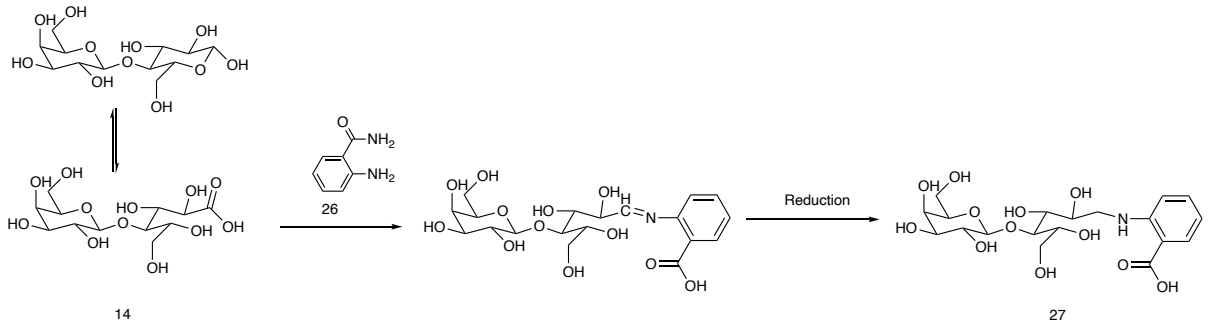

Scheme 4.1 The labelling reaction of **5** (A) and **26** (B) with lactose

4.3.2 The relative between the concentration and HPLC-fluorescence peak area of the standards 16 and 27

Standards **16** and **27** were prepared to a concentration of between 2-250 nmol/ml and 0.5-250 nmol/ml, respectively, in HPLC-grade water. Samples were analysed using an Agilent 1100 HPLC system applying an analytical method by fluorescence detector developed by Hancox [29]. Linearity plots of standard concentration against peak area were produced. Figure 4.4 shows comparable levels of linearity between standards **16** and **27**. The R^2 values are 0.9997 and 0.9992 for standards **16** and **27**, respectively. From these plots, the response of HPLC's peak area is relative to the concentration of standards **16** and **27** in the wide range of linearity. Figure 4.5 shows the HPLC chromatogram of standards **16** and **27** in different concentrations (A and B), retention times of **5**, **16**, **26** and **27** (C), and the different peak areas of standards **16** and **27** in the same concentration (D). However, the different labelling reagents show that different lower concentrations are detectable.

(A)

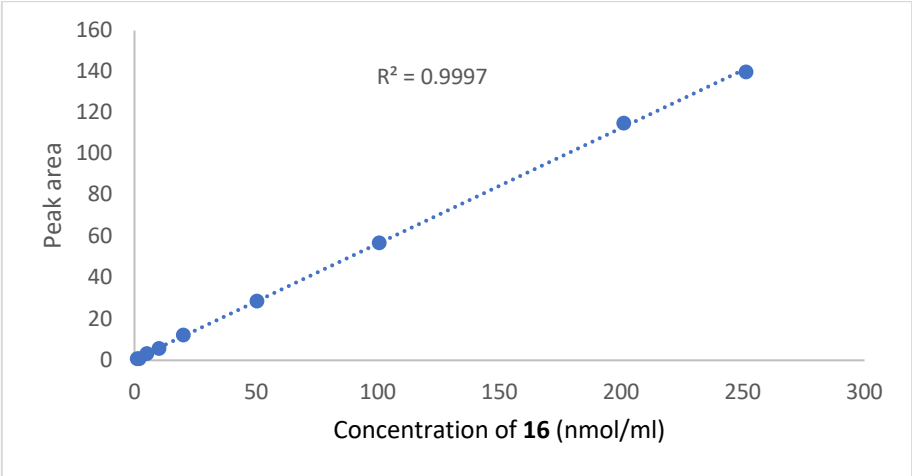

(B)

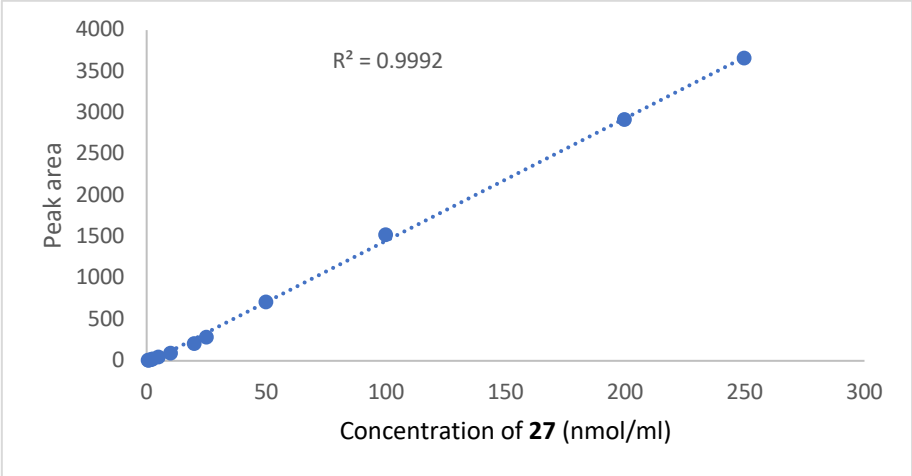

Figure 4.4 Linearity plots of standards **16** (A) and **27** (B) showing peak area versus concentration for quantitative analysis.

(A)

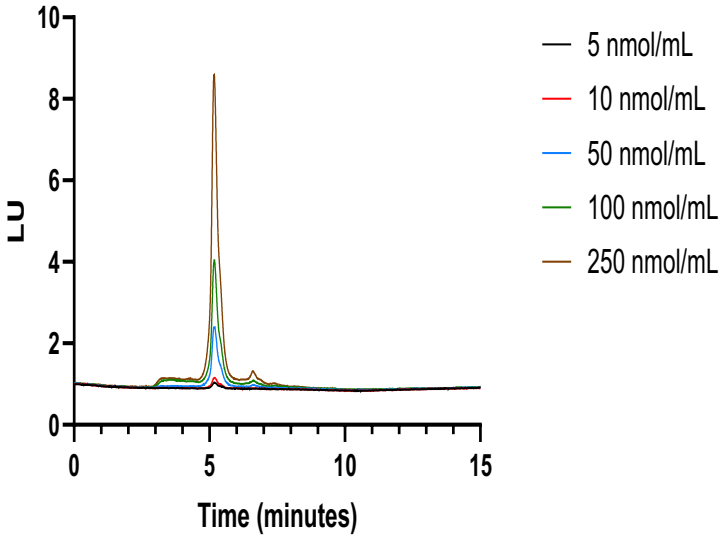
10
8
6
4
2
0
LU
0
5
10
15
Time (minutes)
5 nmol/mL
10 nmol/mL
50 nmol/mL
100 nmol/mL
250 nmol/mL

(B)

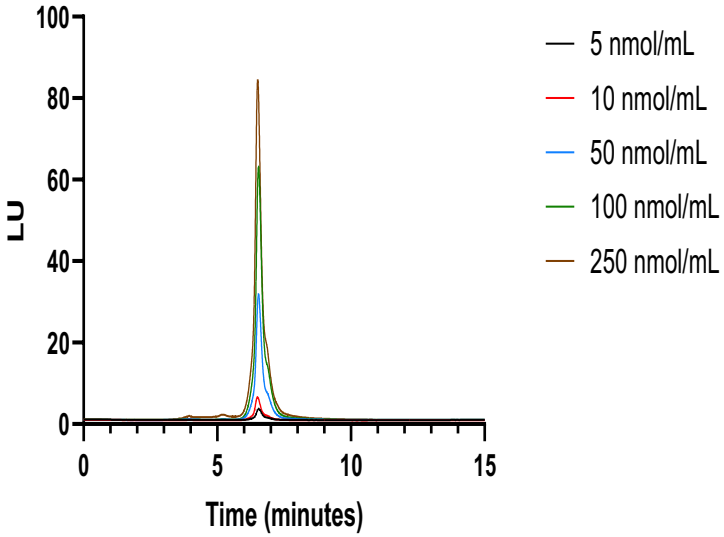
100
80
60
40
20
0
LU
0
5
10
15
Time (minutes)
5 nmol/mL
10 nmol/mL
50 nmol/mL
100 nmol/mL
250 nmol/mL

(C)

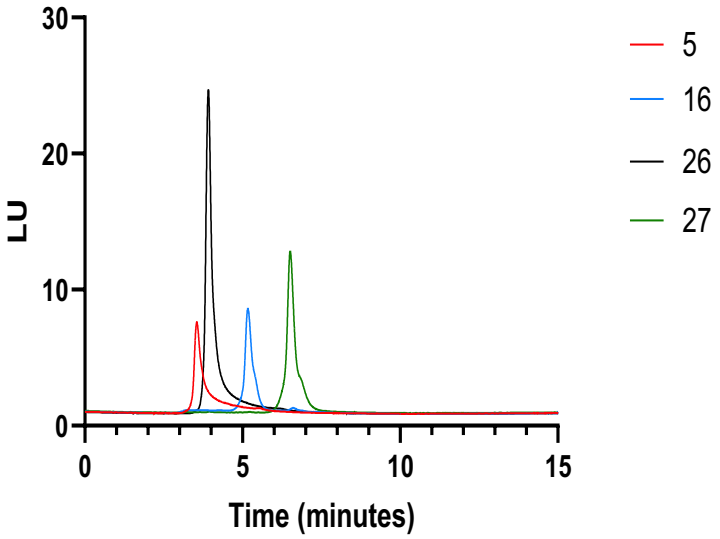

(D)

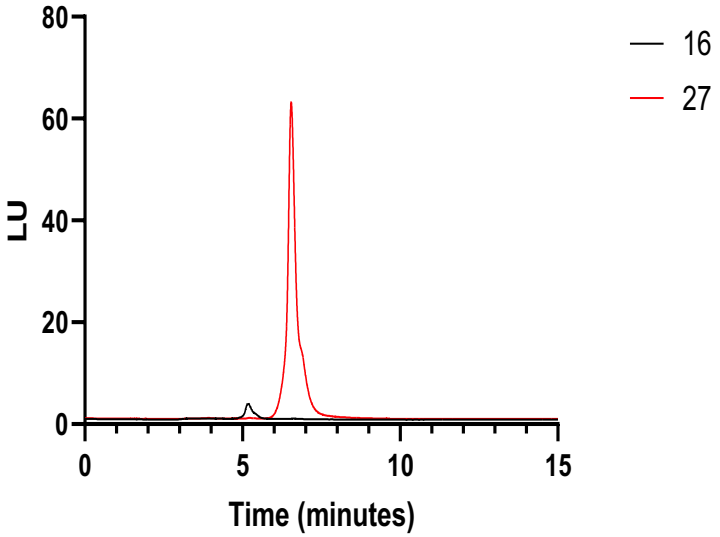

Figure 4.5 The HPLC chromatogram of **5**, **16**, **26**, and **27**. (A) standard **16**, (B) standard **27** with the concentration between 0.5-250 nmol/ml and 2-250 nmol/ml, respectively. (C) The chromatogram compares of the retention time of **5**, **16**, **26,** and **27**, and (D) comparison between 100 nmol/ml of standards **16** and **27.**

The results show that the HILIC HPLC conditions can be used to separate the labelling reagent from the labelled carbohydrate. However, from Figure 4.5 (D), the peak areas of standard **16** are lower by approximately 10 times than standard **27** in the same concentration.

4.3.3 Optimisation of the enrichment methods using various SPE types and brands for 27

In glycan analysis, the removal of the impurities or excess chemical reagents from the sample is required before analysis. SPE is the most common method for achieving enrichment of glycans, with various types of SPE being used to purify or enrich the unlabelled and labelled glycans, for

example, C18, PGC, and HILIC SPE. This study was focused on the labelling of glycan enrichment before HPLC analysis by SPE. In this study, the types and brands of SPE utilised were C18 (4 brands; A, B, C, and D), C8 (1 brand), Amide (2 brands; A and B), PGC (1 brand), Superco Discovery glycan brand, Porous Polystyrene DVB (1 brand), SAX (1 brand), and Strong Cation-exchange (SCX) (1 brand). The standards **27** and **16** were chosen to optimise the type and condition of the SPE enrichment. The conditions of enrichment for each SPE are shown in Table 4.4. The study started by using 1 mL of 100 nmol/ml of standard 27 in every SPE condition. All SPE purifications were performed at least in triplicate. The SPE enrichment methods that found standard **27** only at the eluting step were chosen. The chosen SPE types and conditions were repeated with the labelling reagents (**5** and **26**) for the enrichment. The labelling reagent should not be found in the eluting step. To confirm the results, the SPE types and conditions that can separate **5** and **26** before the eluting step were applied to standard **16**. The selected SPE enrichment condition was applied to the labelled complex glycans (maltotriose and dextran ladder) after being labelled with **5** and **26** before HPLC analysis. Table 4.5 shows the results of percentage recovery with a standard deviation of standard **27** in each type and brand of SPE in this study.

Table 4.4 Condition for each type of SPE investigated

SPE Type	Method 1	Method 2	Method 3
C8 and C18	**Condition**: 1 mL of Acetonitrile	**Condition**: 1 mL of ACN	**Condition**: 1 mL of 80% ACN with 0.1% TFA
	Equilibration: 4 mL of water	**Equilibration**: 1 mL of water	**Equilibration**: 1 mL of water
	Load: 1 ml of sample in water	**Load**: 1 ml of sample in water	**Load**: 1 ml of sample in water
	Wash: 2 mL of water	**Wash**: 2 mL of water	**Wash**: 2 mL of water
	Elute: 1 mL of 25% v/v ACN in water	**Elute**: 1 mL of 4% ACN in 0.1% TFA	**Elute**: 2 mL of 80% ACN in 0.1% TFA
	Reference: [17] *Method for Labelled glycan	**Reference**: [21]	**Reference**: [31]
Amide (HILIC)	**Equilibration**: 2 mL of MeOH	-	-
	Load: 1 mL of sample in ACN		
	Wash1: 5 mL of 1% water in ACN		
	Wash2: 5 mL of 3% water in ACN		
	Elute: 0.8-1.0 mL of water		
	Reference: [29] *Method for Labelled glycan		
PGC	**Condition**: 1 mL of 80% ACN in water	**Condition**: 1 mL of 80% ACN in 0.1%TFA	**Condition**: 1 mL of 80% ACN in 0.1%TFA
	Equilibration: 1 mL of water and 1 mL of ACN in 0.1% TFA	**Equilibration**: 1 mL of water	**Equilibration**: 1 mL of water
	Load: 1 ml sample in water	**Load**: 1 ml sample in water	**Load**: 1 ml sample in water
	Wash: 2 mL of water	**Wash**: 2 mL of water	**Wash**: 2 mL of water
	Elute: 2 mL of 40% ACN in water	**Elute**: 2 mL of 80% ACN in 0.1%TFA	**Elute**: 2 mL of 20% ACN in water
	Reference: [17]	**Reference**: [20]	**Reference**: [22]
Superco Discovery glycan	**Equilibration**:1 mL of 1% water in ACN	-	-
	Load: 1 mL of sample in 1%water in ACN		
	Wash: 3 mL of 1% water in ACN		
	Elute: 1 mL of 20% ACN in water		
	Reference: according to the manufacturer's instruction		

SPE Type	Method 1	Method 2	Method 3
Porous polystyrene DVB	**Condition**: 3 mL of MeOH	**Condition**: 3 mL of MeOH	-
	Equilibration: 3 mL of water	**Equilibration**: 3 mL of water	
	Load: 1 mL of sample in water	**Load**: 1 mL of sample in water	
	Wash: 3 mL of 5% MeOH in water	**Wash**: 3 mL of 5% MeOH in water	
	Elute: 3 mL of MeOH	**Elute**: 3 mL of ACN	
	Reference: according to the manufacturer's instruction	**Reference**: according to the manufacturer's instruction	
SAX	**Condition**: 3 mL of 0.1% TFA in water	**Condition**: 3 mL of MeOH	-
	Equilibration: 3 mL of 95% ACN in 0.1% TFA	**Equilibration**: 3 mL water	
	Load: 1 mL of sample in water	**Load**: 1 mL of sample in water	
	Wash 1: 0.5 mL of 95% ACN in 0.1% TFA **Wash 2**: 6 mL of 95% ACN in 0.1% TFA	**Wash 1**: 1 mL of 50 mM Sodium acetate pH 7 **Wash 2**: 2 mL of MeOH	
	Elute 1: 2 mL of 50% ACN in 0.1% TFA **Elute 2**: 2 mL of 5% ACN in 0.1% TFA	**Elute**: 2 mL of 2% FA in MeOH	
	Reference: [36]	**Reference**: according to the manufacturer's instruction	
SCX	**Condition**: 3 mL of ACN	**Condition**: 3 mL of 0.1% FA in MeOH	-
	Equilibration: 3 mL water, 3 mL of 100 mM triethylammonium acetate, and 3 mL of 95% ACN in 0.1% TFA	**Equilibration**: 3 mL of 2% FA in water	
	Load: 1 mL of sample in 1% FA	**Load**: 1 mL of sample in 1% FA	
	Wash: 3 mL of 95% ACN in 1% TFA	**Wash 1**: 1 mL of 2% FA in water **Wash 2**: 2 mL of MeOH	
	Elute: 800 μL of 50% ACN in 1% TFA	**Elute**: 6 mL of 10% ammonium hydroxide in MeOH	
	Reference: [37]	**Reference**: according to the manufacturer's instruction	

Table 4.5 Percentage recovery with the various types of SPE using 100 nmol of **27**, all data were collected in triplicate.

SPE	Brand	Method 1					Method 2					Method 3				
		Load	Wash 1	Wash 2	Elute	Total of %Recovery	Load	Wash 1	Wash 2	Elute	Total of %Recovery	Load	Wash 1	Wash 2	Elute	Total of %Recovery
C18	A	0± 0.00	34±0.72	ND	16±0.52	50	0± 0.00	37±1.59	ND	10±0.23	47	0± 0.00	34±4.78	ND	11±0.83	45
	B	0± 0.00	0± 0.00	ND	4± 0.16	4	0± 0.00	0± 0.00	ND	1± 0.14	1	0± 0.00	0± 0.00	ND	2±0.27	2
	C	0± 0.00	0± 0.00	ND	5± 1.01	5	0± 0.00	0± 0.00	ND	1± 0.05	1	0± 0.00	0± 0.00	ND	1±0.07	1
	D	0± 0.00	2± 0.47	ND	5± 0.70	7	0± 0.00	2± 0.13	ND	2± 0.61	4	0± 0.00	0± 0.00	ND	2±0.30	2
C8	A	1± 0.05	3± 0.76	ND	1± 0.04	5	0± 0.00	2± 0.68	ND	0± 0.00	2	0± 0.00	2± 0.21	ND	0± 0.00	2
Amide	A	0± 0.00	0± 0.00	1± 0.08	98±0.66	99	ND	ND	ND	ND	ND	-	-	-	-	-
	B	0± 0.00	0± 0.00	0± 0.00	66±4.02	66	ND	ND	ND	ND	ND	-	-	-	-	-
PGC	A	0± 0.00	0± 0.00	ND	79±5.23	79	0± 0.00	0± 0.00	ND	70±3.84	70	0± 0.00	0± 0.00	ND	55±13.01	55
Superco Discovery glycan	A	5± 0.44	22±1.14	ND	63±6.77	90	ND	ND	ND	ND	ND	-	-	-	-	-
Hypersep Retain PEP	A	1± 0.11	43±1.01	ND	47±2.15	91	1± 0.09	43±2.23	ND	44±0.92	88	-	-	-	-	-
SAX	A	54±1.91	45±2.71	0± 0.00	0± 0.00	99	45±2.71	45±4.76	3± 1.90	0± 0.00	93	-	-	-	-	-
SCX	A	0± 0.00	0± 0.00	0± 0.00	0± 0.00	0.00	0± 0.00	0± 0.00	0± 0.00	87±2.55	87	-	-	-	-	-

*ND = Not Detected.

**Amide, Superco Discoversy glycans, Hypersep Retain PEP, SAX, and SCX were tested in 2 methods.

The recovery results for each step are shown in Table 4.5 and Figure 4.6. The best method was determined as the one that allows a maximum recovery of standard **27** at the eluting step. From the results, Amide brand A, PGC-method 1 and SCX-method 2 were chosen for further study as they allowed more than 90% recovery at the eluting step. On the other hand, in the other types and conditions of SPE, the standard is found in the loading and washing steps, or not in any steps for some of the SPE, which would be detrimental for enrichment and recovery. The HPLC chromatograms from the eluting step for Amide SPE brand A, PGC SPE-method 1, and SCX SPE-method 2 are shown in Figure 4.6. The results show differences in percentage recovery in each step between brands in C18 and Amide SPE.

(A)

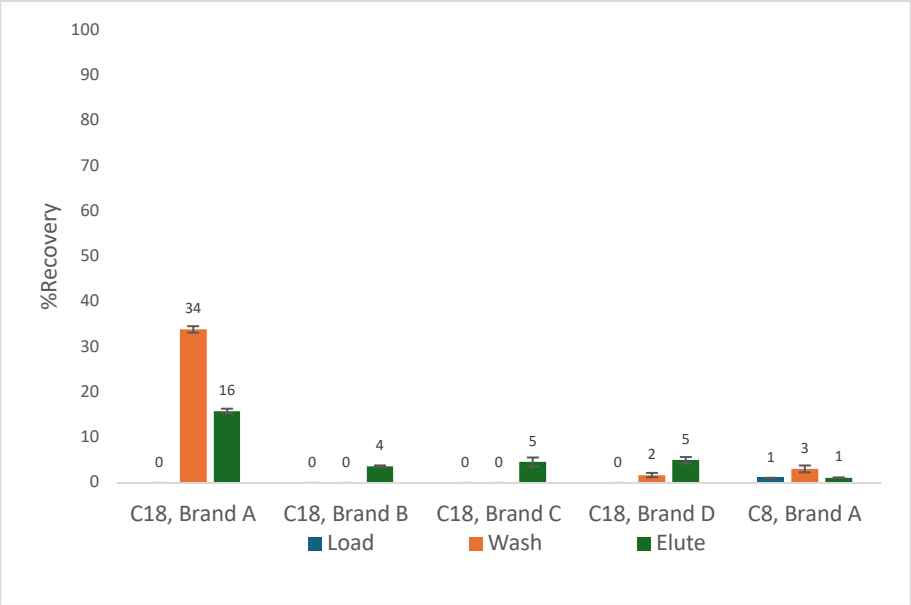

(B)

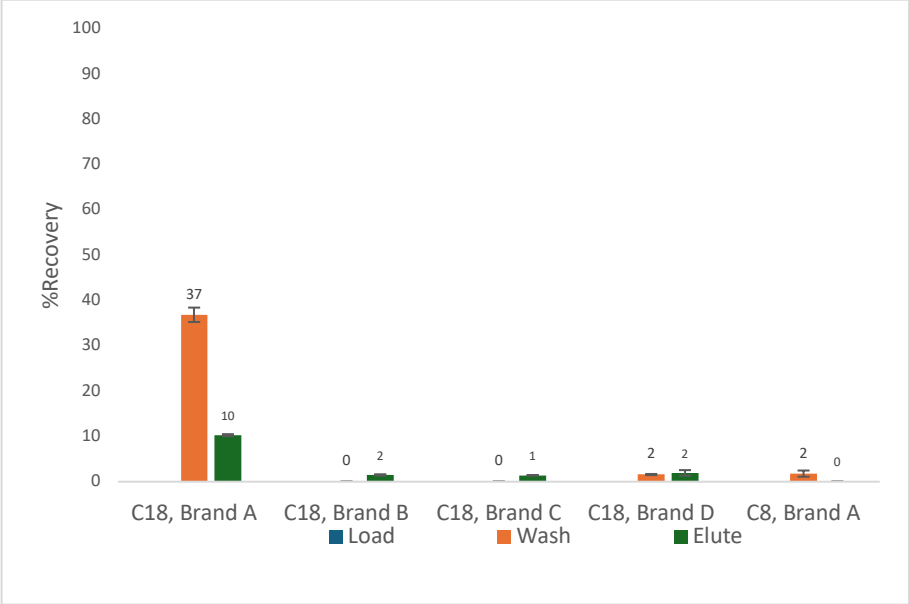

(C)

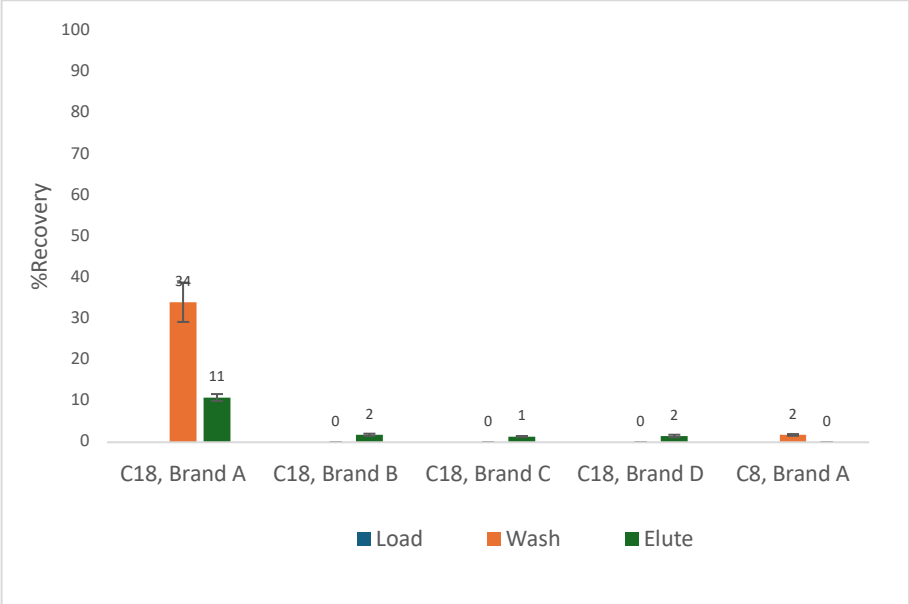
100
90
80
70
60
50
40
30
20
10
0
%Recovery
34
11
0
2
0
1
0
2
2
0
C18, Brand A
C18, Brand B
C18, Brand C
C18, Brand D
C8, Brand A
Load
Wash
Elute

(D)

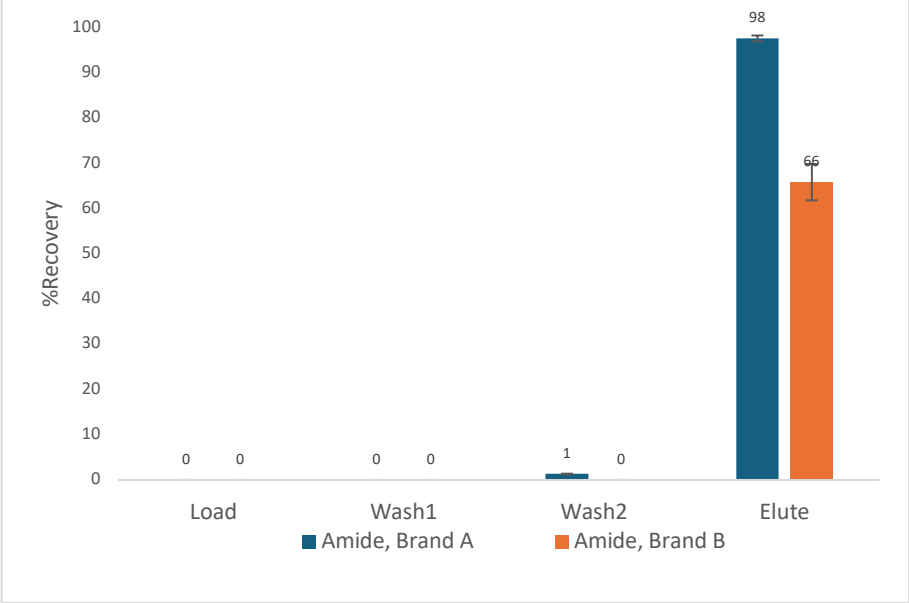
100
90
80
70
60
50
40
30
20
10
0
%Recovery
0
0
0
0
1
0
98
66
Load
Wash1
Wash2
Elute
Amide, Brand A
Amide, Brand B

(E)

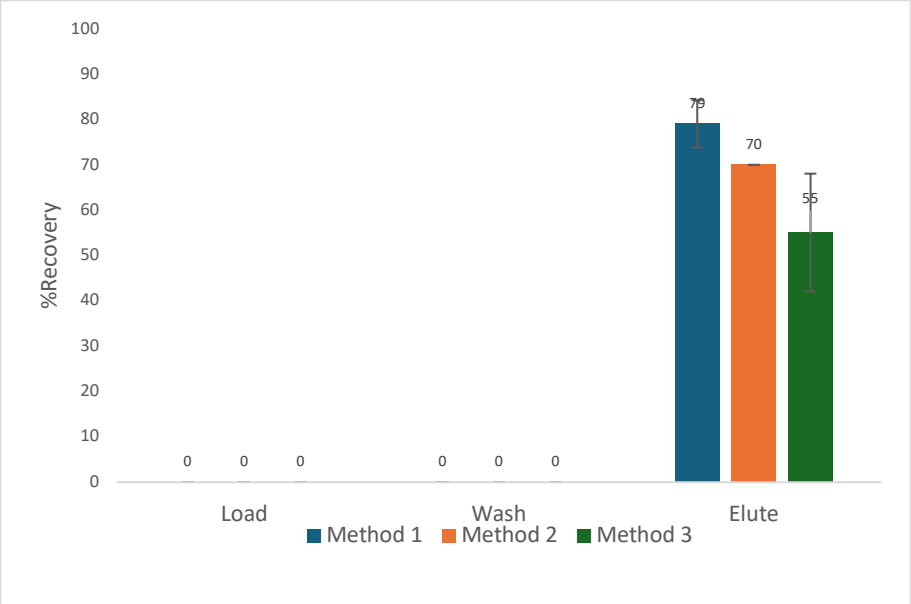
100
90
80
70
60
50
40
30
20
10
0
%Recovery
0
0
0
0
0
0
79
70
55
Load
Wash
Elute
Method 1
Method 2
Method 3

(F)

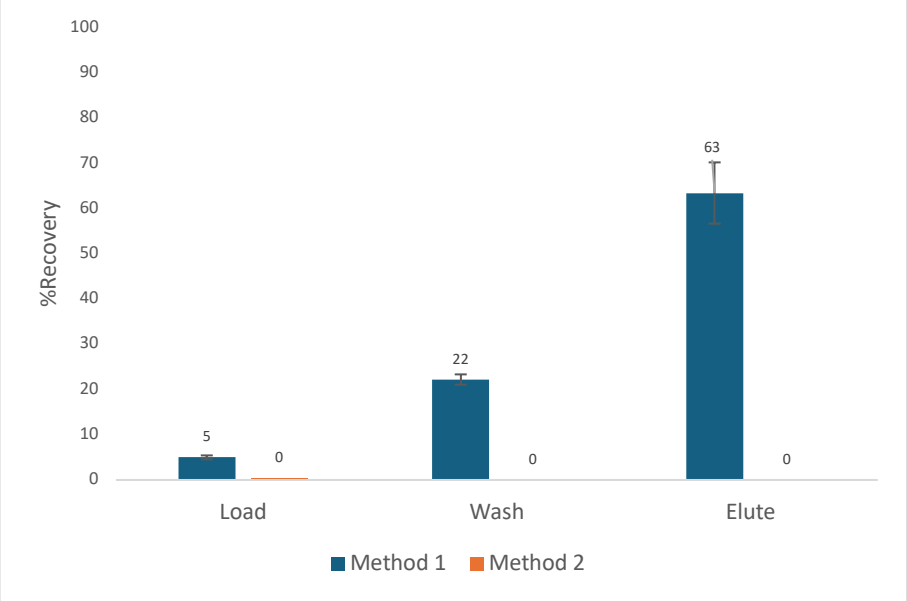
100
90
80
70
60
50
40
30
20
10
0
%Recovery
5
0
22
0
63
0
Load
Wash
Elute
Method 1
Method 2

(G)

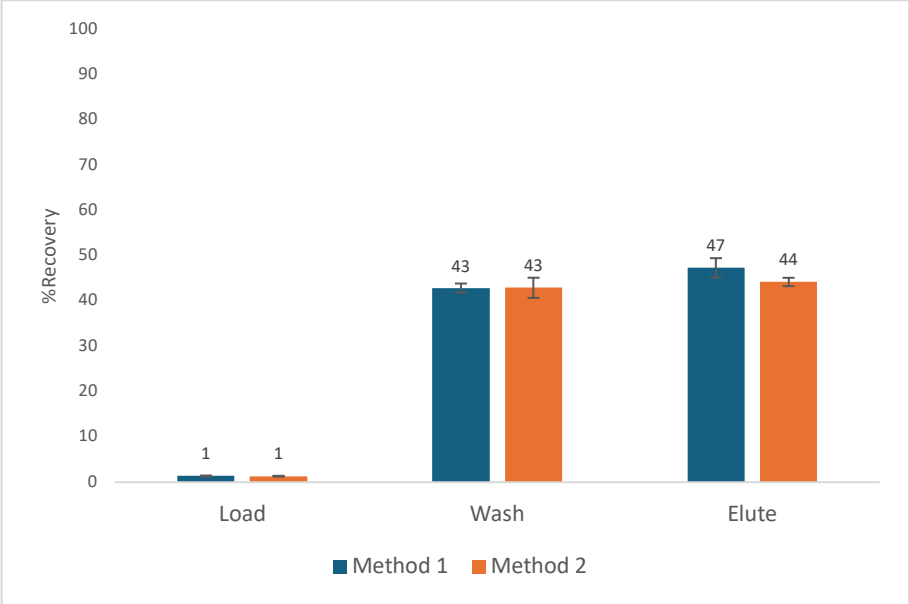
100
90
80
70
60
50
40
30
20
10
0
%Recovery
1
1
43
43
47
44
Load
Wash
Elute
Method 1
Method 2

(H)

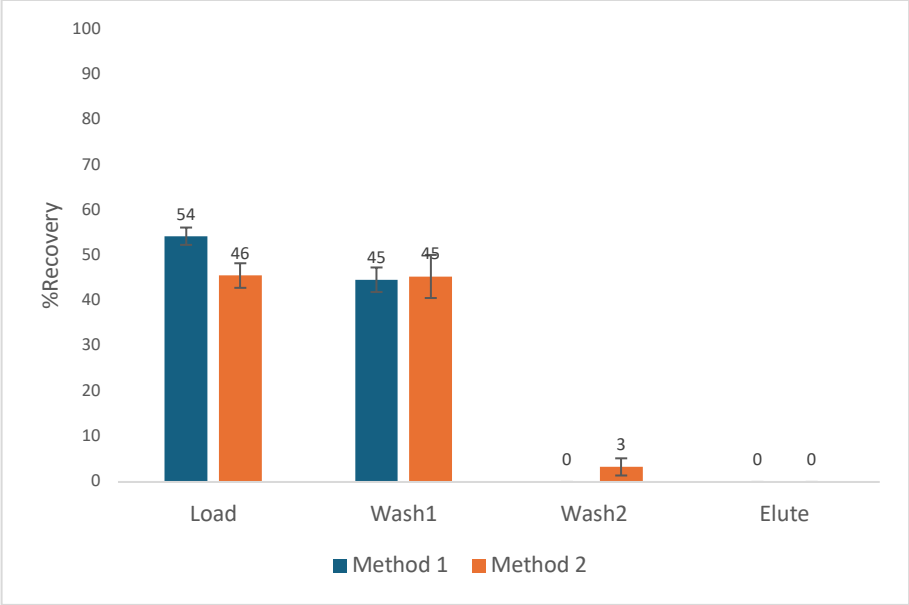
100
90
80
70
60
50
40
30
20
10
0
%Recovery
54
46
45
45
0
3
0
0
Load
Wash1
Wash2
Elute
Method 1
Method 2

(I)

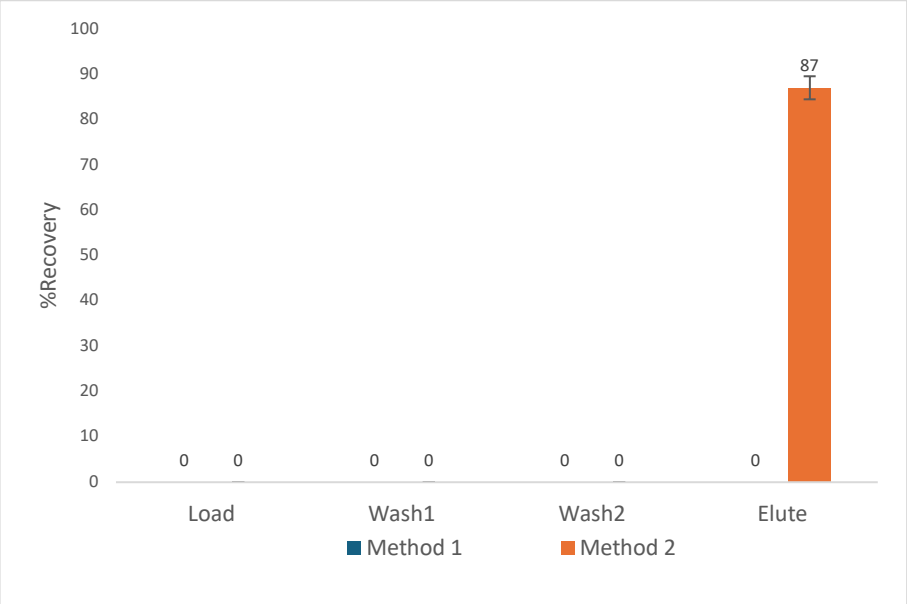

Figure 4.6 The bar chart of percentage recovery of standard **27** in the various types and conditions of SPE. (A) C18 SPE, 4 brands and C18, method 1, (B) C18 SPE, 4 brands and C18 method 2, (C) C18 SPE, 4 brands and C18 method 3, the results from C18 and C8 all brands and C18 methods show most of the standard compound pass through in the wash steps. D) Amide SPE brands A and B, the results show both brands can elute most of the standard in the elute steps. However, Brand A has higher recovery than Brand B. (E) PGC SPE in 3 methods. The results show that all methods can elute the standard in the elute steps. However, method 1 has higher recovery than others. (F) Superco Discovery Glycan SPE, the results show that the standard appeared in all steps (G) Hypersep Ratain PEP SPE, 2 methods, the results show that the standard appeared in all steps (H) SAX SPE, 2 methods, the results show that the standard comes through the cartridge in the load and wash step. (I) SCX SPE, 2 methods, the results show that only method 2 allowed recovery of the standard in the eluting step.

4.3.4 Confirmation of the SPE condition for separating the excess labelling reagent from the labelled glycan

The conditions selected from 4.3.3 section were then applied for analysis of **5** and **26** to determine whether the selected conditions could remove excess labelling reagents from the labelled glycans. If so, the conditions should afford the labelling reagent in the load or wash steps rather than in the eluting step.

The results show that only Amide SPE can remove the excess labelling reagents in the load and wash step, with no labelling reagents in the eluting fractions. The PGC and SCX methods afforded the labelling reagents in the eluting fragments. The chromatograms for recovery of the labelling reagents in each step for the Amide SPE, PGC SPE-method 1, and SCX SPE method 2 are shown in Figure 4.7.

(A)

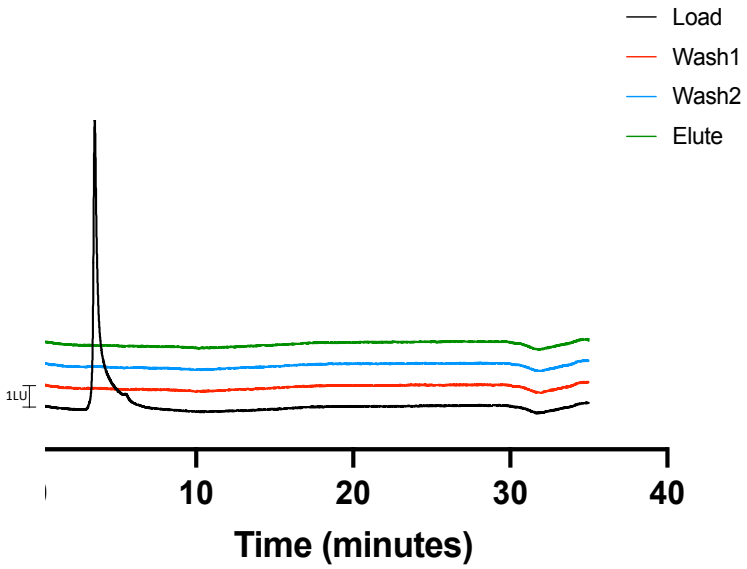
Load
Wash1
Wash2
Elute
1LU
10
20
30
40
Time (minutes)

(B)

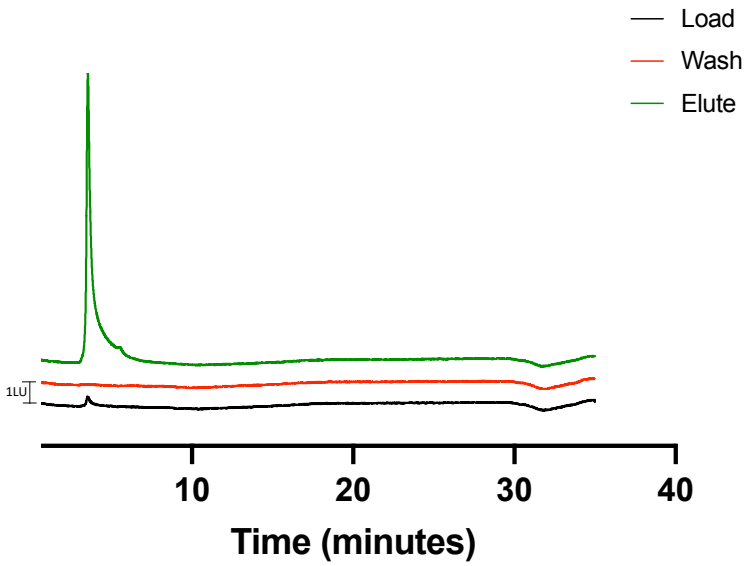
Load
Wash
Elute
1LU
10
20
30
40
Time (minutes)

(C)

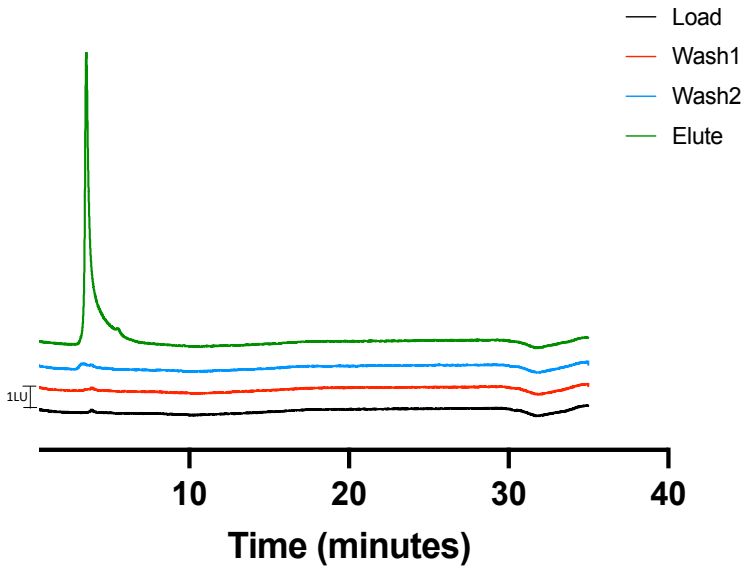
Load
Wash1
Wash2
Elute
1LU
10
20
30
40
Time (minutes)

(D)

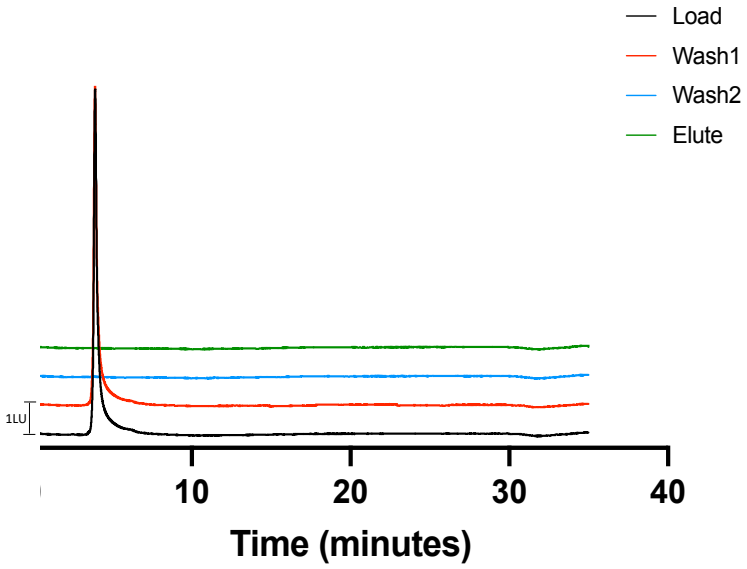
Load
Wash1
Wash2
Elute
1LU
10
20
30
40
Time (minutes)

(E)

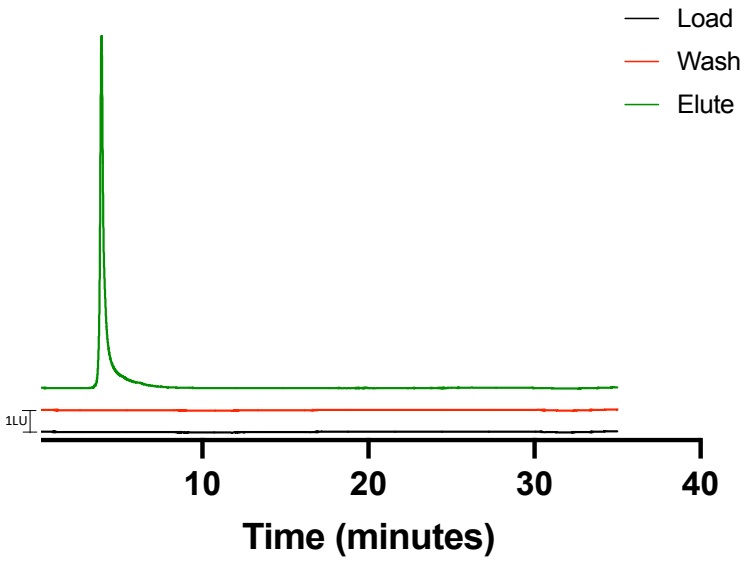

(F)

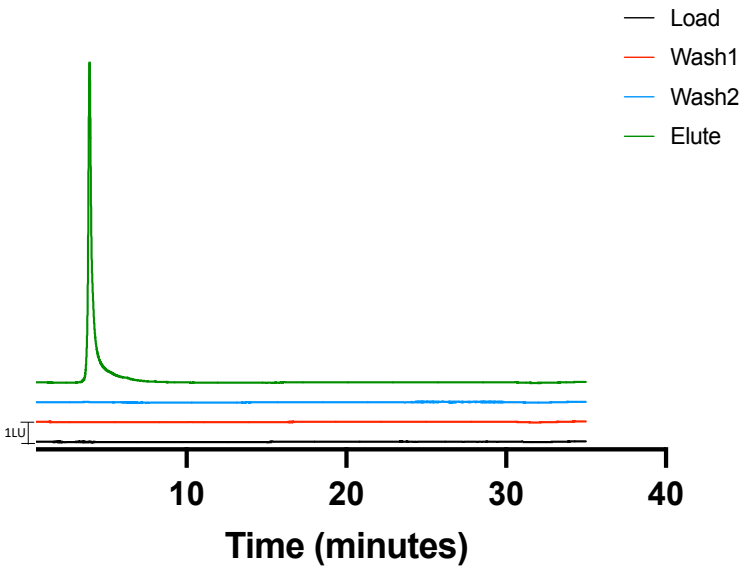

Figure 4.7 The chromatogram of each step of the chosen SPE method of the labelling reagents (A) **5** with Amide SPE, (B) **5** with PGC SPE-method 1, (C) **5** with SCX SPE-method 2, (D) **26** with Amide SPE, (E) **26** with PGC SPE-method 1, and (F) **26** with SCX SPE-method 2.

The results show only Amide SPE can separate the labelling reagents in the load and wash steps before the eluting step. On the other hand, PGC SPE-method 1 and SCX SPE-method 2 found the labelling reagents in the eluting step. According to the theory, the enrichment method should separate the impurities before the eluting step. The Amide SPE was chosen for the confirmation enrichment method of labelled glycans.

4.3.5 Confirmation of selected SPE condition using standard 16.

The Amide SPE brand A gave the same result using different labelling reagents. Standard **16** (100 nmol/ml) was selected to confirm the enrichment condition of standard **27**. The results of

standard **16** enrichment correspond to standard **27** using the amide SPE brand A. Changing the labelling reagent does not affect the enrichment property of the selected SPE methods. Standard **16** found in the eluting step has a yield greater than 90%, as shown in Figures 4.8 and 4.9.

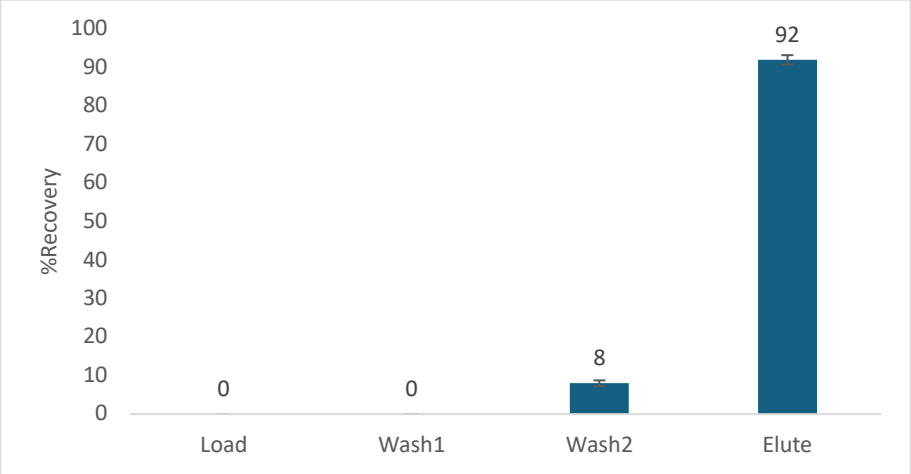

Figure 4.8 Percentage recovery of standard **16** in Amide SPE brand A, all data were collected in triplicate

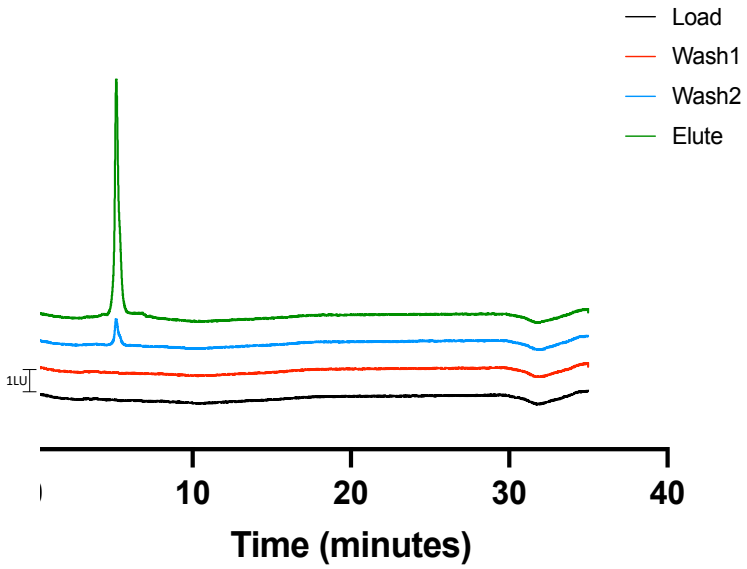

Figure 4.9 The HPLC chromatogram of standard **16** of Amide SPE brand A.

The Amide SPE brand A shows the most effectiveness in enriching labelled glycan standards. This condition is the only system that can remove the labelling reagents (**5** and **26**) from the standards (**16** and **27**). However, the different brands give different results in the same enrichment condition. The Amide SPE brand B has different results from brand A. The Amide SPE brand A was chosen to compare the enrichment property to cotton wool SPE in the same standard (**16** and **27**) and labelled complex glycans (maltotriose and dextran ladder) in the next part of this chapter.

4.3.6 Optimisation of cotton wool (HILIC mode) enrichment methods.

As with the cotton wool in the previous study, unlabelled glycans are enriched by cotton wool during HILIC SPE [10, 30, 31, 34]. A suitable system for labelled glycans using cotton wool is

developed in this experiment. As for the HILIC SPE study, water was used for the activation and elute steps in order to release the sample from the adsorbent. ACN or less than 10% water in ACN was used in the equilibration, load, and wash steps in order to remove the other components from the labelled-glycan samples. Absorbent cotton wool pads of three different brands were purchased from the local store in Reading, UK. According to the manufacturers, cotton wool consists of 100% pure cotton. The cotton wool was cut and weighed to afford 5±0.5 mg samples that were pushed into 200 µL pipette tips tightly by other pipette tips, as shown in Figure 4.10. The tips were stored in a closed box until use. This section used 200 µL of 500 nmol/ml of **27** to optimise the methods at least in triplicate. The methods are illustrated in Table 4.6.

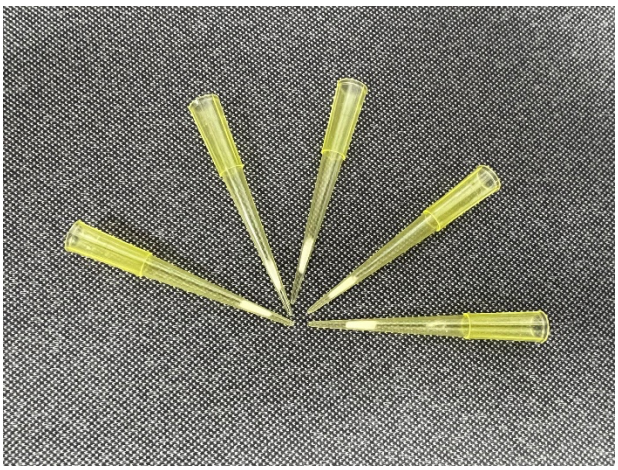

Figure 4.10 The cotton wool tips for use in labelled sugar enrichment experiment.

Table 4.6 The conditions for the purification of standard **27**, using 200 µL of 500 nmol/ml by cotton wool SPE using cotton wool brand A

Method 1	Method 2	Method 3
Condition: 200 µL of water **Equilibration**: 200 µL of 80% ACN **Load**: 200 µL of sample in ACN by pipet up and down 20 times **Wash**: 2x200 µL of 80% ACN in 0.1% TFA in water **Elute**: 200 µL of water	**Equilibration**: 2x200 µL of MeOH **Load**: 200 µL of sample in ACN by pipet up and down 20 times **Wash1**: 5x100 µL of 1% water in ACN **Wash2**: 5x100 µL of 3% water in ACN **Elute**: 3x100 µL of water	**Equilibration**: 3x100 µL of 80% ACN in water **Load**: 200 µL of sample in ACN by pipet up and down 20 times **Wash1**: 5x100 µL of 1% water in ACN **Wash2**: 5x100 µL of 3% water in ACN **Elute**: 3x100 µL of water
Reference: [10, 30, 31, 34]	**Reference**: Modified from Amide SPE method 1 [29]	**Reference**: Modified from results of Method 1 and 2

The recovery results in each step are shown in Table 4.7 and Figure 4.11. The best condition for the enrichment of standard **27** is method 3, as this affords the highest percentage recovery in the elute steps. The results correspond to the study from Selman, M.H.J., *et al*. [10] where it was noted that the percentage of water affects the elution of the labelled glycan. Method 1 used more than 10% of water in the wash step. Most of standard **27** was eluted in the wash step. Methods 2 and 3 used less water content in the wash step than method 1. Standard **27** was eluted with water in the elute step. A comparison of the activated cotton wool in the condition and equilibration steps in methods 2 and 3 shows that method 3 presented a higher percentage recovery at the elute steps than method 2. Table 4.7 shows the results of percentage recovery in each step from the three methods. The comparison of the percentage recovery of the three methods is shown in Figure 4.11 below. The chromatograms of each step in the three methods are shown in Figure 4.12.

Table 4.7 Percentage recovery in the various conditions of cotton wool purification using 100 nmol of standard **27**, all data were collected in triplicate.

Method	%recovery				Total of % recovery
	Load	Wash 1	Wash 2	Elute	
Method 1	1 ± 0.09	76 ± 4.74	-	2 ± 0.13	79
Method 2	3 ± 0.37	4 ± 0.38	2 ± 0.27	89 ± 1.70	98
Method 3	2 ± 1.73	3 ± 0.99	2 ± 0.53	92 ± 2.21	99

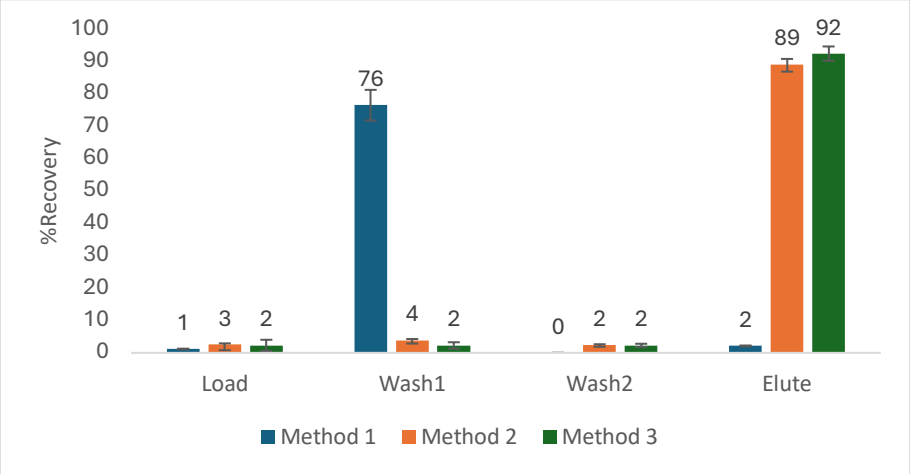

Figure 4.11 Comparison of percentage recovery of standard **27** in three cotton wool (Brand A) enrichment methods.

(A)

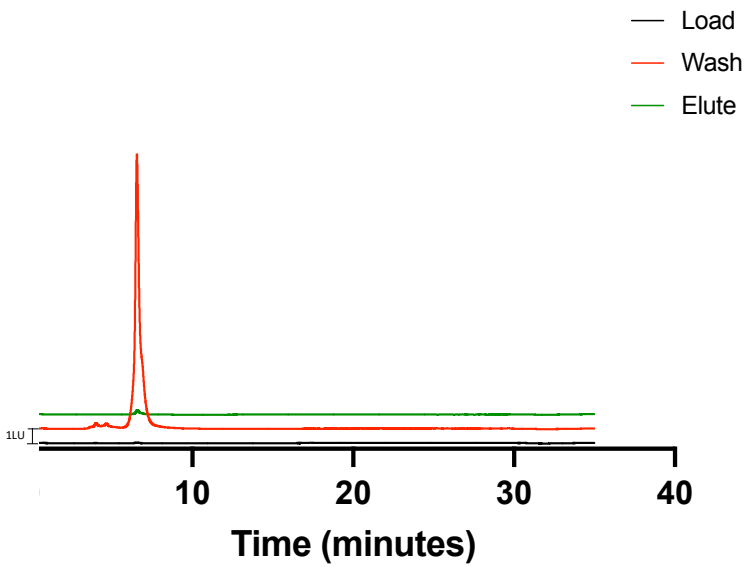
Load
Wash
Elute
1LU
10
20
30
40
Time (minutes)

(B)

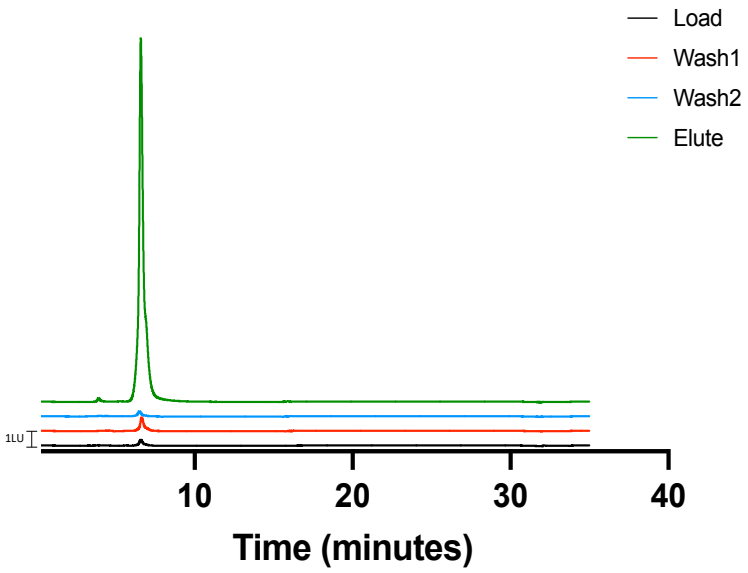
Load
Wash1
Wash2
Elute
1LU
10
20
30
40
Time (minutes)

(C)

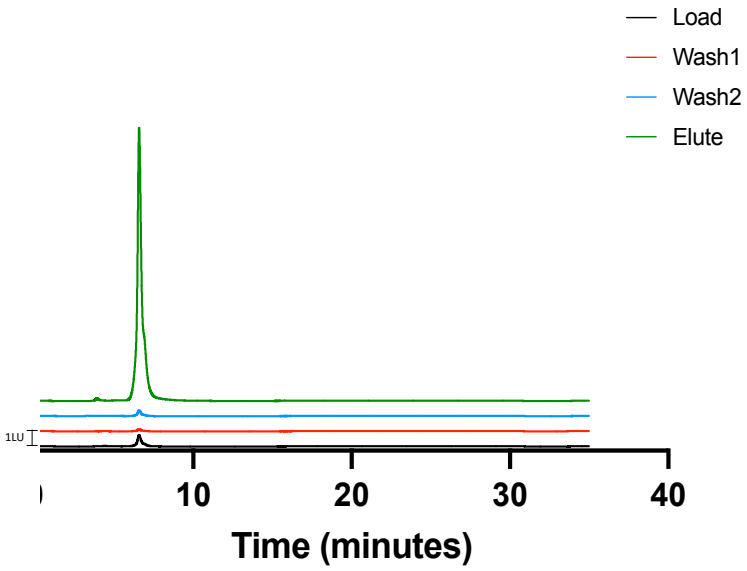

Figure 4.12 The HPLC chromatogram of three methods from cotton wool enrichment in standard **27**; (A) method 1, (B) method 2 and (C) method 3.

The cotton wool enrichment method 3 was chosen. Separating the impurities from the labelled glycans was next tested by using labelling reagents (**5** and **26**) in three different brands of cotton wool. Figure 4.3 shows all brands of cotton wool afforded in the labelling reagents in the load and wash step.

(A)

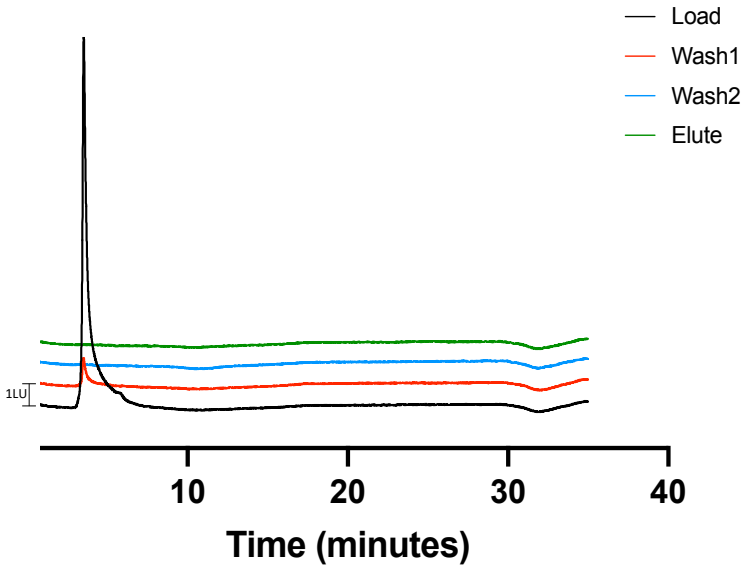

(B)

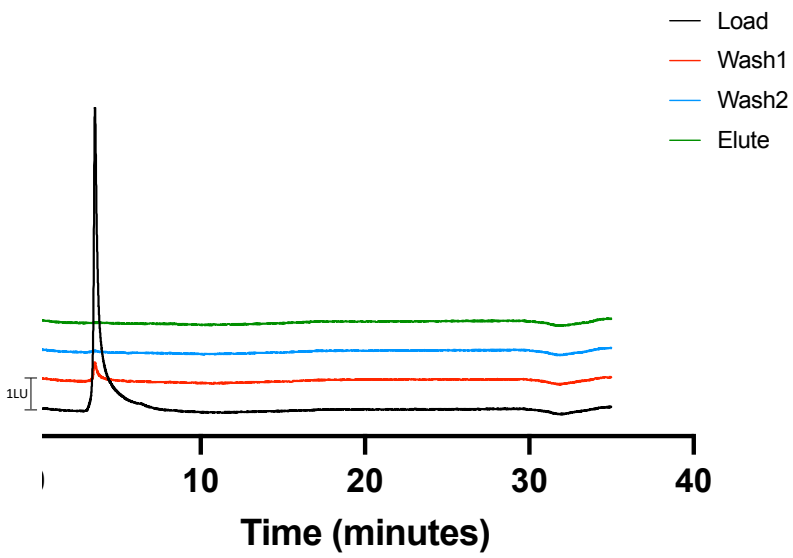
Load
Wash1
Wash2
Elute
1LU
10
20
30
40
Time (minutes)

(C)

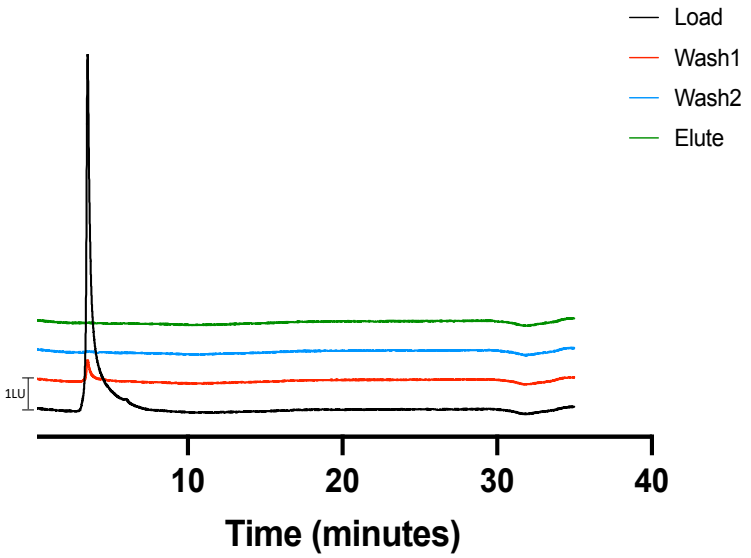
Load
Wash1
Wash2
Elute
1LU
10
20
30
40
Time (minutes)

(D)

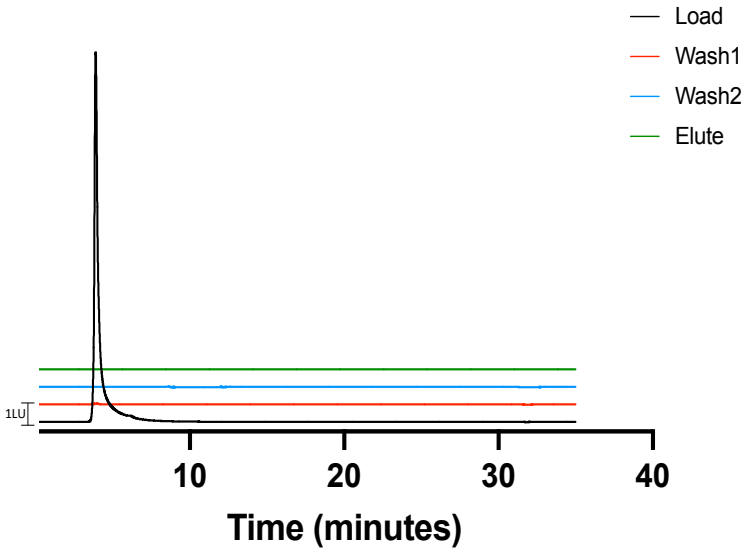
Load
Wash1
Wash2
Elute
1LU
10
20
30
40
Time (minutes)

(E)

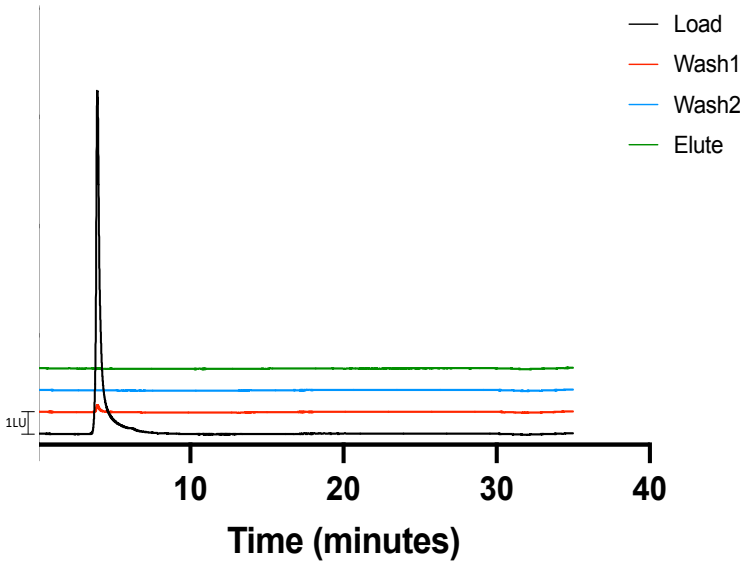
Load
Wash1
Wash2
Elute
1LU
10
20
30
40
Time (minutes)

(F)

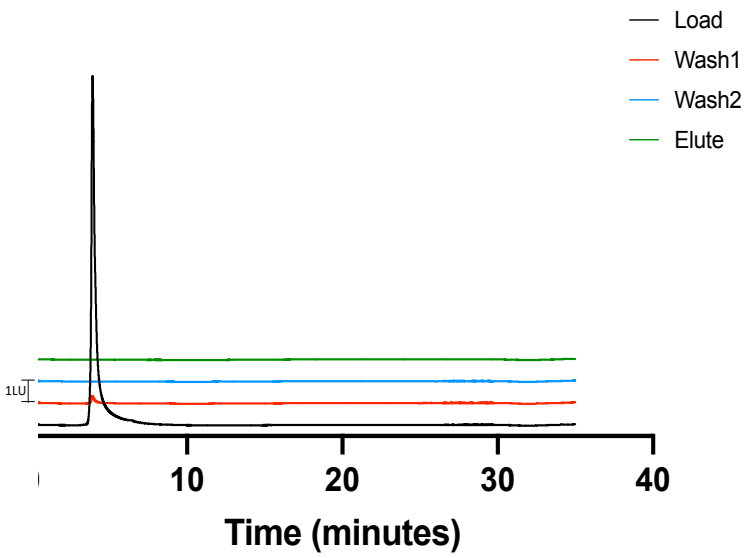

Figure 4.13 The HPLC chromatogram of the labelling reagents (**5** and **26**) in the enrichment process with various brands of cotton wool. (A) **5** with cotton wool brand A, (B) **5** with cotton wool brand B, (C) **5** with cotton wool brand C, (D) **26** with cotton wool brand A, (E) **26** with cotton wool brand B, (F) **26** with cotton wool brand C.

Figure 4.13 shows the effect of removing excess labelling reagents from the labelled carbohydrate by cotton wool using method 3. The excess labelling reagents are removed in the load and wash step. These results will be confirmed by using standard **16** in the next part of this chapter.

4.3.7 Effect of water content in the activated cotton wool (HILIC) condition in the equilibration step.

As shown in section 4.3.6, methods 2 and 3 can elute the standard **27**. However, the standard's percentage recovery differs more in the eluting step from method 3 than in method 2. The difference between the two methods is in the activating cotton wool steps (condition and equilibration). The study of the effect of activating cotton wool on the recovery during the elute step was next developed. As in the previous study, the water content affects the elution property of cotton wool. The study focuses on the variation of water content in the equilibration step. The water content in the study was between 0-100%. The results are shown in Table 4.8 and Figure 4.14. The best condition for the equilibration step used 80% acetonitrile in water, due to the maximum percentage of standard **27** in the elute step.

Table 4.8 Effect of water content variation in the equilibration step of cotton wool purification on percentage recovery, using 100 nmol of standard **27**, all data were collected in triplicate.

Equilibration solution	%recovery of 27				Total %recovery
	Load	Wash 1	Wash 2	Elute	
100% ACN	1 ± 0.10	7 ± 0.83	3 ± 0.87	80 ± 6.06	91
80% ACN in water	2 ± 1.73	2 ± 0.99	2 ± 0.53	92 ± 2.21	98
60% ACN in water	1 ± 0.25	1 ± 0.34	1 ± 0.21	91 ± 1.84	94
40% ACN in water	1 ± 1.54	1 ± 0.13	1 ± 0.18	84 ± 2.49	87
20% ACN in water	3 ± 1.54	1 ± 0.12	1 ± 0.34	89 ± 2.19	94
100% Water	3 ± 0.20	1 ± 0.55	1 ± 0.14	87 ± 4.02	92

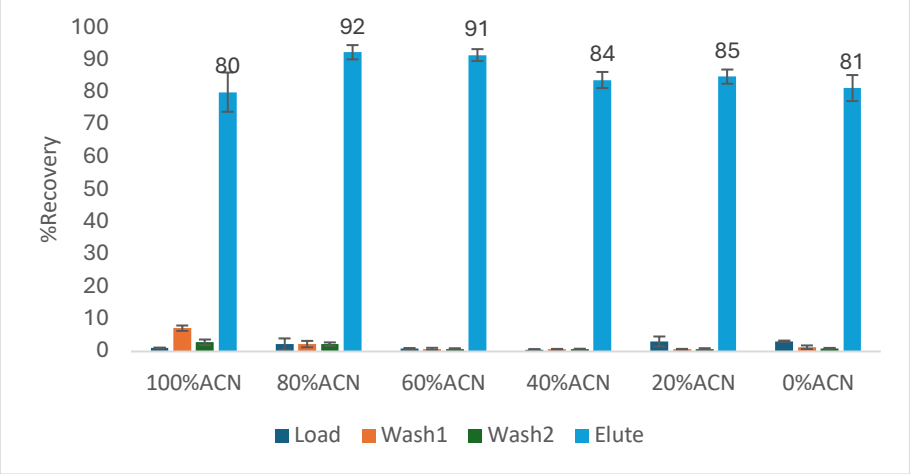

Figure 4.14 Comparison of water content to the percentage recovery of standard **27** in the cotton wool (Brand A) enrichment.

4.3.7 Optimisation of maximum loading capacity of cotton wool (HILIC).

The results from section 4.3.6 showed that standard **27** is found in the loading step in all conditions. Next, the maximum loading capacity of cotton wool was investigated using a standard **27** concentration between 10-100 nmol in method 3 by equilibrating the cotton wool (brand A) with 80% ACN in water. In theory, the cotton wool's maximum loading capacity should be the maximum concentration of the standard that is not found in the other steps except eluting. The results show that the standard was found in the loading step for all concentrations, as shown in Table 4.9 and Figure 4.15.

Table 4.9 Percentage recovery in the load and elute step of cotton wool purification between 10-100 nmol of standard **27**, all data were collected in triplicate.

Standard 27 content	%recovery	
	load	Elute
10 nmol	5 ± 2.53	65 ± 1.77
20 nmol	3 ± 2.01	67 ± 2.01
30 nmol	2 ± 1.58	72 ± 1.63
40 nmol	3 ± 1.82	73 ± 1.45
50 nmol	1 ± 0.78	64 ± 0.99
60 nmol	1 ± 0.88	76 ± 0.72
70 nmol	2 ± 0.67	81 ± 0.33
80 nmol	1 ± 0.11	76 ± 2.73
90 nmol	1 ± 0.03	94 ± 3.50
100 nmol	2 ± 1.73	92 ± 2.21

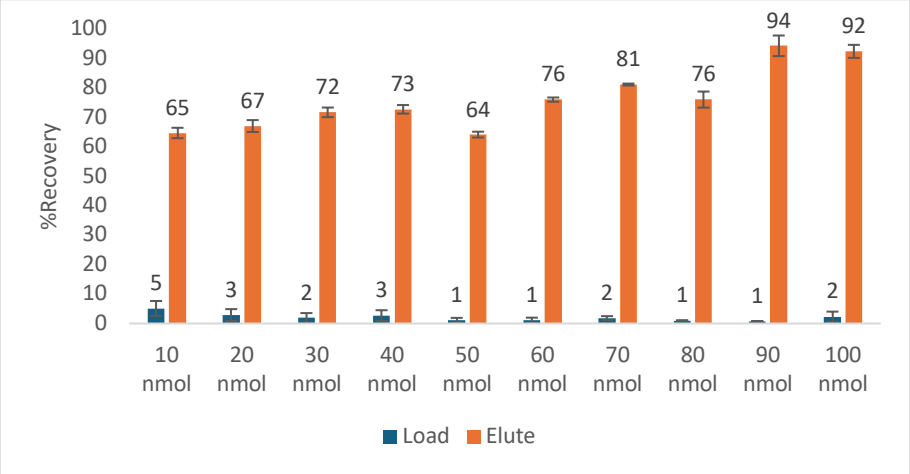

Figure 4.15 Absorption activity of the cotton wool in the various concentrations of standard **27** in the cotton wool (Brand A) between the loading and eluting step.

4.3.8 Comparison of the various brands of cotton wool for enrichment of the labelled sugar.

The three brands of cotton wool from different crops areas and manufacturing countries (India, Netherlands, and Bulgaria) were used for the enrichment of three different concentrations of standard **27** (20, 60 and 100 nmol) with the conditions from method 3. The results show that brands A and B provide a similar pattern and recovery in their load and elute steps. On the other hand, cotton wool brand C shows lower recovery than brands A and B for all concentrations, as shown in Figure 4.16.

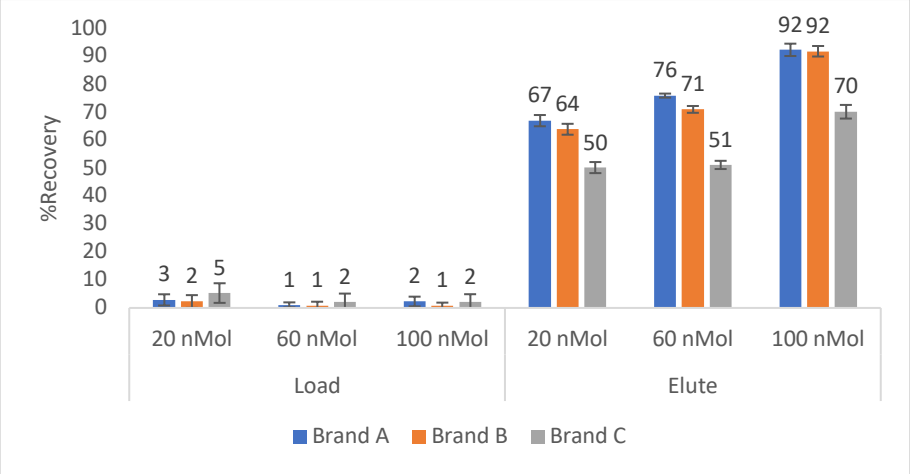

Figure 4.16 Comparison of percentage recovery of the content of standard **27** using different brands of cotton wool, all data collected in triplicate.

4.3.9 Cotton wool enrichment activity using other labelling reagents

The cotton wool enrichment method results from standard **27** were confirmed by using standard **16**. The results from standard **16** at 20-100 nmol corresponded to standard **27**. Brand C demonstrated a lower recovery than brands A and B. The cotton wool brands A and B also have similar results to **27**, as shown in Figures 4.17 and 4.18. However, the higher the polarity, the greater the recovery of standard **27** versus standard **16**.

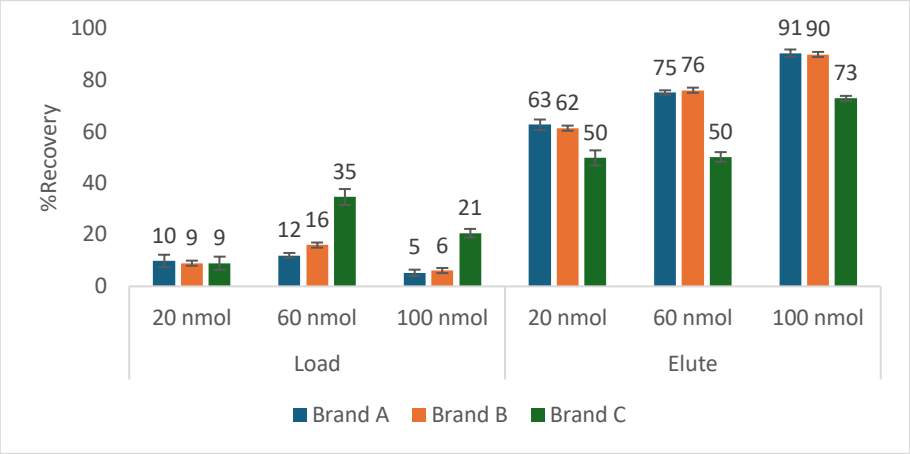

Figure 4.17 Comparison of percentage recovery of the content of standard **16** using different brands of cotton wool, all data were collected in triplicate.

(A)

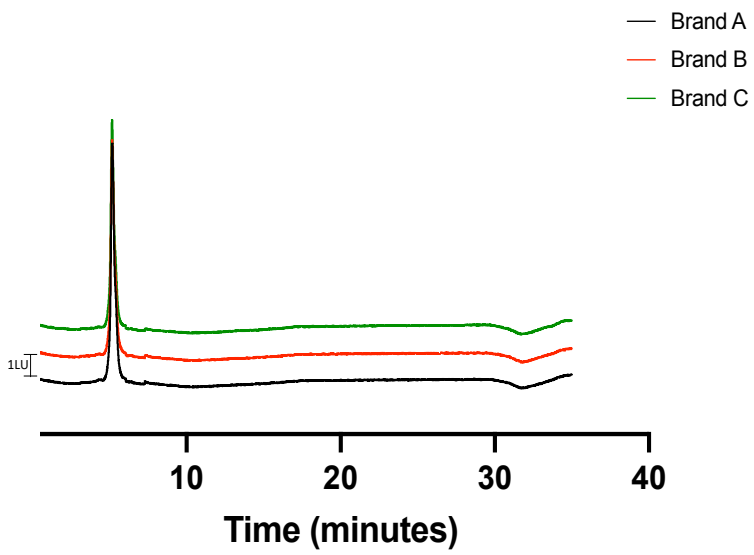

(B)

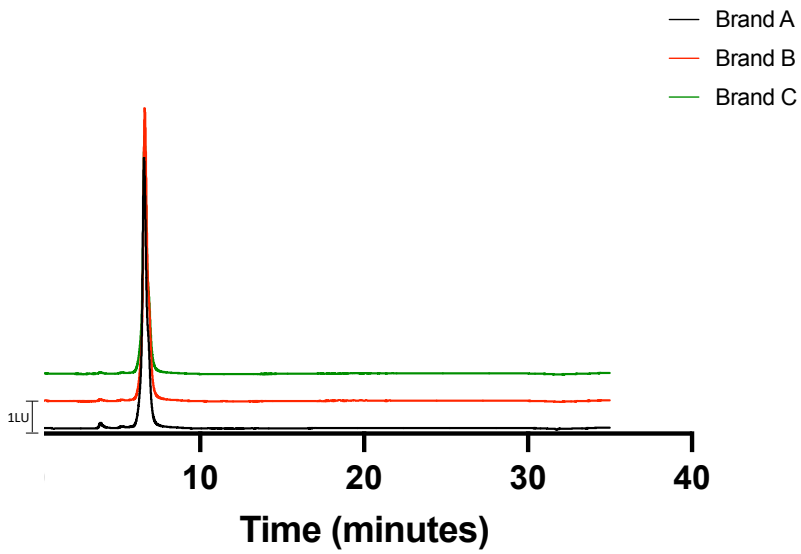

Figure 4.18 The chromatogram of standard **16** (A) and **27** (B) in elute step using three brands of cotton wool.

The results for standards **16** and **27** show that different brands of cotton wool have different capacities to enrich labelled carbohydrates. Brand C had less enrichment capacity than others.

4.3.10 Extension of SPE and cotton wool enrichment methods to other labelled glycans.

The successful methods (Amide SPE-brand A, cotton wool method 3) provided a proof of concept for the enrichment of labelled glycans. This was then probed further using the trisaccharide, Maltotriose (3GU), and the dextran ladder (mixture of linear glucose oligomers obtained by the partial hydrolysis of dextran). Compounds **5** and **26** were again used as labelling reagents.

The results show that both methods can separate the labelling reagents from the labelled Maltotriose and dextran ladder. A small amount of labelled maltotriose was found in the wash solution using Amide SPE and in the load and wash solution using cotton wool. The results have a similar pattern with Compounds **16** and **27**. The structure and chromatograms of **5**-maltotriose (**28**) and **26**-maltotriose (**29**) are shown in Figure 4.19, and the retention time is in Table 4.10. The comparison of the labelled dextran ladder by **5** and **26** enrichment was shown by the HPLC chromatogram in Figure 4.20. The results show that the enrichment property of cotton wools has an enrichment efficiency similar to Amide SPE.

(A)

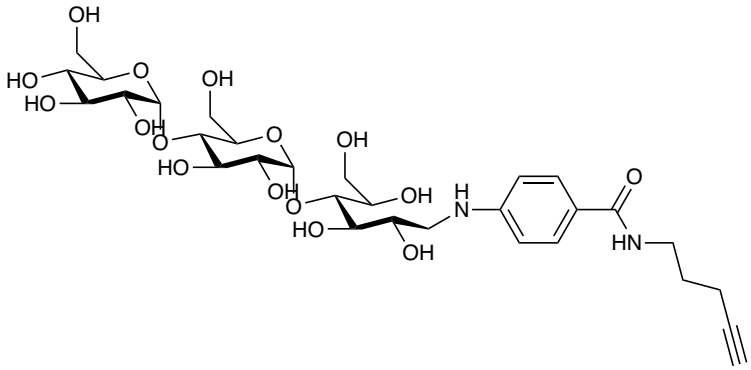

(B)

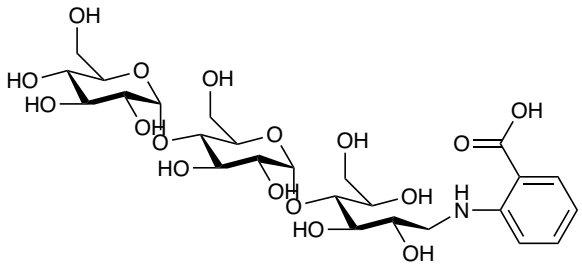

(C)

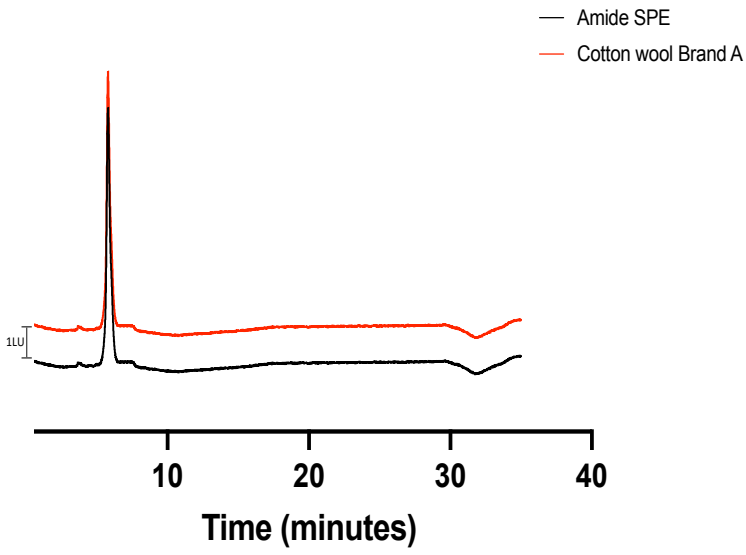

(D)

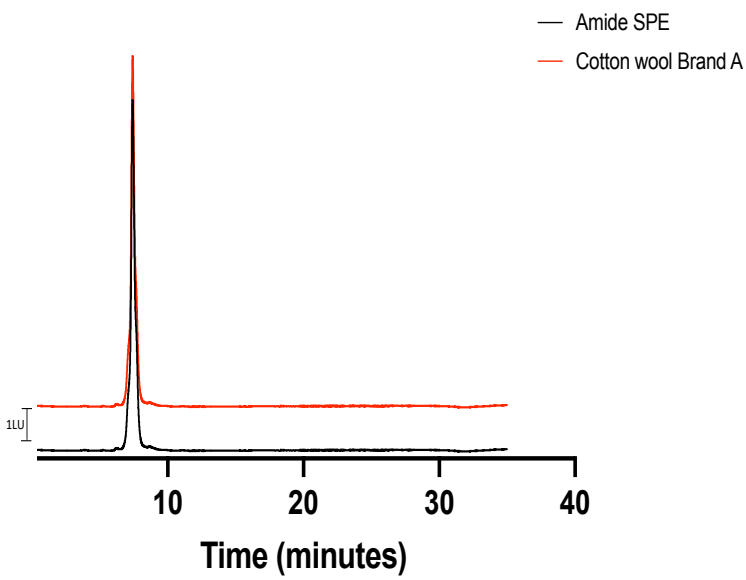

Figure 4.19 Structure of **28** (A), **29** (B), and HPLC chromatograms demonstrating the retention time of different labelling reagents and sugar: (C) chromatogram of **28**, and (D) chromatogram of **29**.

Table 4.10 The retention time of the labelled maltotriose

Compound	Retention time (min)
16	5.17
27	6.55
28	5.77
29	7.39

(A)

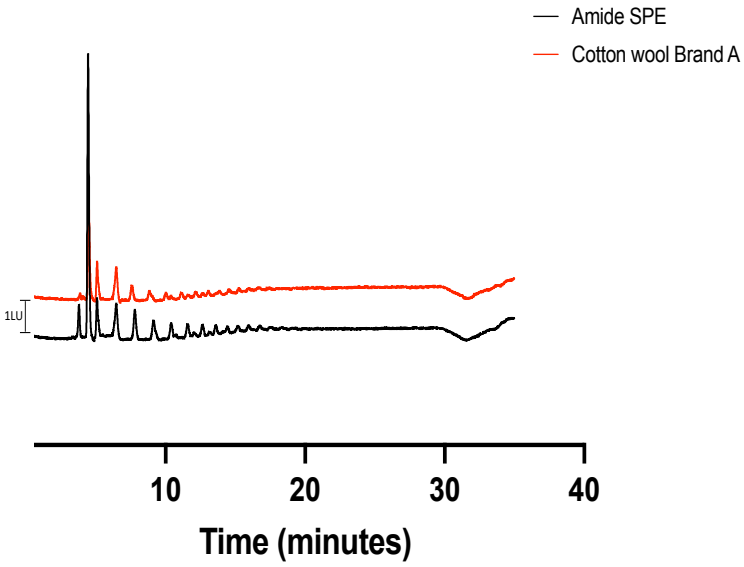

(B)

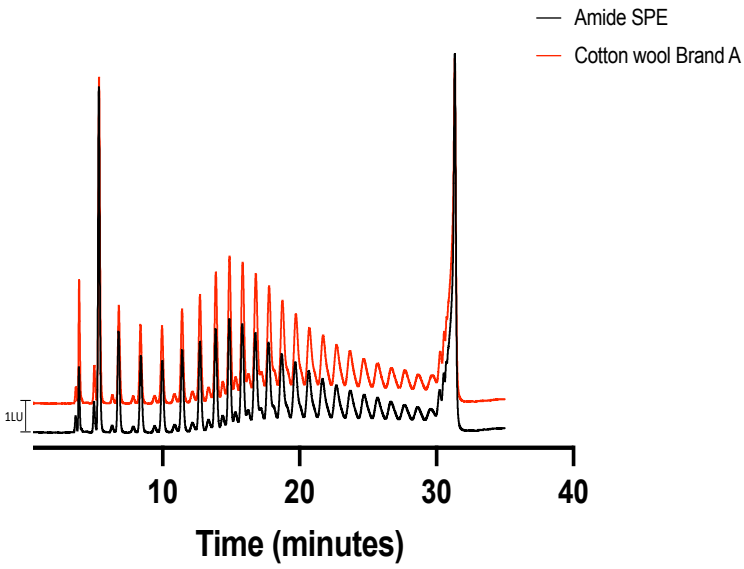

Figure 4.20 The HPLC chromatogram demonstrating the retention times of different labelling reagents and different glucose units of sugar in labelled dextran ladder by (A) **5** and (B) **26**.

4.4 Conclusions and Future Work

Methods for the enrichment of labelled carbohydrates have been developed to remove impurities from the carbohydrate sample before analysis to facilitate analysis of the sample of interest via HPLC. The main focus of enrichment is to remove impurities (such as proteins and lipids) after glycan releasing steps, to accomplish desalting, and to remove excess labels after the labelling step. This chapter aimed to determine enrichment methods suitable for labelled glycans using SPE and cotton wool. Commercially available cotton wool pads are derived from natural sources and are easy to prepare in the laboratory. This study used standards **16** and **27** as the labelling reagents. Various types and modes of SPE were used to find the best conditions. The developed enrichment method from the cotton wool was included in the study to compare the results with the commercial SPE.

It was demonstrated that three types of SPE resulted in the maximum recovery of the standard during the eluting step. However, results using the labelling reagent found that PGC and SCX elute the labelling reagent in the same step as the labelled carbohydrate. The Amide SPE was the only medium that afforded the labelling reagent in the load and washing step. Therefore, the Amide SPE was selected to enrich the labelled carbohydrate in the labelling reaction. The results of the same condition with different brands of the Amide SPE found different recovery in the eluting step. The selected Amide SPE brand and conditions were repeated in triplicate. The results show high accuracy and precision, a percentage recovery of more than 95%, and a standard deviation of less than 1.00. The benefit of the selected condition was confirmed using different labelling reagents (**16**). Similar results between standards **16** and **27** were confirmed.

For the second objective, to optimise the cotton wool enrichment method for labelled glycans, the Amide SPE condition was developed since this had demonstrated the highest percentage recovery in the eluting step. Although the standard was found in fractions from all steps, the highest concentration was found in the eluted fraction. Different conditions and equilibration solvents were studied to optimise the conditions using cotton wool. 80% ACN in water in the equilibration steps led to the best recovery of standard **27**. The maximum absorbent capacity of the cotton wool was studied using concentrations of the standard of 10-100 nmol/200 µL. The optimum conditions for cotton wool were applied to standard **16** (20, 60,100 nmol/200 µL). This allowed for more than 90% recovery. The high precision in the method is demonstrated in the standard deviation which is less than 5.0 for two brands of cotton wool.

In the third objective, the trisaccharide (maltotriose) and dextran ladder were labelled with **5** and **26** in the general fluorescence labelling reaction. The Amide SPE and cotton wool were used to remove the excess labelling reagent from the reaction before analysis by HPLC. The results show that Amide SPE and cotton wool can remove the excess labelling reagent from the sample. The enriched labelled glycans HPLC chromatograms in the eluting step show small amounts of the labelling reagents remain in the sample. One limitation of the study is the different results from the different Amide SPE and cotton wool brands.

In conclusion, HILIC mode SPE is suitable for the enrichment of fluorescence-labelled carbohydrates. Compared with the Amide SPE, the cotton wool method is cheaper and more rapid. Going forward, this study will develop a precise, accurate, robust, and low-cost enrichment method for labelled glycans before HPLC-fluorescence analysis. However, the reliability of cotton wool SPE will require the development of a consistent method for preparing cotton wool tips to ensure consistency of the results and increase the loading capacity.

4.5 Experimental

4.5.1 General experiment

All chemicals used were analytical or HPLC grade, purchased from commercial sources (Sigma-Aldrich, Merk, Fisher Scientific, Alfa Aesar and Acros Organics), and used without further purification. HPLC analytical column (TSKgel Amide-80 HR column) was purchased from Tosoh Bioscience GmbH (Germany). The experiments were monitored by TLC. The TLC plates were aluminium backed 60 F254 silica (Sigma Merk). Visualisation was then carried out under UV light (λ= 254 nm) followed by staining with 5% sulfuric acid in MeOH with 0.3% *N*-1-naphthylenediamine.

All SPE used were purchased from commercial sources (Telos, Applied Separation, Chromabond, and Thermo).

The three brands of absorbent cotton wool pads were purchased from a local store in Reading, UK (Boots, made in India (brand A); Co-op, made in the Netherlands (brand B); and Novon, made in Bulgaria (brand C)).

4.5.2 Cotton wool tip preparation

The cotton wool was cut and weighed to afford 5±0.5 mg samples that were pushed into 200 µL pipette tips tightly by other pipette tips**.** The cotton wool tips were stored in a closed box until used.

4.5.3 Analytical Equipment

Nuclear Magnetic Resonance
Both proton (δ_H) and carbon (δ_C) nuclear magnetic resonance spectra were recorded according to the methods in chapter 2.

Mass Spectrometry
Electrospray Ionization Fourier Transform Mass Spectrometry (FTMS+p ESI) were obtained by either LCMS or direct infusion on a Thermofisher Scientific Orbitrap XL mass spectrometer in ESI+ mode. The scan range is full scan (mass 80.00-2000.00).

High performance liquid chromatography
HILIC mode HPLC was performed on an Agilent 1100 series HPLC system linked to both Agilent G1321A FLD detector and an G1314A variable wavelength detector. Amide HILIC performed the separation of labelled sugars on a TSKgel Amide-80 HR column (250 x 4.6 mm, 5 µM particle size) filled with TSKgel Amide-80 guard column (15 x 3.2 mm, 5 µM particle size). Solvent A was composed of ammonium formate buffer (50 mM pH 4.4), while solvent B consisted of ACN. The flow rate was set at 0.8 mL/ min, and the column was maintained at 40^{o}C for the duration of the run.
Separation of labelled sugars took place over 35 minutes with a linear gradient beginning with 65% phase B at 10 minutes, with a further gradient to 50% in 10 minutes, to 45% in 5 minutes, to 10% in 3 minutes, maintain 10% for 2 minutes before returning to injection condition of 65% B between 31-35 minutes. The column was conditioned with 65% B, 5 minutes before the next injection. The injection volume was 2 µL per injection. The fluorescence detection used the excitation wavelength 240 nm and emission wavelength 420 nm. The Fluorescence absorptivity detection was reported as luminescence unit (LU) represent to the Agilent system.

4.5.4 Solvents and Buffer

2 M Ammonium formate buffer stock solution pH 4.4
Formic acid (184.12 g, 4 mol) was combined with water (1L) and cooled to 0°C in an ice bath. 25% Ammonium solution (200 mL) was then added in 50 mL increments. The pH was adjusted to 4.4 by the 25% ammonium solution. The stock solution was then diluted to 2 L to a final concentration 50 mM and used as a HILIC phase modifier.

Labelling agent stock solution
Labelling reagent (**5** and **26**) were weighed and diluted in methanol to a final concentration of 40 mmol/mL.

Labelling buffer solution
Boric acid (3 g, 0.04 mol) and sodium acetate trihydrate (6 g, 0.045 mol) were dissolved in MeOH (100 mL).

Sodium cyanoborohydride solution
Sodium cyanoborohydride solution was prepared at 0.42 mM in labelling buffer solution.

4.5.5 Synthesis of GU2 labelled carbohydrate standard [29]

***N*-(Pent-4-yn-1-yl)-4-((2,3,5,6-tetrahydroxy-4-(((*2S,3R,4S,5S,6R*)-3,4,5-trihydroxy-6-(hydroxymethyl)tetrahydro-2H-pyran-2-yl)oxy)hexyl)amino)benzamide (16)**

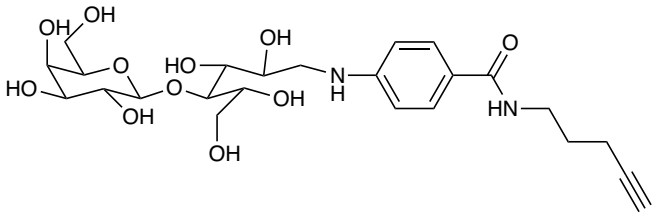

Compound **14** (20 mg, 0.058 mmol) was dissolved in water (200 µL), and sodium cyanoborohydride (36.72 mg, 0.58 mmol, 10 eq) in borate acetate buffered MeOH was added. The solution was heated to 50°C, and **5** (58.6 mg, 0.29 mmol, 5 eq) was added in MeOH (1 mL). The solution was stirred overnight and monitored by TLC until completion. The reaction mixture was dried under reduced pressure and dry loaded onto silica before being loaded onto a 10 cm silica flash column run with a mobile phase consisting of water, isopropanol and EtOAc in the ratio (1:2.5:6). Compound **16** was isolated as a pale yellow solid (24 mg, 0.045 mmol, 78% yield)

^{1}H NMR (**400 MHz, D_2O**) δ 7.56 (d, *J* = 8.8 Hz, 2H Ar 2 X CH), 6.75 (d, *J* = 8.7 Hz, 2H Ar 2 X CH), 3.98-3.03 (m, 18H Carbohydrate), 2.72 (d, *J* = 7.0 Hz, 1H C≡CH), 2.29-2.15 (m, 2H CH_2), 1.73 (p, *J* = 6.8 Hz, 2H CH_3). **^{13}C NMR** (**101 MHa, D_2O**) δ 219.36 (**C**-ONH), 196.25 (CH-**C**NH-CH Ar), 191.54(2CH Ar), 128.77 (**C**-CONH Ar), 113.61 (CH-**C**-2O), 102.74 (CH-**C**O-CH), 84.62 (CH_2-**C**H-CH), 84.38 (CH-**C**HCH2-O), 75.88 (CH-**C**HOH-CH), 75.63 (CHO-**C**HOH-CH), 75.14 (CH-**C**HOH-CH_2), 69.93 (CH-**C**HOH-CH), 68.53 (CH_2-CH), 68.04 (CHOH-**C**HOH-CH), 65.26 (CHOH-**C**HOH-CH_2), 62.91 (**C**HCH_2-OH), 57.95 (CH_2OH-CH), 57.43 (CH_2OH-CH), 53.92 (NH-CH_2-CH_2), 53.43 (CH_2-CH_2-N), 48.46 (N-CH_2-CH_3), 44.94(CH_2OH-CH), 37.86 (CHOH-**C**H_2-NH), 15.21 (CH_2-**C**H_2-CH_2). **FTMS**: ESI+ve $C_{24}H_{36}N_2O_{11}$ expected: 529.2390[M+H] found: 529.2392 [M+H]. HPLC retention time was 6.5 minutes.

2-((2,3,5,6-Tetrahydroxyl-4-(((2S,3R,4S,5S,6R)-3,4,5-trihydroxy-6-(hydroxymethyl)tetrahydro-2H-pyran-2-yl)oxy)hexyl)amino)benzoic acid (27)

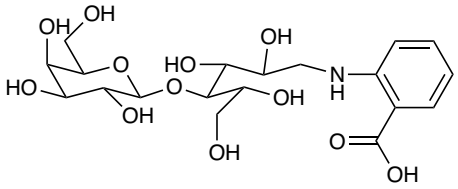

Lactose (**14**) (20 mg, 0.058 mmol) was dissolved in water (200 µL) and sodium cyanoborohydride (36.72 mg, 0.58 mmol, 10 eq) in borate acetate buffered MeOH was added. The solution was heated to 50°C and **26** (40.0 mg, 0.29 mmol, 5 eq) was added in MeOH (1 mL). The solution was stirred overnight and monitored by TLC until completion. The reaction mixture was dried under reduced pressure and dry loaded onto silica before being loaded onto a 10 cm silica flash column run with a mobile phase consisting of water, isopropanol and EtOAc in the ratio (1:2.5:6). This afforded **27** as a white solid (19 mg, 0.041 mmol, 71% yield)

^{1}H NMR (**400 MHz**, **D_2O**) δ 7.48 (t, *J* = 9.0 Hz, 1H), 7.37 (t, *J* = 7.7 Hz, 1H), 6.85 (t, *J* = 87.1 Hz, 1H), 6.71 (q, *J* = 7.5 Hz, 1H), 4.28 (d, *J* = 4.3 Hz, 1H), 4.14-3.49 (m, 15H). **^{13}C NMR** (**101 MHz, D_2O**) δ181.50 (C-ONH_2), 140.48 (C-NHC Ar), 133.55 (CH Ar), 129.10 (CH Ar), 113.15 (CH Ar), 110.53 (C-$CONH_2$ Ar), 101.11 (O-**C**H-CH), 79.23 (CH-**C**O-OH), 74.80 (CH-**C**HCH_2-O), 71.10 (CH-**C**HOH-CH), 70.61 (CH-**C**HOH-CH),68.87 (CH-**C**HOH-CH), 64.24 (CH-**C**HCH_2-OH), 61.99 (CHOH-**C**H_2-NH), 60.61 (**C**H2OH-CH), 45.46 (CHOH-**C**H_2-NH)) **FTMS**: ESI+ve $C_{19}H_{30}N_2O_{11}$ expected: 463.1922 [M+H] found: 463.1922 [M+H]. HPLC retention time was 7.3 minutes.

4.5.6 General labelling procedure for glycans (Maltotriose and dextran ladder)

Glycan solution (1 mM in MeOH for maltotriose and 0.1 mg/mL of dextran ladder), 100 µL, was applied to a 1.5 mL centrifuge tube and mixed with 100 µL of labelling buffer and 15 µL of sodium cyanoborohydride solution. The labelling solution (40 mmol/mL in MeOH) was added (100 µL). The reaction mixture was then vortexed and centrifuged for 10 seconds before being heated at 65°C for 180 minutes. The reaction solution was quenched with the addition of ACN (950 µL), producing a white precipitate. The quenched solution was transferred for enrichment with the selective method for comparison (Amide SPE and cotton wool). The elute solution from the enrichment method was dried and reconstituted with 500 µL of HPLC water before injection into HPLC. The retention time of **28** (maltotriose-**5**) and **29** (maltotriose-**26**) is 5.7 and 7.4 minutes, respectively.

4.5.7 General enrichment of labelled glycan with Amide SPE

The Amide SPE was equilibrated with 1 mL of MeOH twice. The labelled glycan sample from the labelling reaction (1 mL in MeOH) was loaded after equilibrating. Let the solvent dripped through the cartridge. The first wash was 1 mL of 99% ACN (aq), 5 times. The second wash was 1 mL of 97% ACN (aq), 5 times. In the last wash, let the cartridge dry before eluting the labelled glycans with 800 µL of HPLC water. The eluted solution from the enrichment method was dried and kept at -20°C until redissolved with 0.5 mL of HPLC water for HPLC analysis.

4.5.8 General enrichment of labelled glycan with C8 and C18 SPE

Method-1: The C8 and C18 SPE were conditioned with 1 mL of ACN and equilibrated with 1 mL of water, 4 times. The labelled glycan sample from the labelling reaction (1 mL in water) was loaded after equilibrating. Let the solvent dripped through the cartridge. The cartridge was washed with 1 mL of water twice. In the last wash, let the cartridge dry before eluting the labelled glycans with 1 mL of 25% v/v ACN (aq).

Method-2: The C8 and C18 SPE were conditioned with 1 mL of ACN and equilibrated with 1 mL of water, 4 times. The labelled glycan sample from the labelling reaction (1 mL in water) was loaded after equilibrating. Let the solvent dripped through the cartridge. The cartridge was washed with 1 mL of water twice. In the last wash, let the cartridge dry before eluting the labelled glycans with 1 mL of 4% ACN in 0.1% TFA.

Method-3: The C8 and C18 SPE were conditioned with 1 mL of 80% ACN in 0.1% TFA and equilibrated with 1 mL of water. After equilibrating, the labelled glycan sample from the labelling reaction (1 mL in water) was loaded. The solvent dripped through the cartridge. The cartridge was washed with 1 mL of water twice. In the last wash, the cartridge dried before eluting the labelled glycans with 2 mL of 80% ACN in 0.1% TFA twice.

The eluted solution from all enrichment methods was dried and kept at -20^{o}C until redissolved with 0.5 mL of HPLC water for HPLC analysis.

4.5.9 General enrichment of labelled glycan with PGC SPE

Method-1: The PGC SPE was conditioned with 1 mL of 80% ACN (aq) and equilibrated with 1 mL of water, then 1 mL of ACN in 0.1% TFA. The labelled glycan sample from the labelling reaction (1 mL in water) was loaded after equilibrating. Let the solvent dripped through the cartridge. The cartridge was washed with 1 mL of water twice. In the last wash, let the cartridge dry before eluting the labelled glycans with 2 mL of 40% ACN (aq).

Method-2: The PGC SPE was conditioned with 1 mL of 80% ACN in 0.1%TFA and equilibrated with 1 mL of water. The labelled glycan sample from the labelling reaction (1 mL in water) was loaded after equilibrating. Let the solvent dripped through the cartridge. The cartridge was washed with 1 mL of water twice. In the last wash, let the cartridge dry before eluting the labelled glycans with 2 mL of 80% ACN in 0.1%TFA.

Method-3: The PGC SPE was conditioned with 1 mL of 80% ACN in 0.1%TFA and equilibrated with 1 mL of water. The labelled glycan sample from the labelling reaction (1 mL in water) was loaded after equilibrating. Let the solvent dripped through the cartridge. The cartridge was washed with 1 mL of water twice. In the last wash, let the cartridge dry before eluting the labelled glycans with 2 mL of 20% ACN (aq).

The eluted solution from all enrichment methods was dried and kept at -20^{o}C until redissolved with 0.5 mL of HPLC water for HPLC analysis.

4.5.10 General enrichment of labelled glycan with Superco Discovery glycan SPE

The Superco Discovery glycan SPE was equilibrated with 1 mL of 99%ACN (aq). The labelled glycan sample from the labelling reaction (1 mL in 99%ACN (aq)) was loaded after equilibrating. Let the solvent dripped through the cartridge. The cartridge was washed with 1 mL of 99%ACN (aq). In the last wash, let the cartridge dry before eluting the labelled glycans with 1 mL of 20% ACN (aq). The eluted solution from the enrichment method was dried and kept at -20^{o}C until redissolved with 0.5 mL of HPLC water for HPLC analysis.

4.5.11 General enrichment of labelled glycan with Porous polystyrene DVB SPE

Method-1: The Porous polystyrene DVB SPE was conditioned with 1 mL of MeOH, 3 times and equilibrated with 1 mL of water, 3 times. The labelled glycan sample from the labelling reaction (1 mL in water) was loaded after equilibrating. Let the solvent dripped through the cartridge. The cartridge was washed with 1 mL of 5% MeOH (aq), 3 times. In the last wash, let the cartridge dry before eluting the labelled glycans with 3 mL of MeOH.

Method-2: The Porous polystyrene DVB SPE was conditioned with 1 mL of MeOH, 3 times and equilibrated with 1 mL of water, 3 times. The labelled glycan sample from the labelling reaction (1 mL in water) was loaded after equilibrating. Let the solvent dripped through the cartridge. The cartridge was washed with 1 mL of 5% MeOH (aq), 3 times. In the last wash, let the cartridge dry before eluting the labelled glycans with 3 mL of ACN.

The eluted solution from all enrichment methods was dried and kept at -20^{o}C until redissolved with 0.5 mL of HPLC water for HPLC analysis.

4.5.12 General enrichment of labelled glycan with SAX SPE

Method-1: The SAX SPE was conditioned with 1 mL of 0.1% TFA in water, 3 times and equilibrated with 1 mL of 95% ACN in 0.1% TFA, 3 times. The labelled glycan sample from the labelling reaction (1 mL in water) was loaded after equilibrating. Let the solvent dripped through the cartridge. The first wash was 0.5 mL of 95% ACN in 0.1% TFA. The second wash was 1 mL of 95% ACN in 0.1%TFA, 6 times. In the last wash, let the cartridge dry before eluting the labelled glycans with 2 mL of 95% ACN in 0.1% TFA, and 2 mL of 5% ACN in 0.1% TFA.

Method-2: The SAX SPE was conditioned with 1 mL of MeOH, 3 times and equilibrated with 1 mL of water, 3 times. The labelled glycan sample from the labelling reaction (1 mL in water) was loaded after equilibrating. Let the solvent dripped through the cartridge. The first wash was 1 mL of 50 mM Sodium acetate pH 7. The second wash was 1 mL of MeOH twice. In the last wash, let the cartridge dry before eluting the labelled glycans with 2 mL of 2% FA in MeOH.

The eluted solution from all enrichment methods was dried and kept at -20^{o}C until redissolved with 0.5 mL of HPLC water for HPLC analysis.

4.5.13 General enrichment of labelled glycan with SCX SPE

Method-1: The SCX SPE was conditioned with 1 mL of ACN, 3 times and equilibrated with 1 mL of water (3 times), 1 mL of 100mM triethylammonium acetate (3 times), and 1 mL of 95% ACN in 0.1% TFA (3 times). The labelled glycan sample from the labelling reaction (1 mL in 1% FA (aq)) was loaded after equilibrating. Let the solvent dripped through the cartridge. The cartridge was washed with 1 mL of 95% ACN in 1% TFA, 3 times. In the last wash, let the cartridge dry before eluting the labelled glycans with 0.8 mL of 50% ACN in 1% TFA.

Method-2: The SCX SPE was conditioned with 1 mL of 0.1%FA in MeOH, 3 times and equilibrated with 1 mL of 2% FA (aq), 3 times. The labelled glycan sample from the labelling reaction (1 mL in 1% FA (aq)) was loaded after equilibrating. Let the solvent dripped through the cartridge. The first wash was 1 mL of % FA (aq). The second wash was 1 mL of MeOH twice. In the last wash, let the cartridge dry before eluting the labelled glycans with 6 mL of 10% ammonium hydroxide in MeOH.

The eluted solution from all enrichment methods was dried and kept at -20^{o}C until redissolved with 0.5 mL of HPLC water for HPLC analysis.

4.5.14 General enrichment of labelled glycan with Cotton wool.

The cotton wool tip was equilibrated with 3 times 100 µL of 0-100% ACN in water. The sample solution 200 µL was loaded after equilibration by pipet up and down 20 times. The first wash was 100 µL of 99% ACN (aq), 5 times. The second wash was 100 µL of 97% ACN (aq), 5 times. Eluting the labelled glycans used 100 µL of HPLC water 3 times. The combination of eluted solution from the enrichment method was dried and kept at -20^{o}C until redissolved with 0.5 mL of HPLC water for HPLC analysis.

4.5.15 Calculation of percentage recovery of standard from SPE and cotton wool enrichment

The percentage recovery from SPE and cotton wool was calculated by comparing the peak area from the solution in the enrichment of each step obtained from HPLC analysis with the standard curve in the concentration. The dilution factor was then used to calculate the amount of standard, which was compared to the starting concentration used before being added to SPE and cotton wool.

4.6 References

1. Gizaw, S.T., S. Gaunitz, and M.V. Novotny, *Highly Sensitive O-Glycan Profiling for Human Serum Proteins Reveals Gender-Dependent Changes in Colorectal Cancer Patients*. Analytical Chemistry, 2019. **91**(9): p. 6180-6189.
2. Gizaw, S.T., et al., *Glycoblotting method allows for rapid and efficient glycome profiling of human Alzheimer's disease brain, serum and cerebrospinal fluid towards potential biomarker discovery.* Biochimica et Biophysica Acta (BBA) - General Subjects, 2016. **1860**(8): p. 1716-1727.
3. Videira, P.A.Q. and M. Castro-Caldas, *Linking Glycation and Glycosylation With Inflammation and Mitochondrial Dysfunction in Parkinson's Disease*. Frontiers in Neuroscience, 2018. **12**(381): p.1-20
4. McGarrah, R.W., et al., *A Novel Protein Glycan-Derived Inflammation Biomarker Independently Predicts Cardiovascular Disease and Modifies the Association of HDL Subclasses with Mortality.* Clinical Chemistry, 2017. **63**: p. 288-296.
5. Manz, C., et al., *Dextran as internal calibrant for N-glycan analysis by liquid chromatography coupled to ion mobility-mass spectrometry.* Analytical and bioanalytical chemistry, 2022. **414**(17): p. 5023-5031.
6. Daramola, O., et al., *Isomeric separation of native N-glycans using nano zwitterionic- hydrophilic interaction liquid chromatography column*. Journal of Chromatography A, 2023. **1705**: p. 464198.
7. Kayili, H.M. and B. Salih, *Site-specific N-glycosylation analysis of human thyroid thyroglobulin by mass spectrometry-based Glyco-analytical strategies*. Journal of proteomics, 2022. **267**: p. 104700.
8. Zedan, H., et al., *Microheterogeneity and Individual Differences of Human Urinary N -Glycome under Normal Physiological Conditions*. Biomolecules (Basel, Switzerland), 2023. **13**(5): p. 756.
9. Takakura, D., et al., *Selective glycopeptide profiling by acetone enrichment and LC/MS*. Journal of Proteomics, 2014. **101**: p. 17-30.
10. Selman, M.H.J., et al., *Cotton HILIC SPE Microtips for Microscale Purification and Enrichment of Glycans and Glycopeptides*. Analytical Chemistry, 2011. **83**(7): p. 2492-2499.
11. Liu, L., et al., *Preparation of cotton wool modified with boric acid functionalized titania for selective enrichment of glycopeptides*. Talanta (Oxford), 2019. **203**: p. 58-64.
12. Wu, M., et al., *An ultrafast and highly efficient enrichment method for both N-Glycopeptides and N-Glycans by bacterial cellulose*. Analytica chimica acta, 2020. **1140**: p. 60-68.
13. Zhang, D., L. Zhang, and T. Liu, *A magnetic cellulose-based carbon fiber hybrid as a dispersive solid-phase extraction material for the simultaneous detection of six bisphenol analogs from environmental samples*. Analyst (London), 2018. **143**(13): p. 3100-3106.
14. Zhang, Y., et al., *A rapid 2AB-UHPLC method based on magnetic beads extraction for N-glycan analysis of recombinant monoclonal antibody*.

Journal of chromatography. B, Analytical technologies in the biomedical and life sciences, 2022. **1192**: p. 123139-123139.
15. Liu, Y., et al., *Facile Synthesis of Hydrophilic Magnetic Mesoporous Silica Microspheres for Selective Enrichment of Glycopeptides and Glycans*. Analytical letters, 2021. **54**(6): p. 966-978.
16. Verostek, M.F., C. Lubowski, and R.B. Trimble, *Selective Organic Precipitation/Extraction of Released N-Glycans Following Large-Scale Enzymatic Deglycosylation of Glycoproteins*. Analytical Biochemistry, 2000. **278**(2): p. 111-122.
17. Kim, B.J. and D.C. Dallas, *Systematic examination of protein extraction, proteolytic glycopeptide enrichment and MS/MS fragmentation techniques for site-specific profiling of human milk N-glycoproteins*. Talanta (Oxford), 2021. **224**: p. 121811-121811.
18. Nwosu, C.C., et al., *Comparison of the Human and Bovine Milk N-Glycome via High-Performance Microfluidic Chip Liquid Chromatography and Tandem Mass Spectrometry*. Journal of Proteome Research, 2012. **11**(5): p. 2912-2924.
19. Barboza, M., et al., *Region-Specific Cell Membrane N-Glycome of Functional Mouse Brain Areas Revealed by nanoLC-MS Analysis*. Mol Cell Proteomics, 2021. **20**: p. 100130.
20. Seo, Y., et al., *Comprehensive Characterization of Biotherapeutics by Selective Capturing of Highly Acidic Glycans Using Stepwise PGC-SPE and LC/MS/MS*. Analytical Chemistry, 2019. **91**(9): p. 6064-6071.
21. Robinson, R.C., et al., *An improved method for the purification of milk oligosaccharides by graphitised carbon-solid phase extraction*. International dairy journal, 2018. **80**: p. 62-68.
22. Barboza, M., et al., *Region-Specific Cell Membrane N-Glycome of Functional Mouse Brain Areas Revealed by nanoLC-MS Analysis*. Molecular & cellular proteomics, 2021. **20**: p. 100130-100130.
23. Lauber, M.A., et al., *Rapid Preparation of Released N-Glycans for HILIC Analysis Using a Labeling Reagent that Facilitates Sensitive Fluorescence and ESI-MS Detection*. Analytical Chemistry, 2015. **87**(10): p. 5401-5409.
24. Trbojević-Akmačić, I., et al., *Plasma N-glycome composition associates with chronic low back pain*. Biochimica et Biophysica Acta (BBA) - General Subjects, 2018. **1862**(10): p. 2124-2133.
25. Yang, W., et al., *Comparison of Enrichment Methods for Intact N- and O-Linked Glycopeptides Using Strong Anion Exchange and Hydrophilic Interaction Liquid Chromatography*. Anal Chem, 2017. **89**(21): p. 11193-11197.
26. Yang, W., et al., *Comparison of Enrichment Methods for Intact N- and O-Linked Glycopeptides Using Strong Anion Exchange and Hydrophilic Interaction Liquid Chromatography*. Analytical Chemistry, 2017. **89**(21): p. 11193-11197.
27. Wang, Y., et al., *Glycan reductive amino acid coded affinity tagging (GRACAT) for highly specific analysis of N-glycome by mass spectrometry*. Analytica chimica acta, 2019. **1089**: p. 90-99.

28. Liu, X., Q. Wang, and M.A. Lauber, *High sensitivity acidic N-glycan profiling with MS-enhancing derivatization and mixed mode chromatography*. Journal of chromatography. B, Analytical technologies in the biomedical and life sciences, 2022. **1191**: p. 123120-123120.
29. Hancox, O.G.A., *Integrated workflows for Carbohydrate Analysis - Artificial Glycoconjugates as Tools for Glycan Analysis*, in *School of Pharmacy*. 2023, University of Reading. p. 242.
30. Peng, Y., et al., *A streamlined strategy for rapid and selective analysis of serum N-glycome*. Analytica chimica acta, 2019. **1050**: p. 80-87.
31. Han, J., et al., *Purification of N- and O-glycans and their derivatives from biological samples by the absorbent cotton hydrophilic chromatographic column*. Journal of Chromatography A, 2020. **1620**: p. 461001.
32. Qin, W., et al., *Serum Protein N-Glycosylation Signatures of Neuroblastoma*. Frontiers in oncology, 2021. **11**: p. 603417-603417.
33. Xin, M., et al., *Evaluation of absorbent cotton for glycopeptide enrichment*. Analytical and bioanalytical chemistry, 2022. **414**(29-30): p. 8245-8253.
34. Javeed, R., et al., *Apo-H (beta-2-glycoprotein) intact N-glycan analysis by MALDI-TOF-MS using sialic acid derivatization*. Anal Bioanal Chem, 2021. **413**(30): p. 7441-7449.
35. Reiding, K.R., et al., *High-Throughput Profiling of Protein N-Glycosylation by MALDI-TOF-MS Employing Linkage-Specific Sialic Acid Esterification*. Analytical Chemistry, 2014. **86**(12): p. 5784-5793.
36. Bermudez, A. and S. Pitteri, *Enrichment of Intact Glycopeptides Using Strong Anion Exchange and Electrostatic Repulsion Hydrophilic Interaction Chromatography*. Methods in molecular biology (Clifton, N.J.), 2021. **2271**: p. 107-120.
37. Anumula, K.R., *Rapid Quantitative Determination of Sialic Acids in Glycoproteins by High-Performance Liquid Chromatography with a Sensitive Fluorescence Detection*. Analytical Biochemistry, 1995. **230**(1): p. 24-30.

Chapter 5
Analysis of the Glycan profile for human neurological cells (SH-SY5Y)

5.1 Introduction

Neurodegenerative diseases are characterised by progressive loss of cognitive function, behavioural impairment (e.g., mood change), problems with communication, loss of thinking skill, brain imaging scans (computed tomography scan (CT scan), or magnetic resonance imaging (MRI)), and markers from brain pathology. Diagnosis of diseases such as Alzheimer's disease (AD), Parkinson's disease (PD), Huntington's disease (HD), Amyotrophic Lateral Sclerosis (ALS), frontotemporal dementia, and multiple sclerosis all measure the progressive loss of neurons in the central nervous system (CNS). However, neurodegenerative biomarkers are investigated using invasive methods from the brain and CSF, which leads to low patient compliance [1-10]. Therefore, a reliable, non-invasive method of diagnosis is required.

5.1.1 Glycans in neurodegenerative diseases

Glycosylation is an important modification that regulates cell function. Importantly, glycans are also associated with neuron development, migration, and regeneration. The study of glycans as a neurodegenerative disorder biomarker focuses on CSF glycan levels. However, there is great interest in using serum samples to detect biomarkers, as this method should increase patient compliance in the diagnostic process. Studies have shown that glycan levels in healthy populations differ from those with neurodegenerative diseases [11-13], as shown in Table 5.1.

Most commonly studied glycans as biomarkers are the glycans in the lipocalin-type prostaglandin D2 synthase (L-PGDS), transferrin (Tf), N-acetylglucosamine- terminated glycans (GlcNAc-Tf), and Serum Tf carries sialic acid-terminated glycans (Sia-Tf) [11, 12]. *N*- and *O*-glycan profiles are studied and compared with the normal biomarkers of neurodegenerative disease, such as Aβ or tau protein. The results show the patients' glycans levels related to Aβ and tau protein levels compared to normal groups [10, 14]. The hypothesis is that the activity of neuron function in neurodegenerative cells is higher than that of normal neurons. The protein biomarkers generated are related to glycan levels. The expression of different glycan types is an altered pattern in neurodegenerative disease. The different types of glycan levels studied in CSF and blood samples compared between normal biomarkers (Aβ, tau, and inflammatory factors) in neurodegenerative patients and healthy people are in Table 5.1.

Glycan analysis in neurodegenerative diseases used lectin blotting [15-17], glycan-specific lectin [12], glycan fluorescence array [13], NMR for tau and cell-surface glycan heparin sulphate (HS) [18, 19], HPLC-fluorescence [20-22], LC-MS or LC-MS/MS [11, 12, 14, 15, 21-29], and MS/MS [30], as shown in Table 5.1.

Table 5.1 The relationship between neurodegenerative diseases and glycan levels

Disease	Glycan types	Sample specimen	Difference in the glycan profile for the disease group compared with the control group	Relation between diseases and glycan levels	Glycan analysis method	References
AD	- *N*-Glycan (high mannose, hybrid complex, antenna fucose, Gal/GlcNAc, Man-Tf, and sialylation) - *O*-glycan (*O*-GalNAc core 1-3)	- Cell lines from the patient. - Hippocampus and cortex from patient and control brain. - CSF	- Decrease: high mannose hybrid, antenna fucose, 2,3 sialylation, and core 3 *O*-glycans. - Increase: *N*-glycan complex type, Gal/GlcNAc,2,6 sialylation level, core 1 and 2 of *O*-glycans.	The *N*- and *O*-glycan results are related to the Golgi activity of Aβ levels in the patient's cells. - *N*-glycan and high mannose were reduced in patients' cells as the Golgi had more activity in the neurodegenerative state. - Core 2, *O*-glycan level related to Aβ levels from the protein processing of synapse development and processing of the Golgi fragments. - Changing the tau and cell-surface glycan heparin sulphate (HS) binding site. - The Man-Tf levels in CSF are related to the p-tau level.	- LC-MS/MS - NMR between tau and cell-surface glycan heparin sulphate (HS)	[12, 14, 18, 19, 23, 24, 28]

Disease	Glycan types	Sample specimen	Difference in the glycan profile for the disease group compared with the control group	Relation between diseases and glycan levels	Glycan analysis method	References
PD	- *O*-Glycans in sialylated, GalNAc and mannose core - *N*-Glycan	- Striatum and substantia nigra tissue - Plasma - Urine	The level of *O*-sialylation glycans is significantly increased. The level of glycans containing core fucose, sialic acid and bisecting *N*-acetyl glucosamine increased compared to the control group. The total abundance of *N*-glycans (containing core fucose, sialic acid, and bisecting GlcNAc) in the urine of patients were significantly decreased.	The peripheral nervous system's abnormal myelination and axonal degeneration increase the sialylation *O*-glycans generated. For *N*-glycans, the peripheral inflammation induces the glycosylation change.	LC-fluorescence LC-MS MS/MS	[21, 30, 31]
HD	Brain-ganglioside glycans	Plasma	The glycans level in HD patients is higher than in the control group.	The glycan levels of the pre-HD group are higher than those of the HD group. The control group has the lowest glycan levels.	Specific glycan array kits	[13]
Dementia/MCI	IgG *N*-glycans (sialylation, fucosylation and GlcNAc)	Blood	In patient groups, there was a decrease in sialylation and core fucosylation and	The *N*-glycan levels correlate to inflammation factors. In MCI patients, the anti-inflammatory (IL-4	HPLC-fluorescence LC-MS or LC-MS/MS	[20, 25]

Disease	Glycan types	Sample specimen	Difference in the glycan profile for the disease group compared with the control group	Relation between diseases and glycan levels	Glycan analysis method	References
			increased bisecting GlcNAc.	and IL-100) and proinflammation (CRP, TNF-α and IFN-γ) increased, correlated to *N*-glycan levels.		
Multiple sclerosis	Plasma *N*-glycan and IgG *N*-glycans (fucosylation and high mannose)	Plasma	The patient's group found increasing high-branched structures bearing multiple galactose and sialic acid residues of the plasma *N*-glycome. The fucosylation and high mannose *N*-glycan in IgG have significantly increased in the patients compared to the control group.	Multiple sclerosis has the inflammation of neuron cells. The increasing immune cells in the CNS increased the *N*-glycans in the blood through the Blood-Brain Barrier (BBB) system.	HPLC-fluorescence-MS/MS	[22]
Spontaneous Intracranial hypotension (SIH)	Man-Tf GlcNAc-Tf L-PGDS Sia-Tf	CSF	All glycan markers in the patient group are higher than those in the control group.	All glycan markers in this study are produced in the choroid plexus and then secreted to CSF. SIH is caused by CSF leakage. This is why this glycan level is higher than in healthy people in CSF.	Glycan-specific Lectin	[12]

Disease	Glycan types	Sample specimen	Difference in the glycan profile for the disease group compared with the control group	Relation between diseases and glycan levels	Glycan analysis method	References
Idiopathic normal pressure hydrocephalus (iNPH)	Man-Tf GlcNAc-Tf L-PGDS Sia-Tf	CSF	The GlcNAc-Tf and L-PGDS levels of the patients' group were significantly higher than those of the control group.	In iNPH, patients have a reduced absorption of CSF. This is related to the high level of GlcNAc-Tf and L-PGDS in CSF.	Glycan-specific Lectin	[12]

5.1.2 SH-SY5Y Cell culture in neurodegenerative studies

Human neuroblastoma cell lines are used to replace samples from patients in the *in vitro* model of neurodegenerative diseases. An example of cell culture in neurodegenerative disorder is human cells such as primary neurons, organoids and human dermal fibroblasts [14, 32-34] or subclones of neurodegenerative human cells (such as SH-SY5Y, human keratinocyte cells, human-induced pluripotent stem cells, human embryonic kidney (HEK) 293 FT cells, and human microglial cells (HMC3)) [27, 35-42].

The SH-SY5Y (ATCC® CRL-2266™) cell line is the third subclone of the neuroblastoma cell line SK-N-SH (ATCC® HTB-11™), which was established in 1970 from the metastatic bone marrow of 4 years old cancer patient. SK-N-SH cells were subcloned thrice from SH-SY to SH-SY5 and finally to SH-SY5Y [43]. As the third subclone, these cells do not require human ethics. SH-SY5Y can differentiated from neuroblastoma to mature neuronal types by using all-trans retinoic acid (ATRA), phorbol ester, and specific neurotrophins, such as brain-derived neurotrophic factor (BDNF) [43-46]. Depending on the media conditions, these cells can be differentiated towards a cholinergic, dopaminergic, or adrenergic phenotype; for example, using only ATRA is differentiated to a primary cholinergic neuronal phenotype [45, 47]. Using ATRA in combination with growth factors (B-27 and dibutyryl cyclic AMP (db-cAMP)) can promote the complete differentiation of the SH-SY5Y to neuron type [44, 48-50].

The difference between undifferentiated and differentiated states of SH-SY5Y is shown in Figure 5.1. Undifferentiated SH-SY5Y cells exhibit an epithelial-like morphology or "*S*" type. The cells grow in clusters and form clumps of flat cells with short neurites. In contrast, differentiated cells exhibit a neuron-like morphology or "*N*" type. The cells become similar to primary neurons, expressing the neuronal projections and promoting networking between the cells [43, 44, 49].

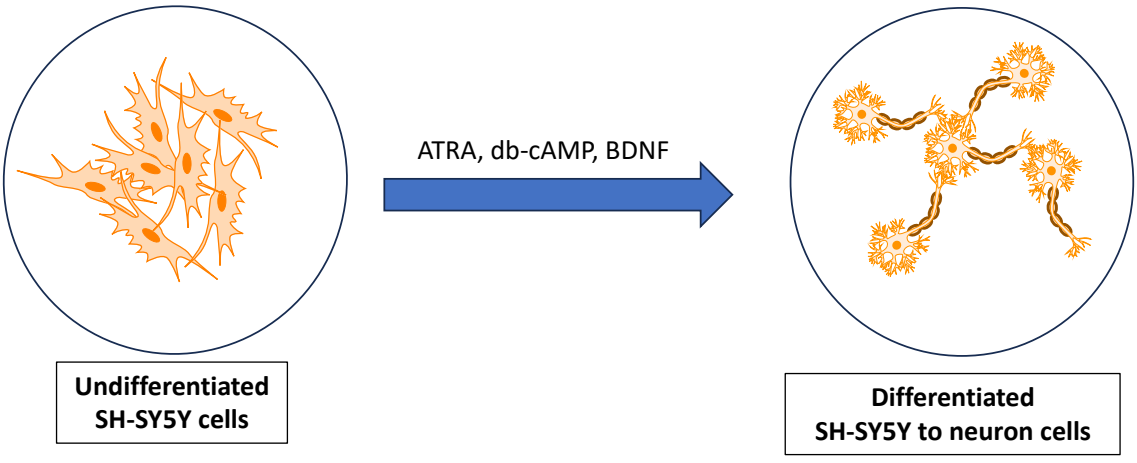

Figure 5.1 The differentiated process of SH-SY5Y from "*S*" type to "*N*" type. The undifferentiated SH-SY5Y cells grow in clusters and form clumps of flat phenotype with short neurites (*S* type). The differentiated cells become more neuronal-like with elongated neurotic projections between the cells (*N* type).

SH-SY5Y cells have been selected for *in vitro* studies on neurodegenerative diseases such as AD and PD due to their ability to differentiate into the cholinergic phenotype [49-61]. In these studies, biomarkers like tau protein [37, 49, 54, 62-64], β tubulin [65-67], amyloid beta (Aβ) [50, 53, 56, 58, 59, 61, 63], and inflammatory factors (IL-6, IL-1β, TNFα and IL-8) [52] have been

utilized for screening SH-SY5Y cells. However, there is limited research on the glycan profiles produced by SH-SY5Y cells.

5.1.3 Glycan levels in SH-SY5Y studies and analysis methods

Table 5.1 illustrates the types of glycans used as biomarkers in neurodegenerative disease studies from human specimens. The glycan levels generated by SH-SY5Y cells were developed in the study as the biomarker of the *in vitro* neurodegenerative state [68-70]. Examples of glycan levels studied in SH-SY5Y cells include terminal and total monosaccharide profiles of reeling glycoproteins (extracellular matrix glycoprotein for brain formation, cell aggregation, and dendrite formation) [68], extracellular *N*-linked glycans [69], and total *N*-linked glycan profiles [70]. Examples of analytical methods for detecting glycans from SH-SY5Y are lectin or blotting [68], capillary liquid chromatography-ESI-MS/MS [68], and HPLC-MS/MS [70]. Most studies focused on the qualitative analysis of carbohydrates from the SH-SY5Y. The molecular mass of glycans generated from SH-SY5Y was reported. However, the number of glycans in quantitative studies is limited. Studying different glycan levels between undifferentiated and differentiated states of SH-SY5Y as a biomarker will benefit the pre-clinical phase of neurodegenerative medicine development by following the cha glycan levels of the cells generated during drug treatment.

5.2 Aims and Objective

This work aims to apply the developed glycan analysis workflow from Chapters 2-4 to analyse the glycan profile from a complex biological sample, namely the undifferentiated and differentiated SH-SY5Y cell line. PNGase F was chosen to release the total *N*-glycan content from undifferentiated and differentiated SH-SY5Y cell lysates. Compound **26** was chosen as the glycan labelling reagent. The results from Chapter 4 show that the Amide SPE enrichment method was used prior to HPLC-fluorescence analysis. The dextran ladder labelled with **26** is used as the standard for quantitative and qualitative analysis of the glycan profile.

This research is summarised in Figure 5.2, which outlines the schemes of work carried out within this chapter.

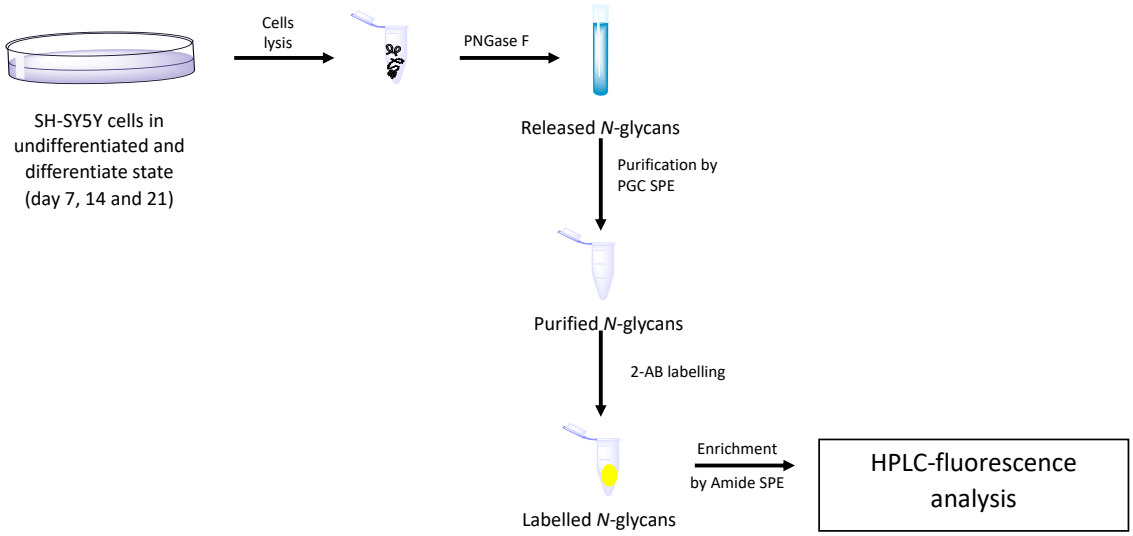

Figure 5.2 Workflow for glycan analysis by HPLC-fluorescence *in vitro* neurodegenerative cells.

5.3 Results and Discussion

5.3.1 Testing the activity of PNGase F

PNGase F was expressed from the bacterial cells, and its activity was checked before being used for the release of *N*-glycans from the SH-SY5Y cells. Figure 5.3 presents the activity testing results from 5 samples. Two samples were demonstrated to have good activity for use in SH-SY5Y cell lines.

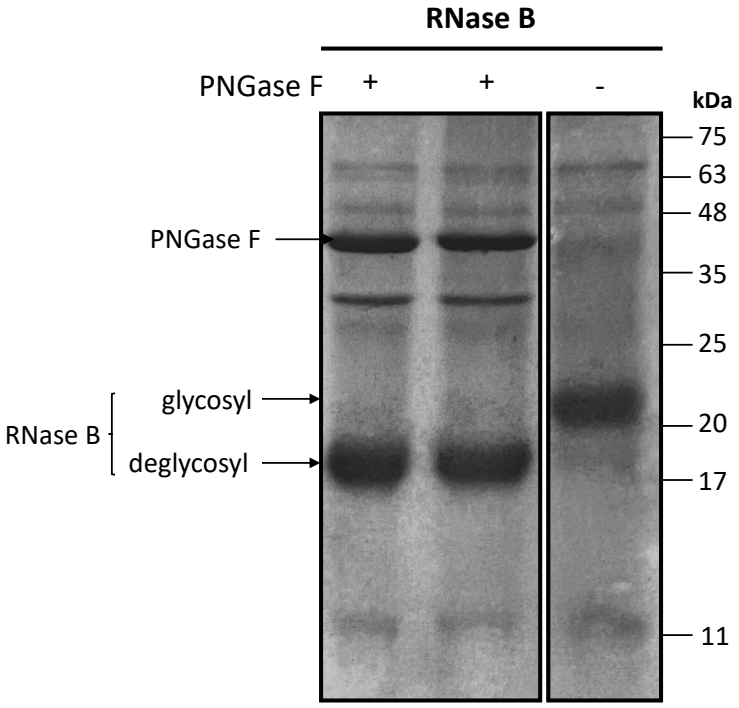

Figure 5.3 SDS-PAGE analysis of PNGase F activity using RNase B as substrate. RNase alone or RNase B with two different aliquots of in-house produced PNGase F were incubated at 37°C for 120 minutes and then analysed by SDS-PAGE. Both aliquots PNGase F showed activity and deglycosylated (deglycosyl) RNase B. In the absence of PNGase F, RNase B remained glycosylated (glycosyl), confirming the specificity of activity.

5.3.2 SH-SY5Y differentiation

The differentiation protocol from Mackenzie M. Shipley *et al*. [44] was used, and this is summarised in Table 5.2 and Figure 5.4. The differentiation media included ATRA, BDNF, and db-cAMP to promote differentiation, and a reduced concentration of foetal bovine serum (FBS). The cell culture media formulations are shown in Table 5.8. Undifferentiated and differentiated cells were grown under the same conditions (37°C, 5% CO_2). The neuronal characteristics of fully differentiated SH-SY5Y cells are apparent by the change in the morphology of the cell and by the detection of a specific protein using immunofluorescence. The cells were stained every 7 days with an antibody to β-III tubulin.

Table 5.2 SH-SY5Y differentiation protocol

Day	Activity
0	Plate two 100 mm cell culture dishes ($6x10^5$ cells/plate) and one 6-well plate with two coated coverslips per well ($1x10^5$ cells/well). All plates and wells use basic growth media.
1	Change the media to differentiation media #1.
2	
3	Change media (differentiation media #1).
4	
5	Change media (differentiation media #1).
6	
7	1. Collect the cells from one 100 mm dish for glycan profile analysis. 2. Passage the other 100 mm dish at a ratio of 1:1. 3. Perform bright field imaging and immunocytochemistry using cells in the 6-well plate. Stain for β-III tubulin.
8	Change the media to differentiation media #2.
9	
10	1. Passage the cells in the 100 mm dish at a ratio of 1:4 into two 100 mm petri dishes (coated with extracellular matrix (ECM) solution (1:100) with MEM/F12 (1:1) in differentiation media #2. 2. Plate remaining cells into two 6-well plates ($1x10^5$ cells/well) with two coated coverslips (with poly-D-lysine and ECM) in differentiation media #2.
11	Change the media to differentiation media #3.
12	
13	
14	1. Collect the cells from one 100 mm dish for glycan profile analysis. 2. Perform bright field imaging and immunocytochemistry using cells in one 6-well plate. Stain for β-III tubulin.
15	Change media (differentiation media #3).
16	
17	
18	Change media (differentiation media #3).
19	
20	
21	1. Collect the cells from one 100 mm dish for glycan profile analysis. 2. Perform bright field imaging and immunocytochemistry using cells in one 6-well plate. Stain for β-III tubulin.

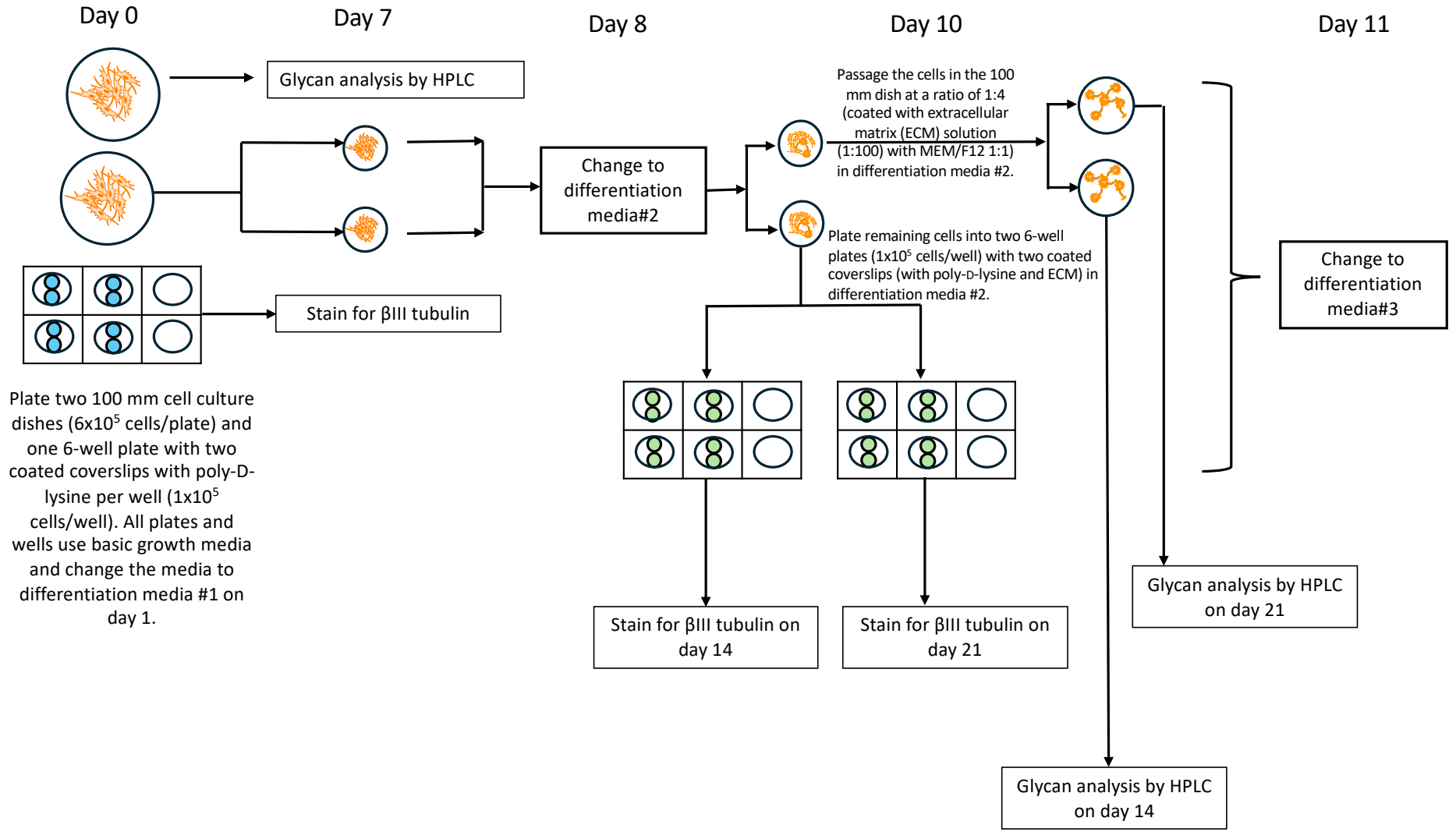

Figure 5.4 SH-SY5Y differentiation workflow over 21 days.

The morphological progression of SH-SY5Y differentiation over 21 days is depicted in Figure 5.5. Initially, on day 0, SH-SY5Y cells exhibit an undifferentiated state resembling an epithelial-like or neuroblastoma morphology, cells grow in clusters with numerous short processes extending (indicated by arrows). By days 7 and 14, cells assume a more pyramidal shape (marked by stars) and become more rounded (marked by circles) with extended neuronal projections (indicated by arrowheads). By day 21, complete neuronal differentiation is evident, with cells displaying long interconnecting neurites (arrowheads) and adopting a round shape.

The proteins generated from the SH-SY5Y neuron types were reported as tau, neurofilament, and β-III tubulin [48, 71-74]. Staining with β-III tubulin antibodies of the SH-SY5Y differentiated process (days 0, 7, 14, and 21) show more protein generation during the time. Figure 5.6 presents the immunofluorescence staining of the production of β-III tubulin. The fluorescence of β-III tubulin-producing staining is increasing intensity from the undifferentiated (day 0) to 21 days. The neuron projection (arrow) can be detected by the staining between the differentiation processes. The results from morphology and β-III tubulin production prove that the SH-SY5Y cells completely differentiated to neuron type in 21 days using this differentiation protocol [44].

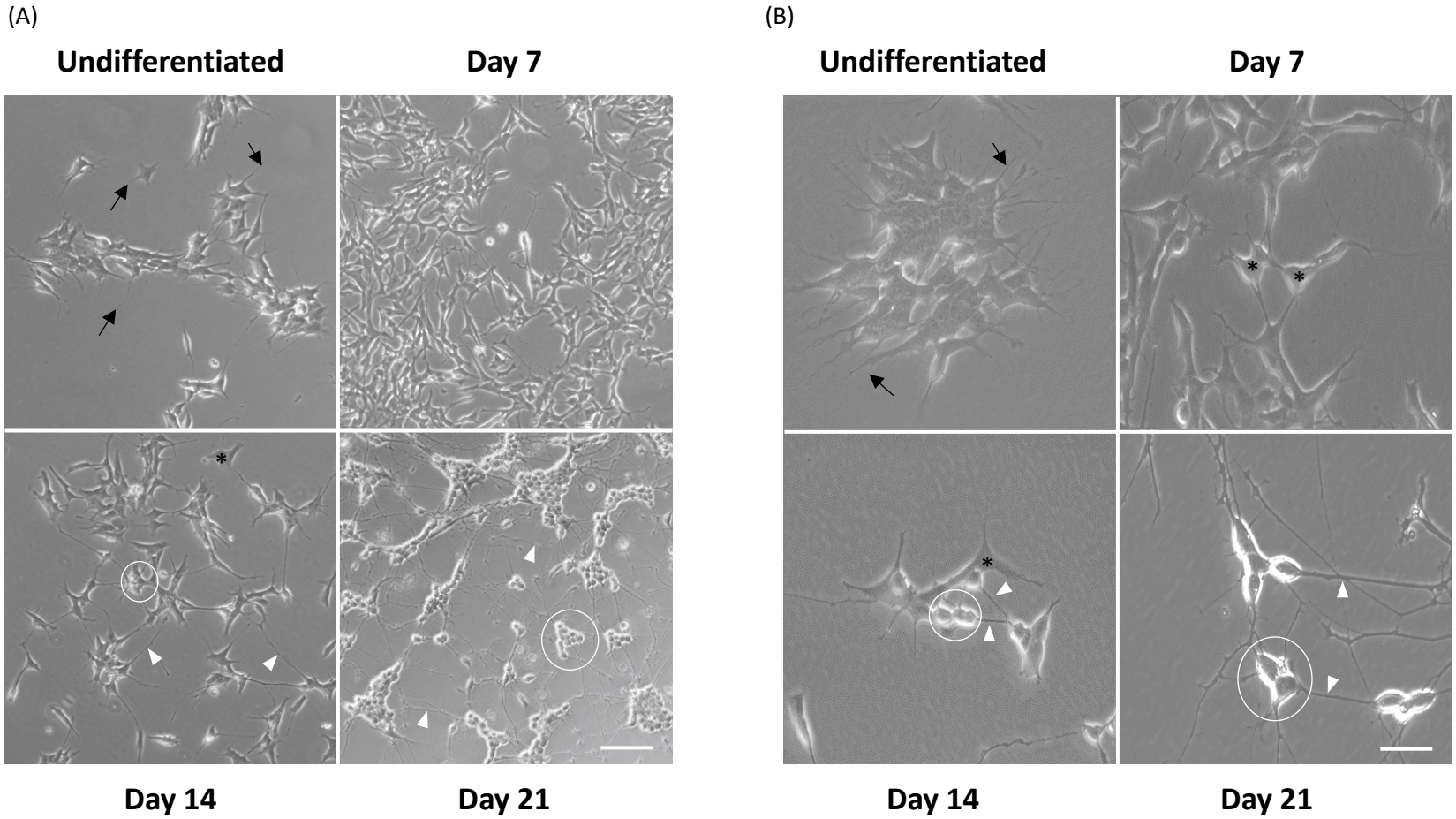

Figure 5.5 Morphology of SHSY-5Y cells during differentiation. SHSY-5Y cells were imaged with a bright field microscope and a 10x objective (A) and a 40x objective (B) prior to and during differentiation. At day 0 (undifferentiated) SHSY-5Y cells were observed to have an epithelial-like cell morphology with short projections (arrows). At day 7, cells started to exhibit longer projections, but still maintained an epithelial-like cell body with the pyramidal shape (star). At, say, 14, the projections are clearly seen between different cells, and by day 21, a network of projections (arrowhead) with round neuron-like cell bodies (circle) is apparent. Scale bar, 100 µm.

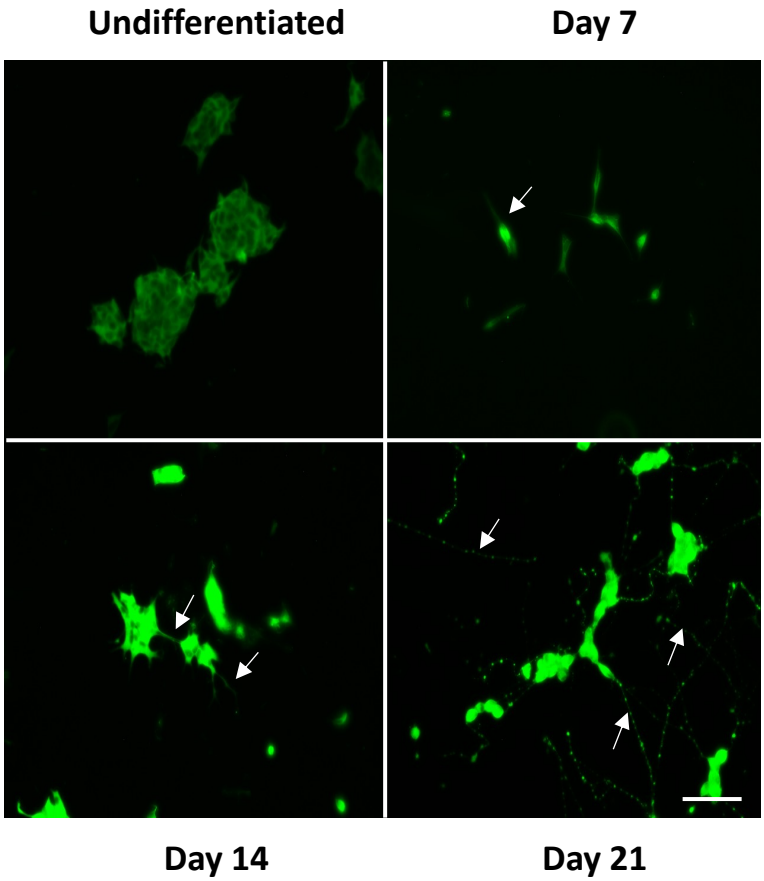

Figure 5.6 β-III tubulin staining of SH-SY5Y cells during differentiation. SHSY-5Y cells were fixed, permeabilized, incubated with an antibody to β-III tubulin followed by incubation with a fluorescently labelled secondary antibody and imaged by epifluorescent microscopy with a 20x objective. The intensity of the staining for β-III tubulin increased from the undifferentiated (day 0) to differentiated (day 21) cells. In addition, neuron-like projections (arrows) can clearly be detected following initiation of the differentiation processes. Scale bar, 100 µm.

5.3.3 Glycan analysis from SH-SY5Y cell lysates

After the collection of SH-SY5Y cells from the plate, cells were lysed by freeze-thaw in three cycles and heated at 80°C for 1 hour before being kept at -20°C until further use. After the *N*-glycans releasing step, the cell lysates were centrifuged at 10,000 *g*, 5 min at 4°C and then 100 µL of the supernatant was moved to a 1.5 mL tube. The denaturing buffer (40 mM DTT in 0.5% SDS, 30 µL) was added to the reaction tube and heated at 95°C for 10 minutes. The mixture was cooled before adding 20 µL of PNGase F. The sample was then incubated at 37°C for 12 hours. The reaction was stopped by heating at 90°C for 10 minutes and was kept at -20°C until enrichment by PGC SPE before labelling and analysis.

5.3.3.1 Optimisation of enrichment method after *N*-glycan release

After releasing the *N*-glycans from the core using PNGase F, the lipids, proteins, salts, and other substances must be removed before labelling with a fluorophore, as these substances interfere with the labelling reaction. SPE (C18 and PGC) and acetone precipitation were chosen to optimise the enrichment of the unlabelled glycans before the labelling step to remove interferences. Table 5.3 illustrates the selected enrichment conditions.

The first set of differentiated SH-SY5Y lysis cells on day 7 was chosen as the model sample for the removal of impurities from glycans before labelling.

Table 5.3 Enrichment condition for unlabelled glycans

Method	Conditions	Remarks	Reference
Acetone precipitation	1. The sample from the released glycan step was taken, 20 µL, then 100 µL of cold Acetone (-20^{o}C) and kept at -20^{o}C for 18 hours. 2. The cold sample was centrifuged at 18,000xg, 4^{o}C for 10 minutes. 3. The aqueous layer was collected for analysis of glycans.	- This method can be used for in all types of glycans. - This method has low precision. The glycans can be found in all fragments.	[75]
SPE (C18)	**Equilibration**: 5 mL of 80% ACN in 0.1% TFA **Condition**: 5 mL of water **Load**: 20 µL of sample diluted to 1 mL with water **Wash**: 5 mL of water **Elute**: 5 mL of 80% ACN in 0.1% TFA	The method included acid in the system which was suitable for acidic glycans, such as sialic acid glycans.	[76]
SPE (PGC) method 1	**Equilibration**: 5 mL of 80% ACN in 0.1% TFA **Condition**: 5 mL of water **Load**: 20 µL of sample diluted to 1 mL with water **Wash**: 5 mL of water **Elute**: 5 mL of 80% ACN in 0.1% TFA	The method included acid in the system which was suitable for acidic glycans, such as sialic acid glycans.	[76]
SPE (PGC) method 2	**Equilibration**: 3 mL of 80% ACN in water **Condition**:3 mL of water **Load**: 20 µL of sample diluted to 1 mL with water **Wash**: 5 mL of water **Elute**:1 mL of 40% ACN in water	The method without the acid in the solvent is neutral and suitable for neutral or basic glycan types.	[77]

The solutions in each step were collected for labelling with **26**, and the excess labelling reagent was removed by the developed method (Amide SPE) in Chapter 4.

Figure 5.7 illustrates the HPLC chromatograms of all enrichment methods. The results from the acetone precipitate found the glycans in all fragments. C18-SPE did not afford any glycan peaks in any steps. PGC SPE found the glycans only in the eluting step. PGC SPE-method 1 is suitable for acidic glycans, and method 2 is suitable for basic and neutral glycans. The glycans peak from PGC SPE-method 1 appeared less than for method 2. PGC SPE-method 2 was chosen for the enrichment of the released neutral *N*-glycans sample before labelling with **26** for analysis of the glycan profile pattern between differentiated SH-SY5Y cells.

(A)

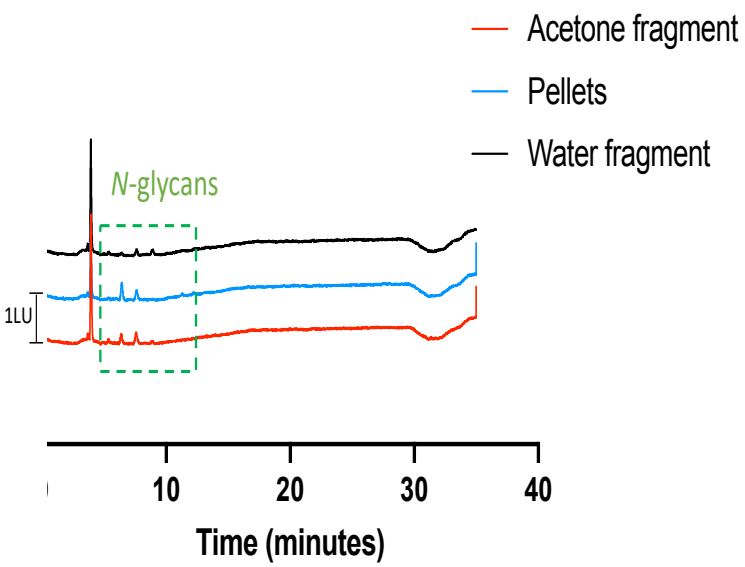
Acetone fragment
Pellets
Water fragment
N-glycans
1LU
10
20
30
40
Time (minutes)

(B)

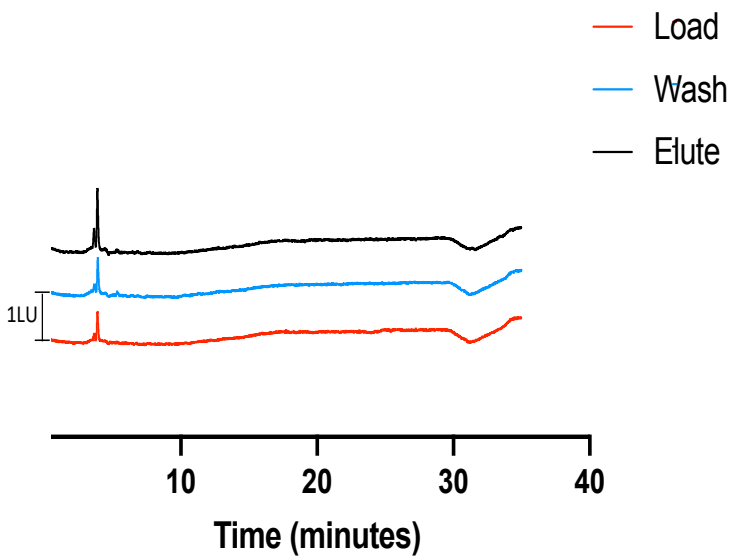
Load
Wash
Elute
1LU
10
20
30
40
Time (minutes)

(C)

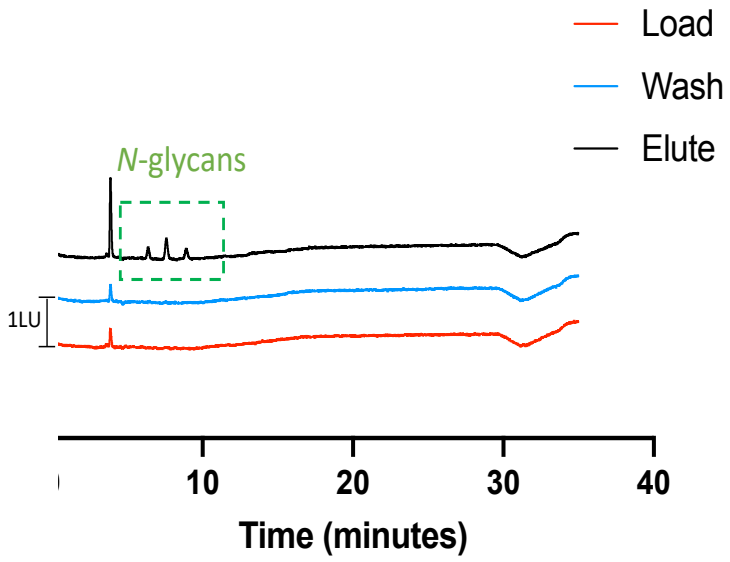

(D)

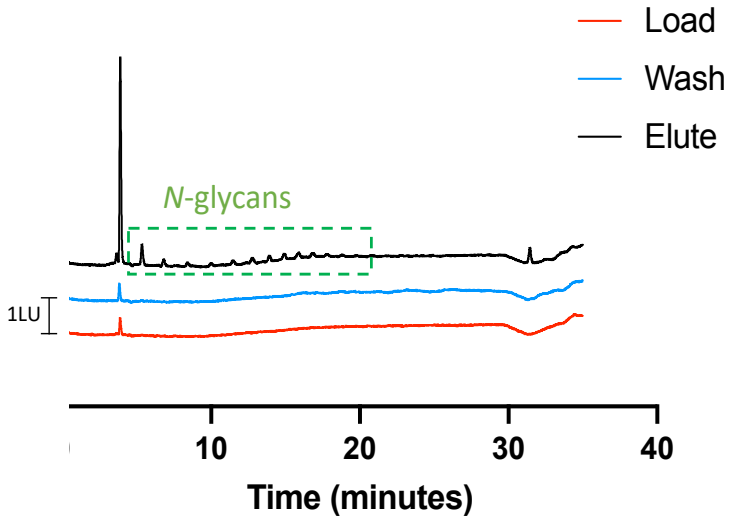

Figure 5.7 HPLC chromatograms of enriched released glycans before labelling (A) acetone precipitate, (B) C18 SPE, (C) PGC SPE-method 1, and (D) PGC SPE-method 2.

5.3.2.1 The relationship between the glucose units (GU) and retention time by dextran ladder HPLC-fluorescence analysis

Dextran ladder is the term used for the products from partial hydrolysis of dextran to glucose homopolymer and is often used as the external standard glycan for HPLC analysis [78-81]. The 200 μL of dextran ladder standard solution (0.1 mg/mL) was taken and labelled with **26** before HPLC analysis using the protocols from Chapter 4. The HPLC chromatogram of the labelled dextran ladder is shown in Figure 5.8. The relationship between the GU and retention time is shown in Table 5.4 and Figure 5.9. The calculated amount of each GU per injection is shown in Table 5.4. The final amount of total dextran is 40 ng from the labelling procedure. The equation and coefficient of determination (r^2) in Figure 5.9 show the linear relationship between the

retention time and GU length. The retention time of glucose unit homopolymer was used for qualitative analysis. The percentage of peak area in Table 5.4 was used for quantifying the percentage of the GU of glycans generated from SH-SY5Y between differentiation on Days 0, 7, 14, and 21.

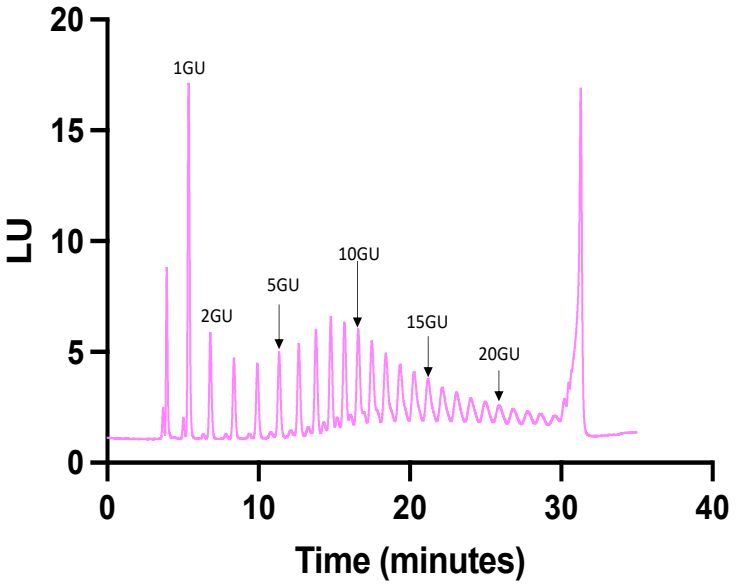

Figure 5.8 The chromatogram of labelled dextran ladder with **26**.

Table 5.4 The relationship between GU from the labelled dextran ladder's retention time and the calculated amount of each GU homopolymer per injection, and all data were collected in triplicate.

Homopolymer length	Retention time (min)	Average peak area	Peak area (%)	Calculated of amount of GU (ng)
1GU	5.35 ± 0.01	210.22 ± 6.70	11.78	4.71
2GU	6.79 ± 0.01	75.32 ± 2.65	4.22	1.69
3GU	8.39 ± 0.02	64.51 ± 0.33	3.61	1.45
4GU	9.96 ± 0.01	64.86 ± 2.42	3.63	1.45
5GU	11.43 ± 0.01	70.84 ± 5.84	4.39	1.76
6GU	12.73 ± 0.01	87.38 ± 9.36	4.90	1.96
7GU	13.89 ± 0.02	98.64 ± 13.38	5.53	2.21
8GU	14.89 ± 0.02	105.19 ± 16.58	5.89	2.36
9GU	15.84 ± 0.03	106.75 ± 17.52	5.98	2.39
10GU	16.80 ± 0.02	106.14 ± 17.53	5.95	2.38
11GU	17.76 ± 0.03	113.93 ± 16.16	6.38	2.55
12GU	18.73 ± 0.03	106.00 ± 13.48	5.94	2.38
13GU	19.71 ± 0.02	95.69 ± 11.98	5.36	2.14
14GU	20.70 ± 0.02	84.01 ± 9.26	4.71	1.88
15GU	21.70 ± 0.02	73.18 ± 9.07	4.10	1.64
16GU	22.71 ± 0.02	65.35 ± 8.44	3.55	1.42
17GU	23.71 ± 0.02	55.04 ± 7.31	3.08	1.23
18GU	24.72 ± 0.03	47.57 ± 4.82	2.67	1.07
19GU	25.70 ± 0.01	41.50 ± 4.26	2.33	0.93
20GU	26.67 ± 0.04	35.40 ± 3.63	1.98	0.79

Homopolymer length	Retention time (min)	Average peak area	Peak area (%)	Calculated of amount of GU (ng)
21GU	27.66 ± 0.03	30.04 ± 4.11	1.68	0.67
22GU	28.64 ± 0.04	25.69 ± 2.65	1.44	0.58
23GU	29.62 ± 0.07	15.71 ± 1.20	0.88	0.35

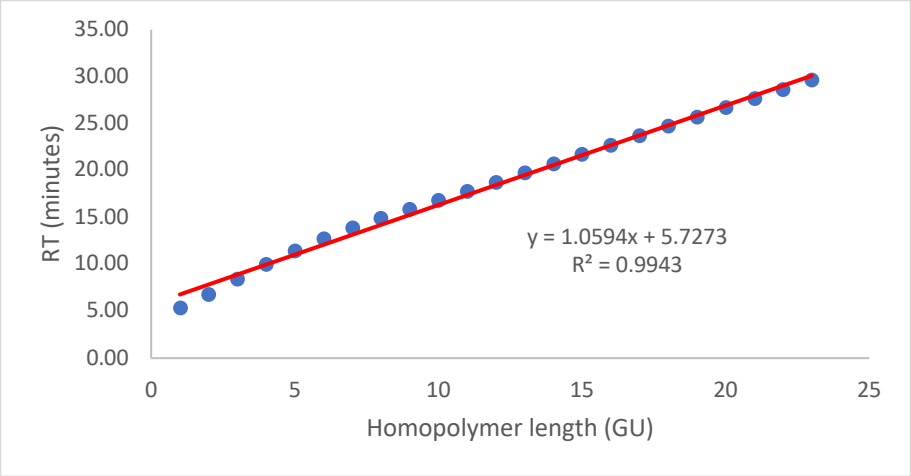

Figure 5.9 The retention linearity of a dextran-derived glucose homopolymer labelled with **26**, separated by HILIC mode LC over a 35-minute runtime following a 2 µL sample injection.

5.3.3.3 Glycan profile analysis from SH-SY5Y over 3 weeks

The HPLC analysis of glycan profiles from SH-SY5Y cells differentiated over 21 days is shown in Figure 5.10 and Table 5.5. The data from the triplicate sets of differentiated cells each show the same pattern. In undifferentiated cells, only two glycan peaks were detected without the glucose homopolymer unit. Following the differentiation processes, there was a decrease in the levels of unknown glycans (highlighted by the red square in Figure 5.10), while an increase in the generation of glucose homopolymers was observed. In order to make sure this was not simply due to an increase in the amount of sample loaded onto the column, the protein concentration from cell lysate samples was determined using a bicinchoninic acid (BCA) and Micro BCA assay. Representative standard curves from each of the protein assays are illustrated in Figure 5.11, while the total protein content for each of the cell lysate samples is detailed in Table 5.6.

(A)

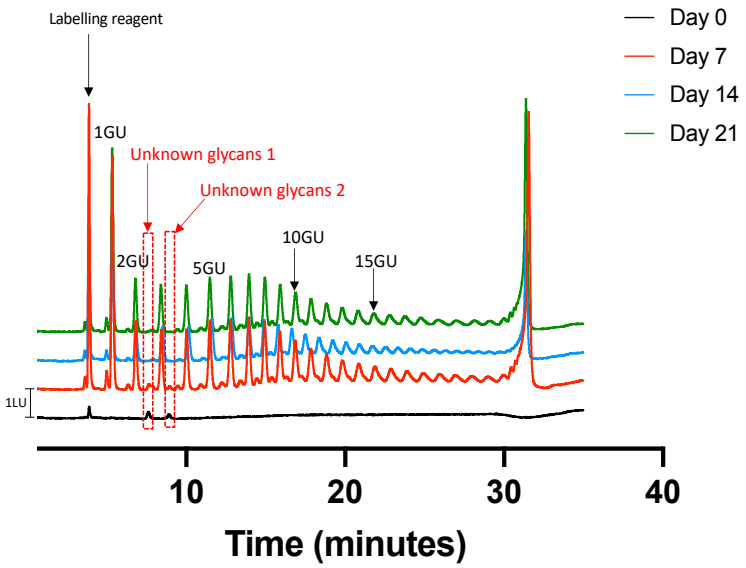
Labelling reagent
1GU
Unknown glycans 1
Unknown glycans 2
2GU
5GU
10GU
15GU
1LU
Day 0
Day 7
Day 14
Day 21
10
20
30
40
Time (minutes)

(B)

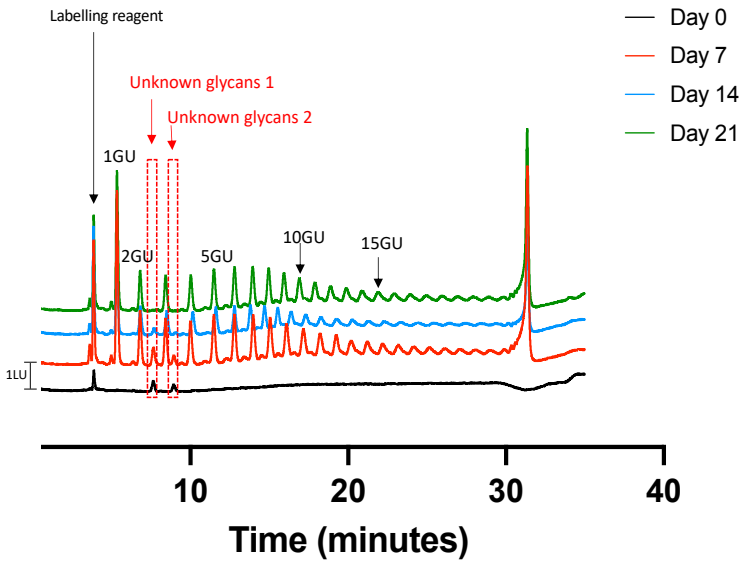
Labelling reagent
Unknown glycans 1
Unknown glycans 2
1GU
2GU
5GU
10GU
15GU
1LU
Day 0
Day 7
Day 14
Day 21
10
20
30
40
Time (minutes)

(C)

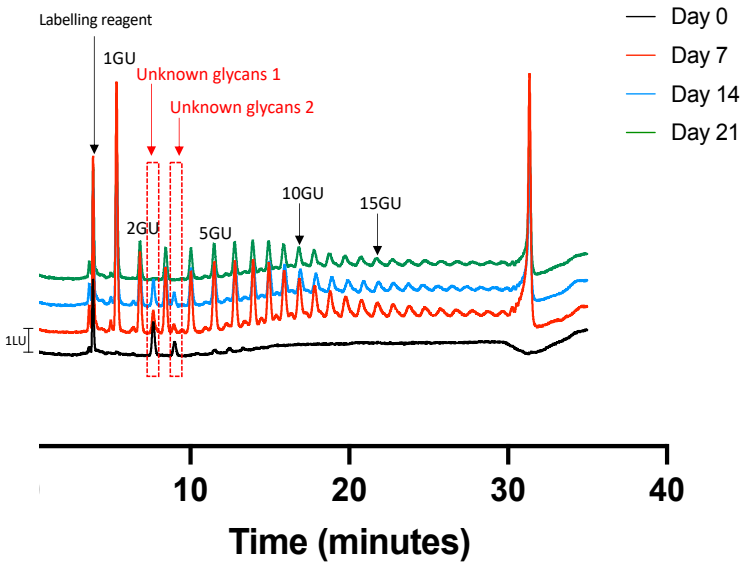

Figure 5.10 HPLC chromatogram comparing the glycan in SH-SY5Y differentiated between 21 days. (A) set 1 (B) set 2, and (C) set 3.

Table 5.5 The glucose homopolymer unit from the SH-SY5Y generated during the differentiation process, all data were collected in triplicate.

Cells collection days	Set 1			Set 2			Set 3		
	RT (min)	Homopolymer length	Average peak area	RT (min)	Homopolymer length	Average peak area	RT (min)	Homopolymer length	Average peak area
Day 0	7.622	Unknown glycan 1	2.47 ± 0.59	7.583	Unknown glycan 1	1.97 ± 0.43	7.631	Unknown glycan 1	4.14 ± 0.94
	8.913	Unknown glycan 2	1.76 ± 0.35	8.839	Unknown glycan 2	1.61 ± 0.27	8.934	Unknown glycan 2	2.10 ± 0.43
Day 7	5.361	1GU	74.09 ± 0.14	5.352	1GU	29.18 ± 0.80	5.335	1GU	25.58 ± 1.06
	6.801	2GU	26.42 ± 0.13	6.813	2GU	111.43 ± 0.21	6.809	2GU	9.92 ± 0.25
	7.629	Unknown glycan 1	3.39 ± 0.74	7.650	Unknown glycan 1	14.59 ± 0.12	7.651	Unknown glycan 1	3.32 ± 0.19
	8.386	3GU	25.66 ± 0.40	8.421	3GU	10.35 ± 0.16	8.435	3GU	8.87 ± 0.23
	8.911	Unknown glycan 2	1.38 ± 0.07	8.938	Unknown glycan 2	12.21 ± 0.11	8.961	Unknown glycan 2	1.19 ± 0.03
	9.975	4GU	27.34 ± 0.51	10.002	4GU	10.50 ± 0.20	10.047	4GU	9.09 ± 0.28
	11.442	5GU	32.24 ± 0.54	11.462	5GU	12.09 ± 0.17	11.525	5GU	10.41 ± 0.37
	12.731	6GU	32.21 ± 0.51	12.763	6GU	11.49 ± 0.18	12.843	6GU	10.01 ± 0.29
	13.838	7GU	31.27 ± 0.31	13.917	7GU	11.3 ± 0.21	13.994	7GU	9.69 ± 0.26
	14.796	8GU	28.64 ± 0.25	14.939	8GU	10.44 ± 0.57	15.004	8GU	8.77 ± 0.21
	15.688	9GU	25.81 ± 0.39	15.917	9GU	9.30 ± 0.35	15.962	9GU	7.88 ± 0.27
	16.570	10GU	23.50 ± 1.06	16.897	10GU	8.69 ± 0.84	16.928	10GU	7.08 ± 0.39
	17.699	11GU	20.76 ± 1.96	17.882	11GU	7.53 ± 0.57	17.902	11GU	6.26 ± 0.30
	18.584	12GU	17.94 ± 2.05	18.858	12GU	7.21 ± 0.19	18.896	12GU	6.01 ± 0.31
	19.721	13GU	14.74 ± 3.19	19.821	13GU	6.46 ± 0.46	19.885	13GU	5.35 ± 0.19
	20.618	14GU	12.74 ± 2.81	20.818	14GU	5.58 ± 0.18	20.883	14GU	4.73 ± 0.09
	21.827	15GU	10.56 ± 2.21	21.781	15GU	4.88 ± 0.31	21.882	15GU	4.06 ± 0.09
	22.974	16GU	8.87 ± 2.51	22.813	16GU	4.38 ± 0.31	22.858	16GU	3.58 ± 0.13
	23.880	17GU	7.77 ± 2.24	23.824	17GU	3.88 ± 0.18	23.823	17GU	3.24 ± 0.17
	24.796	18GU	6.70 ± 1.99	24.863	18GU	3.50 ± 0.16	24.842	18GU	2.87 ± 0.07
	25.672	19GU	6.02 ± 1.76	25.829	19GU	3.04 ± 0.22	25.855	19GU	2.36 ± 0.30
	26.787	20GU	5.08 ± 2.01	26.823	20GU	2.80 ± 0.10	26.832	20GU	2.16 ± 0.32
	27.696	21GU	4.42 ± 1.68	27.527	21GU	2.57 ± 0.12	27.819	21GU	2.08 ± 0.10

Cells collection days	Set 1			Set 2			Set 3		
	RT (min)	Homopolymer length	Average peak area	RT (min)	Homopolymer length	Average peak area	RT (min)	Homopolymer length	Average peak area
	28.563	22GU	3.77 ± 1.48	28.809	22GU	2.08 ± 0.08	28.785	22GU	1.71 ± 0.11
	29.613	23GU	2.65 ± 1.19	29.815	23GU	1.44 ± 0.13	29.719	23GU	1.34 ± 0.22
Day 14	5.364	1GU	42.49 ± 1.23	5.340	1GU	14.75 ± 0.99	5.352	1GU	15.76 ± 0.57
	6.825	2GU	14.84 ± 0.42	6.818	2GU	5.75 ± 0.41	6.817	2GU	5.92 ± 0.28
	7.551	Unknown glycan 1	O.23 ± 0.01	7.659	Unknown glycan 1	1.91 ± 0.11	7.655	Unknown glycan 1	3.92 ± 0.29
	8.434	3GU	14.75 ± 0.42	8.448	3GU	5.50 ± 0.43	8.426	3GU	5.32 ± 0.22
	8.962	Unknown glycan 2	0.16 ± 0.06	8.975	Unknown glycan 2	0.77 ± 0.05	8.951	Unknown glycan 2	2.01 ± 0.09
	10.013	4GU	15.21 ± 0.46	10.055	4GU	5.33 ± 0.39	10.023	4GU	5.55 ± 0.26
	11.433	5GU	17.67 ± 0.50	11.518	5GU	5.94 ± 0.51	11.491	5GU	6.38 ± 0.16
	12.674	6GU	17.79 ± 0.46	12.783	6GU	5.61 ± 0.32	12.803	6GU	5.98 ± 0.26
	13.750	7GU	17.10 ± 0.59	13.888	7GU	5.53 ± 0.28	13.953	7GU	5.66 ± 0.23
	14.693	8GU	15.56 ± 0.62	14.855	8GU	4.94 ± 014	14.943	8GU	5.18 ± 0.25
	15.584	9GU	14.29 ± 0.38	15.771	9GU	4.55 ± 0.04	15.893	9GU	4.73 ± 0.31
	16.495	10GU	13.71 ± 0.99	16.690	10GU	4.06 ± 0.34	16.834	10GU	4.25 ± 0.28
	17.410	11GU	12.54 ± 0.18	17.637	11GU	3.87 ± 0.43	17.771	11GU	3.99 ± 0.27
	18.372	12GU	10.86 ± 0.13	18.598	12GU	3.46 ± 0.12	18.776	12GU	3.46 ± 0.22
	19.348	13GU	9.22 ± 0.25	19.589	13GU	3.06 ± 0.08	19.757	13GU	3.37 ± 0.26
	20.328	14GU	7.97 ± 0.26	20.567	14GU	2.85 ± 0.15	20.767	14GU	2.85 ± 0.09
	21.588	15GU	6.60 ± 0.52	21.558	15GU	2.51 ± 0.07	21.767	15GU	2.55 ± 0.21
	22.572	16GU	5.83 ± 0.69	22.547	16GU	2.25 ± 0.17	22.736	16GU	2.47 ± 0.35
	23.545	17GU	5.13 ± 0.73	23.564	17GU	1.63 ± 0.44	23.712	17GU	2.01 ± 0.26
	24.557	18GU	4.47 ± 0.76	24.625	18GU	1.80 ± 0.29	24.703	18GU	1.86 ± 0.02
	25.752	19GU	3.65 ± 1.08	25.564	19GU	1.63 ± 0.44	25.710	19GU	1.41 ± 0.27
	26.768	20GU	3.28 ± 0.98	26.579	20GU	1.49 ± 0.42	26.585	20GU	1.33 ± 0.03
	27.838	21GU	2.86 ± 0.99	27.467	21GU	1.23 ± 0.09	27.624	21GU	1.22 ± 0.14
	28.783	22GU	2.45 ± 0.75	28.529	22GU	1.35 ± 0.28	28.649	22GU	1.23 ± 0.18
	29. 581	23GU	1.73 ± 0.37	29.713	23GU	1.40 ± 0.07	29.514	23GU	1.26 ± 0.14

Cells collection days	Set 1			Set 2			Set 3		
	RT (min)	Homopolymer length	Average peak area	RT (min)	Homopolymer length	Average peak area	RT (min)	Homopolymer length	Average peak area
Day 21	5.347	1GU	58.00 ± 0.27	5.352	1GU	23.38 ± 0.62	5.350	1GU	13.09 ± 0.67
	6.786	2GU	20.59 ± 0.12	6.807	2GU	8.18 ± 0.22	6.806	2GU	4.77 ± 0.30
	7.595	Unknown glycan 1	0.05 ± 0.01	7.616	Unknown glycan 1	0.39 ± 0.14	7.529	Unknown glycan 1	0.18 ± 0.08
		3GU	20.25 ± 0.11	8.412	3GU	7.96 ± 0.18	8.419	3GU	4.45 ± 0.33
	8.865	Unknown glycan 2	0.03 ± 0.01	8.944	Unknown glycan 2	0.15 ± 0.01	8.880	Unknown glycan 2	0.17 ± 0.02
	9.960	4GU	21.17 ± 0.06	10.002	4GU	8.36 ± 0.23	10.008	4GU	4.46 ± 0.18
	11.421	5GU	24.93 ± 0.06	11.467	5GU	9.94 ± 0.19	11.468	5GU	4.98 ± 0.37
	12.711	6GU	25.07 ± 0.04	12.768	6GU	9.86 ± 0.19	12.760	6GU	5.03 ± 0.34
	13.853	7GU	24.45 ± 0.11	13.911	7GU	9.60 ± 0.23	13.893	7GU	4.71 ± 0.28
	14.850	8GU	22.54 ± 0.14	14.912	8GU	8.67 ± 0.13	14.881	8GU	4.17 ± 0.35
	15.795	9GU	20.13 ± 0.27	15.865	9GU	7.89 ± 0.22	15.819	9GU	3.96 ± 0.19
	16.734	10GU	18.08 ± 0.37	16.823	10GU	7.00 ± 0.14	16.777	10GU	3.59 ± 0.14
	17.692	11GU	17.41 ± 0.32	17.791	11GU	6.73 ± 0.51	17.735	11GU	3.47 ± 0.50
	18.657	12GU	15.18 ± 0.31	18.758	12GU	6.08 ± 0.10	18.778	12GU	3.22 ± 0.29
	19.625	13GU	13.17 ± 0.14	19.736	13GU	5.34 ± 0.18	19.802	13GU	2.72 ± 0.26
	20.623	14GU	11.31 ± 0.18	20.722	14GU	4.74 ± 0.25	20.775	14GU	2.56 ± 0.18
	21.612	15GU	9.77 ± 0.15	21.710	15GU	4.27 ± 0.32	21.788	15GU	2.45 ± 0.19
	22.631	16GU	8.58 ± 0.09	22.721	16GU	3.63 ± 0.21	22.816	16GU	1.79 ± 0.60
	23.631	17GU	7.73 ± 0.11	23.687	17GU	3.38 ± 0.13	23.816	17GU	1.69 ± 0.29
	24.640	18GU	6.84 ± 0.06	24.686	18GU	2.98 ± 0.21	24.896	18GU	1.30 ± 0.33
	25.688	19GU	5.96 ± 0.15	25.670	19GU	2.53 ± 0.08	25.888	19GU	1.33 ± 0.13
	26.729	20GU	5.13 ± 0.22	26.681	20GU	1.90 ± 0.30	26.702	20GU	1.11 ± 0.36
	27.774	21GU	4.52 ± 0.22	27.615	21GU	1.92 ± 0.42	27.577	21GU	1.24 ± 0.07
	28.897	22GU	3.66 ± 0.34	28.603	22GU	1.56 ± 0.42	28.673	22GU	1.06 ± 0.30
	29.720	23GU	2.64 ± 0.07	29.540	23GU	1.47 ± 0.25	29.547	23GU	1.00 ± 0.08

(A)

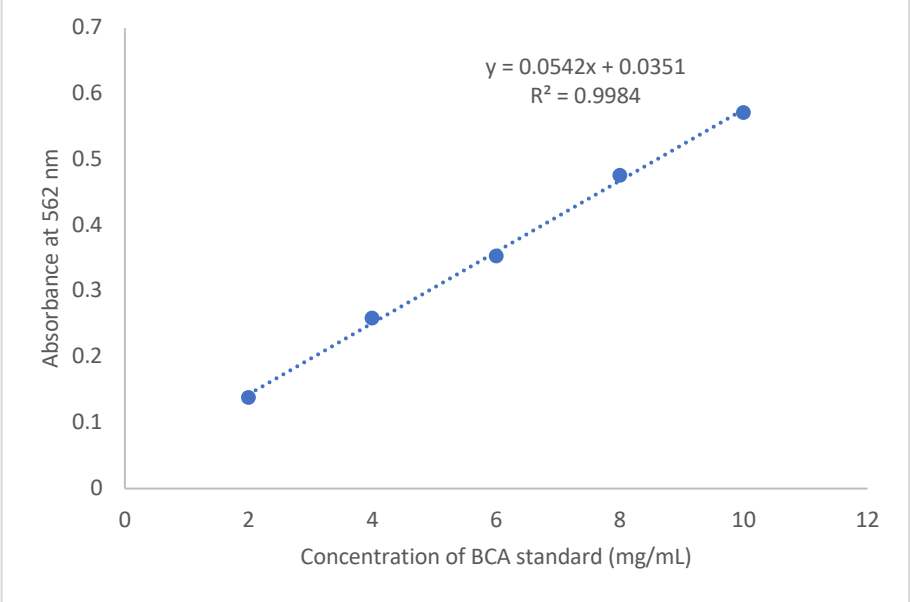

(B)

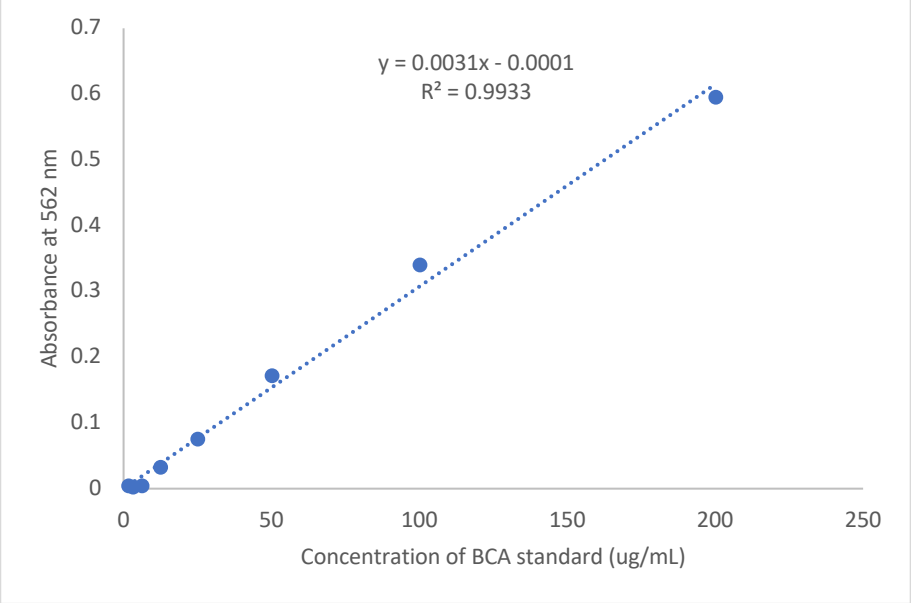

Figure 5.11 Standard curve between the concentration of protein standard in BCA (A) and Micro BCA (B) assay and absorbance at 562 nm.

Table 5.6 The total protein assay from the SH-SY5Y generated during the differentiation process

Collection days	Total protein (µg/mL)		
	Set 1	**Set 2**	**Set 3**
Day 0	6527.000	170.594	191.957
Day 7	4193.000	131.069	82.626
Day 14	154.784	48.948	66.522
Day 21	4021.000	115.03	73.893

The protein assay results show the correlation between the protein level in the SH-SY5Y differentiated triplicate set between 21 days. The protein level data was used to adjust the

glycan levels in each sample before comparing the glycan levels of SH-SY5Y produced between the differentiated processes.
The adjusted *N*-glycan profile levels between 1-23GU and unknown glycans 1 and 2 from the triplicate SH-SY5Y differentiated are shown in Table 5.7, and Figure 5.12 presents the *N*-glycan profile level changing over 21 days of SH-SY5Y differentiation.

Table 5.7 The percentage of each GU in the glycans profile generated between the differentiated over 21 days after adjusting with the total protein levels

Cells collection days	Set 1		Set 2		Set 3	
	Homopolymer length	Adjusted glycans level (ng)	Homopolymer length	Adjust glycans amount (ng)	Homopolymer length	Adjusted glycans level (ng)
Day 7	1GU	0.0792	1GU	0.9979	1GU	1.3876
	2GU	0.0282	2GU	0.3911	2GU	0.5382
	3GU	0.0274	3GU	0.3540	3GU	0.4813
	4GU	0.0292	4GU	0.3590	4GU	0.4935
	5GU	0.0345	5GU	0.4134	5GU	0.5647
	6GU	0.0344	6GU	0.3929	6GU	0.5431
	7GU	0.0334	7GU	0.3806	7GU	0.5258
	8GU	0.0306	8GU	0.3571	8GU	0.4760
	9GU	0.0276	9GU	0.3179	9GU	0.4275
	10GU	0.0251	10GU	0.2972	10GU	0.3839
	11GU	0.0222	11GU	0.2575	11GU	0.3396
	12GU	0.0192	12GU	0.2466	12GU	0.3260
	13GU	0.0158	13GU	0.2210	13GU	0.2905
	14GU	0.0136	14GU	0.1910	14GU	0.2569
	15GU	0.0113	15GU	0.1668	15GU	0.2204
	16GU	0.0095	16GU	0.1499	16GU	0.1941
	17GU	0.0083	17GU	0.1328	17GU	0.1755
	18GU	0.0072	18GU	0.1196	18GU	0.1559
	19GU	0.0064	19GU	0.1041	19GU	0.1282
	20GU	0.0054	20GU	0.0957	20GU	0.1172
	21GU	0.0047	21GU	0.0880	21GU	0.1127
	22GU	0.0040	22GU	0.0712	22GU	0.0930
	23GU	0.0028	23GU	0.0492	23GU	0.0725
	Total glycans	**0.4802**	**Total glycans**	**6.1546**	**Total glycans**	**8.3042**
Day 14	1GU	1.2307	1GU	1.3507	1GU	1.0619
	2GU	0.4300	2GU	0.5269	2GU	0.3990
	3GU	0.4271	3GU	0.5038	3GU	0.3584
	4GU	0.4406	4GU	0.4880	4GU	0.3739
	5GU	0.5118	5GU	0.5440	5GU	0.4296
	6GU	0.5152	6GU	0.5139	6GU	0.4029
	7GU	0.4952	7GU	0.5065	7GU	0.3814
	8GU	0.4505	8GU	0.4523	8GU	0.3494
	9GU	0.4138	9GU	0.4164	9GU	0.3190
	10GU	0.3972	10GU	0.3721	10GU	0.2864
	11GU	0.3633	11GU	0.3540	11GU	0.2686
	12GU	0.3146	12GU	0.3164	12GU	0.2335

Cells collection days	Set 1		Set 2		Set 3	
	Homopolymer length	**Adjusted glycans level (ng)**	**Homopolymer length**	**Adjust glycans amount (ng)**	**Homopolymer length**	**Adjusted glycans level (ng)**
	13GU	0.2669	13GU	0.2802	13GU	0.2272
	14GU	0.2310	14GU	0.2606	14GU	0.1923
	15GU	0.1911	15GU	0.2303	15GU	0.1720
	16GU	0.1688	16GU	0.2061	16GU	0.1663
	17GU	0.1486	17GU	0.1493	17GU	0.1352
	18GU	0.1294	18GU	0.1650	18GU	0.1250
	19GU	0.1057	19GU	0.1387	19GU	0.0954
	20GU	0.0951	20GU	0.1363	20GU	0.0899
	21GU	0.0829	21GU	0.1125	21GU	0.0825
	22GU	0.0708	22GU	0.1232	22GU	0.0829
	23GU	0.0501	23GU	0.1286	23GU	0.0849
	Total glycans	**7.5305**	**Total glycans**	**8.2759**	**Total glycans**	**6.3177**
Day 21	1GU	0.0647	1GU	0.9113	1GU	0.7940
	2GU	0.0230	2GU	0.3187	2GU	0.2895
	3GU	0.0226	3GU	0.3104	3GU	0.2702
	4GU	0.0236	4GU	0.3257	4GU	0.2706
	5GU	0.0278	5GU	0.3875	5GU	0.3020
	6GU	0.0280	6GU	0.3841	6GU	0.3052
	7GU	0.0273	7GU	0.3741	7GU	0.2856
	8GU	0.0251	8GU	0.3380	8GU	0.2528
	9GU	0.0224	9GU	0.3073	9GU	0.2403
	10GU	0.0202	10GU	0.2727	10GU	0.2180
	11GU	0.0194	11GU	0.2624	11GU	0.2107
	12GU	0.0169	12GU	0.2368	12GU	0.1956
	13GU	0.0147	13GU	0.2083	13GU	0.1648
	14GU	0.0126	14GU	0.1846	14GU	0.1554
	15GU	0.0109	15GU	0.1663	15GU	0.1486
	16GU	0.0096	16GU	0.1412	16GU	0.1089
	17GU	0.0086	17GU	0.1317	17GU	0.1026
	18GU	0.0076	18GU	0.1163	18GU	0.0787
	19GU	0.0066	19GU	0.0984	19GU	0.0808
	20GU	0.0057	20GU	0.0740	20GU	0.0672
	21GU	0.0050	21GU	0.0748	21GU	0.0752
	22GU	0.0041	22GU	0.0609	22GU	0.0646
	23GU	0.0029	23GU	0.0573	23GU	0.0608
	Total glycans	**0.4093**	**Total glycans**	**5.7427**	**Total glycans**	**4.7422**

(A)

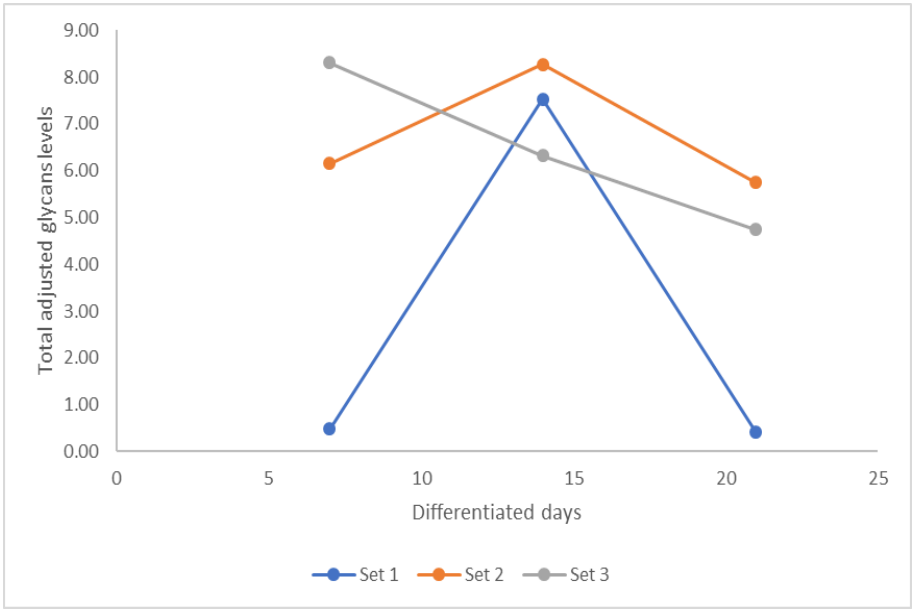
9.00
8.00
7.00
6.00
5.00
4.00
3.00
2.00
1.00
0.00
Total adjusted glycans levels
0
5
10
15
20
25
Differentiated days
Set 1
Set 2
Set 3

(B)

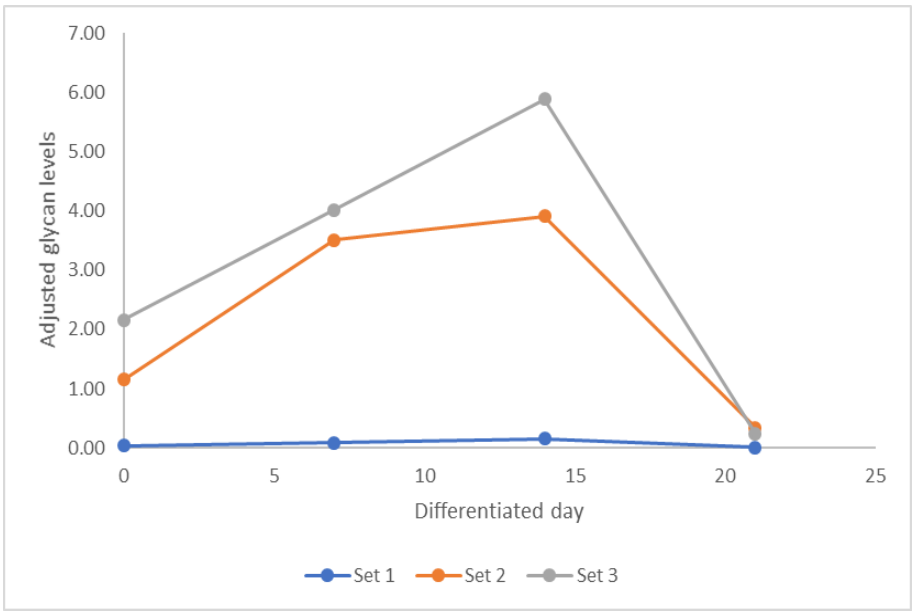
7.00
6.00
5.00
4.00
3.00
2.00
1.00
0.00
Adjusted glycan levels
0
5
10
15
20
25
Differentiated day
Set 1
Set 2
Set 3

(C)

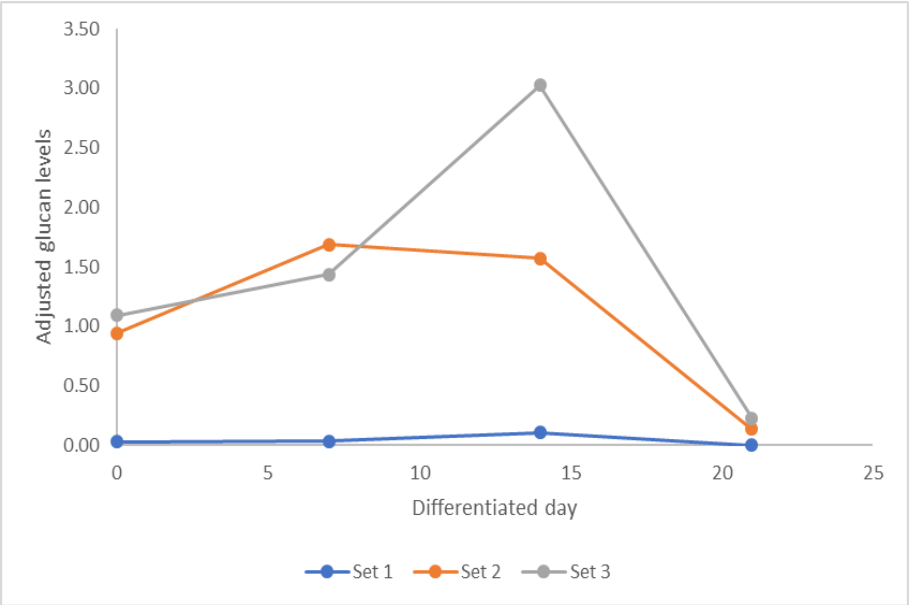

Figure 5.12 The changing of glycans profile generated during the triplicate set differentiation of SH-SY5Y over 21 days. (A) the total glycans contains 1-23GU, (B) the unknown glycan 1, and (C) the unknown glycan 1.

The data show the similarity of total glycan levels in the set 1 and 2 cell differentiated experiment. The *N*-glycan profile levels were increased from day 7 to day 14 and then decreased on day 21, while on the third set, the total glycan levels continued decreasing. The unknown glycans 1 and 2 show a similar pattern during differentiation. The levels of unknown glycans increased until day 14 and then suddenly dropped to a very low level on day 21 compared to the undifferentiated state.

5.4 Conclusions and Future Work

Cell cultures are used for study in the pre-clinical phase of the drug development process to avoid using animal testing. SH-SY5Y cell lines are a commonly used model for neurodegenerative disease studies. Most of the biomarkers in neurodegenerative diseases in SH-SY5Y studies are specific proteins expressed as the cells transition from an undifferentiated to a differentiated (neuron-like) state. This chapter aimed to determine the qualitative and quantitative glycans profile for SH-SY5Y cells in undifferentiated and differentiated states. Protein concentration levels were chosen to normalise all glycan levels in three sets of differentiated cells to the same level before comparing the level of glycans in the differentiated state. All homopolymer glycans were produced in the differentiated process compared to the undifferentiated state. The *N*-glycans profile in sets 1 and 2 increased to the highest level on day 14, and the level dropped on day 21 to near the levels on day 7. The third set is different; the glycans level is highest on day 7 and continues to decrease until day 21. The interesting point is the levels of unknown glycan 1 and 2. These glycans were found in the undifferentiated cells and continued to increase until day 14, then dramatically dropped to nearly zero on day 21.

In conclusion, the protocol developed in this thesis determined that differentiated SH-SY5Y cells produced a radically different glycans profile compared to undifferentiated states-SY5Y cells. The workflow of labelled glycan enrichment in Chapter 4 can be used to remove other components from the labelled glycans before HPLC-fluorescence analysis. Future work will continue studying the glycan profile level as cells differentiate into neuron-like cells. Also worth further study is the significant decrease in the unknown glycans 1 and 2 as the cells progressed from undifferentiated to differentiated cells. It will be of great interest to identify the structures of these glycans. These glycans could be developed as glycan biomarkers for neurodegenerative disease in the future.

5.5 Experimental

5.5.1 General experiment

All chemicals used were analytical or HPLC grade, purchased from commercial sources (Sigma-Aldrich, Merk, Fisher Scientific, Alfa Aesar and Acros Organics), and used without further purification.

All sterile cell culture media and supplements used were purchased from commercial sources (Corning, Fisher Scientific, Sigma-Aldrich, REF, Peprotech, and Gibco). The SH-SY5Y cell was purchased from the European Collection of Authenticated Cell Cultures (ECACC).

5.5.2 Analytical Equipment

High performance liquid chromatography
HILIC mode HPLC was performed on an Agilent 1100 series HPLC system linked to both Agilent G1321A FLD detector and an G1314A variable wavelength detector. Amide HILIC performed the separation of labelled sugars on a TSKgel Amide-80 HR column (250 x 4.6 mm, 5 µM particle size) filled with TSKgel Amide-80 guard column (15 bufferx 3.2 mm, 5 µM particle size). Solvent A was composed of ammonium formate buffer (50 mM pH 4.4), while solvent B consisted of ACN. The flow rate was set at 0.8 mL/ min, and the column was maintained at 40^{o}C for the duration of the run.

Separation of labelled sugars took place over 35 minutes with a linear gradient beginning with 65% phase B at 10 minutes, with a further gradient to 50% in 10 minutes, to 45% in 5 minutes, to 10% in 3 minutes, maintain 10% for 2 minutes before returning to injection condition of 65% B between 31-35 minutes. The column was conditioned with 65% B, 5 minutes before the next injection. The injection volume was 2 µL per injection. The fluorescence detection used the excitation wavelength 240 nm and emission wavelength 420 nm. The Fluorescence absorptivity detection was reported as luminescence unit (LU) represent to the Agilent system.

5.5.3 Solvents and Buffer

4% Paraformaldehyde (PFA) solution
Distilled deionised water (DDW, 70 mL) was warmed in a microwave for approximately 30 seconds. 10x PBS (10 mL), paraformaldehyde (PFA, 4 g) and 10 M NaOH (2-3 drops) were added and the solution stirred until the PFA dissolved. The solution was then allowed to cool to room temperature and the pH adjusted to 7.4 using 1 M HCl. The solution was adjusted to a volume of 100 mL with DDW. Finally, the solution was filtered through a 0.2 µm bottle top filter.

Immunocytochemistry Blocking Buffer
A 5x stock (500 mL) of blocking buffer was made as follows: Normal horse serum (NHS, 50 mL), 10x PBS (250 mL), Saponin (2.5 g). The solution was stirred until the saponin dissolved, filtered through a 0.2 µm bottle top filter and stored at -20°C in 10 mL aliquots. For 1x blocking buffer, a single 10 mL aliquot of 5x stock was diluted to 50 mL using DDW.

5 mM all-trans retinoic acid (ATRA)
ATRA (5 mg, 0.0167 mmol) was dissolved in ethanol (3.33 mL). This solution is sensitive to heat, light, and air and was stored in a dark tube at 4°C for a maximum of 6 weeks.

1 M Potassium chloride solution

Potassium chloride (18.6 g, 0.25 mol) was dissolved in water (250 mL). The solution was sterilised by autoclaving and stored at 4°C until used.

5.5.4 Media formulation

The formulation of basic growth media, differentiation media #1, #2, and #3 is shown in Table 5.8. Table 5.9 illustrates the concentration of each component in the formulation [44].

Table 5.8 The volume of each component in the SH-SY5Y growth media

Component	Basic Growth Media (Total volume 50 mL)	Differentiation Media #1 (Total volume 50 mL)	Differentiation Media #2 (Total volume 50 mL)	Differentiation Media #3 (Total volume 50 mL)
Minimum Essential Medium (MEM)	22.25 mL	24 mL	24.45 mL	-
Nutrient Mixture F-12 Ham	22.5 mL	24 mL	24.45 mL	-
Foetal bovine serum (FBS)	5 mL	1.3 mL	500 µL	-
Glutamine (100x)	500 µL	500 µL	500 µL	500 µL
ATRA stock solution (5 mM)	-	100 µL	100 µL	100 µL
Neurobasal medium (NB)	-	-	-	46.15 mL
B-27 supplement (50x)	-	-	-	1 mL
BDNF (10 µg/mL)	-	-	-	250 µL
db-cAMP (100 mmol/mL)	-	-	-	1 mL
1 M Potassium chloride	-	-	-	1 mL

Table 5.9 The final concentration of each component in the SH-SY5Y growth media (50 mL)

Component	Basic Growth Media	Differentiation Media #1	Differentiation Media #2	Differentiation Media #3
Minimum Essential Medium (MEM)	44.5% v/v	48% v/v	48.9% v/v	-
Nutrient Mixture F-12 Ham	44.5% v/v	48% v/v	48.9% v/v	-
Foetal Bovine Serum (FBS)	15% v/v	2.5% v/v	1% v/v	-
Glutamine (100x)	2 mM (1x)	2 mM (1x)	2 mM (1x)	2 mM (1x)
ATRA stock solution (5 mM)	-	10 µM	10 µM	10 µM
Neurobasal medium (NB)	-	-	-	92.3% v/v
B-27 supplement (50x)	-	-	-	1x
BDNF (10 µg/mL)	-	-	-	50 ng/mL
db-cAMP (100 mmol/mL)	-	-	-	2 mmol
1 M Potassium chloride	-	-	-	20 mM

2 M Ammonium formate buffer stock solution pH 4.4
Formic acid (184.12 g, 4 mol) was combined with water (1L) and cooled to 0°C in an ice bath. 25% Ammonium solution (200 mL) was then added in 50 mL increments. The pH was adjusted to 4.4 by the 25% ammonium solution. The stock solution was then diluted to 2 L to a final concentration 50 mM and used as a HILIC phase modifier.

Labelling agent stock solution
Compound **26** was weighed and diluted in MeOH to a final concentration of 40 mmol/mL.

Labelling buffer solution
Boric acid (3 g, 0.04 mol) and sodium acetate trihydrate (6 g, 0.045 mol) were dissolved in MeOH (100 mL).

Sodium cyanoborohydride solution
Sodium cyanoborohydride solution was prepared at 0.42 mM in the labelling buffer solution.

5.5.5 General Cell Culture Condition

5.5.5.1 Reviving cells from long-term liquid nitrogen storage
The basic growth media was prepared under aseptic conditions and warmed at 37°C before thawing the vial frozen cells in a 37°C waterbath. Once thawed, the cells were added to basic growth media (9 mL) in a 15 mL conical tube and centrifuged (100 *g*, 5 minutes). The supernatant was discarded, the cell pellet was resuspended basic growth media (10 mL) and the cells transferred to a T-75 culture flask. The cells were cultivated in a humidified incubator

at 37°C with 5% CO_2. The basic growth media was replaced every 2-3 days, and cells were monitored for confluence. Cells were sub-cultured when they reached 80-90% confluency.

5.5.5.2 Sub-culture Conditions for Maintenance Cultures
Cells were passaged upon reaching 80-90% confluency (every 3-5 days). The old media was removed from the flask and then rinsed once with approximately 10 mL of PBS (without magnesium chloride and calcium chloride). After aspirating PBS, the warm (37°C) of 0.05% trypsin-EDTA (1x), 5 mL was added into the flask. The cells were incubated with the trypsin solution at 37°C for 2-3 minutes until the cells were all detached. 5 mL of basic growth media was added to stop the trypsin activity, and the cell suspension was transferred to a 15 mL tube. The solution was centrifuged at 1,00 *g* for 5 minutes, and then the supernatant was aspirated. The cell pellet was resuspended with 10 mL of basic growth media, and cells were subcultured at a ratio of 1:5 in a T75 flask before being incubated at 37°C, 5% CO_2.

5.5.5.3 Preparation of cells for storage in liquid nitrogen.
Following sub-culturing, cells were collected by centrifugation (100 *g*, 5 min) and then resuspended in basic growth media (1 mL per 2 mL of original solution) containing DMSO (10% v/v) in a 1.5 mL cryovial. Cells were transferred to a Mr. Frosty container and placed at -80°C for ~24 h before transferring the vial to liquid nitrogen for long-term storage.

5.5.5.4 Cell lysis
The cell culture dish (100 mm) was placed on the ice before removing the media. The cells were washed with ice-cold PBS (containing calcium and magnesium chloride, 5 mL). Cells were then collected into ice-cold PBS (1 mL) using a cell scraper and transferred to a 1.5 mL microcentrifuge tube. The cells were lysed by several repeated freeze-thaw cycles, and denatured at 80°C for 1 hour. The cell lysate solution was kept at -20°C until required.

5.5.6 Immunocytochemistry

SHSY-5Y cells were grown on glass coverslips (13 mm round, German glass, #1) coated with high molecular mass poly-d-lysine (20 µg/mL) for 15 minutes at room temperature and then rinsed with sterile DDW. SH-SY5Y cells were seeded $1x10^5$ cells/well (6-well plate) on the coated coverslips.

At the appropriate time point, the media from the cells was removed, the cells were carefully washed with PBS containing calcium and magnesium chloride and then cells were fixed by incubating in 4% PFA (4°C, 20 min, room temperature). After that, the cells were washed with blocking buffer (3 times for 5 mins). Coverslips were transferred to a humidified tray with parafilm, primary antibody in blocking buffer (40-50 µL) added to the cells and incubated overnight at 4°C. To remove excess primary antibody the coverslips were washed with blocking buffer (3 times for 5 mins), before adding secondary antibody in blocking buffer (2 h, room temperature) on the parafilm-coated tray. The coverslips were then washed 3 times for 5 minutes with blocking buffer and then rinsed 3 times with 1x PBS. Finally, excess PBS from the underside of the coverslip was removed using a soft tissue and the coverslip was mounted in a glass microscope slide using mounting media containing the nuclear stain, DAPI.

5.5.7 Activity testing PNGase F

All PNGase F enzymes were tested for the deglycosylation activity of RNase B before use. A sample solution of RNase B (20 µg, 9 µL) in water was added to denaturing buffer (1 µL 40 mM DTT in 0.5% SDS) and held at 95°C for 10 minutes. The mixture was cooled, and PNGase F was added to the sodium phosphate buffer solution (50 mM, pH 7) to a final volume of 20 µL. The sample was incubated at 37°C for 120 minutes. The digestion was stopped by adding 4x loading

dye (4 µL) before samples were analysed by SDS-PAGE (15%) at 150V. The gel was then stained with Coomassie stain (2 hours) before being rinsed and destained for 6 hours, revealing a >1 kDa mass change.

5.5.8 Preparation of glycans standard and sample

5.5.8.1 Dextran ladder

Dextran from *Leuconostoc mesenteroides* (Mr ~ 200,000, 1 g) was dissolved in a solution of 0.1 M HCl (10 mL) and heated to 100°C under reflux conditions. The conditions were maintained for 4 hours while stirring. The solution was then cooled on ice to room temperature, and pH was neutralised using Amberlite IRA 157 (1.5 g). The solution containing ion exchange resin was stirred until neutrality was achieved, pH 7. The solution was then filtrated and collected before being diluted to 0.1 mg/mL in water.

5.5.8.2 Release of *N*-linked glycans of SH-SY5Y lysates

A cell lysate of SH-SY5Y (200 µL), the lysate protocol from 5.5.5.4, was added to denaturing buffer (40 mM DTT in 0.5% SDS, 30 µL) and was held at 95°C for 10 minutes. The mixture was cooled, and PNGase F (100 µg) and PBS (300 µL) were added. The sample was then incubated at 37°C for 12 hours. The solution was then made up to 1 mL with an 18Ω H_2O centrifuge at 10,000 rpm for 10 minutes. The supernatant was loaded to PGC SPE to enrich glycans before being labelled with Compound **26**.

5.5.8.3 General enrichment of released *N*-glycans before labelling with PGC SPE

The PGC SPE was conditioned with 1 mL of 80% ACN in water 3 times and then equilibrated with 1 mL of water 3 times. The released *N*-glycan sample from the PNGase F released reaction 1 mL was loaded after equilibrating. Let the solvent drip through the cartridge. The wash step was 1 mL of water, 5 times. In the last wash, let the cartridge dry before eluting the unlabelled glycans with 1 mL of 40% ACN in water. The solution from the eluting step was dried with a speed vac and kept at -20°C until redissolved with 100 µL of MeOH for labelling with **26**.

5.5.8.4 General labelling procedure of glycans

Released glycan from SH-SY5Y cells after enrichment by PGC SPE was redissolved with 100 µL of MeOH in the centrifuge tube and mixed with the 100 µL of labelling buffer and 15 µL of sodium cyanoborohydride solution. The labelling solution (**26**, 40 mmol/mL in MeOH) was added (100 µL). The reaction mixture was then vortexed and centrifuged for 10 seconds before being heated at 65°C for 180 minutes. The reaction solution was quenched with the addition of ACN (950 µL), producing a white precipitate. The quenched solution was transferred for enrichment with Amide SPE. The elute solution from the enrichment method was dried and kept at 20°C until redissolved with 500 µL of HPLC water before injection into HPLC.

5.5.8.5 General enrichment of labelled glycan with Amide SPE

The Amide SPE was equilibrated with 1 mL of methanol twice. The labelled glycan sample from the labelling reaction (1 mL) was loaded after equilibrating. Let the solvent dripped through the cartridge. The first wash was 1 mL of 99% ACN (aq), 5 times. The second wash was 1 mL of 97% ACN (aq), 5 times. In the last wash, let the cartridge dry before eluting the labelled glycans with 800 µL of HPLC water. The eluted solution from the enrichment method was dried and kept at -20°C until redissolved with 0.5 mL of HPLC water for HPLC analysis.

5.5.9 Quantification of protein from SH-SY5Y cell lysates

5.5.9.1 BCA assay

Reagents for the assay were purchased from Thermo Scientific. The BCA standards were prepared in the concentration between 2-10 mg/mL by DDW and used DDW as blank and then pipet all concentrations 10 μL duplicated per concentration to the 96 well-plate. The sample was prepared and diluted with DDW before adding 10 μL triplicate to the 96 well-plate. The mixture of BCA and 4% copper sulphate in the ratio of 50:1 was prepared before adding 200 μL per well. The 96 well-plate was incubated at 37^{o}C for 30 minutes before reading the absorbance at 562 nm with a microplate reader.

5.5.9.2 Micro BCA assay

Reagents for the assay were purchased from Thermo Scientific. The BSA standards were prepared in a concentration between 40-200 μg/mL from the stock solution (2.0 mg/mL) with DDW and used DDW as blank. 100 μL of all concentrations (duplicate) of standards and samples (triplicate) were pipetted to the 96 well-plate. The Micro BCA working reagent (Reagent MA:MB:MC 25:24:1) 100 μL was added per well. The 96 well-plate was incubated at 60^{o}C for 60 minutes before reading the absorbance at 562 nm with a microplate reader.

5.6 References

1. Bellenguez, C., et al., *New insights into the genetic etiology of Alzheimer's disease and related dementias.* Nature Genetics, 2022. **54**(4): p. 412-436.
2. Ronge, R., et al., *Alzheimer's Disease Diagnosis via Deep Factorization Machine Models.* 2021. p.624-633.
3. Koníčková, D., et al., *Cerebrospinal fluid and blood serum biomarkers in neurodegenerative proteinopathies: A prospective, open, cross-correlation study.* J Neurochem, 2023. **167**(2): p. 168-182.
4. Delvenne, A., et al., *Cerebrospinal fluid proteomic profiling of individuals with prodromal Alzheimer's disease classified using two different neurodegenerative biomarkers (N) in A/T/N classification.* Alzheimer's & Dementia, 2021. **17**(S3): p. e053030.
5. Frontera, J.A., et al., *Comparison of serum neurodegenerative biomarkers among hospitalized COVID-19 patients versus non-COVID subjects with normal cognition, mild cognitive impairment, or Alzheimer's dementia.* Alzheimer's & dementia, 2022. **18**(5): p. 899-910.
6. Mohamed, S.A., et al., *Evaluation of Sodium (Na) MR-imaging as a biomarker and predictor for neurodegenerative changes in patients with alzheimer's disease.* In vivo (Athens), 2021. **35**(1): p. 429-435.
7. Johnson, S.C., et al., *Identifying clinically useful biomarkers in neurodegenerative disease through a collaborative approach: the NeuroToolKit.* Alzheimer's Research & Therapy, 2023. **15**(1): p. 25.
8. Fan, L., et al., *New Insights Into the Pathogenesis of Alzheimer's Disease.* Front Neurol, 2019. **10**: p. 1312.
9. Kim, S.-W., et al., *Unified framework for brain connectivity-based biomarkers in neurodegenerative disorders.* Frontiers in Neuroscience, 2022. **16**: p.975299
10. Cvetkovska, V., et al., *Neurexin-β Mediates the Synaptogenic Activity of Amyloid Precursor Protein.* The Journal of neuroscience, 2022. **42**(48): p. 8936-8947.
11. Baerenfaenger, M., et al., *Glycoproteomics in Cerebrospinal Fluid Reveals Brain-Specific Glycosylation Changes.* International journal of molecular sciences, 2023. **24**(3): p. 1937.
12. Hoshi, K., et al., *Brain-Derived Major Glycoproteins Are Possible Biomarkers for Altered Metabolism of Cerebrospinal Fluid in Neurological Diseases.* International Journal of Molecular Sciences, 2023. **24**(7): p. 6084.
13. Lin, T.W., et al., *Ganglioside-focused Glycan Array Reveals Abnormal Anti-GD1b Auto-antibody in Plasma of Preclinical Huntington's Disease.* Mol Neurobiol, 2023. **60**(7): p. 3873-3882.
14. Haukedal, H., et al., *Golgi fragmentation – One of the earliest organelle phenotypes in Alzheimer's disease neurons.* Frontiers in neuroscience, 2023. **17**: p. 1120086-1120086.
15. Williams, S.E., et al., *Mammalian brain glycoproteins exhibit diminished glycan complexity compared to other tissues.* Nature Communications, 2022. **13**(1): p. 275.
16. Bürgi, M., et al., *Novel erythropoietin-based therapeutic candidates with extra N-glycan sites that block hematopoiesis but preserve neuroplasticity.* Biotechnology Journal, 2021. **16**(5): p. 2000455.
17. Rebelo, A.L., et al., *An optimized protocol for combined fluorescent lectin/immunohistochemistry to characterize tissue-specific glycan distribution in human or rodent tissues.* STAR protocols, 2021. **2**(1): p. 100237.
18. Faris, S., et al., *Small-molecule compound from AlphaScreen disrupts tau-glycan interface.* Frontiers in molecular biosciences, 2022. **9**: p. 1083225-1083225.
19. Murray, A., et al., *Proline-Rich Region II (PRR2) Plays an Important Role in Tau-Glycan Interaction: An NMR Study.* Biomolecules, 2022. **12**(11): p.1573

20. Gu, Y., et al., *Serum IgG N-glycans enable early detection and early relapse prediction of colorectal cancer.* International journal of cancer, 2023. **152**(3): p. 536-547.
21. Wilkinson, H., et al., *The O-Glycome of Human Nigrostriatal Tissue and Its Alteration in Parkinson's Disease.* Journal of Proteome Research, 2021. **20**(8): p. 3913-3924.
22. Cvetko, A., et al., *Glycosylation Alterations in Multiple Sclerosis Show Increased Proinflammatory Potential.* Biomedicines, 2020. **8**(10): p.410.
23. Gaunitz, S., L.O. Tjernberg, and S. Schedin-Weiss, *The N-glycan profile in cortex and hippocampus is altered in Alzheimer disease.* J Neurochem, 2021. **159**(2): p. 292-304.
24. Peng, Y., et al., *A streamlined strategy for rapid and selective analysis of serum N-glycome.* Analytica chimica acta, 2019. **1050**: p. 80-87.
25. Gutierrez Reyes, C.D., et al., *LC-MS/MS Isomeric Profiling of N-Glycans Derived from Low-Abundant Serum Glycoproteins in Mild Cognitive Impairment Patients.* Biomolecules (Basel, Switzerland), 2022. **12**(11): p. 1657.
26. Helm, J., et al., *Bisecting Lewis X in Hybrid-Type N-Glycans of Human Brain Revealed by Deep Structural Glycomics.* Analytical Chemistry, 2021. **93**(45): p. 15175-15182.
27. Kimura, K., et al., *Glycoproteomic analysis of the changes in protein N-glycosylation during neuronal differentiation in human-induced pluripotent stem cells and derived neuronal cells.* Sci Rep, 2021. **11**(1): p. 11169.
28. Yu, L., et al., *Human Brain and Blood N-Glycome Profiling in Alzheimer's Disease and Alzheimer's Disease-Related Dementias.* Frontiers in Aging Neuroscience, 2021. **13**: p.765259
29. Lee, J., et al., *Spatial and temporal diversity of glycome expression in mammalian brain.* Proceedings of the National Academy of Sciences, 2020. **117**(46): p. 28743-28753.
30. Xu, M., et al., *Mass Spectrometry-Based Analysis of Serum N-Glycosylation Changes in Patients with Parkinson's Disease.* ACS chemical neuroscience, 2022. **13**(12): p. 1719-1726.
31. Xu, M., et al., *Mass Spectrometric Analysis of Urinary N-Glycosylation Changes in Patients with Parkinson's Disease.* ACS chemical neuroscience, 2023. **14**(18): p. 3507-3517.
32. McCaughey-Chapman, A., et al., *Reprogramming of adult human dermal fibroblasts to induced dorsal forebrain precursor cells maintains aging signatures.* Frontiers in cellular neuroscience, 2023. **17**: p. 1003188-1003188.
33. Kraskovskaya, N., et al., *Protocol Optimization for Direct Reprogramming of Primary Human Fibroblast into Induced Striatal Neurons.* International journal of molecular sciences, 2023. **24**(7): p. 6799.
34. Slanzi, A., et al., *In vitro Models of Neurodegenerative Diseases.* Frontiers in Cell and Developmental Biology, 2020. **8**: p.328.
35. Maniv, I., et al., *Altered ubiquitin signaling induces Alzheimer's disease-like hallmarks in a three-dimensional human neural cell culture model.* Nature communications, 2023. **14**(1): p. 5922-5922.
36. Polini, B., et al., *T1AM/TAAR1 System Reduces Inflammatory Response and β-Amyloid Toxicity in Human Microglial HMC3 Cell Line.* International journal of molecular sciences, 2023. **24**(14): p. 11569.
37. Chen, Y., et al., *Dexmedetomidine protects SH-SY5Y cells against MPP+-induced declining of mitochondrial membrane potential and cell cycle deficits.* European Journal of Neuroscience, 2021. **54**(1): p. 4141-4153.
38. Kyunai, Y.M., et al., *Fucosyltransferase 8 (FUT8) and core fucose expression in oxidative stress response.* PLOS ONE, 2023. **18**(2): p. e0281516.
39. Pereira, I., M.J. Lopez-Martinez, and J. Samitier, *Advances in current in vitro models on neurodegenerative diseases.* Frontiers in bioengineering and biotechnology, 2023. **11**: p.1260397

40. Vahsen, B.F., et al., *C9orf72-ALS human iPSC microglia are pro-inflammatory and toxic to co-cultured motor neurons via MMP9.* Nature communications, 2023. **14**(1): p. 5898-5898.
41. Buijsen, R.A.M., et al., *Spinocerebellar Ataxia Type 1 Characteristics in Patient-Derived Fibroblast and iPSC-Derived Neuronal Cultures.* Movement disorders, 2023. **38**(8): p. 1428-1442.
42. Cetin, S., et al., *Cell models for Alzheimer's and Parkinson's disease: At the interface of biology and drug discovery.* Biomedicine & Pharmacotherapy, 2022. **149**: p. 112924.
43. Kovalevich, J. and D. Langford, *Considerations for the use of SH-SY5Y neuroblastoma cells in neurobiology.* Methods Mol Biol, 2013. **1078**: p. 9-21.
44. Shipley, M.M., C.A. Mangold, and M.L. Szpara, *Differentiation of the SH-SY5Y Human Neuroblastoma Cell Line.* Journal of visualized experiments : JoVE, 2016(108): p. 53193-53193.
45. Teppola, H., et al., *Morphological Differentiation Towards Neuronal Phenotype of SH-SY5Y Neuroblastoma Cells by Estradiol, Retinoic Acid and Cholesterol.* Neurochem Res, 2016. **41**(4): p. 731-47.
46. Magalingam, K.B., et al., *Influence of serum concentration in retinoic acid and phorbol ester induced differentiation of SH-SY5Y human neuroblastoma cell line.* Mol Biol Rep, 2020. **47**(11): p. 8775-8788.
47. Dwane, S., E. Durack, and P.A. Kiely, *Optimising parameters for the differentiation of SH-SY5Y cells to study cell adhesion and cell migration.* BMC Res Notes, 2013. **6**: p. 366.
48. Martin, E.-R., J. Gandawijaya, and A. Oguro-Ando, *A novel method for generating glutamatergic SH-SY5Y neuron-like cells utilizing B-27 supplement.* Frontiers in Pharmacology, 2022. **13**: p.943627.
49. Bell, M. and H. Zempel, *SH-SY5Y-derived neurons: a human neuronal model system for investigating TAU sorting and neuronal subtype-specific TAU vulnerability.* Reviews in the Neurosciences, 2022. **33**(1): p. 1-15.
50. de Medeiros, L.M., et al., *Cholinergic Differentiation of Human Neuroblastoma SH-SY5Y Cell Line and Its Potential Use as an In vitro Model for Alzheimer's Disease Studies.* Mol Neurobiol, 2019. **56**(11): p. 7355-7367.
51. Costanti, F., et al., *A Deep Learning Approach to Analyze NMR Spectra of SH-SY5Y Cells for Alzheimer's Disease Diagnosis.* Mathematics, 2023. **11**(12): p. 2664.
52. Xiong, W.-P., et al., *BMSCs-exosomes containing GDF-15 alleviated SH-SY5Y cell injury model of Alzheimer's disease via AKT/GSK-3β/β-catenin.* Brain Research Bulletin, 2021. **177**: p. 92-102.
53. Blanco-Míguez, A., et al., *Microbiota-Derived β-Amyloid-like Peptides Trigger Alzheimer's Disease-Related Pathways in the SH-SY5Y Neural Cell Line.* Nutrients, 2021. **13**(11): p. 3868.
54. Löffler, T., et al., *Stable mutated tau441 transfected SH-SY5Y cells as screening tool for Alzheimer's disease drug candidates.* J Mol Neurosci, 2012. **47**(1): p. 192-203.
55. Radagdam, S., et al., *Evaluation of dihydrotestosterone and dihydroprogesterone levels and gene expression of genes involved in neurosteroidogenesis in the SH-SY5Y Alzheimer disease cell model.* Frontiers in Neuroscience, 2023. **17**: p.1163806.
56. Wang, P., et al., *Midazolam alleviates cellular senescence in SH-SY5Y neuronal cells in Alzheimer's disease.* Brain and Behavior, 2023. **13**(1): p. e2822.
57. Snoderly-Foster, L.J., et al., *Regulation of Parkinson's disease-associated genes by Pumilio proteins and microRNAs in SH-SY5Y neuronal cells.* PLoS One, 2022. **17**(9): p.e0275235.
58. Elham Rezvani, B., et al., *Soluble Prion Peptide 107–120 Protects Neuroblastoma SH-SY5Y Cells against Oligomers Associated with Alzheimer's Disease.* International Journal of Molecular Sciences, 2020. **21**(19): p. 7273.

59. Guyon, A., et al., *The protective mutation A673T in amyloid precursor protein gene decreases A[beta] peptides production for 14 forms of Familial Alzheimer's Disease in SH-SY5Y cells.* PLoS ONE, 2020. **15**: p. e0237122.
60. Pokusa, M., et al., *Vulnerability of Subcellular Structures to Pathogenesis Induced by Rotenone in SH-SY5Y Cells.* Physiological Research, 2021. **70**(1): p. 89-99.
61. Grimm, M.O.W., et al., *The impact of capsaicinoids on APP processing in Alzheimer's disease in SH-SY5Y cells.* Scientific reports, 2020. **10**(1): p. 9164-9164.
62. Uberti, D., et al., *Characterization of tau proteins in human neuroblastoma SH-SY5Y cell line.* Neurosci Lett, 1997. **235**(3): p. 149-53.
63. Yirün, A., et al., *Evaluation of the effects of herpes simplex glycoprotein B on complement system and cytokines in in vitro models of Alzheimer's disease.* J Appl Toxicol, 2023. **43**(9): p. 1368-1378.
64. Boban, M., et al., *Human neuroblastoma SH-SY5Y cells treated with okadaic acid express phosphorylated high molecular weight tau-immunoreactive protein species.* J Neurosci Methods, 2019. **319**: p. 60-68.
65. Nasu, R., et al., *The Effect of Glyceraldehyde-Derived Advanced Glycation End Products on β-Tubulin-Inhibited Neurite Outgrowth in SH-SY5Y Human Neuroblastoma Cells.* Nutrients, 2020. **12**(10): p.2958.
66. Mundhara, N. and D. Panda, *β-II tubulin isotype directs stiffness and differentiation of neuroblastoma SH-SY5Y cells.* Molecular and cellular biochemistry, 2023. **478**(9): p. 1961-1971.
67. Kumari, A., S.S. Prassanawar, and D. Panda, *β-III Tubulin Levels Determine the Neurotoxicity Induced by Colchicine-Site Binding Agent Indibulin.* ACS chemical neuroscience, 2023. **14**(1): p. 19-34.
68. Demir, R., U. Şahar, and R. Deveci, *Determination of terminal glycan and total monosaccharide profiles of reelin glycoprotein in SH-SY5Y neuroblastoma cell line by lectin blotting and capillary liquid chromatography electrospray ionization-ion trap tandem mass spectrometry system.* Biochim Biophys Acta Proteins Proteom, 2021. **1869**(2): p. 140559.
69. Birol, M., et al., *Identification of N-linked glycans as specific mediators of neuronal uptake of acetylated α-Synuclein.* PLOS Biology, 2019. **17**(6): p. e3000318.
70. Hu, Y., et al., *N-linked glycan profiling in neuroblastoma cell lines.* Journal of proteome research, 2015. **14**(5): p. 2074-2081.
71. Forster, J.I., et al., *Characterization of Differentiated SH-SY5Y as Neuronal Screening Model Reveals Increased Oxidative Vulnerability.* J Biomol Screen, 2016. **21**(5): p. 496-509.
72. Cai, A., et al., *Neuroblastoma SH-SY5Y Cell Differentiation to Mature Neuron by AM580 Treatment.* Neurochemical Research, 2022. **47**(12): p. 3723-3732.
73. Dravid, A., et al., *Optimised techniques for high-throughput screening of differentiated SH-SY5Y cells and application for neurite outgrowth assays.* Scientific Reports, 2021. **11**(1): p. 23935.
74. Kaya, Z.B., et al., *Optimizing SH-SY5Y cell culture: exploring the beneficial effects of an alternative media supplement on cell proliferation and viability.* Scientific Reports, 2024. **14**(1): p. 4775.
75. Wang, J., et al., *An Efficient and Economical N-Glycome Sample Preparation Using Acetone Precipitation.* Metabolites, 2022. **12**(12): p.1285.
76. Kim, B.J. and D.C. Dallas, *Systematic examination of protein extraction, proteolytic glycopeptide enrichment and MS/MS fragmentation techniques for site-specific profiling of human milk N-glycoproteins.* Talanta (Oxford), 2021. **224**: p. 121811-121811.

77. Barboza, M., et al., *Region-Specific Cell Membrane N-Glycome of Functional Mouse Brain Areas Revealed by nanoLC-MS Analysis.* Molecular & cellular proteomics, 2021. **20**: p. 100130-100130.
78. Hilliard, M., et al., *Glycan characterization of the NIST RM monoclonal antibody using a total analytical solution: From sample preparation to data analysis.* MAbs, 2017. **9**(8): p. 1349-1359.
79. Zhang, R., et al., *GlycanGUI: Automated Glycan Annotation and Quantification Using Glucose Unit Index.* Frontiers in Chemistry, 2021. **9**: p.707382.
80. Campbell, M.P., et al., *GlycoBase and autoGU: tools for HPLC-based glycan analysis.* Bioinformatics, 2008. **24**(9): p. 1214-1216.
81. Ashwood, C., et al., *Standardization of PGC-LC-MS-based glycomics for sample specific glycotyping.* Analyst (London), 2019. **144**(11): p. 361-3612.

Chapter 6

Conclusions and Future Work

6.1 Conclusions

A glycan analysis workflow using HPLC-fluorescence for investigating the *N*- and *O*-linked glycans in neurodegenerative diseases was developed in this thesis. Chapter 2 used the synthetic labelling reagent (**5**) to label *N*- and *O*-linked glycans by a reductive amination and a CuAAc reaction, respectively. Chapter 3 optimised the protein cleavage method for labelling the amino glycans in the amino acids' sidechain. Chapter 4 compared the SPE enrichment of the labelled glycans method with alternative methods (using cotton wool as the sorbent base). Finally, Chapter 5 implemented all processes to develop the analysis workflow for the glycan profile levels generated from SH-SY5Y cells (human neurological cell lines) during differentiation to the complete neuron types.

Chapter 2 aimed to determine that the synthetic alkyne labelling reagent (**5**) can label the *N*- and *O*-linked glycans for HPLC-fluorescence analysis. The *O*-linked glycans required conversion of the amino acid side chain to amino azide before being labelled by the CuAAc reaction, as shown in Figure 6.1 (A). The *N*-linked glycans can be labelled with **5** by reductive amination (Figure 6.1 (B)) or CuAAc reaction at the amino azide side chain. The HPLC chromatogram using **5** as the labelling reagent in *N*- and *O*-linked glycan models (**16** and **25**) in different reactions is shown in Figure 6.1 (C). The HPLC chromatogram showed different retention times of 1 and 2 GU (5.3 and 6.5 minutes, respectively) of different linkage types of glycans. This result means **5** can be used as the labelling reagent for different linkage types for HPLC-fluorescence analysis in different labelling reactions for the general form of glycans and the amino azide form of glycans. However, most of the CuAAc reaction studies of glycans in living cells focus on introducing the azide functional group to the sugar moieties. The monosaccharide that attaches with amino acids is GlcNAc for *N*-linked and GalNAc for *O*-linked glycans. Using the CuAAc reaction to label the fluorophore at the azide sugar side chain still needs to release glycan from the cores as labelled by reductive amination reaction. The problems with the O-linked glycans, which have no specific enzymes for all cores releasing and peeling by-products, continue to exist. Modifying the amino azide side chain labelled by CuAAc was developed in this Chapter as the alternative method. Labelling the fluorophore at the amino acids side chain can analyse all core *N*- and *O*-linked glycans simultaneously without releasing the glycan from the cores. However, this method needs to hydrolyse the protein to a single amino acid and glycoprotein before labelling and enriching the labelled glycoprotein from the labelled amino acids for HPLC analysis. The protein hydrolysis and enrichment methods were studied in Chapters 3 and 4 of this thesis, respectively.

Chapter 3 aimed to optimise methods to analyse *N*- and *O*-linked glycans simultaneously without releasing the glycans from the core by cleavage from the peptide to a single amino acid. RNase A was used as the simple protein model for investigation and does not contain glycans in its structure. A combination of enzymes (pepsin, trypsin, LAP, and pronase) and acid concentrations (1-5 M HCl) were chosen for the cleavage of the protein to single amino acids. DNS, which is a fluorescence labelling reagent for the amine group, was selected to label the amino acids' side chains to prove the cleavage results. However, the results in this section did not complete the objective. The four enzymes and 5 M HCl were unable to cleave the simple protein model to single amino acids completely. The peptide peaks were still found in the chromatogram.

Chapter 4 aimed to develop and optimise the enrichment of labelled glycans using SPE and compare the results with cotton wool enrichment using **5** and **26** as the labelling reagents. Lactose was used as the model substrate. The high concentration of the excess labelling reagents interfered with the sample peaks in the HPLC chromatogram by decreasing the resolution between the labelling reagent and nearby sample peaks. The high intensity of labelling reagent can decrease the appearance of the sample peaks, especially with a low concentration of samples.

The first objective is optimaisation the type of SPE for enrichment the labelled glycans. Standard **16** and **27** (100 nmol/ml) as the labelled *N*-glycan model and **5** and **26** as the labelling reagents were used for optimising the types and conditions of SPE enrichment. The various types and brands of SPE (C8, C18, Amide, PGC, Specific SPE for glycans analysis (Superco Discovery glycans), porous polystyrene DVB, SAX, and SCX) were studied for selecting the optimum method for enriching the labelled glycans. In theory, the best SPE condition for enriching labelled glycans can remove all the excess labelling reagents in the loading and washing steps. Moreover, the labelled glycans should be found in the eluting step with more than 95% recovery. Amide SPE brand A was chosen to enrich labelled glycans. The results showed that only Amide SPE brand A could remove the labelling reagents (**5** and **26**) during the loading and washing steps. Standards **16** and **27** were found in the eluting steps in more than 95% yield. Figure 6.1 (F and G) shows the standards **16** and **27** chromatograms from the Amide-SPE enrichment results in each step. This phenomenon represents the theory that only the target molecule can make the bond with the absorbent of the SPE and break that bond by the eluting solvent. However, the interfered molecules cannot make the bond with the absorbent and are removed from the SPE cartridge before the eluting step. Some standards **16** and **27** (less than 5%) were found in the washing step from the water content (1-3%) in the washing step solvent system. However, the two brands of the Amide SPE afforded different recovery percentages.

The second objective in this Chapter is developing the alternative enrichment labelled glycans by using the cotton wool as the sorbent base. This method was developed and compared to the commercial Amide SPE for the enrichment of the labelled glycans. The results showed that the efficiency of cotton wool (brand A) enrichment of the labelled glycan standards (**16** and **27**) from the excess labelling reagents (**5** and **26**) in the studied condition was equivalent to Amide SPE (brand A), as shown in Figure 6.1 (H and I). However, the results showed that the water content in the loading and washing step affected the bond between the labelled glycans and cotton wool. The cotton wool was defined as the HILIC SPE system [1-4]. The differences in enrichment efficiency between the three cotton wool brands showed the different results in brand C from brands A and B. The cotton wool brand C had lower recovery percentages of standards in the eluting step than brands A and B.

The enrichment results from Amide SPE and cotton wool were confirmed using more complex glycans (maltotriose and dextran ladder) that had been labelled using **5** and **26**, as shown in Figures 6.1 (J and K for maltotriose, and L and M for dextran ladder). The results showed that enrichment from the cotton wool brand A could enrich the labelled glycans in the different labelling reagents and glucose units equivalent to the Amide SPE for the same amount of labelled glycans. Cotton wool can be developed as the alternative cheap, accurate and precise enrichment protocol for labelled glycans to replace SPE. However, the absorption and enrichment capacity of cotton wool depended on the weight and brand of cotton wool. As in this study, the weight of cotton wool 5 ± 0.5 mg per tip can enrich the labelled glycan between 10-100 nmol.

Chapter 5 aimed to apply the developed glycan analysis workflow from Chapters 2-4 to analyse the glycan profile from a complex biological sample. The *N*-glycan profile levels were chosen as

a potential biomarker in neurodegenerative disorders. The SH-SY5Y cell line was chosen as the neurodegenerative model. In this study, SH-SY5Y cells were stimulated from the epithelial-like morphology (*S* type) to the neuron-like morphology (*N* type) by adding ATRA, B-27, db-cAMP, and BDNF in the differentiation media over 21 days, as shown in Figure 6.1 (N). The neuronal characteristics of fully differentiated SH-SY5Y cells are apparent by the change in the morphology of the cell and by the detection of a specific protein using immunofluorescence. The cells were stained every 7 days with an antibody to β-III tubulin. The glycan profiles were analysed every 7 days by HPLC-fluorescence. The glycan profiles between the differentiated and undifferentiated states of SH-SY5Y were studied using **26** as the labelling reagent and the enrichment method using SPE, as reported in Chapter 4. The results showed SH-SY5Y generated the glycans between 1-23 GU in the differentiated and undifferentiated states, as shown in Figures 6.1 (O). The glycan between 1-23 GU was not found in the undifferentiated state. All homopolymer glycans were produced in the differentiated process. The two unknown glycans were found in the undifferentiated state and decreasing levels when differentiated to neuron-like morphology on day 21.

In conclusion, carbohydrate analysis for biomedical workflow for neurodegenerative disorders was developed using HPLC-fluorescence to analyse the total *N*-glycans produced during differentiation of neuron cell lines. The results show the different levels of *N*-glycans between the undifferentiated and differentiated states. The calculation of the total *N*-glycans demonstrated that there are increases of 1-23 GU and decreases of unknown glycans 1 and 2 between the cells differentiated to the neuron type. This thesis's outcomes are summarised in Figure 6.5, which summarises the main findings from each chapter.

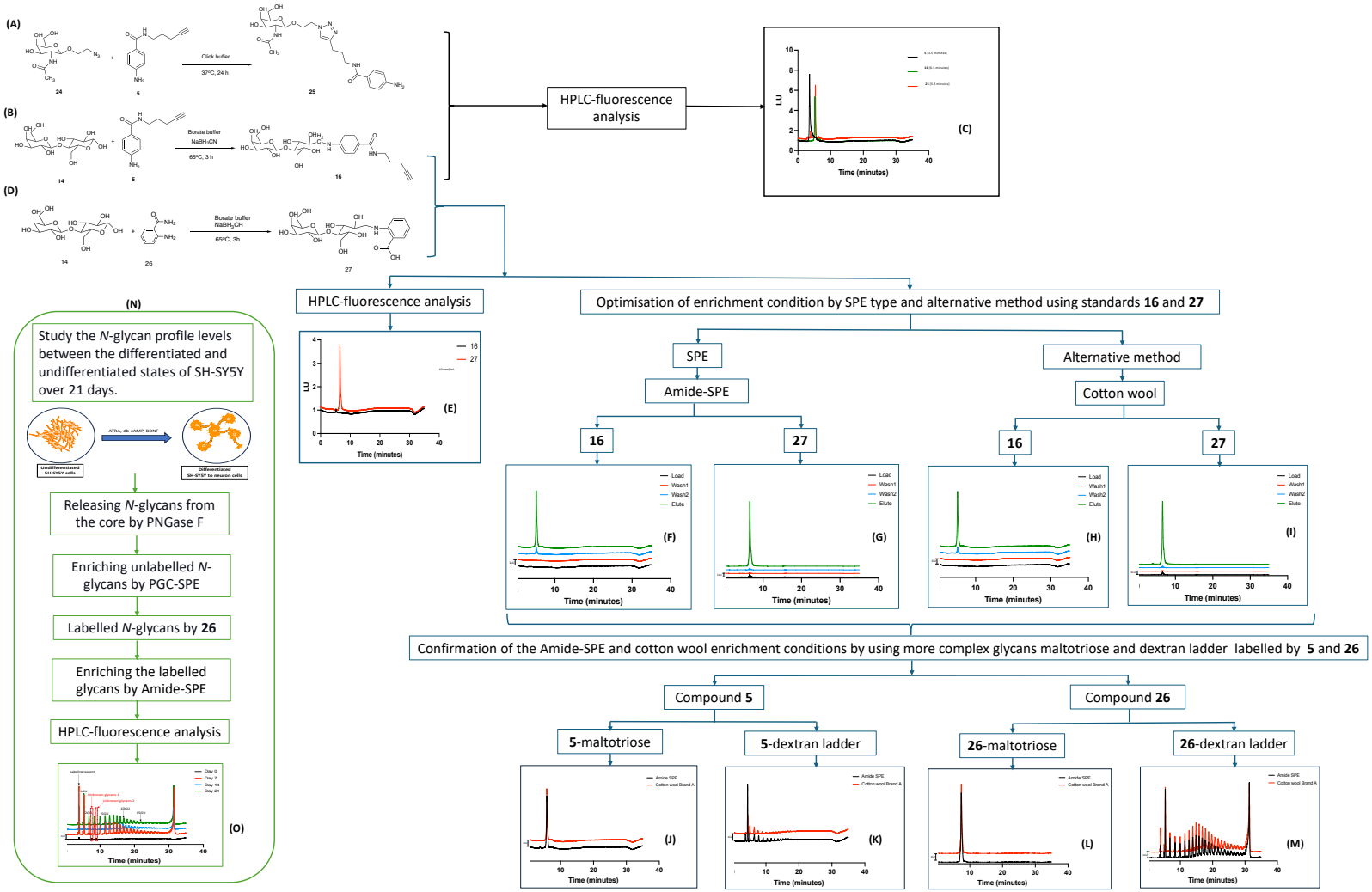

Figure 6.1 The summary of workflow and results of this thesis, (A)–(C) according to Chapter 2 results, (B) and (D)-(M) according to Chapter 4 results, and (N)-(O) according to Chapter 5 results.

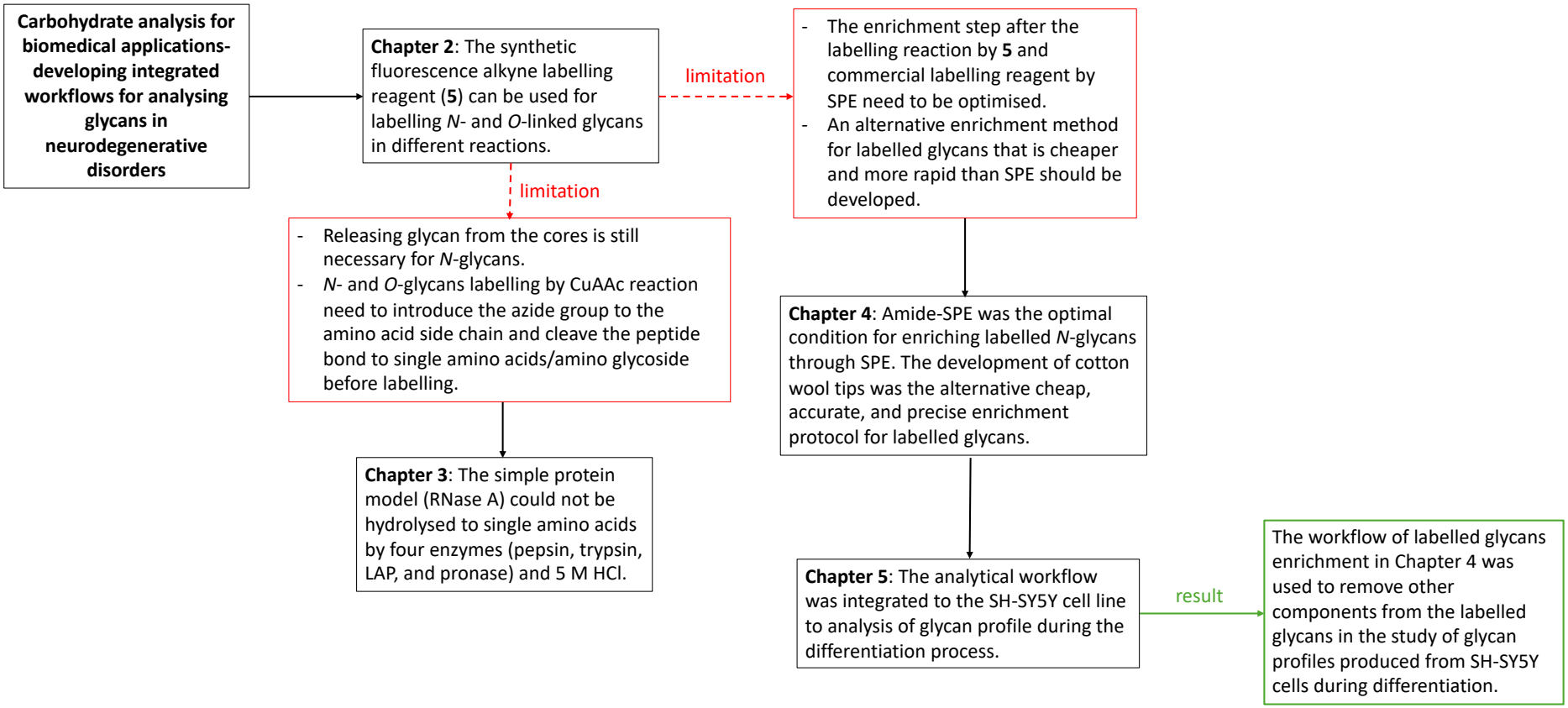

Figure 6.2 Schematic representation of the conclusion within this thesis

6.2 Future work

Figure 6.3 summarizes the future work and suggestions for this thesis**.** Chapter 2 studied using the synthetic alkyne labelling reagent **(5)** to label the glycans for HPLC analysis. Compound **5** can be labelled glycan by reductive amination reaction for normal glycan and CuAAc reaction for azido-glycans. There are researches on using azido-modified monosaccharides, such as azido-sialic acid or azido-mannose [5, 6], or introducing the alkyne functional group to the sugar structure [7] to label the fluorescence of the glycan by CuAAc reaction for HPLC analysis. These methods were developed for cell activity tracking in living cells *in vitro*. The CuAAc reaction for glycan labelling should be developed workflow for future work by introducing the azide to the amino acids, cleaving the protein to single amino acids, labelling the azido-glycoproteins by CuAAc reaction for adding the fluorophore and enriching the labelled azido-glycoproteins before HPLC analysis. This developed workflow can analyse the *N*- and *O*-linked glycans simultaneously. However, the limitation of **5** was lower fluorescence absorptivity than the commercial labelling reagent (**26**), shown in Figure 6.1 (F). Improving the **5** structure to increase the fluorescence absorption is needed to increase the sensitivity and lower the limit of detection for quantitative analysis of the labelled glycans.

For Chapter 3, the protein hydrolysis method needs improvement to complete the protein digestion to single amino acids. This approach can then analyse the *N*- and *O*-amino glycans in the protein sequences. In theory, cleavage of the protein to single amino acids and labelled fluorophore at the amino acid side chain can analyse the amino glycans without releasing the glycan from the cores. However, the studies of protein hydrolysis used strong conditions, such as high temperatures (> 100 ^{o}C) with strong acids, such as 4-12 M HCl, 88% FA [8-14] or a combination of simulated human digestive fluid (including amylase, pepsin, pancreatin, trypsin, bile or commercial simulated digestive fluid) [15-17]. For stabilising the glycans, simulated human digestion juices should be selected as the first choice of complete protein digestion to complete the purpose of this Chapter in future research.

Chapter 4, the alternative enrichment of labelled carbohydrates by cotton wool tips, requires the development of a consistent method for preparing cotton wool tips to ensure consistency of the results and increase the loading capacity. Moreover, the different SPE and cotton wool brands gave different results. The standard preparation of the SPE absorbent materials should be developed to ensure consistency between the brands. For the cotton wool SPE, studying the physical and chemical properties of the different brands can define the different enrichment properties. The results can be used to select the cotton wool to prepare as the SPE tip to avoid the different enrichment properties.

From Chapter 5, the unknown glycans 1 and 2 were interesting glycans as biomarkers in neurodegenerative disease, as the levels decrease during the SH-SY5Y differentiation, as shown in Figures 6.1 (O). The study should be repeated to confirm the increase of total *N*-glycans and decrease of unknown glycans 1 and 2.

The purification and elucidation of unknown glycans 1 and 2 structures are required. After clarifying the two unknown glycan structures, the levels of *N*- glycan profile and these two unknown glycans should be investigated by comparing the neurodegenerative patients and healthy people's biological samples (for example, blood, serum, or CSF) to be the potential biomarkers. If the results are correlated between the *in vitro* and *in vivo* about the *N*-glycan and two unknown glycan levels. The SH-SY5Y cell line can be used in the pre-clinical phase study of the neurodegenerative medicines development process by following the changing of glycan levels.

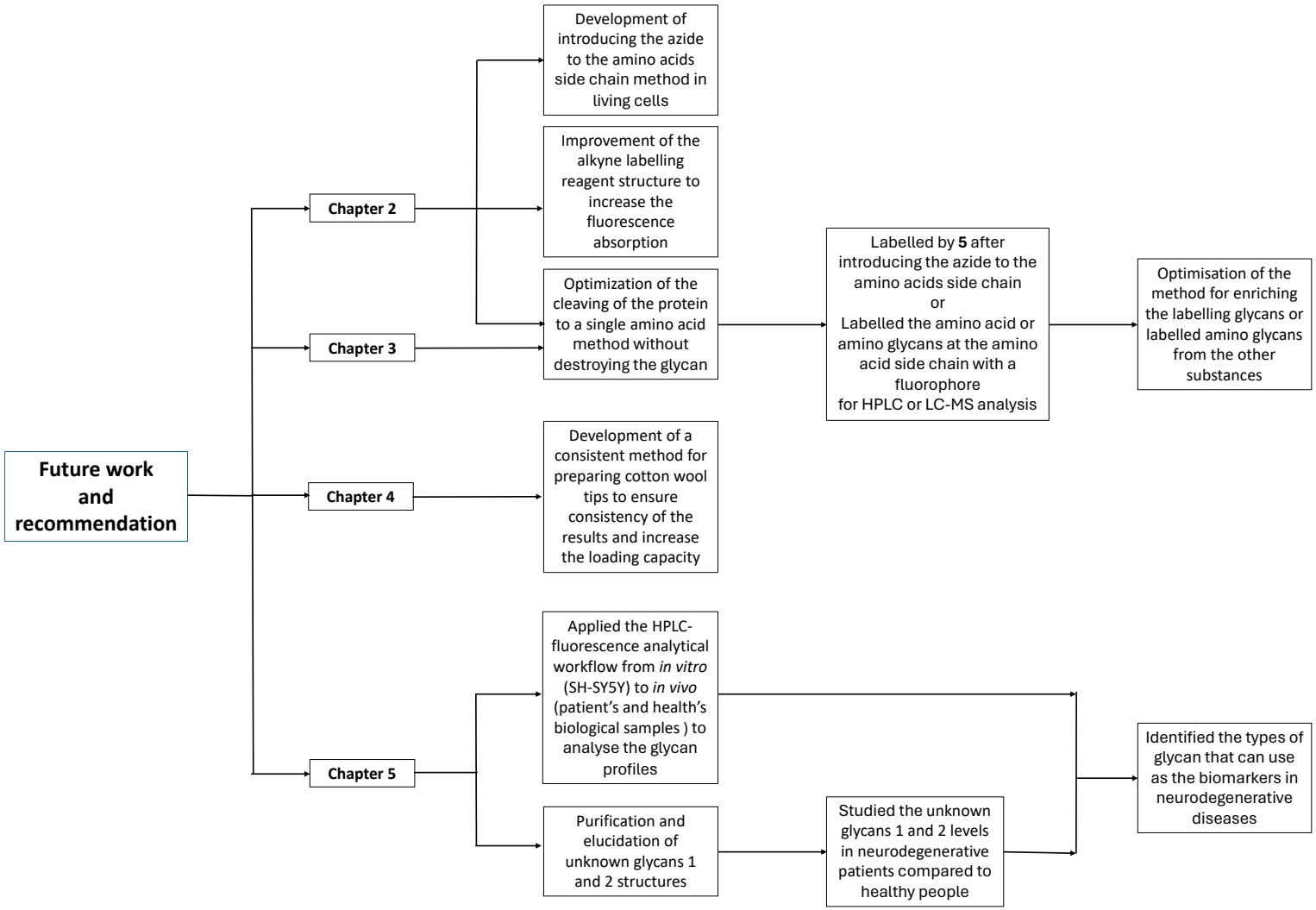

Figure 6.3 Schematic representation of the future work and suggestions.

6.3 References

1. Selman, M.H.J., et al., *Cotton HILIC SPE Microtips for Microscale Purification and Enrichment of Glycans and Glycopeptides.* Analytical Chemistry, 2011. **83**(7): p. 2492-2499.
2. Peng, Y., et al., *A streamlined strategy for rapid and selective analysis of serum N-glycome.* Analytica chimica acta, 2019. **1050**: p. 80-87.
3. Han, J., et al., *Purification of N- and O-glycans and their derivatives from biological samples by the absorbent cotton hydrophilic chromatographic column.* Journal of Chromatography A, 2020. **1620**: p. 461001.
4. Qin, W., et al., *Serum Protein N-Glycosylation Signatures of Neuroblastoma.* Frontiers in oncology, 2021. **11**: p. 603417-603417.
5. Darabedian, N., et al., *O-Acetylated Chemical Reporters of Glycosylation Can Display Metabolism-Dependent Background Labeling of Proteins but Are Generally Reliable Tools for the Identification of Glycoproteins.* Frontiers in Chemistry, 2020. **8**: p.318.
6. Lee, D.J., et al., *A synthetic approach to 'click' neoglycoprotein analogues of EPO employing one-pot native chemical ligation and CuAAC chemistry.* Chemical Science, 2019. **10**(3): p. 815-828.
7. Ivanova, I.M., et al., *Fluorescent mannosides serve as acceptor substrates for glycosyltransferase and sugar-1-phosphate transferase activities in Euglena gracilis membranes.* Carbohydrate research, 2017. **438**: p. 26-38.
8. Davila, M. and X. Du, *Primary exploration of mushroom protein hydrolysis and cooking impact on the protein amino acid profiles of Agaricus bisporus and Lentinula edodes mushrooms.* International Journal of Gastronomy and Food Science, 2023. **32**: p. 100710.
9. Luparelli, A.V., et al., *Development of a Quantitative UPLC-ESI/MS Method for the Simultaneous Determination of the Chitin and Protein Content in Insects.* Food analytical methods, 2023. **16**(2): p. 252-265.
10. Abd El-Rady, T.K., et al., *Effect of different hydrolysis methods on composition and functional properties of fish protein hydrolysate obtained from Bigeye tuna waste.* International journal of food science & technology, 2023. **58**(12): p. 6552-6562.
11. Ortega, A.F., H. Zhao, and M.E. Van Amburgh, *Development and Validation of a Method for Hydrolysis and Analysis of Amino Acids in Ruminant Feeds, Tissue, and Milk Using Isotope Dilution Z-HILIC Coupled with Electrospray Ionization Triple Quadrupole LC-MS/MS.* Journal of agricultural and food chemistry, 2024. **72**(1): p. 833-844.
12. Araya, M., et al., *Determination of free and protein amino acid content in microalgae by HPLC-DAD with pre-column derivatization and pressure hydrolysis.* Marine chemistry, 2021. **234**: p. 103999.
13. Reddy, P., et al., *High-Throughput Analysis of Amino Acids for Protein Quantification in Plant and Animal-Derived Samples Using High Resolution Mass Spectrometry.* Molecules (Basel, Switzerland), 2021. **26**(24): p. 7578.
14. Gargano, E.M., et al., *Development and validation of a method for simultaneous analysis of hair underivatized amino acids and damage biomarkers, using liquid*

chromatography-tandem mass spectrometry. Talanta (Oxford), 2021. **233**: p. 122584-122584.
15. Sousa, R., et al., *Comparison of in vitro digestibility and DIAAR between vegan and meat burgers before and after grilling.* Food research international, 2023. **166**: p. 112569-112569.
16. Wang, R., et al., *In vitro protein digestibility of edible filamentous fungi compared to common food protein sources.* Food bioscience, 2023. **54**: p. 102862.
17. Liu, D., et al., *The necessity of walnut proteolysis based on evaluation after in vitro simulated digestion: ACE inhibition and DPPH radical-scavenging activities.* Food chemistry, 2020. **311**: p. 125960-125960.